Development of a Continuous Calcium Looping Process for CO_2 Capture

By
Robert Symonds

Thesis submitted to the
Faculty of Graduate and Postdoctoral Studies
In partial fulfillment of the requirements
For the Degree of Ph.D. in Chemical Engineering

Department of Chemical and Biological Engineering
University of Ottawa
2017

Statement of Contribution of Collaborators

I am the sole author of all the chapters of this thesis, except for Chapter 7 which was co-written by myself and Dr. Firas Ridha under my guidance. My academic supervisors, Dr. Arturo Macchi of the Department of Chemical and Biological Engineering and Dr. Edward John Anthony of Natural Resources Canada – CanmetENERGY and Cranfield University provided editorial comments and supervised my overall work.

Chapter 3 is an article which was submitted to Fuel in 2017. This article was written by me. The work was a collaboration with Natural Resources Canada – CanmetENERGY. Dr. Dennis Lu and Dr. Robin Hughes provided editorial corrections and overview for my work while working at CanmetENERGY.

Chapter 4 is an article which was published in Industrial & Engineering Chemistry Research in 2012. This article was written by me. The work was a collaboration with Natural Resources Canada – CanmetENERGY. Dr. Dennis Lu and Dr. Vasilije Manovic provided editorial corrections and overview for my work while working at CanmetENERGY.

Chapter 6 is an article which was published in Powder Technology in 2016. This article was written by me. The work was a collaboration with Natural Resources Canada – CanmetENERGY. Dr. Dennis Lu provided editorial corrections and overview for my work while working at CanmetENERGY, whereas Mr. Scott Champagne and Dr. Firas Ridha provided editorial corrections.

Chapter 7 is an article which was published in Powder Technology in 2016. This article was co-written by myself and Dr. Firas Ridha under my guidance. The work was a collaboration with Natural Resources Canada – CanmetENERGY. Dr. Dennis Lu provided editorial

corrections and overview for my work while working at CanmetENERGY. Mr. Scott Champagne provided editorial corrections.

Signature: _____ Date: _____

Abstract

Carbon capture and storage technologies are required in order to reduce greenhouse gas emissions, while continuing to utilize existing fossil-fueled power generation stations. Of the many developing post-combustion CO_2 capture technologies, calcium looping appears promising due to its high thermal efficiency, technical feasibility at commercial-scale, and low sorbent cost. Calcium looping has now been performed at the larger-scale, but there is still a significant quantity of information about sorbent performance, the fate of trace pollutant emissions (specifically SO_2 and HCl), dual fluidized bed operating configurations, and impact of realistic operating conditions that still needs to be determined. Based on an economic analysis of the process, three key parameters serve to have the largest potential economic impact: (1) the sorbent deactivation rate, (2) the Ca/C molar ratio, and (3) the rate of sorbent attrition. Therefore, a series of bench-scale, pilot-scale, and continuous pilot-scale testing were conducted to not only explore these parameters from an improvement standpoint, but accurately determine them under conditions expected at the commercial-scale.

The presence of HCl did not have a significant impact on sorbent performance provided that steam is present during calcination, although issues with downstream corrosion could be a factor. High CO_2 partial pressures during calcination, coupled with high temperatures and the presence of SO_2, resulted in dramatically lower cyclic carbonation conversions and a reduced high CO_2 capture efficiency regime. Continuous pilot-scale testing generated realistic, and more detrimental, values for sorbent carrying capacity, Ca/C molar ratio, sorbent make-up rates, and rate of sorbent elutriation, that can now be utilized for techno-economic evaluations and scale-up of the technology.

Sommaire

Les technologies de capture et séquestration du CO_2 sont nécessaires pour réduire les émissions de gaz à effet de serre tout en continuant l'utilisation de centrales thermiques à combustible fossile existantes. Parmi les nombreuses technologies post-combustion de capture du CO_2 en développement, le bouclage du calcium semble être prometteur en raison de son efficacité thermique élevée, de sa faisabilité technique à l'échelle commerciale et du faible coût du sorbant. Le bouclage du calcium a maintenant été réalisé à relativement grande échelle, mais il manque encore une quantité importante d'informations sur la performance du sorbant, le sort des émissions de polluants mineures (spécifiquement SO_2 et HCl), les configurations d'opérations des lits fluidisés doubles et l'impact de conditions d'opérations réalistes. Sur une base d'analyse économique du procédé, trois paramètres clés ont potentiellement le plus grand impact économique: (1) le taux de désactivation du sorbant, (2) le rapport molaire Ca/C et (3) le taux d'attrition du sorbant. Par conséquent, une série d'essais à l'échelle laboratoire, à l'échelle pilote et à l'échelle pilote en continu ont été réalisés pour explorer ces paramètres d'un point de vue d'amélioration et afin de les déterminer avec exactitude pour les conditions prévues à l'échelle commerciale.

La présence de HCl n'a pas eu d'impact significatif sur la performance du sorbant, à condition que la vapeur soit présente lors de la calcination, bien que des problèmes avec la corrosion en aval puissent être un facteur. Des pressions partielles élevées de CO_2 pendant la calcination, couplées à des températures élevées et à la présence de SO_2, ont entraîné des conversions de carbonatation cyclique considérablement plus faibles et un régime réduit d'efficacité de capture de CO_2. Des essais en continu à l'échelle pilote ont généré des valeurs réalistes, et plus nuisibles, pour la capacité de charge du sorbant, le rapport molaire Ca/C requis, les taux d'appoint du sorbant et les taux elutriés du sorbant, qui peuvent maintenant être utilisés pour les évaluations techno-économiques et la mise à l'échelle de la technologie.

Acknowledgements

I would like to express my most sincere gratitude to my academic co-supervisors, Dr. Arturo Macchi and Dr. E.J. 'Ben' Anthony, for their guidance, support, and patience throughout my graduate studies, and for giving me the opportunity to continue my education while working at Natural Resources Canada – CanmetENERGY.

I would also like to thank Dr. Dennis Lu and Dr. Robin Hughes from CanmetENERGY for encouraging me to continue my graduate studies and for providing direction and assistance with my research. I also appreciate all the help I received from the engineering and technical staff at CanmetENERGY, which allowed me to complete all my experimental work.

Lastly, I would like to express my appreciation to my wife, Katie, family, and friends for their endless support and encouragement.

Table of Contents

List of Tables

List of Figures

Acronyms

ASU	Air Separation Unit
BET	Brunauer-Emmett-Teller
BFB	Bubbling Fluidized Bed
BJH	Barrett-Joyner-Halenda
CaL	Calcium Looping
CAPEX	Capital Expenditures
CCS	Carbon Capture and Storage
CFB	Circulating Fluidized Bed
CFBC	Circulating Fluidized Bed Combustor
CLC	Chemical Looping Combustion
DFB	Dual Fluidized Bed
EDX	Energy Dispersive X-Ray
GHG	Greenhouse Gas
HHV	Higher Heating Value
ID	Induced Draft
IEA	International Energy Agency
IPCC	Intergovernmental Panel on Climate Change
ITRI	Industrial Technology Research Institute
LOF	Loss on Fusion
MEA	Monoethanolamine
OC	Oxygen Carrier
O&M	Operations and Maintenance
OPEX	Operating Expenditures

PAH	Polycyclic Aromatic Hydrocarbon
PC	Pulverized Fuel Combustor
PCC	Post-combustion CO_2 Capture
PSD	Particle Size Distribution
RDF	Refuse Derived Fuel
SEM	Scanning Electron Microscopy
TGA	Thermogravimetric Analyzer
XFR	X-Ray Florescence

Chapter 1 – Introduction

1.1 – Carbon Capture and Storage (CCS)

1.1.1 – Background

CO_2 emissions from fossil-fuelled power stations are believed to be a major contributor to global warming and climate change (IPCC, 2013) (Pachauri & Reisinger, 2007). One method for reducing CO_2 emissions would be *via* a carbon capture and storage (CCS) technology. The rationale for the use of CCS on fossil-fuelled power plants is that, when deployed with other technologies (e.g., renewables), the overall cost of electricity would be minimized. Since the use of renewable sources of electricity (e.g., wind, solar, etc.) are intermittent, the implementation of CCS to coal-fired power plants would reduce the need for large-scale energy storage systems.

At this time, CCS has been proposed for combustion (related to power generation) and gasification, where the CO_2 is captured at a particular point within the overall process. Other industries such as cement production, iron / steel making, and natural gas treatment could also be adapted with CO_2 capture technologies. After the CO_2 has been captured, it is then compressed to 80 bar (or potentially higher), prior to being transported to a storage site. Once at one of the many types of stable geological sites, the CO_2 is injected underground (or deep ocean) trapping it and preventing its subsequent emission into the atmosphere (Bachu, 2008) (Beer, 2000) (Metz, Davidson, de Conninck, Loos, & Meyer, 2005).

To date, all the individual elements of the CCS chain including capture, compression, transportation, and sequestration have been demonstrated at or close to the commercial scale (Krebs, 2012). However, the integration of these elements into a single process still represents a significant scientific / engineering challenge. The subsequent sections will give a brief overview of the current CO_2 capture technologies associated with large-scale combustion or gasification

systems. Typically, the technologies are categorised into three main areas: (1) pre-combustion, (2) oxy-fuel combustion, and (3) post-combustion (Berger, 2004).

Pre-combustion CO_2 capture systems eliminate carbon from the fuel prior to final combustion. An example of this type of system is the production of syngas (mainly CO and H_2) from gasification (solid or liquid fuel), which is further reacted to produce H_2 (typically generated using a water-gas shift reactor). Oxy-fuel combustion systems capture CO_2 within the process itself by replacing air with high purity oxygen as the oxidant; thus, producing a concentrated CO_2 stream ready for compression. It should be noted that the oxygen required for combustion can be supplied either by cryogenic separation from air or by using a metal oxide (chemical looping). Oxy-fuel systems can be applied to both pulverized fuel combustors (PC) and circulating fluidized bed combustors (CFBC). The final type of CO_2 capture systems are those that are targeted at removing CO_2 at the back end of existing fossil-fuelled power stations. These separation technologies include chemical and physical solvents, membranes, low-temperature physical adsorbents, and calcium looping. Capture technologies such as solvent scrubbing, oxy-fuel combustion, chemical looping combustion, and calcium looping are expected to be commercialized within the next 10-20 years pending the implementation of greenhouse gas (GHG) regulations.

1.1.2 – Power Generation

Although there has recently been a significant reduction in the world-wide demand for oil and gas, the demand for coal has steadily increased over the past decade. As of 2010, the total demand for coal was 5000 Mt and is expected to increase to more than 7500 Mt by the year 2035 (IEA, 2010). It should be mentioned at this point that the entirety of this growth is in non-OECD (Organization for Economic Co-operation and Development) countries.

In 2008, approximately 41% of total global electricity production was provided from coal-fired plants which equates to over 8200 TWh. Although the share of power production from coal-fired plants is expected to drop over the next few decades, the total power production is still expected to increase to over 11000 TWh. This increase in total coal consumption is attributed to non-OECD countries, as OECD nations are moving towards the use of shale gas (and other unconventional sources) and policies encouraging the reduction of the carbon intensity of power generation (IEA, 2010). One example of minimizing the intensity of power generation and / or increasing energy efficiency is by displacing sub-critical boilers (30-45% efficiency) with super-critical and ultra-supercritical. Super-critical power plants operate with a higher base-load efficiency (48-52%) and ultra-supercritical higher still (Viswanathan, et al., 2001). Although some of these technologies are still under development, and the associated capital costs are relatively high due to high priced materials (Nalbandian, 2008) (Nalbandian, 2009), coal-fired power generation can remain economical even with energy penalties associated to CCS.

1.2 – Overview of Current CO_2 Capture Technologies

The following sections provide a brief overview of the CO_2 capture technologies that are believed to be the most promising and are closest to commercialization: (1) solvent scrubbing, (2) oxy-fuel combustion, (3) chemical looping combustion, and finally (4) calcium looping, which is the focus of this thesis.

1.2.1 – Solvent Scrubbing

In this post-combustion CO_2 capture (PCC) process, the CO_2 is separated from the flue gas using chemical absorption, such as monoethanolamine (MEA), ammonia, Rectisol, and Selexol (Mohammed, Samah, Mohamed, & Sabina, 2014) (Yeh & Bai, 1999). Figure 1.2.1

shows the process flow diagram of the technology. Although this technique has been used for CO_2 separation in the natural gas industry for over 60 years, the size and cost of the required scrubber would be on par to that of a SO_2 scrubber and would consume up to one third of the total steam production of the power plant. In a year 2000 study performed by the National Energy Technology Laboratory (NETL), it was determined that addition of a MEA solvent scrubbing system would increase the cost of electricity by as much as 70%, while the footprint of the existing power plant could expect to grow by nearly 60% (Elwell and Grant, 2006).

The MEA absorption process has been the most extensively studied CO_2 absorption technology. Other solvents such as diethanolamine (DEA) and methyl-diethanolamine (MDEA) have also been explored to overcome the inherent disadvantages of the solvent scrubbing CO_2 capture technologies. These disadvantages include (Fauth, Frommell, Hoffman, Reasbeck, & Pennline, 2005) (Resnik, Yeh, & Pennline, 2004) (Yeh, Resnik, Rygle, & Pennline, 2005):

- Low CO_2 carrying capacity
- High equipment corrosion rates
- Amine degradation by trace fuel contaminants (i.e., SO_2, NO_2, HCl, HF, and O_2)
- High energy consumption during high temperature absorbent regeneration
- Loss of solvent during regeneration

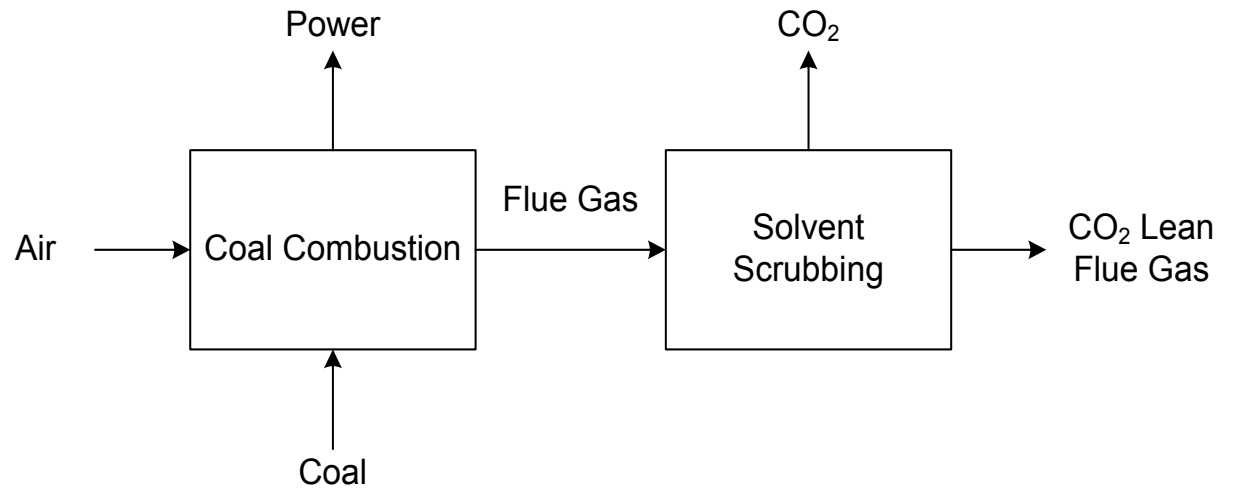

Figure 1.2.1: Process flow diagram for solvent scrubbing CO_2 capture technology.

1.2.2 – Oxy-fuel Combustion

Oxy-fuel combustion is one of the most developed technologies for CO_2 capture (Jia, et al., 2012). Oxy-fuel combustion refers to a fuel (in most cases coal) being burned in a mixture of O_2 and recycled flue gas, used to moderate the combustion temperature. Dissimilar to conventional fossil fuel-fired power plants, an air separation unit (ASU) is required to produce a relatively pure (>98%) O_2 stream (Stewart, Symonds, Manovic, Macchi, & Anthony, 2012). Figure 1.2.2 shows the process flow diagram of the technology.

Until recently, the main application of oxy-fuel combustion was for conventional PC boiler technology, where this technology has already been demonstrated at the 30 MW_{th} scale (Faber, Yan, Stark, & Priesnitz, 2011). Future commercial demonstration-scale oxy-fuel combustion plants have been announced including a 250 MW_{th} unit in Germany and a 200 MWth unit in the United States (Wall, Stanger, & Santos, 2011). Recently, oxy-fuel CFBC has gained significant attention as a method for CO_2 capture because of its fuel flexibility and for the possibility of co-firing with renewable fuels such as biomass (Hughes, Atkinson, Symonds, Wu, & Jia, 2015). CFBC operation has the advantage of increased heat flux inside the combustor,

which is a used means of transferring heat from the combustor. The capability of a CFBC to remove large quantities of heat from the reactor greatly reduces the required flow of recycled flue gas moderator, reducing the costs associated with operation (Symonds, McCalden, Hughes, & Champagne, 2015). Other advantages of this technology include: the elimination of NO_x control equipment and CO_2 separation step, boiler size reduction, and SO_2 scrubber size reduction (Yang, et al., 2008).

Demonstration tests are currently underway at the 30 MW_{th} scale in Spain (Hack, Lupion, Hotta, Lantto, Kuivalainen, & Alvarez, 2012) (Hack, et al., 2012) and Alstom has announced intentions of constructing a 100 MW_e demonstration facility in the near future (Suraniti, Nsakala, & Darling, 2009). It should be noted at this point that maintenance and capital costs for oxy-fuel combustion systems are comparable to that of solvent scrubbing technologies, with between 23 and 27% of the total plant power production consumed *via* the air separation unit. Another disadvantage of this technology is the requirement of a greenfield facility (new build); whereas retrofits of existing power generation facilities is an option for post-combustion CO_2 capture technologies.

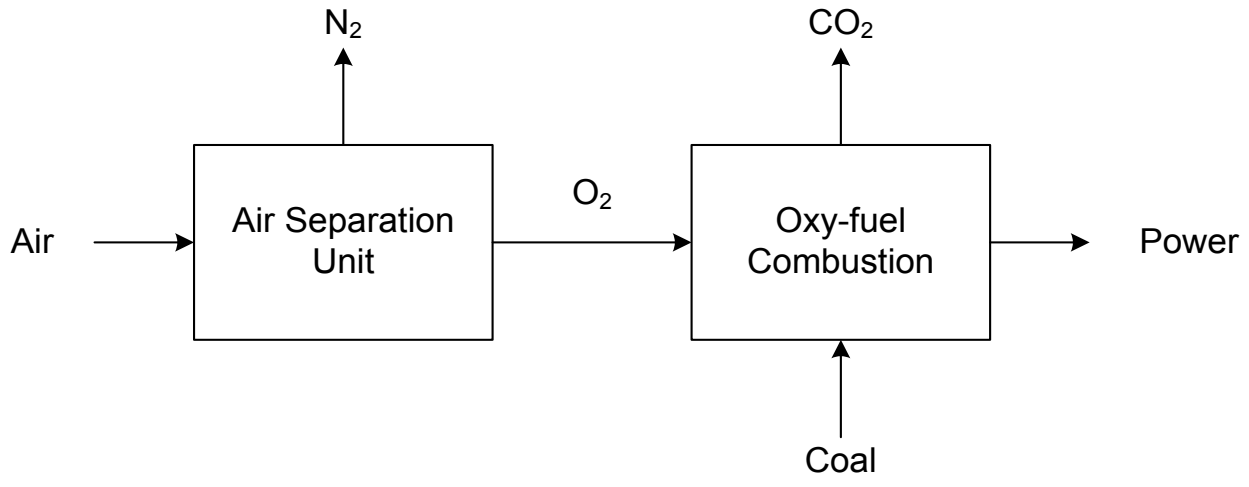

Figure 1.2.2: Process flow diagram for oxy-fuel combustion.

1.2.3 – Chemical Looping Combustion

Chemical looping combustion (CLC) is a novel process with inherent CO_2 capture. Figure 1.2.3 shows the process flow diagram of the technology. In this process, an oxygen carrier (OC) brings the required O_2 from air to the fuel reactor without direct contact (i.e., no N_2 input in the flue reactor). Several oxygen carriers such as Fe_2O_3, NiO, CuO, and Mn_2O_3 have been shown to be suitable for this application (Ryden & Lyngfelt, 2006). The oxygen carrier is circulated between the air and fuel reactor, where by the carrier is oxidized (Equation 1.1) and reduced (Equation 1.2), respectively. It should be acknowledged that, in principle, all major fuels can be utilized for CLC including natural gas, syngas, and solid fuels (coal, coke, biomass, etc.).

$$O_2 + 2Me \rightarrow 2MeO \quad (1.1)$$

$$C_nH_m + (2n + 0.5m)MeO \rightarrow nCO_2 + 0.5mH_2O + (2n + 0.5m)Me \quad (1.2)$$

Chemical looping combustion has several advantages compared to that of conventional combustion processes:

- Exhaust gas from air reactor is inert
- No formation of thermal NO_x since regeneration takes place without flame and at moderate temperatures (<950^oC)
- Minimized energy penalty from CO_2 separation from H_2O (only condensation required)

CLC technology has been successfully demonstrated in a number of smaller pilot-plants and the technology should be ready to scale up to the 1 or 10 MW_{th} size. Unfortunately, current systems operate under atmospheric conditions and temperature between 800 and 950^oC, which would limit the overall efficiency of power generation (Duhoux, et al., 2016). Moreover, the

metal oxide carrying capacity degrades over repeated cycles. Higher pressure and temperature CLC systems will require development before large-scale demonstration can be practically considered (Symonds, Hughes, Navarri, Lu, & Ashrafi, 2017) (Tan, Symonds, Rihda, Lu, & Hughes, 2017) (Navarri, Ashrafi, Symonds, Hughes, & Lu, 2016).

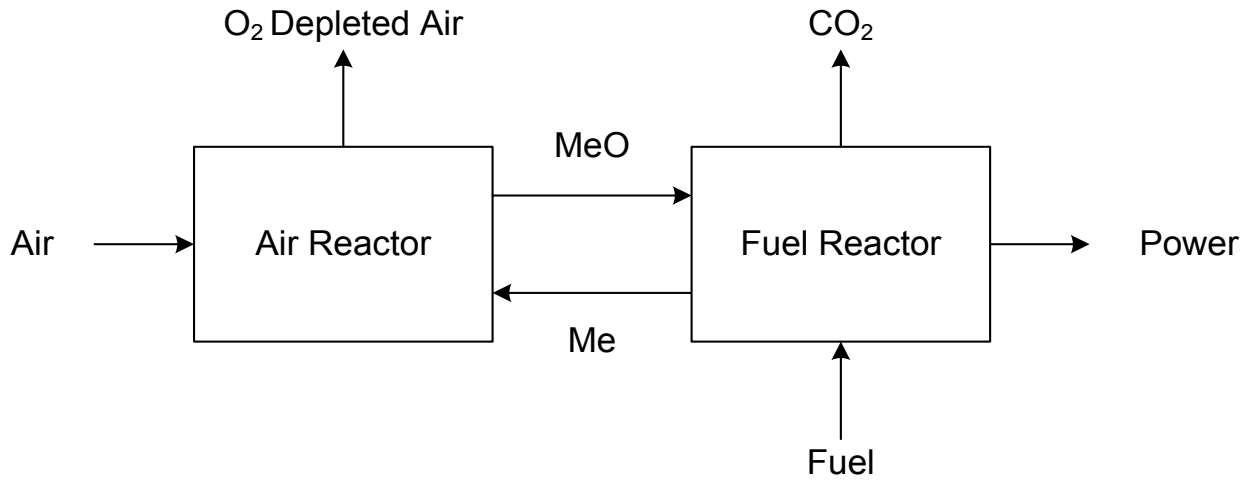

Figure 1.2.3: Process flow diagram for chemical looping combustion.

1.2.4 – Calcium Looping

Of the many developing CO_2 capture technologies, post-combustion CO_2 absorption processes such as calcium looping (CaL) appear to be promising. Calcium looping is considered technically feasible at an industrial scale, economical (MacKenzie, Granatstein, & Anthony, 2007) (Abanades, Grasa, Alonso, Rodriguez, Anthony, & Romeo, 2007), and environmentally benign because of the relatively inert nature of the solid residues produced by the process. Moreover, the spent residues could also be used in cement manufacturing, for example (Harrison, 2004) (Yang, et al., 2008) (Blamey, Anthony, Wang, & Fennell, 2010). Calcium looping has now been performed at the larger scale (up to 1.9 MW_{th}), but there is still a significant quantity of information about sorbent performance, the fate of trace pollutant emissions (specifically SO_2 and HCl), dual fluidized bed operating configurations, and the effect

of realistic operating conditions that still needs to be determined. To date, there is a considerable amount of data of calcium looping that has been generated at the bench-scale, but unfortuntely, this information cannot accurately represent what is observed at the pilot-scale (Symonds & Hughes, 2016). Chapter 2 will provide an indepth process description of calcium looping, along with the current status of the technology.

1.3 – Thesis Objectives

The focus of this work was to bridge the gap between bench-scale testing and what can be expected at the commercial-scale; specifically the effects of proper gas-solid contacting, high heating rates, realistic reactive environments, and sorbent attrition. Based on an economic analysis of the calcium looping process, it was determined that three key parameters serve to have the largest potential benefits to the economics of calcium looping for post-combustion CO_2 capture, namely: (1) the sorbent deactivation rate, (2) the Ca/C ratio, and (3) the rate of attrition. Therefore, not only were these parameters explored from an improvement standpoint, but significant efforts were made to accurately determine them under conditions expected at the commercial-scale. Experimental measurements of the key parameters were conducted *via* a combination of bench-scale, batch pilot-scale, and continuous pilot-scale testing. This also included the design, construction, and commissioning of a 100 kW_{th} dual fluidized bed reactor system capable of operating over a wide range of operating conditions and configurations. The results of each test campaign were broken into individual phases with the following objectives:

Phase I – Bench-scale Experimentation

1) Determine the effect of HCl on CO_2 capture using calcium-based sorbents
    a. CaO-$CaCO_3$-$CaCl_2$ phase equilibria analysis

b. Impact of HCl capture on overall sorbent CO_2 carrying capacity over repeated cycles

c. Fate of HCl within the overall CaL process (calcination / carbonation)

2) Determine the effect of H_2O on overall sorbent CO_2 carrying capacity during both carbonation and calcination over repeated cycles

Phase II – Batch Pilot-scale Experimentation

1) Determine the effect of SO_2 addition during calcination and H_2O addition during carbonation on calcium-based sorbent performance over repeated cycles

2) Determine the effect of oxy-fuel calcination on calcium-based sorbent performance over repeated cycles

3) Compare results to bench-scale data (both generated as a part of this experimental program and from literature) to determine operating parameters for fully continuous CaL system operation under realistic conditions

Phase III – System Design, Construction, and Commissioning of a Dual Fluidized Bed System for CaL

1) Prove the capabilities of several reactor configurations

a. Circulating fluidized bed vs. bubbling bed operation

b. Pneumatic vs. mechanical sorbent transfer system

2) Determine acceptable operating conditions and practical operational limits for all the configurations

3) Demonstrate continuous CO_2 capture using calcium-based sorbents under realistic operating conditions

Phase IV – Continuous Pilot-scale Experimentation

1) Determine the effect of oxy-fuel calcination on calcium based sorbent performance, including rate of attrition, for long duration continuous operation

2) Determine the effect of H_2O addition during carbonation on calcium based sorbent performance, for long duration continuous operation

3) Allow for the validation of process modeling and scale-up activities

As indicated above, Chapter 2 will provide an indepth process description of calcium looping, along with background theory on fluidized beds and how they have been implemented within the calcium looping process. Chapter 3, entitled "**The Effect of HCl and Steam on Cyclic CO_2 Capture Performance in Calcium Looping Systems**," investigates the effect of HCl and steam in both the carbonator and calciner on CO_2 capture using calcium-based sorbents *via* bench-scale experimental testing. A series of batch pilot-scale tests conducted to examine the impact of the presence of SO_2 and steam on the calcium looping process are presented in Chapter 4, entitled "**Pilot-Scale Study of CO_2 Capture by CaO-Based Sorbents in the Presence of Steam and SO_2.**" This work also provided the required operating parameters for the design and operation of a fully continuous calcium looping system capable of operating under realistic conditions. Chapter 5, entitled "**System Design, Construction, and Commissioning of a Dual Fluidized Bed System for Calcium Looping**," provides detailed information of the design and operation of a dual fluidized bed system for calcium looping, along with demonstration of continuous CO_2 capture using calcium-based sorbents under realistic operating conditions. A test campaign utilizing the continuous dual fluidized bed system for calcium looping and the resulting CO_2 capture performance under realistic conditions are presented in Chapters 6 and 7, entitled "**CO_2 Capture Performance of CaO-Based Pellets in a**

0.1 MW_{th} Pilot-Scale Calcium Looping System" and "**Attrition of CaO-Based Pellets in a 0.1 MW_{th} Dual Fluidized Bed Pilot Plant for Post-Combustion CO_2 Capture**," respectively. This work provides information about long-term sorbent performance, sorbent make-up rates, and rate of attrition required for the validation of process modeling and scale-up activities. Finally, Chapter 8 contains concluding remarks and recommendations for future work.

1.4 – References

Abanades, J. C., Grasa, G., Alonso, M., Rodriguez, N., Anthony, E. J., & Romeo, L. M. (2007). Cost Structure of a Postcombustion CO2 Capture System Using CaO. *Environ. Sci. Technol.*, 41, 5523-5527.

Bachu, S. (2008). CO2 Storage in Geological Media: Role, Means, Status, and Barriers to Deployment. *Prog. Energy Combust. Sci.*, 34, 254-273.

Beer, J. M. (2000). Combution Technology Development in Power Generation in Response to Environment Challenges. *Prog. Energy Combust. Sci.*, 25, 301-327.

Berger, R. (2004). *Calcium Cycle for Efficient and Low Cost CO2 Capture in Fluidized Bed System.* University of Stuttgart, Germany: European Union Specified Targeted Research Project.

Blamey, J., Anthony, E. J., Wang, J., & Fennell, P. (2010). The Use of the Calcium Looping Cycle for Post-combustion CO2 Capture. *Prog. Energy Combust. Sci.*, 36, 260-279.

Duhoux, B., Mehrani, P., Lu, D., Symonds, R. T., Anthony, E. J., & Macchi, A. (2016). Combined Calcium Looping and Chemical Looping Combustion for Post-Combustion Carbon Dioxide Capture: Process Simulation and Sensitivity Analysis. *Energy Technology*, 4 (19), 1158-1170.

Elwell, L. C., & Grant, E. S. (2006). technology options for capturing CO2-Special reports. *Power*, 150(8).

Faber, R., Yan, J. Y., Stark, F., & Priesnitz, S. (2011). Flue gas desulphurization for hot recycle Oxyfuel combustion: Experiences from the 30MWth Oxyfuel pilot plant in Schwarze Pumpe. *Int. J. Greenhouse Gas Control*, 5, S210-S223.

Fauth, D., Frommell, E. A., Hoffman, J. S., Reasbeck, R. P., & Pennline, H. W. (2005). Eutectic salt promoted lithium zirconate: Novel high temperature sorbent for CO2 capture. *Fuel Process. Technol.*, 86, 1503-1521.

Hack, H., Alvarez, I., Diego, R., Lupion, M., Cortes, V., Hotta, A., et al. (2012). Initial Operation of the CIUDEN Oxy-CFB Boiler Demonstration Project. *The 11th Annual Carbon Capture, Utilization & Sequestration Conference.* Pittsburgh, USA.

Hack, H., Lupion, M., Hotta, A., Lantto, J., Kuivalainen, R., & Alvarez, J. (2012). Tesing in the CIUDEN Oxy-CFB Boiler Demonstration Project. *The 37th International Technical Conference on Clean Coal and Fuel Systems.* Clearwater, USA.

Harrison, D. P. (2004). The Role of Solids in CO2 capture: A Mini Review. *Seventh International Conference on Greenhouse Gas Control Technologies* (pp. 1101-1106). Amsterdam: Elsevier.

Hughes, R., Atkinson, K., Symonds, R. T., Wu, Y., & Jia, L. (2015). Oxy-Fluidized Bed Combustion Using Under Bed Fines Fuel Injection. *22nd International Conference on Fluidized Bed Conversion.* Turku, Finland: IFRF.

IEA. (2010). *World Energy Outlook 2010.* OECD Publishing.

IPCC. (2013). Climate Change 2013: The Physical Science Basis. Contribution of Working Group I to the Fifth Assessment Report of Intergovernmental Panel on Climate Change. Cambridge, United Kingdom and New York, USA: Cambridge University Press.

Krebs, F. (2012). Carbon dioxide - a themed issue. *Energy Environ. Sci.*, 5, 7238-7239.

MacKenzie, A., Granatstein, D. L., & Anthony, E. J. (2007). Economics of CO2 Capture Using the Calcium Cycle with a Pressurized Fluidized Bed Combustor. *Energy Fuels*, 21, 920-926.

Metz, B., Davidson, O., de Conninck, H., Loos, M., & Meyer, L. (2005). *IPCC Special Report on Carbon Dioxide Capture and Storage.* New York: Cambridge University Press.

Mohammed, I. Y., Samah, M., Mohamed, A., & Sabina, G. (2014). Comparison of Selexol and Rectisol Technolgies in an Integrated Gasification Combined Cycle (IGCC) Plant for Clean Energy Production. *International Journal of Engineering Research*, 3 (12), 742-744.

Nalbandian, H. (2008). *Performance and Risks of Advanced Pulverized-Coal Plants.* IEA Coal Research.

Nalbandian, H. (2009). Performance and Risks of Advanced Pulverized-Coal Plants. *Energeia*, 20, 1-3.

Navarri, P., Ashrafi, O., Symonds, R. T., Hughes, R., & Lu, D. (2016). *Heat Integrated PCLC-SAGD Process.* Ottawa, Canada: Natural Resources Canada - CanmetENERGY.

Pachauri, R. K., & Reisinger, A. (2007). *Climate Change 2007: Synthesis Report. Contribution of Working Groups I, II and III to the Fourth Assessment Report of the Intergovernmental Panel on Climate Change.* Geneva, Switzerland: Intergovernmental Panel on Climate Change (IPCC).

Resnik, K. P., Yeh, J. T., & Pennline, H. W. (2004). Aqua ammonia process for simultaneous removal of CO2, SO2 and NOx. *Inter. J. Environ. Technol. Management*, 4, 89-104.

Ryden, M., & Lyngfelt, A. (2006). Using steam reforming to produce hydrogen with carbon dioxide capture by chemical-looping combustion. *International Journal of Hydrogen Energy*, 31, 1271-1283.

Suraniti, S. L., Nsakala, N. Y., & Darling, S. L. (2009). Alstom oxyfuel CFB boilers: A promising option for CO2 capture. *Energy Procedia*, 1, 543-548.

Stewart, M. C., Symonds, R. T., Manovic, V., Macchi, A., & Anthony, E. J. (2012). Effects of steam on the sulfation of limestone and NOx formation in an air- and oxy-fired pilot-scale circulating fluidized bed combustor. *Fuel*, 92, 107-115.

Symonds, R. T., & Hughes, R. (2016). *NGCC CCS using Calcium Looping - Process Simulation, Equipment Desing, and Sizing.* Ottawa, Canada: Natural Resources Canada - CanmetENERGY.

Symonds, R. T., Hughes, R., Navarri, P., Lu, D., & Ashrafi, O. (2017). Systems Analysis of Pressurized Chemical Looping Combustion for SAGD Applications. *Submitted*.

Symonds, R. T., McCalden, D., Hughes, R., & Champagne, S. (2015). *Process simulation and modeling of 1 MWth oxy-PFBC pilot-plant.* Ottawa, Canada: Natural Resources Canada - CanmetENERGY.

Tan, Y., Symonds, R. T., Rihda, F., Lu, D., & Hughes, R. (2017). Reduction kinetics of ilmenite ore as an oxygen carrier for pressurized chemical looping combustion of simulated natural gas. *Submitted*.

Viswanathan, R., Alto, P., Henry, J. F., Chattanooga, A., Tanzosh, J., Stanko, G., et al. (2001). *The advanced supercritical 700oC pulverized coal fired power plant.* Brussels: Power-Gen Europe.

Wall, T., Stanger, R., & Santos, S. (2011). Demonstrations of coal-fired oxy-fuel technology for carbon capture and storage and issues with commercial deployment. *Int. J. Greenhouse Gas Control*, 5, S5-S15.

Yang, H., Xu, Z., Fan, M., Gupta, R., Slimane, R. B., Bland, A. E., et al. (2008). Progress in Carbon Dioxide Separation and Capture: A Review. *J. Environ. Sci.*, 20, 14-27.

Yeh, A. C., & Bai, H. (1999). Comparison of ammonia and monoethanolamine solvents to reduce CO2 greenhouse gas emissions. *Science of the Total Environment*, 228 (2-3), 121-133.

Yeh, J. T., Resnik, K. P., Rygle, K., & Pennline, H. W. (2005). Semi-batch absorption and regeneration studies for CO2 capture by aqueous ammonia. *Fuel Process. Tech.*, 86, 1533-1546.

Chapter 2 – Calcium Looping Process Background

2.1 – Calcium Looping for Post-combustion CO_2 Capture

2.1.1 – Detailed Process Description

Calcium Looping (CaL) for post-combustion CO_2 capture utilizes sorbent particles containing CaO to absorb CO_2 from a flue gas (carbonation) and releases it in a concentrated stream during the decomposition of $CaCO_3$ (calcination), to generate an atmosphere rich in CO_2 (Shimizu, et al., 1999). The reversible reaction is as follows (Equation 2.1):

$$CaO_{(s)} + CO_{2(g)} \leftrightarrow CaCO_{3(s)} \qquad \Delta H_r^0 = -178.2 \text{ kJ/mol} \tag{2.1}$$

The CaO source is often limestone, but other natural occurring sorbents such as dolomites and dolomitic limestones have been investigated (Siliban, Narcida, & Harrison, 1996) (Champagne, Lu, Macchi, Symonds, & Anthony, 2013). Many synthetic, pelletized, and stabilized CaO-based materials that possess a high and cyclically stable CO_2 uptake have also been examined, typically at the bench-scale (Fennel, Pacciani, Dennis, Davidson, & Hayhurst, 2007) (Manovic & Anthony, 2008) (Li, Cai, Huang, & Han, 2005) (Manovic & Anthony, 2011).

During carbonation (forward of Equation (2.1)), flue gas containing CO_2 is passed through the carbonator where it comes into contact with CaO-containing solids, to form $CaCO_3$ and a CO_2 depleted flue gas. Figure 2.1.1 provides a basic process flow diagram of the overall process. The flue gas entering the carbonator typically contains a wide range of CO_2 concentrations depending on the flue gas source. Natural gas combined cycle (NGCC) systems generate flue gas with lower CO_2 concentrations (~4 vol.%), whereas coal-fired power systems can have flue gas containing up to 15 vol.% CO_2. The total CO_2 capture efficiency (kg CO_2 captured/kg CO_2 generated) is governed by two main parameters: (1) the fraction of flue gas sent to the carbonator and (2) the operating temperature of the carbonator. The fraction of flue gas

that is processed would typically be set to meet CO_2 emissions regulations (kg CO_2/MWh) and would vary depending on what country and/or region utilizes the technology. In the Canadian context, this value is set at 420 kg CO_2/MWh (Environment and Climate Change Canada, 2013).

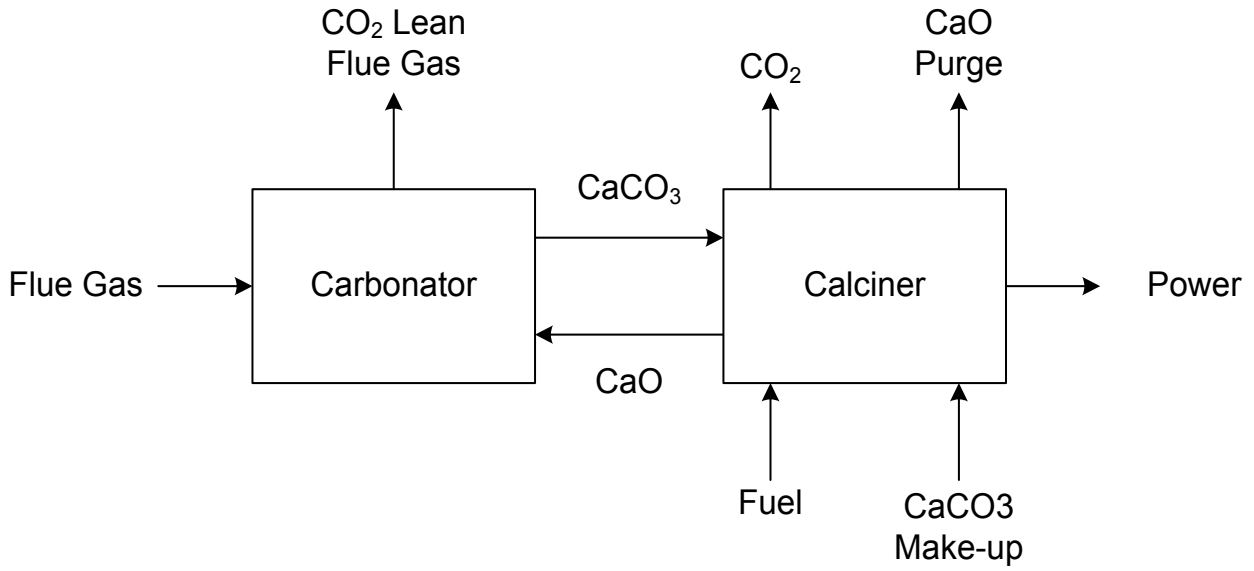

Figure 2.1.1: Process flow diagram for calcium looping.

The operating temperature of the carbonator not only governs the total CO_2 capture efficiency, but also significantly impacts other process parameters such as the carbonation kinetics and the required heat transfer surface area. Experimental testing on the CaO-CO_2 equilibrium system, such as those performed by Baker (1962) and Barin (1989), showed that the optimum space-time yield for carbonation is at lower temperatures between 500-700^{o}C. A temperature must be selected where the kinetics of the reaction are sufficient to drive the reaction forward, but the temperature is low enough that the system is below the equilibrium point for CO_2 to be sorbed. As can be seen in Figure 2.1.2, as the temperature rises, so does the CO_2 equilibrium partial pressure. For systems operating at atmospheric pressure, 90 % CO_2 capture can be achieved at a temperature of roughly 650^{o}C with a flue gas containing 15 vol% CO_2. This temperature is reduced to around 600^{o}C for a flue gas containing 4 vol% CO_2.

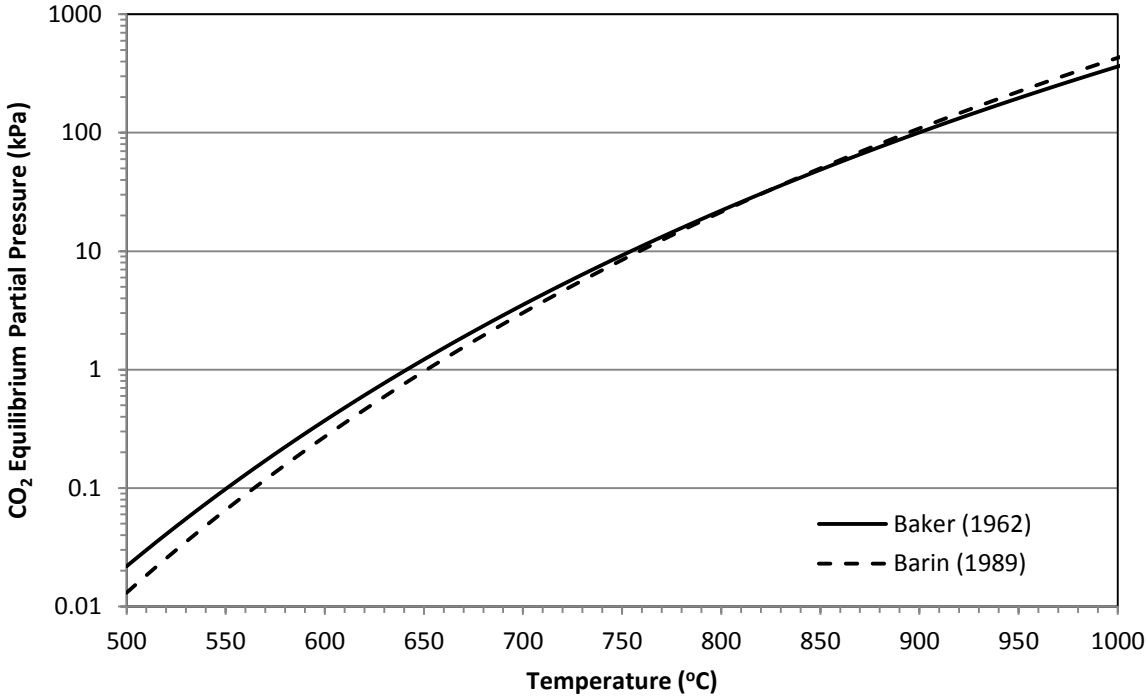

Figure 2.1.2: Equilibrium CO_2 partial pressure versus temperature for the CaO-CO_2 system.

Since the carbonation reaction is exothermic, there is a significant amount of high temperature heat released that could be utilized for steam production. In this arrangement, the carbonator temperature is maintained by boiler components which generate steam for the power cycle using water walls and an external heat exchanger. It should be noted that the lower temperatures found in the carbonator means that the heat exchanger arrangement would require modification in comparison to typical boilers which operate at temperatures above 850^{o}C (Yang, 2003). As such, the minimum operating temperature of the carbonator is most likely limited by the maximum heat transfer surface area that can be accommodated within the reactor.

A fundamental characteristic of calcium looping systems is the design and operation of the two reactors (carbonator and calciner) and their interconnection in order to facilitate continuous flow of solids between reactors and an effective separation of gas atmospheres.

Consequently, the use of fluidized bed reactors for this purpose is today the main option for calcium looping systems. A more detailed discussion on fluidized bed characteristics and selection, along with advantages over fixed beds, will follow in the subsequent sections.

The CO_2 depleted flue gas exiting the carbonator passes through a primary solids separation device, such as a cyclone, where the majority of the entrained sorbent is separated from the gas stream. The sorbent exiting the bottom of the cyclone would typically be passed through an external heat exchanger before being split, where a portion of the solids are transferred to the calciner and the remainder reintroduced into the carbonator *via* a loop seal. The gas stream leaving the cyclone still contains a small fraction of elutriated solids not captured by the cyclone (or multiple cyclones in some cases). These solids are generally made-up of finer particles (<20 micron) and are a result of particle attrition within the reactor. The causes and impact of particle attrition will be discussed in greater detail in the subsequent sections. A baghouse is normally employed to remove the fine particulate before the depleted flue gas is sent to the stack. The gas stream is cooled *via* a convective heat exchanger upstream of the baghouse to both protect the bags from thermal degradation and recover heat that can be used for steam generation. Depending on the upstream flue gas processing performed before entering the carbonator, a blower will either be placed before the carbonator or after the baghouse, since most standard blowers cannot be operated under high temperature and/or fines loading conditions.

The partial carbonated sorbent not reintroduced into the carbonator is directed to the calciner for regeneration (reverse of Equation (2.1)) *via* a refractory-lined duct to minimize heat loss to the surroundings. Depending on the system arrangement and fluidized bed type, such as bubbling or circulating, the use of vertical risers and conveying gas are required for solids transfer. The calciner is operated at temperatures between 850 and 950^{o}C to ensure the

decomposition of $CaCO_3$ will proceed (see Figure 2.1.2). The minimum temperature required for calcination is a function of the exact CO_2 concentration in the reactor, which can vary greatly depending on (1) the fuel source utilized and (2) the recycle gas composition. Combustion of a carbonaceous fuel is required in the calciner to both provide the heat necessary for $CaCO_3$ decomposition (endothermic) and sensible heating of the sorbent up to reaction temperature.

Since the most important design criteria of any post-combustion CO_2 capture technology is the production of a concentrated CO_2 stream with a CO_2 concentration of greater than 95 vol% (IEA, 2013) (IPCC, 2005), the use of air for combustion is not feasible. Instead, to avoid dilution of the product stream, a relatively pure stream of O_2 (95-98 vol%) is utilized. The oxygen stream is produced from an air separation unit (ASU) and is mixed with recycled flue gas prior to entering the refractory-lined calciner. The recycled flue gas is necessary for both bed temperature moderation and as a fluidizing medium. Unlike a typical oxy-fuel combustor, there are no boiler components within the calciner since this would increase the amount of O_2 and fuel required to regenerate the sorbent and would reduce the overall efficiency of the process.

A cyclone is used to separate the majority of the entrained sorbent from the concentrated CO_2 product stream. A portion of this calcined sorbent is directed to the carbonator *via* a refractory-lined duct, in a similar manner as described above, completing the sorbent looping cycle. The CO_2 product steam exiting the cyclone is subsequently cooled, allowing for steam production, and sent to a baghouse for fine particulate removal. A certain percentage of the product stream is recycled back to the calciner *via* a recycle blower and mixed with the O_2 supply, as described above. The quantity of recycled flue gas is dependent on several factors include: (1) wet or dry recycle, (2) the inlet O_2 concentration, and (3) the outlet O_2 concentration, which must be minimized to meet pressurized CO_2 pipeline specifications (World Resources

Institute (WRI), 2008). The balance of the CO_2 product stream is directed to the CO_2 processing unit for compression, water removal, and purification to meet pipeline specifications (IPCC, 2005).

On top of the fine particulate material captured by the carbonator and calciner baghouses, an additional solids purge stream is also required to deal with sorbent deactivation and ash accumulation in the case of solid fuel combustion in the calciner. Provided the ash content is relatively low (Napp, Gambhir, Hills, Florin, & Fennell, 2014) (or zero in the case of natural gas combustion), the waste solids leaving the system are believed to be suitable for cement production (Rodriguez, et al., 2011) (Rodriguez, Murillo, & Abanades, 2012) (Telesca, et al., 2014), soil stabilization, wastewater treatment, agriculture uses, and flue gas desulphurization (Borgwardt, 1970).

2.1.2 – Economics of Calcium Looping

If calcium looping is to be seriously considered as a technology option for carbon capture and sequestration, it must first be compared against what are considered the front runners: oxy-fuel combustion and solvent scrubbing.

- Oxy-fuel combustion = ~10 percentage points efficiency loss
- Solvent (amine-water) scrubbing = ~12 percentage points efficiency loss

There is a target to reduce both efficiency penalties to around 8 percentage points by 2020. Unfortunately, the target for a modern power station is between 42 to 47% (higher heating value (HHV)) total efficiency by 2020, which is only partially met by displacing sub-critical boilers with super- and ultra-supercritical boilers. One major reason to really consider calcium looping for power generation is that the efficiency losses lie around 6 to 8 percentage points. This is

mainly due to effective heat integration, allowing for the energy required to regenerate the sorbent to be subsequently captured into an efficient steam cycle.

To date, there is a relatively large discrepancy when it comes to determining the actual efficiency penalties. Sensitivity analyses have been performed by a range of authors (Abanades, et al., 2007) (Romeo, Lara, Lisbona, & Escosa, 2009) to determine the effect of several parameters on the overall cost of CO_2 captured. One of the first groups to conduct such an analysis (MacKenzie, Granastein, Anthony, & Abanades, 2007) considered the following key parameters:

1) Cost of sorbent
2) Calcium to carbon molar ratio
3) CaO deactivation rate
4) CaO recycle rate
5) Calciner, O_2 plant operations and maintenance (O&M) costs
6) Calciner, O_2 plant capital expenditures (CAPEX)
7) Energy loss in calciner
8) CO_2 credits

It was conclude that the dominant parameters were all related to the sorbent itself, and not surprisingly, the cost of sorbent, Ca/C ratio, CaO deactivation rate, and the CaO recycle rate were all found to be closely related. For example, if the deactivation rate increases (i.e., the average CaO carrying capacity is decreased) this will increase the required Ca/C ratio, since a smaller fraction of the CaO entering the carbonator is capable of capturing CO_2 for a given

residence time. Moreover, the capital cost for both the carbonator and calciner will increase, since larger reactors are required to accommodate the increased sorbent throughput.

Unfortunately, the cost of sorbent (limestone or dolomite) is likely to be outside the control of the calcium looping facility. The sorbent will be required to be sourced from a quarry in relatively close proximity to the power generation facility (or other large-scale stationary CO_2 emitting facility) to avoid large transportation costs. Therefore, the cost to supply the sorbent will be market-driven and there would be limited pathways to decrease this cost over time, but it is a rather plentiful and geographically well distributed resource. It should be noted that, given multiple sorbent selection options, preference should be given to sorbents with relatively high $CaCO_3$ contents and high attrition resistance, all else being equal. This will maximize the sorbent CO_2 carrying capacity, while also reducing the sorbent makeup rate.

The CaO recycle rate is essentially dependant on three main factors (1) the deactivation rate, (2) the rate of attrition, and (3) the waste material purge rate. Although it can be shown that reducing the recycle rate might be advantageous from a reactor sizing perspective, this is significantly outweighed by the sorbent makeup costs. As noted by MacKenzie et al. (2007), levelized cost summaries show the sorbent, in most cases limestone, as the single most expensive plant cost component and the most expensive component of CO_2 capture. Waste material purge rates are typical controlled by the type of fuel utilized as the heat source for calcination. Coals and other solid fuels containing ash lead to significant sorbent loses during ash removal due to solids mixing in the calciner. This negative effect to the process can be minimized by using low ash solid fuels, or even natural gas (Erans, Hanak, Mir, Anthony, & Manovic, 2016) (Cormos, 2015) during calcination, but is solely dependent on the post-combustion CO_2 source fuel, as it would not vary between systems.

This leaves three remaining key parameters, which if reduced, serve to have the largest potential benefits to the economics of calcium looping for post-combustion CO_2 capture: (1) the deactivation rate, (2) the Ca/C ratio, and (3) the rate of attrition. Therefore, not only should these parameters garner the most attention from an improvement standpoint, but significant efforts should be made to accurately determine them under conditions expected at the commercial-scale. This is critical in ensuring that the economics of the process are not over- or underestimated, leading to uncertainty in the competitiveness of calcium looping against other CO_2 capture technologies.

2.1.3 – Sorbent Deactivation

As mentioned above, one of the key parameters driving the economics of calcium looping is the deactivation rate of the CaO-based sorbents. The drop in CO_2 carrying capacity over repeated calcination / carbonation cycles can be modeled using the following semi-empirical equation developed by Grasa and Abanades (2006):

$$X_N = \frac{1}{\frac{1}{1-X_r}+kN} + X_r \tag{2.2}$$

where X_N is the CaO conversion in the Nth cycle, X_r is the residual CaO conversion, and k is a deactivation constant, which varies from 0.28 to 1.96 depending on the sorbent type and test conditions. By examining Equation (2.2), it becomes apparent that the CO_2 carrying capacity drops significantly over the first 10 to 20 cycles and reaches a residual CaO conversion after only 75 to 100 cycles. The residual CaO conversion is typically below 10% for many limestones studied in literature (Grasa & Abanades, 2006).

Sorbent deactivation has been attributed to thermal sintering owing to the low Tammann temperature of $CaCO_3$ (533^{o}C). Sintering causes changes in morphology at the surface of the

sorbents particles. The various peaks and ridges that make up the pore structure start to consolidate, reducing particle surface area and pore volume, limiting the number of active sites available for reaction (Herring, 1950). Along with the thermal sintering observed under typical calcination conditions, the gaseous atmosphere present during calcination has been shown to enhance the sintering effect. Borgwardt (1989) showed that CO_2 and steam enhanced the sintering of CaO in comparison to air or N_2. This result is significant since calcination is performed under oxy-fuel combustion conditions, which produces a CO_2 and steam rich atmosphere.

Along with sintering, another major contributor to sorbent deactivation is caused by the reaction of SO_2, a common by-product of combustion, with the sorbent *via* either indirect (Equation 2.3) or direct (Equation 2.4) sulphation:

$$CaO_{(s)} + SO_{2(g)} + 0.5O_{2(g)} \leftrightarrow CaSO_{4(s)} \qquad \Delta H_r^0 = -502 \text{ kJ/mol} \tag{2.3}$$

$$CaCO_{3(s)} + SO_{2(g)} + 0.5\ O_{2(g)} \leftrightarrow CaSO_{4(s)} + CO_{2(g)} \qquad \Delta H_r^0 = -324 \text{ kJ/mol} \tag{2.4}$$

Unlike $CaCO_3$, $CaSO_4$ will not decompose at typical carbonation / calcination temperatures and permanently reduces the CO_2 carrying capacity of the sorbent by reducing the amount of CaO available for reaction with CO_2 and forming a dense product layer at the particle surface (Sun, Grace, Lim, & Anthony, 2006).

Since both thermal sintering and sorbent sulphation are expected to be more severe at the commercial-scale (i.e., higher heating rates, high CO_2 calcination, and high sulphur containing fuels), it is critical that realistic sorbent deactivation rates be determined for use in calcium looping techno-economic studies. Considering that multi-cycle carbonation conversions

under less severe conditions are already low, a few percentage points decrease can make a relatively large difference on overall viability of this technology.

2.1.4 – Overview of Current Pilot-plant Facilities

The success at the bench-scale initiated a movement towards demonstrating calcium looping at the pilot-scale under more realistic operating conditions. The largest pilot-plant globally for post-combustion CO_2 capture using calcium looping is the 1.9 MW_{th} Industrial Technology Research Institute (ITRI) system in Taiwan, utilizing a bubbling fluidized bed carbonator and diesel as the fuel for calcination (Chang, et al., 2013). Also successfully commissioned are the 1.7 MW_{th} La Pereda facility in Spain treating flue gas from an existing 50 MW_e CFBC power plant (Arias , et al., 2013) and the 1 MW_{th} TU facility in Germany at Darmstadt University (Strohle, Junk, Kremer, Galloy, & Epple, 2014). Both systems are operated using circulating fluidized beds (CFB) for the carbonation and calciner, but differ in the method of solids circulation control. The La Pereda facility use a double loop seal arrangement for solids transfer, whereas the TU facility uses a single loop seal with a screw conveyor to transfer the sorbent from the carbonator to calciner. From an operational standpoint, the use of two circulating fluidized beds with loop seals can be challenging since the solids circulation rate is dependent on the difference in pressure between the reactor and the loop seal and the difference in operating pressure between the two reactors; both of which are functions of bed inventory, gas velocity, and level of sorbent conversion.

Although these facilities represent the most advanced demonstrations of the calcium looping technology, some critical aspects of the process are still being performed under non-realistic operating conditions, including:

- Simulated calcination feed gas (i.e., no flue gas recirculation) which does not include water vapour
- Simulated carbonator feed gas
- Low or zero sulphur containing fuel sources for calcination

Therefore, additional pilot-scale testing is required to both improve the dual fluidized bed system reliability and to provide critical sorbent performance values under operating conditions expected at the commercial-scale.

2.2 – Fluidized Beds

As detailed in the calcium looping process description, large quantities of solids are required to continuously flow between the carbonator and calciner, making the use of fluidized bed reactors ideal for calcium looping systems. By selecting specific reactor geometries, the feed gas can react with the sorbent, while simultaneously be utilized to transfer the now converted solids out of the reactor without the use of any mechanical systems (often used to transfer solid materials). Fluidized beds have several other advantages (Grace, Leckner, Zhu, & Cheng, 2006) in comparison to more traditional gas-solid reactor systems, such as fixed-bed reactors, including:

1) Low pressure drops
2) Temperature uniformity due to exceptional solids mixing
3) Excellent surface-to-bed heat transfer, and
4) The ability to accommodate a wide range of particle properties

All of these advantages can be capitalized on within the process to maximize the overall process efficiency and minimize the CAPEX and operating expenditures (OPEX) for calcium looping systems.

1) The low pressure drops over the reactors minimize the electrical utility demand on the major equipment such as the induced draft (ID) blower for the carbonator and the recycle blower for the calciner.
2) A uniform temperature in the carbonator ensures the target CO_2 capture efficiency can be met (see Figure 2.1.2). This is important due to the exothermic nature of the carbonation reaction that would otherwise result in significant temperature gradients throughout the carbonator height. This phenomenon is equally important in the calciner where the high temperatures from fuel combustion can lead to severe sintering of the sorbents, reducing its maximum CO_2 carrying capacity.
3) One of the key advantages of calcium looping over other post-combustion CO_2 capture technologies is the opportunity to increase the net power production of the overall facility (primary power station plus calcium looping system) *via* the high temperature heat generated in the carbonator. The increased heat transfer rates due to surface-to-bed contact minimize the required heat exchanger surface area, reducing the carbonator size and associated costs.
4) One of the main drivers towards the use of calcium looping is the abundance and relatively low cost of naturally occurring calcium based sorbents (Fang, Li, & Cai, 2009). Unfortunately, the particle properties such as purity (Ca content), density, and friability can vary greatly between sorbent sources. The ability to accommodate a wide range of

particle properties ensures the technologies' applicability regardless of the sorbent source.

One of the most critical parameters of any fluidized bed system is the mean particle diameter. Not only will this affect the fluidization behaviour, it also significantly impacts (1) the cost of solids preparation (e.g., crushing), (2) rate of attrition, (3) overall rate of reaction (e.g., mass diffusion limitations), (4) solids looping controllability, and (5) solids waste product value. Since these parameters can be both positively and negatively affected by particle diameter, careful consideration should be made when selecting particle size from both a process and economic perspective.

2.2.1 – Hydrodynamics of Fluidization

A popular classification scheme for particles fluidized in air under atmospheric conditions was proposed by Gelgart (1973). Under this scheme, all particles being fluidized could be classified into one of four groups based on broad types of behaviour as can be seen in Figure 2.2.1. It should be noted that this classification has been extended to other gas atmospheres, pressures, and temperatures (Grace, 1986), but does not change the particle groups for calcium looping since the particle density, ρ_p, is several orders of magnitude larger than the gas density, ρ_g, in all cases.

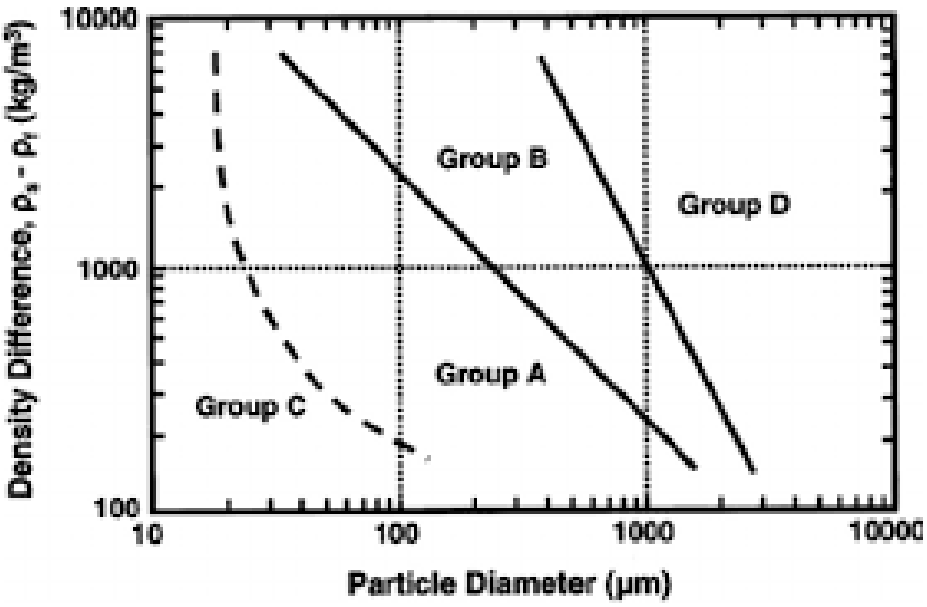

Figure 2.2.1: Geldart powder groups for fluidization by air at room temperature and atmospheric pressure – Mean particle diameter versus difference between particle and gas density.

It has been suggested that Group C and D particles not be selected for fluidized bed applications. Group C particles fluidize poorly due to strong interparticle forces (Visser, 1989) and Group D particles result in large bubbles (decreased mass transfer) and poor solids mixing (Grace, 1986). Therefore, the mean particle diameter, d_p, range should be limited to between approximately 50 to 1600 μm. Furthermore, since most naturally occurring calcium based sorbents have a particle density of around ~3000 kg/m^3, the maximum particle diameter should be reduced to approximately 800 μm to avoid Group D fluidization characteristics.

For a given mean particle diameter, that falls within the Group A and B (and sometimes D) classification, several distinct flow regimes can exist. Figure 2.2.2 shows each flow regime as a function of superficial gas velocity,U, for a column of high height-diameter ratio, ensuring all entrained particles are returned (Grace, Leckner, Zhu, & Cheng, 2006).

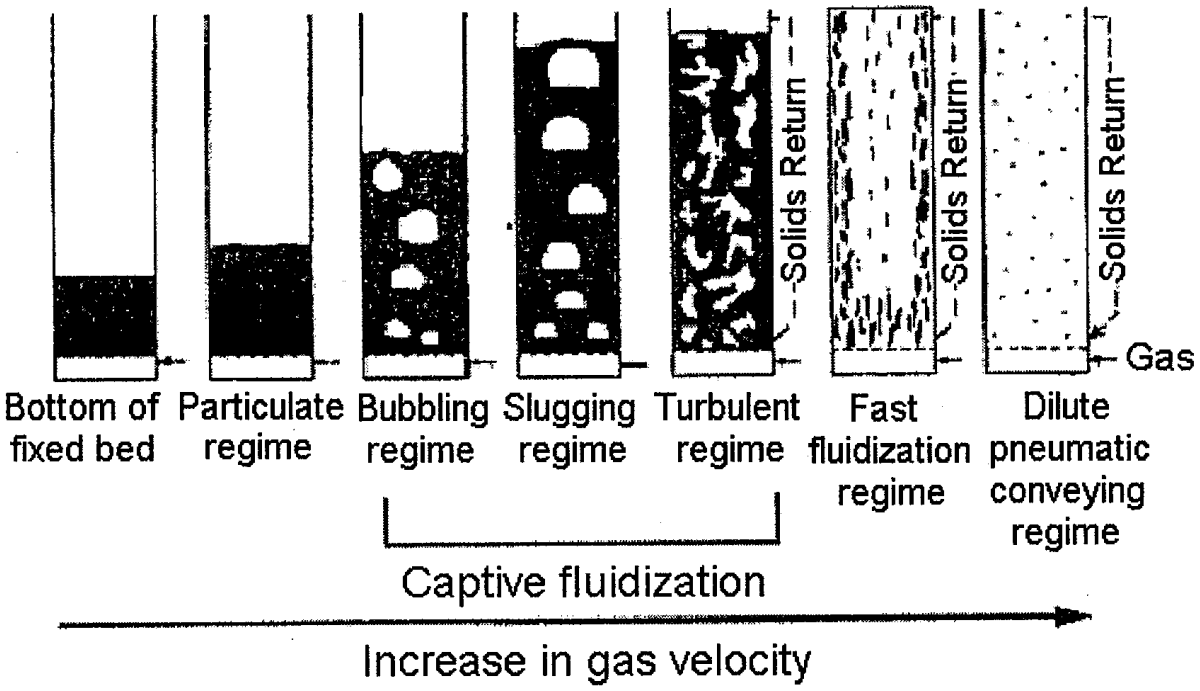

Figure 2.2.2: Schematic representation showing appearance of flow regimes relevant to gas-solid fluidization.

The minimum fluidization velocity,U_{mf}, is reached when the pressure drop across the bed, ΔP_{bed}, is equal to the buoyed weight of the particles, so that:

$$\Delta P_{bed} = \left(\rho_p - \rho_g\right)(1 - \langle\epsilon\rangle_{av})gH \tag{2.5}$$

where $\langle\epsilon\rangle_{av}$ is the bed voidage over the volume of the bed, g is acceleration due to gravity, and H is the bed height. The pressure drop across a fixed bed can be predicted *via* the use of the Ergun equation (Ergun, 1952):

$$\Delta P_{bed} = \frac{150\,\mu_g U(1-\langle\epsilon\rangle_{av})^2}{\varphi^2 d_p^2 \langle\epsilon\rangle_{av}^3} + \frac{1.75\rho_g U^2(1-\langle\epsilon\rangle_{av})}{\varphi d_p \langle\epsilon\rangle_{av}^3} \tag{2.6}$$

where μ_g is the gas viscosity and φ is the particle sphericity. Therefore, the minimum fluidization velocity can be estimated at the transition between a fixed and fluidized bed (Equations (2.5) and (2.6)):

$$\mathrm{Re_{mf}} = \frac{\rho_g d_p U_{mf}}{\mu_g} = \sqrt{C_1^2 + C_2 Ar} - C_1 \tag{2.7}$$

where $\mathrm{Re_{mf}}$ is the Reynolds number at minimum fluidization, C_1 and C_2 are parameters that are a function of the bed voidage, and Ar is defined as follows:

$$Ar = \frac{g\rho_g(\rho_p - \rho_g)d_p^3}{\mu_g^2} \tag{2.8}$$

Several values for C_1 and C_2 exist in the literature, with the most common being 33.7 and 0.0408, respectively (Wen & Yu, 1966). Unfortunately, large errors in the minimum fluidization can be observed when using these values, so it is suggested that simplified versions of Equation 2.7 be used when appropriate:

For cases where $Ar < 10^3$,

$$U_{mf} = 0.00061 * \left(\frac{g(\rho_p - \rho_g)d_p^2}{\mu_g}\right) \tag{2.9}$$

For cases where $Ar > 10^7$,

$$U_{mf} = 0.20 * \sqrt{\frac{g(\rho_p - \rho_g)d_p}{p_g}} \tag{2.10}$$

2.2.2 – Circulating and Bubbling Fluidized Beds for Calcium Looping

As described in Section 2.1.4, there has been some debate about the most appropriate type of fluidized bed to use for the calciner and carbonator (Galloy, Strohle, & Epple, 2011). Circulating fluidized beds are typically operated in the fast fluidized flow regime, where the transition can be predicted *via* the following equation (Bi, Grace, & Zhu, 1995):

$$U_{se} = 1.53 * \sqrt{\frac{g(\rho_p - \rho_g)d_p}{p_g}} \tag{2.11}$$

where $U_{se}$is the significant entrainment velocity. This equation is of the same form as Equation 2.10 and indicates that for $Ar > 10^7$ the transition to fast fluidization is approximately 7 to 8 times higher than that of minimum fluidization. This value is significantly higher when $Ar < 10^3$, which is typically the case for calcium looping where smaller particle sizes are normally used. CFBs are well suited for calcination since they can handle large gas / solids throughputs, without significant pressure drop, and the required sorbent residence is short due to rapid calcination reaction rates at elevated temperatures (Martinez, Grasa, Murillo, Arias, & Abanades, 2012).

Bubbling fluidized beds (BFB) operate between the bubbling and turbulent regimes. For group B and D particles, bubbling begins as soon U becomes greater thanU_{mf}. However, for group A particles, the interparticle forces play a role, so there is an appreciable gap between the minimum bubbling velocity,U_{mb}, and U_{mf}. In this case, the following correlation proposed by Abrahamsen and Geldart (1980) can be used to calculate U_{mb}:

$$U_{mb} = 2.07\exp(0.716\theta)\frac{d_p p_g^{0.06}}{\mu_g^{0.347}} \tag{2.12}$$

where θ is the mass fraction of particles finer than 45 micron in diameter. Turbulent fluidization occurs when the superficial velocity is increased to the point where the bubbles begin to break down. The critical velocity, U_c , which demarcates the transition to turbulent fluidization is typically of the form:

$$\mathrm{Re_c} = \frac{\rho_g d_p U_c}{\mu_g} = BAr^{\gamma} \tag{2.13}$$

where recommended values for B and γ are 0.565 and 0.461, respectively, based on a wide range of experimental data (Bi, Ellis, Abba, & Grace, 2000). Since superficial velocities in BFBs are lower than in CFBs, the level of particle entrainment is very low. This means that particle residence times can be very long if required. In the case of carbonation, the required residence times are on the order of several minutes, which is ideally suited for a bubbling fluidized bed. The short CFB residence times would require that the reactor be very tall (increased CAPEX) or have a large particle recirculation, which can cause issues with system reliability especially with small particles.

By combining the fluidized bed hydrodynamic models, with appropriate carbonation and calcination reaction kinetics, it is then possible to size the calcium looping reactors to (1) provide the appropriate gas-solid residence time to meet the desired CO_2 capture target and (2) select a reactor configuration that provides reliable sorbent circulation, while minimizing particle attrition.

2.3 – Nomenclature

Ar Archimedes number, dimensionless

B empirical constant for Equation 2.13, dimensionless

C_1 empirical constant for Equation 2.7, dimensionless

C_2 empirical constant for Equation 2.7, dimensionless

g acceleration due to gravity, m/s^2

H bed height, m

ΔH_r^0 enthalpy of reaction at standard conditions, kJ/mol

k deactivation constant, dimensionless

N cycle number, dimensionless

ΔP_{bed} bed pressure drop, Pa

$\mathrm{Re_c}$ Reynolds number at the onset of turbulent regime, dimensionless

$\mathrm{Re_{mf}}$ Reynolds number at minimum fluidization, dimensionless

U superficial gas velocity, m/s

U_c onset of turbulent regime velocity, m/s

U_{mb} minimum bubbling velocity, m/s

U_{mf} minimum fluidization velocity, m/s

U_{se} significant entrainment velocity, m/s

X_N CaO conversion, dimensionless

X_r residual CaO conversion, dimensionless

Greek letters

$\langle \epsilon \rangle_{av}$ bed voidage over the volume of the bed, dimensionless

ρ_g gas density, kg/m^3

ρ_p particle density, kg/m^3

μ_g gas viscosity, Pa.s

φ particle sphericity, dimensionless

θ mass fraction of particles finer than 45 micron

γ empirical constant for Equation 2.13, dimensionless

2.4 – References

Abrahamsen, A. R., & Geldart, D. (1980). Behaviour of gas fluidized beds of fine powders. *Powder Technology*, 26, 35.

Arias, B., Diego, M. E., Abanades, J. C., Lorenzo, M., Diaz, L., Martinez, D., . . . Sanchez-Biezma, A. (2013). Demonstration of steady state CO2 capture in a 1.7 MWth calcium looping pilot. *International Journal of Greenhouse Gas Control*, 18, 237-245.

Baker, E. H. (1962). The Calcium Oxide-Carbon Dioxide System in the Pressure Range 1-300 Atmospheres. *J. Chem. Soc*., 464-470.

Barin, I. (1989). Thermochemical data of pure substances. Weinheim: VCH.

Bi, H. T., Ellis, N., Abba, I. A., & Grace, J. R. (2000). A state-of-the-art review of gas-solids turbulent fluidization. *Chem. Eng. Sci*., 55, 4789.

Bi, H. T., Grace, J. R., & Zhu, J. (1995). Regime transitions affecting gas-solids suspensions and fluidized beds. Trans. *Inst. Chem. Eng*., 73, 154.

Borgwardt, R. H. (1970). Kinetics of the Reaction of SO2 with Calcined Limestone. 4, 59-63: *Environ. Sci. Technol*.

Borgwardt, R. H. (1989). Calcium Oxide Sintering in Atmospheres Containing Water and Carbon Dioxide. *Ind. Eng. Chem. Res*., 28, 493-500.

Champagne, S., Lu, D., Macchi, A., Symonds, R. T., & Anthony, E. J. (2013). The influence of steam inject during calcination on the reactivity of CaO-based sorbent for carbon capture. *Industrial & Engineering Chemistry Research*, 52, 2241-2246.

Chang, M. H., Huang, C. M., Liu, W. H., Chen, W. C., Cheng, J. Y., Chen, W., . . . Hsu, H. W. (2013). Design and Experimental Investigation of the Calcium Looping Process for 3-kWth and 1.9-MWth Facilities. *Chemical Engineering Technology*, 36 (9), 1525-1532.

Cormos, C. (2015). Assessment of chemical absorption/adsorption for post-combustion CO2 capture form Natural Gas Combined Cycle (NGCC) power plants. *Applied Thermal Engineering,* 82, 120-128.

Environment and Climate Change Canada. (2013, December 16th). Overview of Coal-fired Electricity Generation. Retrieved from Environment and Climate Change Canada: https://ec.gc.ca/cc/default.asp?lang=En&n=C94FABDA-1

Erans, M., Hanak, D. P., Mir, J., Anthony, E. J., & Manovic, V. (2016). Process Modelling and Techno-Economic Analysis of Natural Gas Combined Cycle Integrated with Calcium Looping. *Thermal Science*, 20, S59-S67.

Ergun, S. (1952). Fluid flow through packed columns. *Chem. Eng. Prog*., 48.

Fang, F., Li, Z. S., & Cai, N. S. (2009). Continuous CO2 Capture from Flue Gases Using a Dual Fluidized Bed Reactor with Calcium-Based Sorbent. *Ind. Eng. Chem. Res*., 48, 11140-11147.

Fennel, P. S., Pacciani, R., Dennis, J. S., Davidson, J. F., & Hayhurst, A. N. (2007). The effects of repeated cycles of calcination and carbonation on a variety of different limestones as measured in a hot fluidized bed of sand. *Energy Fuels*, 21, 2072-2081.

Galloy, A., Strohle, A. J., & Epple, B. (2011). Design and operation of a 1 MWth carbonate and chemical looping CCS test rig. *VGB PowerTech*, 6, 64-68.

Geldart, D. (1973). Types of gas fluidization. *Powder Technol*, 7, 285.

Grace, J. R. (1986). Contacting modes and behaviour classification of gas-solid and other two-phase suspensions. *Can. J. Chem. Eng*., 64, 353.

Grace, J. R., Leckner, B., Zhu, J., & Cheng, Y. (2006). Fluidized Beds. In C. T. Crowe, Multiphase Flow Handbook (pp. 5-1 - 5-93). Boca Raton, Florida: CRC Press.

Grasa, G. S., & Abanades, J. C. (2006). CO2 capture capacity of CaO in long series of carbonation / calcination cycles. *Ind. Eng. Chem. Res*, 45, 8846-8851.

Herring, C. (1950). Effect of change of scale on sintering phenomena. *J. Appl. Phys*., 21, 301.

IEA. (2013). CO2 Pipeline Infrastructure. Stoke Orchard, Cheltenham: IEAGHG.

IPCC. (2005). IPCC Special Report on Carbon Dioxide Capture and Storage. Geneva, Switzerland: IPCC.

Jia, L., Tan, Y., McCalden, D., Wu, Y., He, I., Symonds, R. T., & Anthony, E. J. (2012). Commissioning of a 0.8 MWth CFBC for oxy-fuel combustion. *International Journal of Greenhouse Gas Control*, 7, 240-243.

Li, Z. S., Cai, N. S., Huang, Y. Y., & Han, H. J. (2005). Synthesis, experimental studies, and analysis of a new calcium-based carbon dioxide absorbent. *Energy Fuels*, 19, 1447-1452.

MacKenzie, A., Granastein, D. L., Anthony, E. J., & Abanades, J. C. (2007). Economic of CO2 capture using the calcium cycle with a pressurized fluidized bed combustor. *Energy & Fuels*, 21, 920-926.

Manovic, V., & Anthony, E. J. (2008). Thermal activation of CaO-based sorbent and self-reactivation during CO2 capture looping cycles. *Environmental Science and Technology*, 42, 4170-4174.

Manovic, V., & Anthony, E. J. (2011). Reactivation and remaking of calcium aluminate pellets for CO2 capture. *Fuel*, 90 (1), 233-239.

Martinez, I., Grasa, G., Murillo, R., Arias, B., & Abanades, J. C. (2012). Kinetics of Calcination of Partially Carbonated Particles in a Ca-Looping System for CO2 Capture. *Energy Fuels*, 26, 1432-1440.

Mohammed, I. Y., Samah, M., Mohamed, A., & Sabina, G. (2014). Comparison of Selexol and Rectisol Technologies in an Integrated Gasification Combined Cycle (IGCC) Plant for Clean Energy Production. *International Journal of Engineering Research*, 3 (12), 742-744.

Napp, T. A., Gambhir, A., Hills, T. P., Florin, N., & Fennell, P. S. (2014). A review of the technologies, economics and policy instruments for decarbonising energy-intensive manufacturing industries. *Renewable and Sustainable Energy Reviews*, 30, 616-640.

Rodriguez, N., Murillo, R., & Abanades, J. C. (2012). CO2 capture from cement plants using oxyfired precalcined and/or calcium looping. *Environmental Science & Technology*, 46(4), 2460-2466.

Rodriguez, N., Murillo, R., Alonso, M., Martinez, I., Grasa, G., & Abanades, J. C. (2011). Analysis of a process for capturing the CO2 resulting from the precalcination of limestone in a cement plant. *Industrial & Engineering Chemistry Research*, 50(4), 2126-2132.

Romeo, L. M., Lara, Y., Lisbona, P., & Escosa, J. M. (2009). Optimized make-up flow in a CO2 capture system using CaO. *Chemical Engineering Journal*, 147 (2-3), 252-258.

Shimizu, T., Hirama, T., Hosoda, H., Kitano, K., Inagaki, M., & Tejima, K. (1999). A Twin Fluid-Bed Reactor for Removal of CO2 from Combustion Processes. *Chemical Engineering Research and Design*, 77 (1), 62-68.

Siliban, D. S., Narcida, M., & Harrison, D. P. (1996). Characteristics of the reversible reaction between CO2(g) and calcined dolomite. *Chemical Engineering Communications*, 146, 149-162.

Strohle, J., Junk, M., Kremer, J., Galloy, A., & Epple, B. (2014). Carbonate looping experiments in a 1 MWth pilot plant and model validation. *Fuel*, 127, 13-22.

Sun, P., Grace, J., Lim, C. J., & Anthony, E. J. (2006). Removal of CO2 by Calcium-based Sorbents in the Presence of SO2. *Energy Fuels*, 21, 163-170.

Telesca, A., Calabrese, D., Marroccoli, M., Tomasulo, M., Valenti, G. L., Dueilli, G., & Montagnaro, F. (2014). Spent limestone sorbent from calcium looping cycle as a raw material for the cement industry. *Fuel*, 118, 202-205.

Visser, J. (1989). Van der Waals and other cohesive forces affecting powder fluidization. *Powder Technol*, 58, 1.

Wen, C. Y., & Yu, Y. H. (1966). Generalized method for predicting the minimum fluidization velocity. *AICHe* J., 12, 610.

World Resources Institute (WRI). (2008). CCS Guidelines: Guidelines for Carbon Dioxide Capture, Transport, and Storage. Washington: World Resources Institute.

Yang, W. C. (2003). Handbook of Fluidization and Fluid-Particle Systems. New York: Marcel Dekker Inc.

Chapter 3 – The Effect of HCl and Steam on Cyclic CO_2 Capture Performance in Calcium Looping Systems

Robert T. Symonds[a], Dennis Y. Lu[a], Arturo Macchi[b], Robin W. Hughes[a], Edward J. Anthony[c]

[a]Natural Resources Canada, CanmetENERGY

1 Haanel Drive, Ottawa, Ontario K1A 1M1, Canada

[b]Department of Chemical and Biological Engineering, University of Ottawa

161 Louis Pasteur Street, Ottawa, Ontario K1N 6N5, Canada

[c]School of Applied Science, Cranfield University

Cranfield, Bedfordshire MK43 0AL, United Kingdom

Article submitted to *Chemical Engineering Science* 2017

3.1 – Abstract

Calcium looping is CO_2 capture technology that is considered to be technically feasible at an industrial scale using a variety of fuels such as natural gas, coals, biomass, refuse derived fuels, and biofuels. Unfortunately, many of these fuels contain significant quantities of chlorine which principally converts to gaseous HCl during combustion or gasification. To date, very few studies have examined the effect of HCl on sorbent CO_2 capture performance using calcium-based sorbents under realistic carbonation and calcination conditions. In this work, experiments were conducted using thermogravimetric analysis and fixed bed reactor testing to determine the effect of HCl addition during carbonation and calcination over repeated cycles using a Canadian limestone. The presence of HCl was found to increase sorbent reactivity towards CO_2 capture when steam was injected during calcination. The resulting decomposition of $CaCl_2$ to CaO during calcination caused changes in the particle morphology, which in turn decreased the CO_2 diffusional resistance during carbonation. Fixed bed test results provided confirmation of full sorbent dechlorination under typical oxy-fuel calcination conditions. It was shown that both particle surface area and pore volume were higher during tests where HCl was present during carbonation and that greater than 99% HCl capture could be achieved without adversely affecting sorbent CO_2 capture performance when steam was present during both carbonation and calcination.

3.2 – Introduction

CO_2 emissions from fossil-fuelled power stations are believed to be a major contributor to global warming and climate change (Pachauri & Reisinger, 2007) (IEA, 2010). One method for reducing CO_2 emissions would be *via* a carbon capture, utilization, and storage (CCUS) technology (Boot-Handford, et al., 2014). The rationale for the use of CCS on fossil-fuelled

power plants is that, when deployed with other technologies (e.g., renewables), the overall cost of electricity would be minimized. Since the use of renewable sources of electricity (e.g., wind, solar, etc.) are intermittent, the implementation of CCS to fossil-fueled power plants would reduce the need for large-scale energy storage systems (IEA, 2014) (Fennell & Anthony, 2015). To date, many methods for CO_2 capture have been investigated (Abu-Zahra, Schneiders, Niederer, Feron, & Versteeg, 2007) (Elwell & Grant, 2006) (Fauth, Frommell, Hoffman, Reasbeck, & Pennline, 2005) (Resnik, Yeh, & Pennline, 2004) (Wall, Stanger, & Santos, 2011) (Yang, et al., 2008) (Hack, et al., 2012) (Suraniti, Nsakala, & Darling, 2009) (Ryden & Lyngfelt, 2006), with calcium looping emerging as one of the most promising technologies for large-scale industrial applications.

The calcium looping process is based on the reversible reaction between CaO and CO_2 (Shimizu, et al., 1999) and utilizes a dual-fluidized bed reactor system. CFB and/or BFB systems are particularly suited from processing large quantities of solids and reactions between gas and solid streams are significantly enhanced by superior mixing that maximizes mass and heat transfer (Davidson, Clift, & Harrision, 1985). Therefore, at appropriate temperatures and pressures, a flue gas stream can be decarbonized by being passed through a fluidized bed of calcined limestone or dolomite (CaO) to form $CaCO_3$ (carbonation, Equation 3.1). The carbonated material is then transferred to a second fluidized bed (calciner) where, at higher temperatures and/or lower pressures, the calcination reaction occurs (Equation 3.2). The resulting gas stream is concentrated CO_2 (>90%), which is then suitable for liquefaction and ultimate sequestration. The heat of regeneration is supplied by the combustion of a fuel, such as coal or biomass, with high purity O_2 and a diluent; recycle flue gas or steam. The calciner is

operated as an oxy-fuel CFBC and the high temperature utilized for regeneration allows for the production of high quality steam for electrical power generation.

$$CaO(s) + CO_2(g) \rightarrow CaCO_3(s) \quad (3.1)$$

$$CaCO_3(s) \rightarrow CaO(s) + CO_2(g) \quad (3.2)$$

Calcium looping is considered to be technically feasible at an industrial scale (Fennell & Anthony, 2015) (Sanchez-Biezma, et al., 2013) (Blamey, Anthony, Wang, & Fennell, 2010) (Yang, et al., 2010), relatively energy-efficient (Ball, 2014) (Goto, Yogo, & Higashii, 2013) (Lara, Lisbona, Martinez, & Romeo, 2013) (Martinez, Lara, Lisbona, & Romeo, 2012) (Rodriguez, Alonso, Grasa, & Abanades, 2008), economically competitive (MacKenzie, Granatstein, Anthony, & Abanades, 2007) (Abanades, et al., 2007) (Abanades, Rubin, & Anthony, 2004), and environmentally benign because of the relatively inert nature of the solid residues produced by the process. Moreover, the spent residues could also be used in cement manufacturing or other industrial processes (Dean, Dugwell, & Fennell, 2011) (Dean, Blamey, Florin, Al-Jeboori, & Fennell, 2011) (Rodriguez, Murillo, & Abanades, 2012) (Romeo, Catalina, Lisbona, Lara, & Martinez, 2011).

Many bench-scale studies have demonstrated that naturally occurring limestone sorbents exhibit a rapid decay in CO_2 capture reactivity with increasing calcination/carbonation cycle number attributed mainly to thermal sintering of the particles (Grasa & Abanades, 2006) (Chrissafis, 2007) (Wang, Manovic, Wu, & Anthony, 2010). Due to the adverse effect of sorbent deactivation on the overall process efficiency, intensive research has been focused on CaO reactivation methods and the development of routes to obtain more stable CaO-based CO_2 sorbents (Kierzkowska, Pacciani, & Muller, 2013) (Valverde, Sanchez-Jimenez, & Perez-

Maqueda, 2014). Some of the more researched methods include steam reactivation (Arias, Grasa, & Abanades, 2010) (Fennell, Davidson, Dennis, & Hayhurst, 2007) (Hughes, Lu, Anthony, & Wu, 2004) (Manovic & Anthony, 2007), self-reactivation (Manovic & Anthony, 2008), sorbent doping (Al-Jeboori, Nguyen, Dean, & Fennell, 2013), pelletized / synthetic sorbents (Symonds, Champagne, Firas, & Lu, 2016) (Blamey, Anthony, Wang, & Fennell, 2010) (Chen, Zhao, Yang , & Zhang, 2012), and recarbonation (Arias, Grasa, Alonso, & Abanades, 2012) (Valverde, Sanchez-Jimenez, & Perez-Maqueda, 2014).

The CO_2 carrying capacity of calcium based sorbents is not only reduced by thermal sintering, but also by competitive reactions with other pollutants commonly found in combustion flue gas. One of which is SO_2, which at normal combustor operating conditions irreversibly reacts with both CaO and $CaCO_3$ to form $CaSO_4$, limiting carbonation conversions due to pore blockage (Borgwardt, Kinetics of the reaction of SO2 eith calcined limestone, 1970) (Tullin & Ljungstrom, 1989) (Sun, Grace, Lim, & Anthony, Removal of CO2 by calcium-based sorbents in the presence of SO2, 2006) (Arias, Cordero, Alonso, & Abanades, 2012). Many fuels such as coal, biomass, refuse derived fuel (RDF), and biofuels contain significant quantities of chlorine which principally converts to gaseous HCl during combustion or gasification. Authors Partanen *et al*. (2005) and Chyang *et al*. (2009) suggested that flue gas concentrations of HCl could reach upwards of 2000 ppm, which requires capture in order to avoid corrosion and fouling of boiler components and other downstream equipment. Calcium-based sorbents are commonly used for HCl capture in combustion or gasification systems, as shown in Equations 3.3 and 3.4.

$$CaO(s) + 2HCl(g) \leftrightarrow CaCl_2(s,l) + H_2O(g) \quad (3.3)$$

$$CaCO_3(s) + 2HCl(g) \leftrightarrow CaCl_2(s,l) + H_2O(g) + CO_2(g) \quad (3.4)$$

It has been shown that the optimum HCl capture capacity using CaO is achieved in the temperature range of 500-650^{o}C (Bie, Li, & Yang, 2005) (Chyang, Han, & Zhong, 2009), with the highest capture capacity reported at 550^{o}C (Sun, Yu, Li, Li, & Fan, 2011). Lower conversions reported at temperatures above 800^{o}C have been attributed to the formation of molten $CaCl_2$ product phases. Therefore, it would be expected that both HCl and CO_2 capture would occur simultaneously with calcium-based sorbents in the calcium looping process, since typical carbonation temperatures are in the range of 650-720^{o}C (Manovic & Anthony, 2008) (Grasa, Abanades, Alonso, & Gonzalez, 2008). Several reported investigations have examined the effect of gas atmosphere on HCl capture by calcium-based sorbents. Partanen et al. (2005) discovered that the presence of CO_2 resulted in a higher HCl capture capacity, although it should be noted that both Duo et al. (1996) and Chin et al. (2005) observed the opposite effect. This decrease in HCl capture capacity was attributed to an increase in diffusion resistance due to CO_2 reacting with CaO forming $CaCO_3$. Another major species of interest is steam, which would be present during both carbonation and calcination processes associated with calcium looping. The presence of steam has been shown to decrease the HCl capture capacity of calcium-based sorbents by as much as 50%, with this effect becoming more prominent at higher temperatures (>650^{o}C) (Lawrence & Bu, 2000) (Partanen, Backman, Backman, & Hupa, 2005).

To date, almost all investigations just focus on the effect of CO_2 and steam on HCl capture and do not consider the impact of HCl on CO_2 capture using calcium-based sorbents. In these cases the ultimate goal is to maximize HCl capture by forming $CaCl_2$, which is subsequently removed from the process and not repeatedly cycled as is the case with calcium looping. Wang et al. (2014) addressed this issue by performing multiple calcination/carbonation cycles in the presence of HCl at various calcination and carbonation conditions. Although this

gave significant insight into the effect of HCl on the calcium looping process as a whole, the presence of steam during calcination and carbonation was not considered. Both calcination and carbonation environments would contain some level of steam, which by examining Equations 3.3 and 3.4, should significantly impact the level of $CaCl_2$ formation over repeated cycles. In this present work, the cyclic CO_2 capture behavior of limestone in the presence of HCl during calcination and/or carbonation under more realistic conditions was examined *via* thermogravimetric analysis (TGA). In addition, fixed bed reactor testing was performed to quantify the level of chlorination/de-chlorination expected in a real dual fluidized bed reactor system.

3.3 – Experimental Details

3.3.1 – Thermogravimetric analyzer (TGA) and fixed bed reactor system

Figure 3.3.1 is a schematic diagram of the thermogravimetric analyzer (TGA) and fixed bed reactor systems used for this experimental test work. The TGA system was comprised of a hang-down tube reactor column made of Inconel 625 alloy with an inner diameter of 0.025m. Located centrally within the hang-down tube was a platinum sample tray suspended from a Cahn 1000 Electrobalance with a capacity of 100g and a sensitivity of 1μg. Weight measurements were sent from the balance to the control box, which was controlled by the use of customized Honeywell software. The fixed bed reactor was fabricated out of Hastelloy HT and was outfitted with a 0.013m custom ceramic tube insert capable of holding samples of up to 10g in size. Samples were held in place *via* high temperature ceramic meshing.

Gas cylinders containing N_2, CO_2, and HCl (balance CO_2) were mixed before entering the inlets to both the TGA and fixed bed reactor. Brooks mass flow controllers (0-100 and 500NmL/min) were used to accurately control the gas flow rates to obtain desired feed gas

concentrations. Steam was fed to both systems *via* a Harvard PHD 440 syringe pump and steam generator. Feed lines containing both steam and mixed gas were insulated and electrically heat-traced to ensure no steam condensation occurred. A purge gas (N_2 in all cases) was top-fed through the balance of the TGA to ensure the sensitive balance electronics did not overheat and that the reaction gases did not enter the balance housing. Purge gas was fed to the outlet of the fixed bed reactor for sample gas dilution. Outlet gases from both systems were subsequently cooled, to condense steam, passed through a moisture trap, and finally vented to the atmosphere. Both reactors were heated by means of electric heaters located centrally around the sample holders and can reach temperatures up to 950^{o}C. System temperatures were monitored using K-type thermocouples, as shown in Figure 3.3.1. Honeywell software was used to control all gas flow rates, electric heaters, and heat-tracing and was operated in automatic mode to allow for changes in operating condition set points. All temperatures, flow rates, and weight measurements were recorded every 6s and stored in Microsoft Excel files. During fixed bed reactor testing, a portable GASMET fourier transform infrared (FTIR) spectrometer was employed to measure the outlet gas composition (CO_2, H_2O, and HCl).

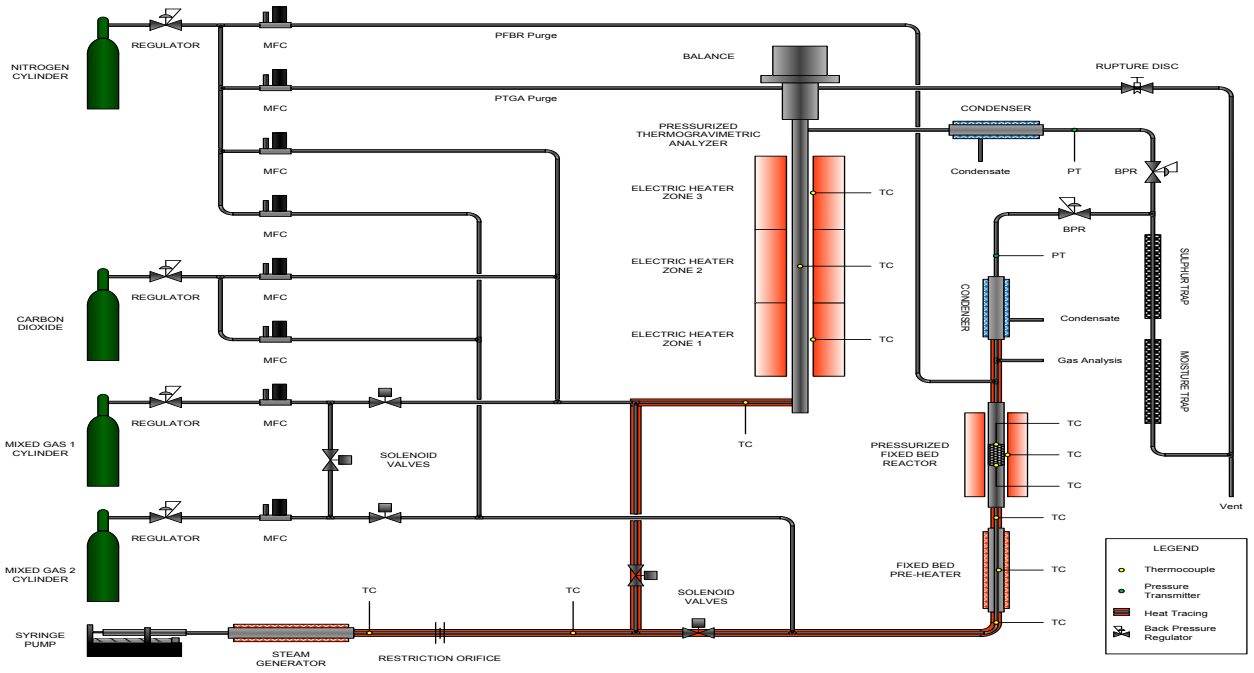

Figure 3.3.1: Schematic diagram of the TGA and fixed bed reactor experimental setup.

3.3.2 – Experimental test conditions

The CaO source for all TGA and fixed bed experiments was a naturally occurring Canadian limestone (Cadomin). The limestone was crushed and sieved to a single particle size range of 250 to 425µm in diameter, as this represents a common particle size range used during dual fluidized bed reactor operation (Ridha, Lu, Symonds, & Champagne, 2016) (Champagne, Lu, Symonds, Macchi, & Anthony, 2016). Approximately 20 to 25mg and 5g of sorbent were used for TGA and fixed bed reactor experiments, respectively. In the case of the TGA testing, this particular sample size was chosen in order to lower potential variance in chemical composition between runs, as individual particles can display different CaO/MgO ratios. Larger fixed bed samples were utilized to allow for post-run SEM/EDX and pore structure analyses.

To determine the effect of HCl on the CO_2 capture behavior of limestone, experiments were performed with and without HCl present during both carbonation and calcination over

repeated cycles. The rationale is that if an existing power generation facility utilizing a high chlorine fuel is retrofitted for post-combustion CO_2 capture using calcium looping, the same fuel would most likely be adopted as the heat source for sorbent regeneration, since the fuel is already on-site. Since the flue gas entering the carbonator would contain some level of steam, its impact on CO_2 capture and chlorination was also tested, both with and without HCl present. In each case, steam was present during calcination as would be the case in any real combustion system, except for two runs where a comparison with a pure N_2 environment was performed. For all TGA tests, a total gas flow rate of 100 NmL/min of reaction gas was used and all tests were performed at atmospheric pressure. Based on previous testing, it has been shown that these conditions limit gas diffusion limitations from the bulk gas to the particle surface (Symonds, Lu, Macchi, Hughes, & Anthony, 2009). The total gas flow rate was increased to 200 NmL/min for fixed bed reactor tests (1) to achieve a relatively quick CO_2 breakthrough and (2) to provide enough sample gas to facilitate the usage of the portable FTIR spectrometer.

As determined by Garcia-Lablano et al. (2002), the equilibrium partial pressure of CO_2, $P_{CO_2,eq}$, over CaO at a temperature, T, is given by the following equation:

$$P_{CO_2,eq} = 4.137 \times 10^{12} \exp\left(-\frac{20474}{T}\right) \tag{3.5}$$

Based on Equation 3.5, the minimum temperature to allow for calcination of the sorbent was determined. It was decided to operate at a temperature slightly higher than equilibrium to ensure a rapid and complete calcination. Carbonation was performed at 650^{o}C for all tests, since it has been determined to be the preferred temperature for CO_2 capture using calcium-based sorbents (Manovic & Anthony, 2008) and represents a greater than 90% CO_2 capture efficiency based on

a typical coal-combustion flue gas composition (~15 vol%). The specific experimental conditions for all TGA and fixed bed reactor tests are presented in Table 3.3.1 and Table 3.3.2, respectively.

Table 3.3.1: Experimental conditions – TGA tests.

Run No.	Carbonation Conditions	Calcination Conditions	Number of Cycles
1	20 mins, 650°C, 15 mol% CO_2/balance N_2	10 mins, 870 °C, 100 mol% N_2	10
2	20 mins, 650°C, 15 mol% CO_2/2000 ppm HCl/balance N_2	10 mins, 870 °C, 100 mol% N_2	10
3	20 mins, 650°C, 15 mol% CO_2/balance N_2	10 mins, 870 °C, 60 mol% CO_2/15 mol% H_2O/balance N_2	10
4	20 mins, 650°C, 15 mol% CO_2/2000 ppm HCl/balance N_2	10 mins, 870 °C, 60 mol% CO_2/15 mol% H_2O/balance N_2	10
5	20 mins, 650°C, 15 mol% CO_2/balance N_2	10 mins, 870 °C, 60 mol% CO_2/15 mol% H_2O/balance N_2	10
6	20 mins, 650°C, 15 mol% CO_2/balance N_2	10 mins, 870 °C, 60 mol% CO_2/15 mol% H_2O/2000 ppm HCl/balance N_2	10
7	20 mins, 650°C, 15 mol% CO_2/15 mol% H_2O/balance N_2	10 mins, 870 °C, 60 mol% CO_2/15 mol% H_2O/balance N_2	10
8	20 mins, 650°C, 15 mol% CO_2/15 mol% H_2O/2000 ppm HCl/balance N_2	10 mins, 870 °C, 60 mol% CO_2/15 mol% H_2O/balance N_2	10

Table 3.3.2: Experimental conditions – fixed bed reactor tests.

Run No.	Carbonation Conditions	Calcination Conditions	Number of Cycles
1	20 mins, 650°C, 15 mol% CO_2/balance N_2	20 mins, 870 °C, 60 mol% CO_2/15 mol% H_2O/balance N_2	6
2	20 mins, 650°C, 15 mol% CO_2/2000 ppm HCl/balance N_2	20 mins, 870 °C, 60 mol% CO_2/15 mol% H_2O/balance N_2	6
3	20 mins, 650°C, 15 mol% CO_2/15 mol% H_2O/balance N_2	20 mins, 870 °C, 60 mol% CO_2/15 mol% H_2O/balance N_2	6
4	20 mins, 650°C, 15 mol% CO_2/15 mol% H_2O/2000 ppm HCl/balance N_2	20 mins, 870 °C, 60 mol% CO_2/15 mol% H_2O/balance N_2	6

For the set of TGA experiments, the carbonation conversion was calculated based on the level of mass change recorded during the calcination step for each cycle, which assumes that all decreases in mass were attributed to the decomposition of $CaCO_3$ to CaO (Equation 3.2). It should be noted that all carbonation conversions were determined based on the mass change after 20 min of carbonation. Therefore, the carbonation conversion for each cycle, $X_{carb,N}$, was calculated as follows:

$$X_{carb,N} = \frac{m_{carb,N} - m_{calc,N}}{m_0 \cdot \beta} \cdot \frac{M_{CaO}}{M_{CO_2}} \cdot 100 \tag{3.6}$$

where N is the carbonation / calcination cycle number, m_{carb} is the mass of sample after carbonation, m_{calc} is the mass of sample after calcination, m_0 is the initial sample mass, β is the content of CaO in the initial sample, M_{CaO} is the molar mass of CaO, and M_{CO_2} is the molar mass of CO_2. Since the melting point of anhydrous $CaCl_2$ is between 772-775^{o}C (Pradyot, 2003), any carbonation conditions that form $CaCl_2$ would have the potential for evaporation and sublimation during calcination. A series of preliminary tests were conducted using chlorinated limestone at 870^{o}C under an atmospheric pressure N_2 environment to quantify the level of $CaCl_2$ evaporation expected during calcination. From these results it was determined that, for such a short calcination period (10 minutes), the level of $CaCl_2$ mass loss was negligible. This outcome is in agreement with the high temperature HCl absorption work performed by Chyang (2009), which showed a $CaCl_2$ mass loss of less than 0.3% over a 10 minute period at temperatures similar to this work. Consequently, the chlorination conversion for each cycle, $X_{chlor,N}$, could be determined *via* the following equation:

$$X_{chlor,N} = \frac{m_{calc,N} - m_0}{m_0 \cdot \beta} \cdot \frac{M_{CaO}}{M_{CaCl_2} - M_{CO_2}} \cdot 100 \tag{3.7}$$

where M_{CaCl_2} is the molar mass of $CaCl_2$.

The carbonation and chlorination conversions for the fixed bed experiments were calculated using the difference between the measured inlet and outlet flowrates of CO_2 and HCl, respectively, over the entire carbonation period, P_{carb}. Taking into account the initial mass and purity of the sample, the fixed bed conversions for each cycle were determined as follows:

$$X_{carb,N} = \frac{(Mass\ CO_2\ In - Mass\ CO_2\ Out)}{m_0 \cdot \beta} \cdot \frac{M_{CaO}}{M_{CO_2}} \cdot 100 \tag{3.8}$$

$$X_{carb,N} = \frac{\rho_{CO_2} \cdot \left((F_{CO_2,0} \cdot P_{carb}) - \left(\int_{t=0}^{t=P_{carb}} F_{Outlet} \cdot C_{CO_2} \right) \right)}{m_0 \cdot \beta} \cdot \frac{M_{CaO}}{M_{CO_2}} \cdot 100 \tag{3.9}$$

$$X_{chlor,N} = \frac{\rho_{HCl} \cdot \left((F_{HCl,0} \cdot P_{carb}) - \left(\int_{t=0}^{t=P_{carb}} F_{Outlet} \cdot C_{HCl} \right) \right)}{m_0 \cdot \beta} \cdot \frac{M_{CaO}}{2 \cdot M_{HCl}} \cdot 100$$

where ρ_{CO_2} is the density of CO_2, ρ_{HCl} is the density of HCl, $F_{CO_2,0}$ is the inlet flowrate of CO_2, $F_{HCl,0}$ is the inlet flowrate of HCl, F_{Outlet} is the total outlet flowrate, C_{CO_2} is the outlet concentration of CO_2, C_{HCl} is the outlet concentration of HCl, and M_{HCl} is the molar mass of HCl.

3.3.3 – Thermodynamic equilibrium predictions

FactSage software predicts equilibrium solid-liquid-gas phases and compositions based on Gibbs free energy minimization (Bale, et al., 2014). Gibbs free energy is calculated from optimized models with parameters based on empirical data with various compositions, temperatures and pressures. This information is contained within compound and solution databases. For thermodynamic equilibrium predictions in this study, the FactSage 6.4 *Reaction*, *Equilib* and *Phase Diagram* modules were utilized with the FactPS and FToxid databases. All

gas, liquid and solid compounds were considered. For compounds found in both the FactPS and FToxid databases, preference was given to the FToxid database to have better thermodynamic consistency with the solution phases data. Note that by default some solid and liquid compound phases are not selected and had to be manually selected. All possible solution phases, neglecting immiscibility, were included in the calculations.

3.3.4 – Sorbent characterization

Physical and chemical characterizations of the sorbent, before and after testing, were carried out using several different analysis techniques. The composition of the raw sorbent was obtained by X-ray fluorescence (XRF) following ASTM D4326 and is provided in Table 3.3.3. Specific surface areas and pore volumes were obtained from N_2 adsorption measurements at -196°C using a porosity analyzer (Micromeritics TriStar II-3020). Surface area was obtained from adsorption data using the multiple point Brunauer-Emmett-Teller (BET) model, while pore volume was derived from the corresponding desorption data using the Barrett-Joyner-Halenda (BJH) model (Lowell, Thomas, & Thommes, 2004). The surfaces of particles were examined using a scanning electron microscope (SEM, Hitachi S-3400 N). Localized elemental composition was obtained with energy dispersive X-ray (EDX) spectrometry on the same instrument. For both SEM and EDX analyses, the sample was coated with a thin layer of palladium (~2 nm).

Table 3.3.3: XRF chemical analysis of Cadomin Limestone (wt.%).

CaO	MgO	SiO_2	Al_2O_3	Fe_2O_3	TiO_2	P_2O_5	SO_3	Na_2O	K_2O	*LOF
50.64	3.28	1.30	0.40	0.11	0.04	<0.03	<0.1	<0.2	0.14	43.99

* LOF = Loss on fusion

3.4 – Results and Discussion

3.4.1 – Effect of HCl on CO_2 capture without the presence of steam

It is well documented that at temperatures around 650^{o}C, both carbonation (Equation 3.1) and chlorination (Equation 3.3) of CaO will separately proceed to form $CaCO_3$ and $CaCl_2$, respectively. What is less understood is how the level of conversion of one species will affect the other, how this will affect the rate of CO_2 uptake, and what can be expected in terms of cyclic CO_2 capture stability over repeated cycles. A preliminary series of tests were conducted to examine the impact of the presence of HCl on the carbonation conversion over repeated cycles to provide baseline data. In these tests, calcination was performed under pure N_2 at 870^{o}C and atmospheric pressure to (1) determine the extent of $CaCl_2$ evaporation and (2) compare the cyclic CO_2 stability to previous studies.

As indicated above, no measurable level of $CaCl_2$ evaporation was observed over the 20-minute calcination period. This conclusion was based on the fact that after calcination of $CaCO_3$ to CaO had completed, no further weight loss was measured. It should be mentioned that $CaCl_2$ evaporation could have taken place during the calcination period, but this is very unlikely since (1) the calcination reaction was completed within a very short period (<2 minutes) and (2) no $CaCl_2$ deposits were found in the TGA system post-run, which would be expected if evaporation had occurred (Chyang, Han, & Zhong, 2009).

The carbonation conversions of the Cadomin limestone after repeated cycles in the absence and presence of HCl are shown in Figure 3.4.1. Over all 10 cycles, the carbonation conversions were lower when HCl was present, with the difference in conversion diminishing with increasing cycle number. From these results, it appears that the formation of $CaCl_2$ on the surface of the CaO particles increases the CO_2 diffusion resistance in comparison to that of

$CaCO_3$. This result is quite plausible since the molar volume of $CaCl_2$ is approximately 1.4 times that of $CaCO_3$ (FactSage). It is also important to point out that any $CaCl_2$ formed during carbonation should increase in total cumulative conversion from cycle to cycle. This can be clearly seen in Figure 3.4.1 where the total CaO conversion to $CaCl_2$ increases from approximately 2.1 to 10.0% over 10 cycles. This is further reinforced by the CaO-$CaCl_2$ phase diagram provided in Figure 3.4.2, where high gas-to-solids ratios have been chosen to represent TGA conditions. Over a wide range of HCl and CO_2 concentrations (balance N_2) thermodynamic phase equilibrium analysis predicts that during carbonation at temperatures below approximately 770^oC, only solid phase $CaCl_2$ should exist. Conversely, during calcination at temperatures above 770^oC only a phase change from solid to liquid $CaCl_2$ is predicted and, assuming the rate of evaporation is negligible over such short calcination periods, no loss in $CaCl_2$ product can be expected. Figure 3.4.2 also indicates that under typical carbonation conditions the formation of $CaCl_2$ is thermodynamically favoured over the formation of $CaCO_3$. Therefore, lower carbonation conversions could be expected if carbonation time periods where increased. After several cycles the impact of the $CaCl_2$ product layer becomes less prominent since thermal sintering of the sorbent during calcination becomes the dominant CO_2 diffusional resistance (Lysikov, Salanov, & Okunev, 2007). It should be noted that the phase equilibrium predictions in Figure 3.4.2 are unaffected by CO_2 concentration ranging from 0 to 80 mol%, which covers all typical CO_2 concentrations in both the carbonation and calcination regimes.

Interestingly, these results are somewhat different from those found by Wang et al. (2014), where it was reported that the carbonation conversions over the first 10 cycles were higher when HCl was present during carbonation. This phenomenon was attributed to a two-step mechanism where the surface of the calcined sorbent is initially converted to $CaCO_3$, then

subsequently reacted with HCl to form $CaCl_2$ (Equation 4). During this process, H_2O and CO_2 release from the product layer could create additional porosity, lowering the CO_2 diffusional resistance to the unreacted CaO core. Alternatively, Partanen *et al*. (2003) and Freidina & Fray (2000) considered the $CaCl_2$-$CaCO_3$ product layer possibly forming a molten phase during carbonation at temperatures around 700^oC. This could reduce the diffusion limitations and explain the increased carbonation conversions in comparison to what is seen in Figure 3.4.1, where carbonation takes place at 650^oC. To investigate this phenomenon further a more detailed look at each carbonation cycle is required.

Presented in Figure 3.4.3 is a comparison of the carbonation conversion versus time data for the 3rd and 9th cycle with and without the presence of HCl. It can be observed that although the total conversion over entire carbonation period is higher without the presence of HCl, the initial rate of reaction in the kinetically controlled regime is greater when HCl is present. This result would suggest that chlorination of both CaO and $CaCO_3$ is kinetically favoured over carbonation, but the release of H_2O during the chlorination of CaO to $CaCl_2$ increases the available surface area for carbonation through the creation of additional porosity as suggested by Wang et al. (2014). Figure 3.4.3 also clearly shows that the fast kinetically controlled regime period is reduced when HCl is present indicating that the formation of $CaCl_2$ eventually has a negative effect on CO_2 capture. This is mostly likely caused when a significant quantity of the active portion of the particle surface becomes covered in a layer of $CaCl_2$, increasing the diffusional resistance. It is interesting to note that the initial rate of reaction remains constant from the 3rd to the 9th cycles when HCl is present, whereas there is a significant drop over repeated cycles in the absence of HCl. As shown by Wang et al. (2014), the residual CO_2 carrying capacity should eventually be reduced to near zero over an increased number of

carbonation / calcination cycles, since more and more sorbent would be irreversibly converted to $CaCl_2$ under these particular carbonation / calcination conditions.

An alternate theory that may help explain the reduced difference between carbonation conversions over repeated cycles with and without the presence of HCl is related to solid state diffusion where Cl migration may occur. The solid state diffusion of $CaCl_2$ is enhanced at the higher calcination temperature when the $CaCl_2$ is in the liquid state with the consequence that it migrates into the interior of the particle to some extent. This migration tends to occur at grain boundaries where solid state diffusion rates can be expected to be highest due to local lattice dislocations. Migration of the Cl into the interior of the particle during calcination results in a portion of the surface sites that had previously been $CaCl_2$ forming CaO, which is subsequently available for reaction with either additional HCl or with CO_2. Due to this effect, the pore blockage that occurs is temporary and does not result in a large degradation in carbonation conversion over a large number of cycles. Thus, after 10 calcination / carbonation cycles, the carbonation conversion both with and without the presence of HCl tend towards the same value (Figure 3.4.1). This occurs despite the fact that the sum of the molar volumes of $CaCO_3$ and $CaCl_2$ in the particles that had been exposed to HCl is greater than the molar volume of $CaCO_3$ in the particles that were not exposed to HCl. Future testing with an extended number of calcination / carbonation cycles should be explored to further reinforce this theory.

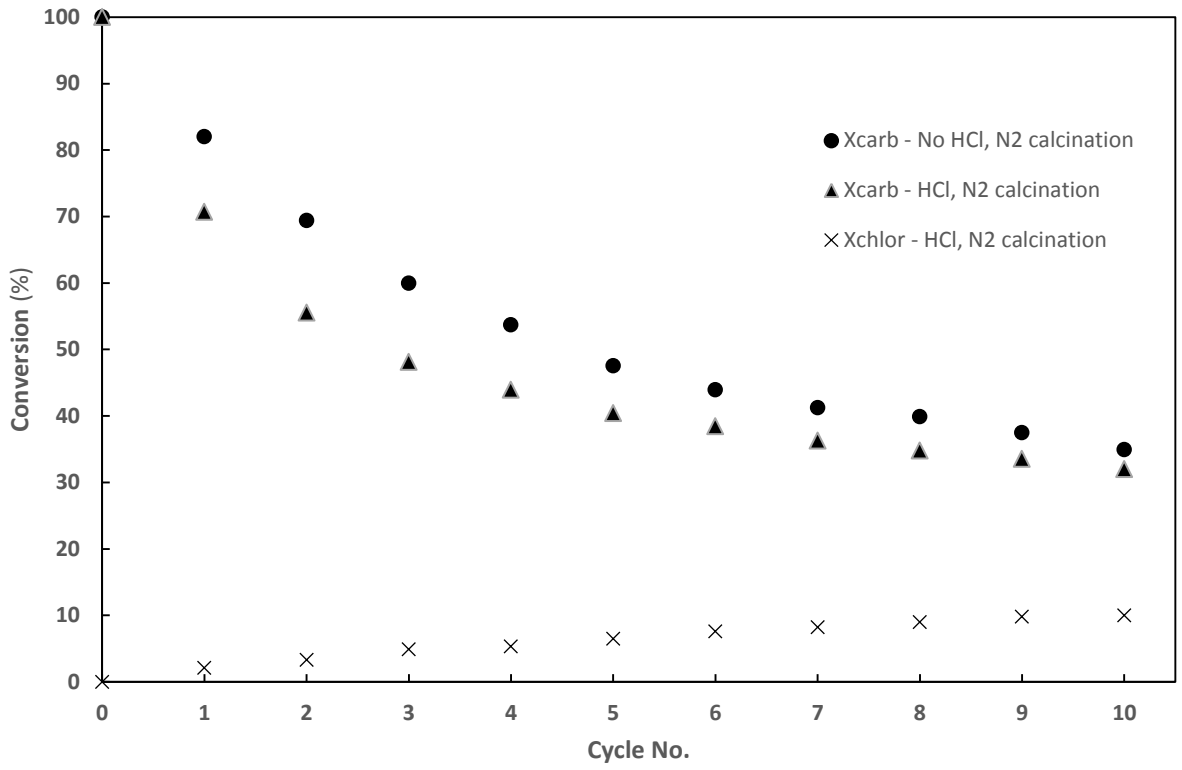

Figure 3.4.1: TGA carbonation and chlorination conversions over repeated calcination / carbonation cycles with and without the presence of HCl – Carbonation at 650°C (0 and 2000 ppm HCl, 15% CO_2, balance N_2) and calcination at 870°C (100% N_2).

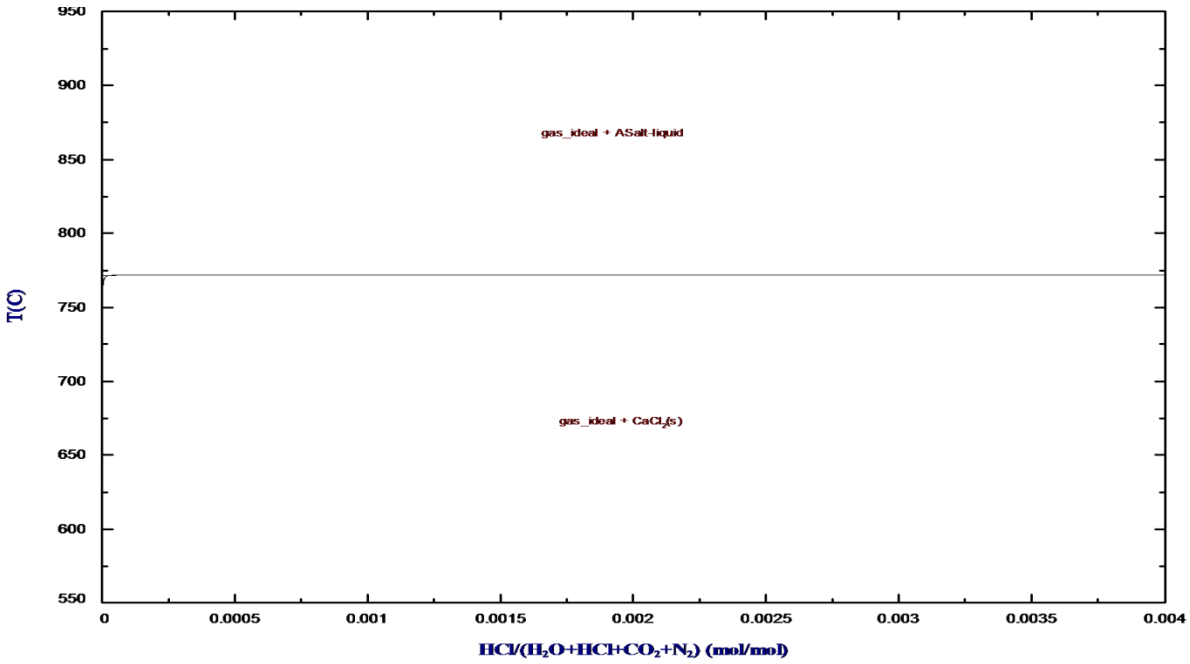

Figure 3.4.2: Thermodynamic phase diagram for the CaO-CaCl2 system – 1 atmosphere, CO_2=0 to 80 mol%, N_2 balance.

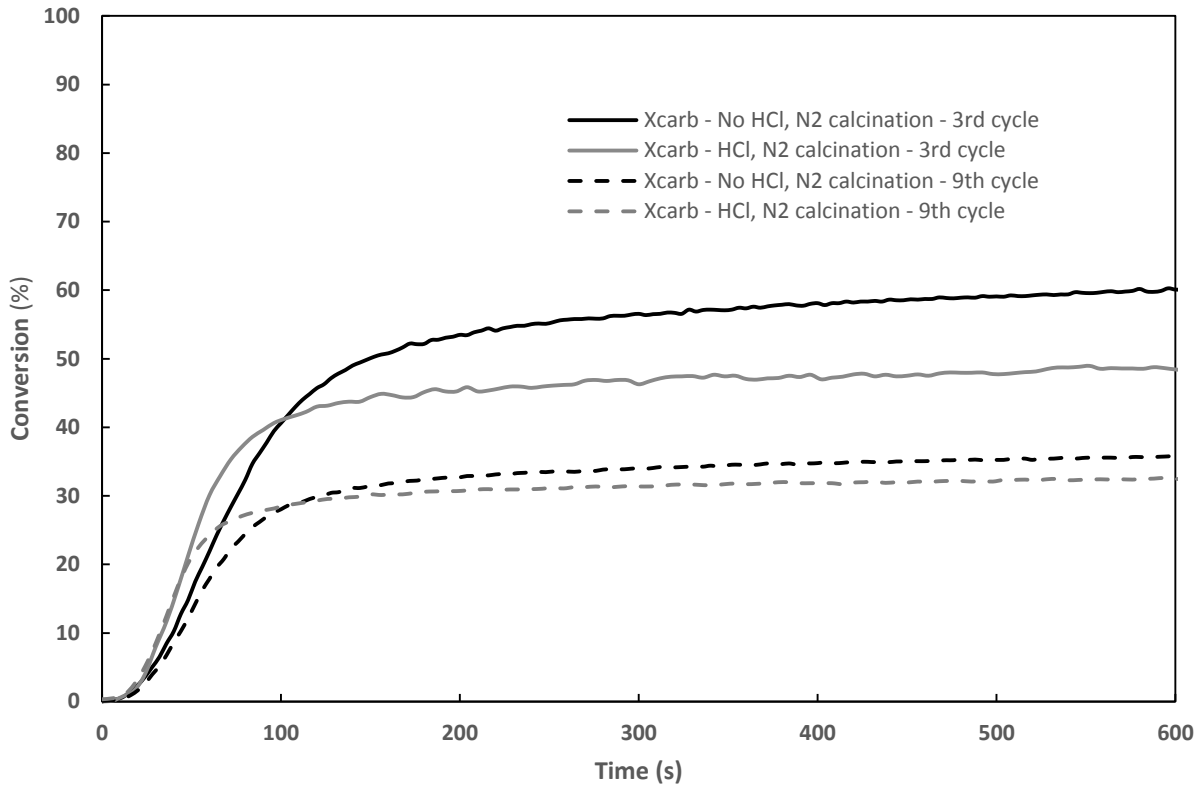

Figure 3.4.3: TGA carbonation conversion vs. time for 3rd and 9th carbonation cycle with and without the presence of HCl – Carbonation at 650°C (0 and 2000 ppm HCl, 15% CO_2, balance N_2) and calcination at 870°C (100% N_2).

3.4.2 – Effect of HCl on CO_2 capture with the presence of steam during calcination

As shown above, the presence of HCl has a dramatic effect on the CO_2 carrying capacity of CaO based sorbents over the first 10 cycles. These results however only consider a calcination environment containing pure N_2, which would not be the case in a real system. The heat required to drive the endothermic calcination reaction would come from a carbonaceous source, meaning both CO_2 and steam would be present during calcination and should be considered when examining the impact of HCl on the calcium looping process. Figure 3.4.4 presents thermodynamic phase equilibrium analysis predictions covering a wide range of HCl concentrations for both (a) 15 mol% H_2O and (b) 30 mol% H_2O with 60 mol% CO_2 and balance N_2. These two steam concentrations represent both a dry and wet flue gas recycle common

during oxy-fuel calcination operation. In comparison to calcination under pure N_2, several key differences exist when steam is present. The first is that the transition from solid phase to liquid phase $CaCl_2$ drops from approximately 770^oC to 750^oC, which could have implications on the process if higher carbonation temperatures were employed. The second major difference, which can be considered the most significant, is that for HCl concentrations below 2000 ppm, no $CaCl_2$ phases are predicted to exist above approximately 830^oC. When the H_2O concentration is increased to 30 mol%, all phases predictions shift to the right; thus, higher HCl concentrations (>3500 ppm) are required to allow for the formation of $CaCl_2$. These results suggest that any $CaCl_2$ formed during the carbonation period, given enough time, would dechlorinate to CaO at typical calcination temperatures when steam is present.

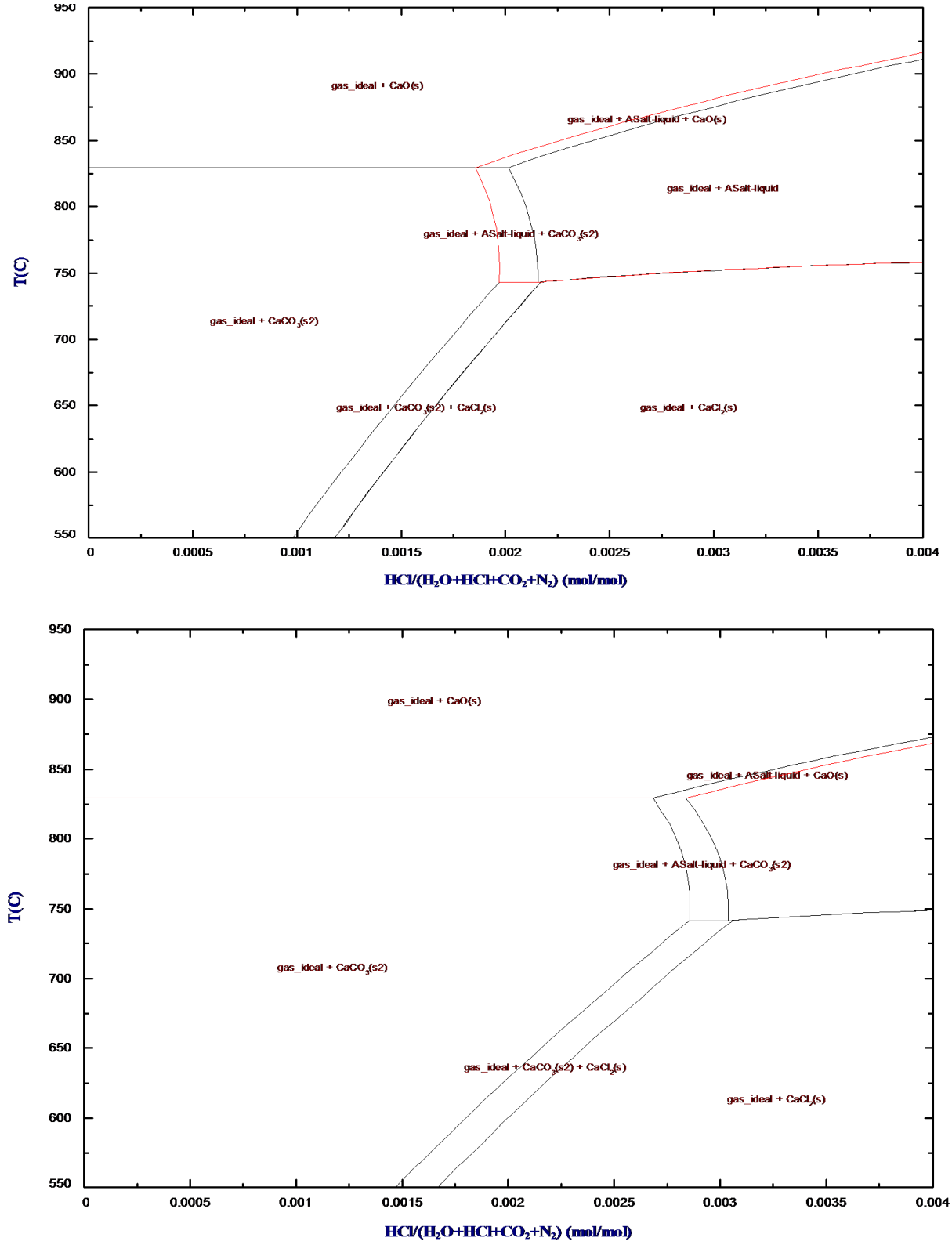

Figure 3.4.4: Thermodynamic phase diagram for the CaO-$CaCl_2$ system – (a) Top - 1 atmosphere, H_2O=15 mol%, CO_2=60 mol%, N_2 balance (b) Bottom - 1 atmosphere, H_2O=30 mol%, CO_2=60 mol%, N_2 balance.

A series of TGA tests were conducted to examine the effect of the presence of steam during calcination on the cyclic CO_2 carrying capacity of Cadomin limestone. Carbonation conversions over repeated cycles with and without HCl present during carbonation (with steam during calcination) are depicted in Figure 3.4.5. In contrast to the results shown in Figure 3.4.1, the presence of HCl not only did not show a negative effect on carbonation conversion, but it in fact showed a positive effect from the 4^{th} cycle onwards. The first point to consider when examining these results is the fact that no increase in mass was recorded after calcination from cycle to cycle. This supports the theory that any $CaCl_2$ formed during carbonation with HCl present is converted back to CaO during calcination, as predicted by thermodynamic phase equilibrium analysis (Figure 3.4.4). Therefore, chlorination conversions could not be determined for TGA tests under these conditions. Further analysis into chlorination conversions and potential residual $CaCl_2$ under these conditions will be discussed in the subsequent Section (3.4), where fixed bed testing was employed.

As expected, the carbonation conversions without the presence of HCl were lower than those where calcination was performed under a pure N_2 gaseous environment (Figure 3.4.1), as CO_2 is known to accelerate sintering of calcium based sorbents especially over the first few cycles (Barker, 1973) (Silaban & Harrison, 1995). This would explain why after the first cycle, the presence of HCl only drops the carbonation conversion by approximately 2.5 percentage points. After the first cycle, carbonation conversions begin to be at par or higher in the presence of HCl, which would suggest that dechlorination during calcination impacts the subsequent carbonation. One explanation for this phenomenon could be the difference in molar volumes between $CaCl_2$ and $CaCO_3$ which causes the formation of larger pores at the particle surface and decreases the CO_2 diffusional resistance during carbonation; a similar phenomenon observed

during CaO hydration to $Ca(OH)_2$ (Blamey, Lu, Fennell, & Anthony, 2011). Presented in Figure 3.4.6 is a comparison of the carbonation conversion versus time data for the 6th cycle with and without the presence of HCl and calcination under 15 mol% steam conditions. The 6th cycle was selected as this is the point where the carbonation conversion with and without HCl present start to significantly diverge. The initial fast kinetically controlled regime period is significantly reduced (~40%) when HCl is present, which is further confirmation that the formation of $CaCl_2$ limits the number of active CaO sites for reaction with CO_2 on the particle surface. In contrast, the diffusion controlled regime period is not only extended, but there is also a substantial increase in the rate of reaction. This result would suggest that morphological changes are occurring, which are likely related to the decomposition of $CaCl_2$ to CaO during calcination.

Identical carbonaceous fuel sources would most likely be used for the generation of the flue gas and for the suppling the required heat for calcination. Therefore, it was of interest to examine the effect of the presence of HCl during calcination on the CO_2 carrying capacity of the sorbent over repeated cycles. Under a calcination temperature of 870^{o}C, the presence of HCl during calcination has little to no effect on carbonation conversion over 10 cycles (Figure 3.4.7). Based on the phase equilibrium predictions in Figure 3.4.4, the formation of $CaCl_2$ is only possible at significantly higher HCl concentrations (>3500 ppm) or at lower H_2O concentrations, both of which were not explored in this work. Since HCl concentrations above 2000 ppm and H_2O concentrations below 15 mol% are never expected under any oxy-fuel combustion operating scenario, no further attention was given to the impact of HCl during calcination.

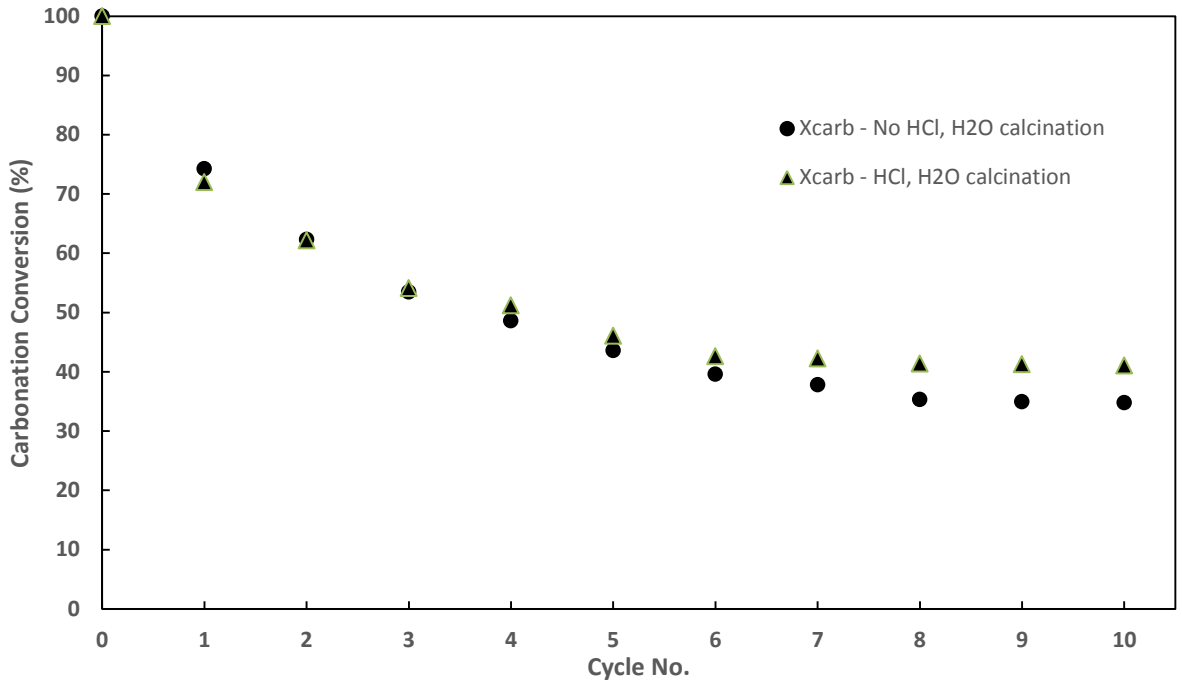

Figure 3.4.5: TGA carbonation conversions over repeated calcination / carbonation cycles with and without the presence of HCl – Carbonation at 650°C (0 and 2000 ppm HCl, 15% CO_2, balance N_2) and calcination at 870°C (60% CO_2, 15% H_2O, balance N_2).

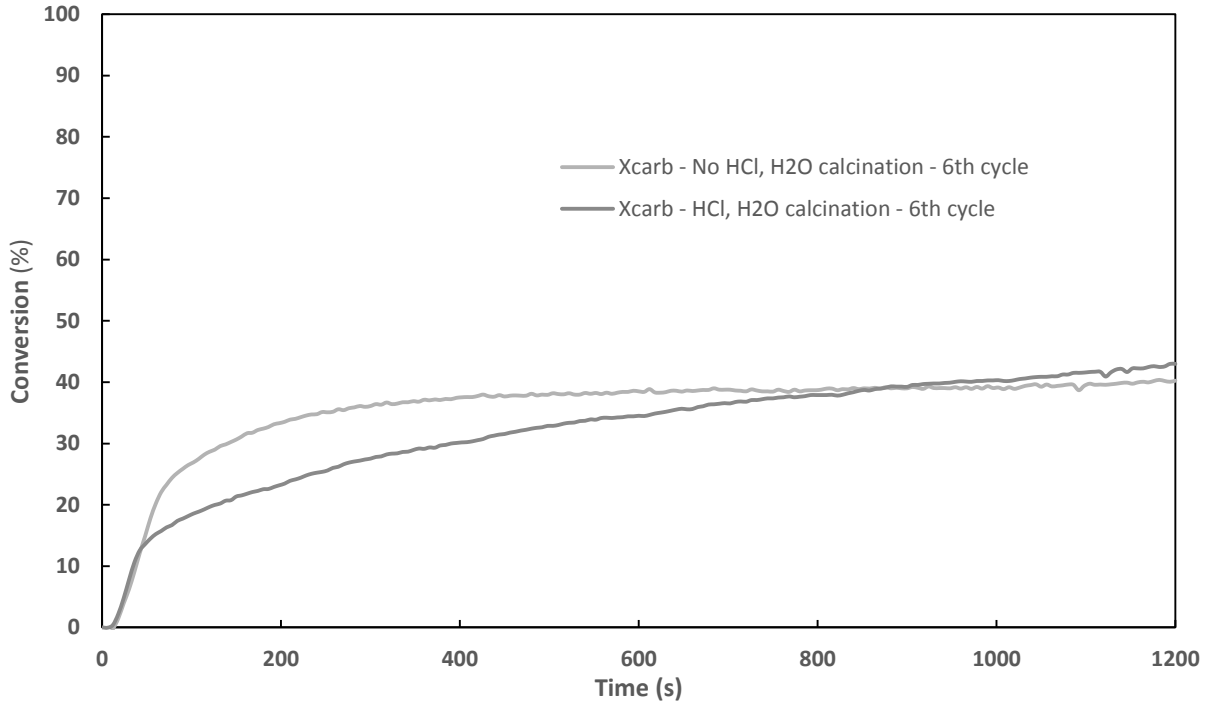

Figure 3.4.6: TGA carbonation conversion vs. time for 6th carbonation cycle with and without the presence of HCl – Carbonation at 650°C (0 and 2000 ppm HCl, 15% CO_2, balance N_2) and calcination at 870°C (60% CO_2, 15% H_2O, balance N_2).

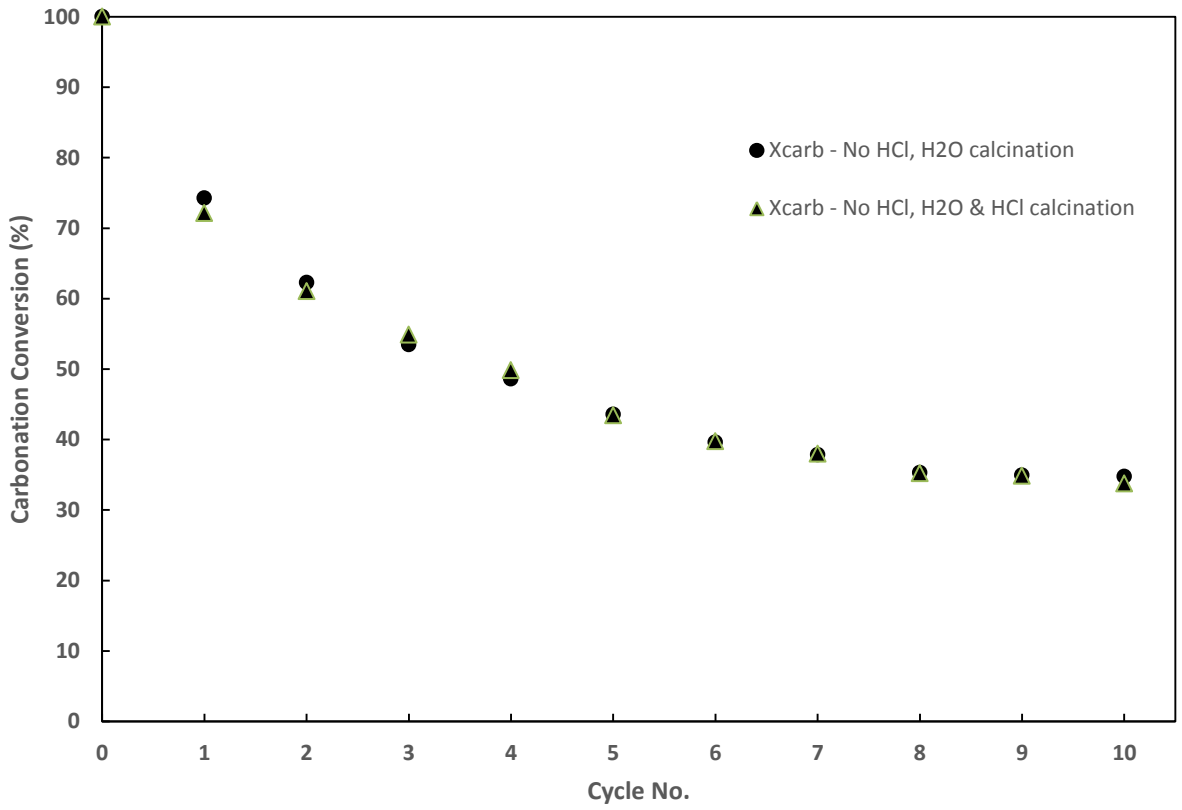

Figure 3.4.7: TGA carbonation conversions over repeated calcination / carbonation cycles with and without the presence of HCl during calcination – Carbonation at 650°C (15% CO_2, balance N_2) and calcination at 870°C (0 and 2000 ppm HCl, 60% CO_2, 15% H_2O, balance N_2).

3.4.3 – Effect of HCl on CO_2 capture with the presence of steam during carbonation

Steam addition during carbonation has been shown to improve sorbent performance, with the effect becoming more pronounced after multiple cycles (Symonds, Lu, Macchi, Hughes, & Anthony, 2009) (Manovic & Anthony, 2010) (Symonds, Lu, Hughes , Anthony, & Macchi, 2009). This phenomenon has been interpreted in several ways including: catalytic improvement of the capture process through hydration of CaO at the surface of the sorbent or enhancement of CO_2 mobility due to reduction in diffusion resistance (Champagne, Lu, Macchi, Symonds, & Anthony, 2012). Numerous more recent studies on the addition of steam during carbonation have also confirmed the previous results, while indicating that steam has little to no influence on the initial reaction rate, but enhances the diffusion controlled regime of carbonation (Dou, Song,

Liu, & Feng, 2010) (Arias, Abanades, Grasa, Manovic, & Anthony, 2012). Figure 3.4.8 depicts the carbonation conversions over 10 cycles with (15 mol% steam) and without steam present during carbonation. As expected, the conversions were substantially higher when steam was present, with the largest enhancements observed after the 5^{th} cycle and onwards (~10 percentage points difference after the 10^{th} cycle). Although not shown here, the initial fast, kinetically controlled regime was unchanged when steam was present.

Also shown in Figure 3.4.8 are the carbonation conversions over repeated cycles for a case where both steam and HCl were present during carbonation. Over all 10 cycles the measured conversions were higher than (1) without HCl and (2) just steam present. This result is in alignment with what was observed in Figure 3.4.5, where it was proposed that the increase in carbonation conversion was caused by the formation of larger pores at the particle surface during the decomposition of $CaCl_2$ to CaO during calcination. It should be noted that when no steam was present during carbonation the effect of HCl was larger than when steam was present. After 10 cycles, the presence of HCl showed a 6.3 and 2.7 percentage point increase in carbonation conversion with and without steam present, respectively. Plausible explanations for this decrease in relative improvement include: (1) the steam enhancement during the diffusion controlled regime significantly outweighs any improvement to the particle morphology during calcination and (2) $CaCl_2$ conversion is suppressed *via* the presence of steam during carbonation.

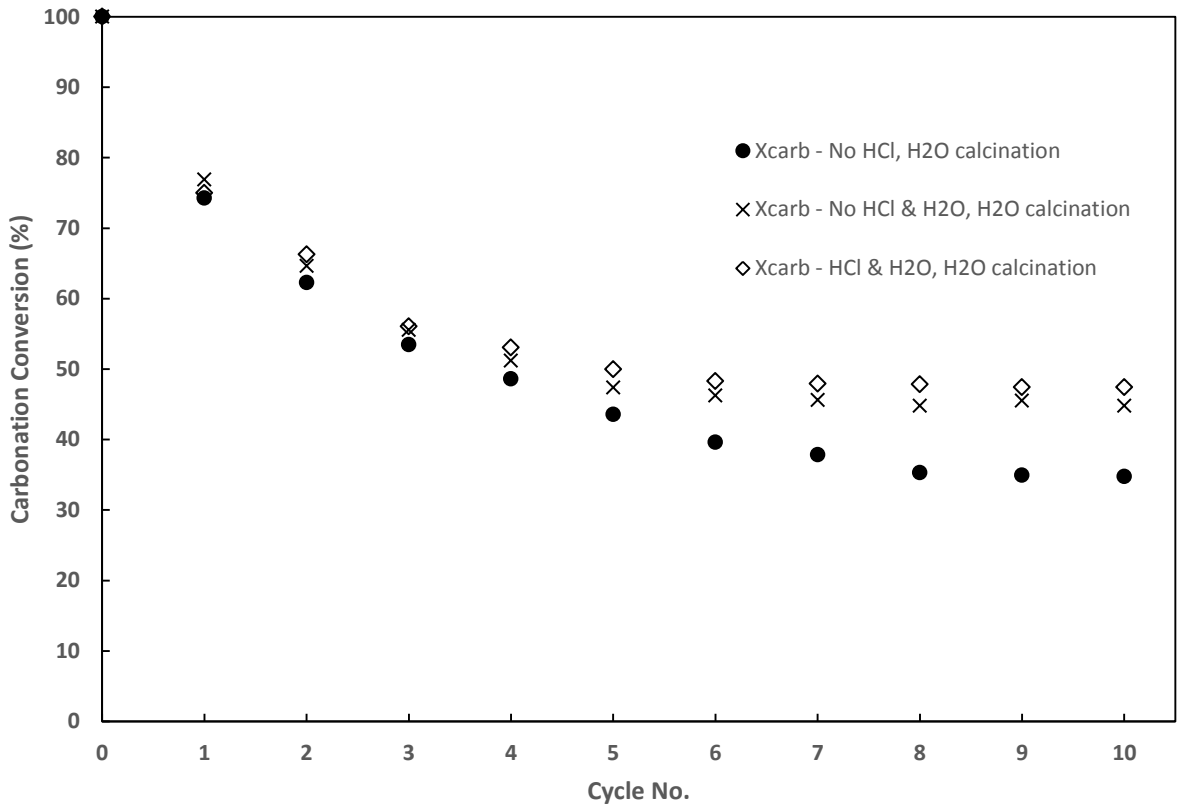

Figure 3.4.8: TGA carbonation conversions over repeated calcination / carbonation cycles with and without the presence of HCl and H_2O during carbonation – Carbonation at 650^oC (0 and 2000 ppm HCl, 0 and 15% H_2O, 15% CO_2, balance N_2) and calcination at 870^oC (60% CO_2, 15% H_2O, balance N_2).

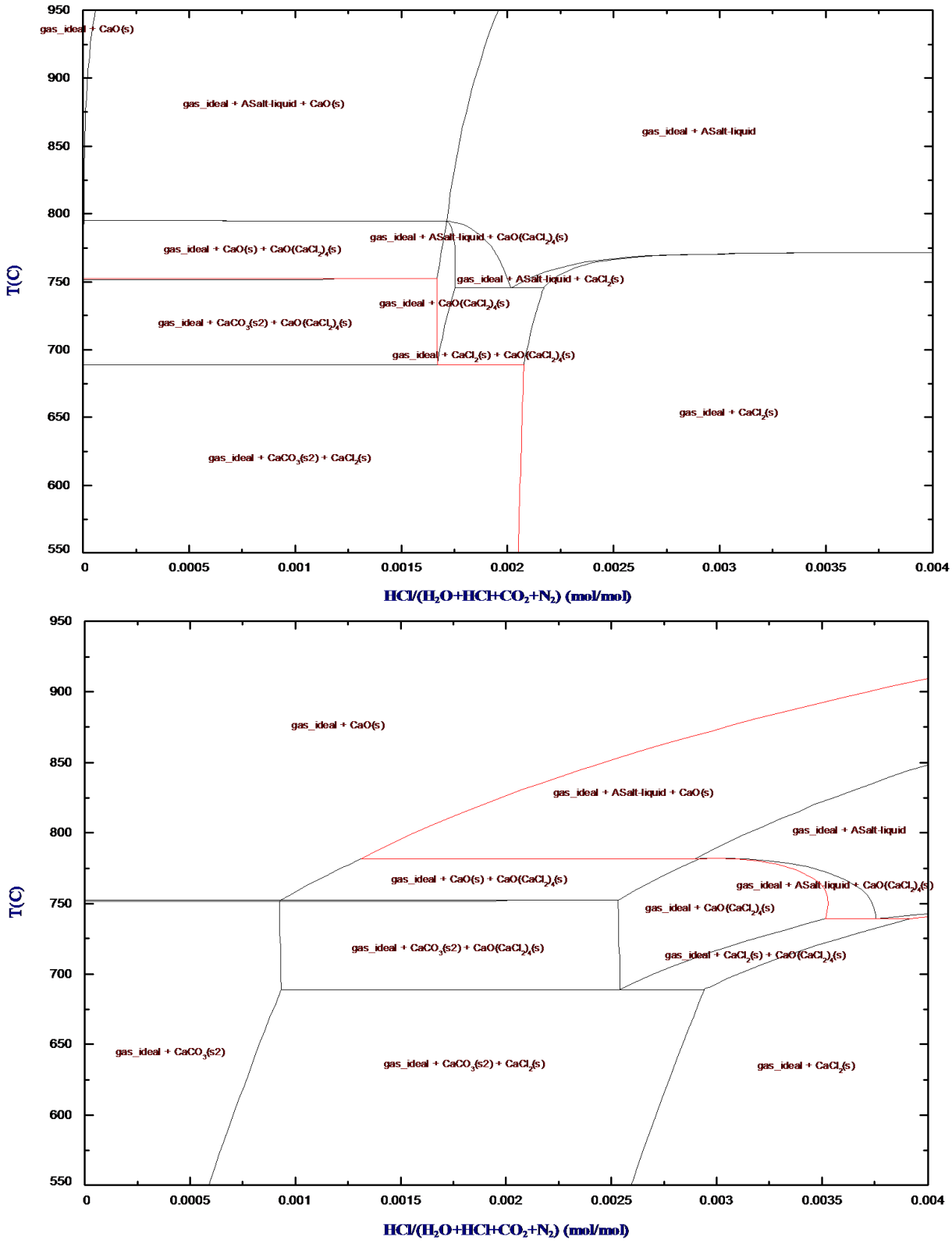

Figure 3.4.9: Thermodynamic phase diagram for the CaO-$CaCl_2$ system – (a) Top - 1 atmosphere, H_2O=0 mol%, CO_2=15 mol%, N_2 balance (b) Bottom - 1 atmosphere, H_2O=15 mol%, CO_2=15 mol%, N_2 balance.

Figure 3.4.9 presents thermodynamic phase equilibrium analysis predictions under typical carbonation conditions, covering a wide range of HCl concentrations for both (a) 0 mol% H_2O and (b) 15 mol% H_2O with 15 mol% CO_2 and balance N_2. From this figure, several key observations can be made. The first is that at carbonation temperatures below approximately 690^oC both $CaCO_3$ and $CaCl_2$ should be formed, but the creation of $CaO(CaCl_2)_4$ is possible at temperatures above 690^oC up to melting point of $CaCl_2$. Although temperatures above 690^oC were not explored in this work, it is believed that such higher carbonation temperatures should be avoided when HCl is present since the formation of $CaO(CaCl_2)_4$ would most likely limit the availability of CaO for CO_2 capture and could cause significant pore blockage. The second key observation is that the presence of steam significantly suppresses the formation of $CaCl_2$. When comparing Figure 3.4.9a to Figure 3.4.9b there is clear shift in the phase envelopes towards the right, and under low enough HCl concentrations (<600 ppm), it is possible to avoid any formation of $CaCl_2$. Increasing the steam concentration further would increase the minimum HCl concentration required for chlorination, although this might not be practical since (1) the presence of HCl has been shown to improve carbonation conversion with steam present during calcination and (2) adding additional steam to the carbonator would most likely reduce the overall process efficiency of the calcium looping process. Nevertheless, minimizing or eliminating HCl capture in the carbonator could be advantageous in cases where HCl removal from the concentrated CO_2 calciner flue gas is difficult or not cost-effective. This issue is especially important since the HCl concentrations in the calciner flue gas would be significantly higher now due to dechlorination, which could lead to corrosion and equipment failure (Hjornhede, Sotkovszki, & Nylund, 2006). In some circumstances, HCl could become the dominant species controlling acid dew point similar to SO_2/SO_3 in most typical combustion

systems. For the HCl concentration utilized in this work (2000 ppm), the formation of $CaCl_2$ is still expected even with the presence of 15 mol% H_2O, as can be seen in Figure 3.4.9b. However, the rate of chlorination should be reduced since the difference between the HCl concentration in the bulk gas and the equilibrium has been decreased. Since all carbonation cycles shown in Figure 3.4.8 were performed at 650°C with 15 mol% CO_2 in the reaction gas, it is expected that there would be a reduction in $CaCl_2$ formation in comparison to without the presence of steam. The lower level of chlorination could explain why a smaller relative improvement in carbonation conversion was measured when steam was present.

3.4.4 – Fixed bed testing and microstructure analysis

A series of fixed bed tests were performed to further explore the effect of HCl on CO_2 capture and to allow for microstructure analysis *via* SEM/EDX and BET/BJH. Figure 3.4.10 shows the carbonation conversions over 6 cycles both with and without HCl and steam present during carbonation at 650°C with 15 mol% CO_2. In each case, calcination was performed at 870°C under a 60 mol% CO_2, 15 mol% H_2O with balance N_2 environment. Like the TGA tests discussed earlier (Figure 3.4.5 and Figure 3.4.8), the presence of HCl improves the carbonation conversion over repeated cycles. The average increase in carbonation conversion over 6 cycles without steam present was only ~1.2 percentage points, which would indicate that the effect of HCl is limited in comparison to the TGA tests. A plausible explanation for the difference between TGA and fixed bed reactor tests could be related to the level of chlorination of the sorbent sample. Based on the results presented in Figure 3.4.1, where the chlorination conversion could be measured, a single cycle chlorination conversion is in the 1 to 2% range under the conditions utilized in this work. The maximum chlorination conversion measured for any fixed bed reactor test was approximately 0.32% for a single cycle. During calcination, this

would limit the formation of larger pores at the particle surface, decreasing the enhancement to CO_2 diffusion during carbonation in comparison to cases where a higher level of $CaCl_2$ formation had occurred. A similar result can also be seen in Figure 3.4.10 for the case where steam is present during carbonation. The addition of steam improves the carbonation conversion, but the presence of HCl only results in a 0.33 percentage point increase in the average carbonation conversion over 6 cycles. It was expected that steam suppression of the chlorination reaction would have caused the limited improvement in carbonation conversion, but as was the case for all fixed bed reactor tests, the chlorination conversion and HCl capture values were nearly identical. For each carbonation cycle the chlorination conversions ranged between 0.30 and 0.32% and the HCl capture was greater than 99%. The high capture efficiencies were due the large excess of sorbent in relation to the total flowrate of HCl sent to the fixed bed reactor. Under these conditions, it is possible that the steam enhancement during the diffusion controlled regime significantly outweighs any improvement to the particle morphology during calcination *via* decomposition of $CaCl_2$ to CaO. It should be noted that, regardless of carbonation condition during fixed bed reactor testing (both with and without HCl and steam), the initial carbonation conversions were significantly lower than during TGA testing and essentially remained constant over all 6 cycles. This phenomenon is in alignment with previous studies which showed that, under more severe calcination conditions (higher local CO_2 concentrations and higher heating rates) seen during fixed bed and pilot-plant testing, carbonation conversions do not decay gradually over several cycles (Grasa & Abanades, 2006), but instead drop immediately (1^{st} cycle) and remain relatively constant over repeated cycles (Champagne, Lu, Symonds, Macchi, & Anthony, 2016) (Symonds, Champagne, Firas, & Lu, 2016).

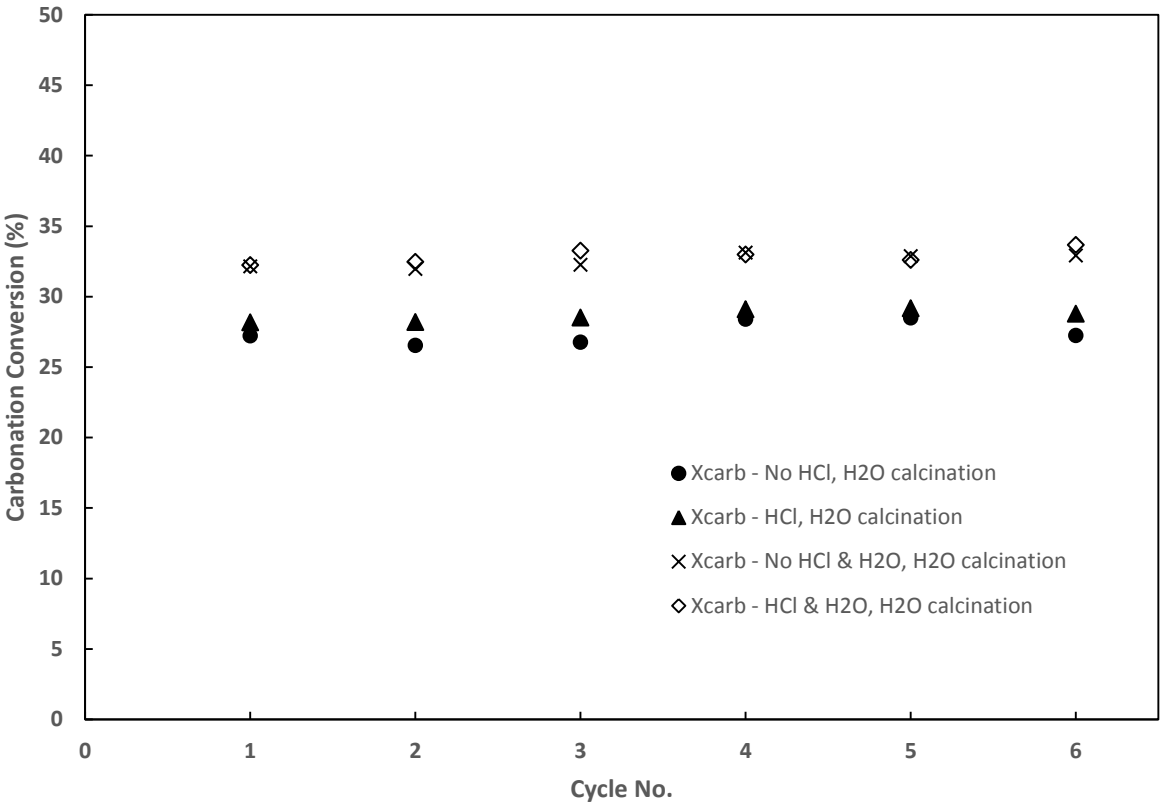

Figure 3.4.10: Fixed bed reactor carbonation conversions over repeated calcination / carbonation cycles with and without the presence of HCl and H_2O during carbonation – Carbonation at 650°C (0 and 2000 ppm HCl, 0 and 15% H_2O, 15% CO_2, balance N_2) and calcination at 870°C (60% CO_2, 15% H_2O, balance N_2).

Figure 3.4.11(a) and (b) present SEM images of the calcined sorbent after 6 carbonation / calcination cycles without and with the presence of HCl during carbonation, respectively. Without the presence of HCl, it was observed that there are a lot of smooth, compact, and non-porous zones on the surface of the particle. In comparison, the particle surface with the presence of HCl showed larger cracks / voids and significantly more porosity on the particle grain surfaces. This result would suggest that the particles that are exposed to HCl during carbonation should have higher surface area and pore volumes, which has been correlated to higher carbonation conversions (Sun, Lim, & Grace, 2008). To further investigate, particle surface area and pore volume measurements were made *via* BET and BJH analyses and are presented Table 3.4.1. Particles carbonated with HCl present showed higher surface area and pore volume after 6

carbonation / calcination cycles which support the results observed in Figure 3.4.11 and is in alignment with the hypothesis that the decomposition of $CaCl_2$ to CaO during calcination improves the particle morphology in terms of CO_2 capture potential. Only ~11.6% and ~28.4% increases in surface area and pore volume, respectively, were measured with the addition of HCl when steam was present. In contrast, the surface area and pore volume where roughly 39% higher (for both) in the absence of steam when HCl was added during carbonation. Interestingly, this observed increase in surface area and pore volume did not result in a significant increase in carbonation conversion (Figure 3.4.10). Similar to the results shown in Figure 3.4.6, the increase in carbonation conversion when HCl is present is only expected to be substantial during the diffusion control regime. Therefore, it is likely that higher carbonation conversion would have been achieved with HCl present if the carbonation period was extended further into this regime. It is uncertain why the surface area and pore volume increase was lower during carbonation with steam, but could be related to the higher carbonation conversion observed during the diffusion controlled regime when steam is present (Champagne, Lu, Macchi, Symonds, & Anthony, 2012). In any case, it can be concluded that, under more realistic operating conditions experienced during fixed bed reactor testing, the presence of HCl has little or no effect on the carbonation conversion over repeated cycles when the flue gas contains steam. This result is significant since (1) this would be the case in any commercial-scale calcium looping facility and (2) high HCl capture efficiencies can still be achieved, reducing up or down stream gas clean-up of the post-combustion flue gas.

Both TGA and thermodynamic phase diagram analyses showed that given enough time at appropriate calcination conditions (high temperature and steam present), any $CaCl_2$ formed during the carbonation period should decompose. Therefore, it was of interest to determine if

any residual $CaCl_2$ remained after calcination for fixed bed reactor tests performed with the presence HCl during carbonation. Since it was anticipated that the majority of $CaCl_2$ formed during the carbonation period would be on the surface of the particle under these conditions, EDX analysis was performed on the surface of several particles after the final calcination. In all cases, no Cl was detected on the surface of any particle. This confirms that (1) the concentration of steam (15 mol%) is suitable for the full decomposition of $CaCl_2$, which is in alignment with FactSage phase predictions, and (2) the decomposition of $CaCl_2$ is fast enough to be completed within the $CaCO_3$ calcination time frame. This is important since calcination times are significantly shorter (~1-minute time scale) in circulating fluidized beds (CFB) systems utilized in commercial-scale operation. Any residual $CaCl_2$ not decomposed during the calcination period could severely reduce the sorbent CO_2 carrying capacity over repeated cycles as shown in this work and by Wang et al. (2014).

Table 3.4.1: Surface area and pore volume of calcined sorbent particles after 6 fixed bed reactor cycles (down to 2nm).

Run No.	Carbonation Condition	BET Surface Area (m^2/g)	BJH Pore Volume (cm^3/g)
-	Starting material	10.42	0.01580
1	No HCl, no steam	3.21	0.00447
2	HCl, no steam	4.47	0.00625
3	No HCl, steam	3.51	0.00504
4	HCl, steam	3.92	0.00647

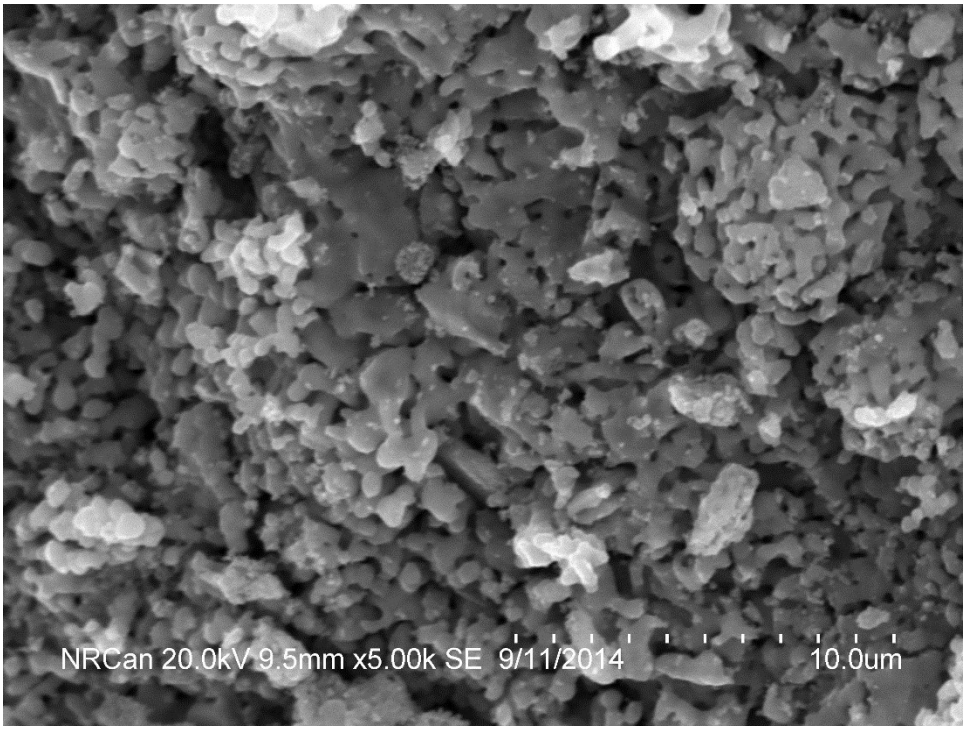

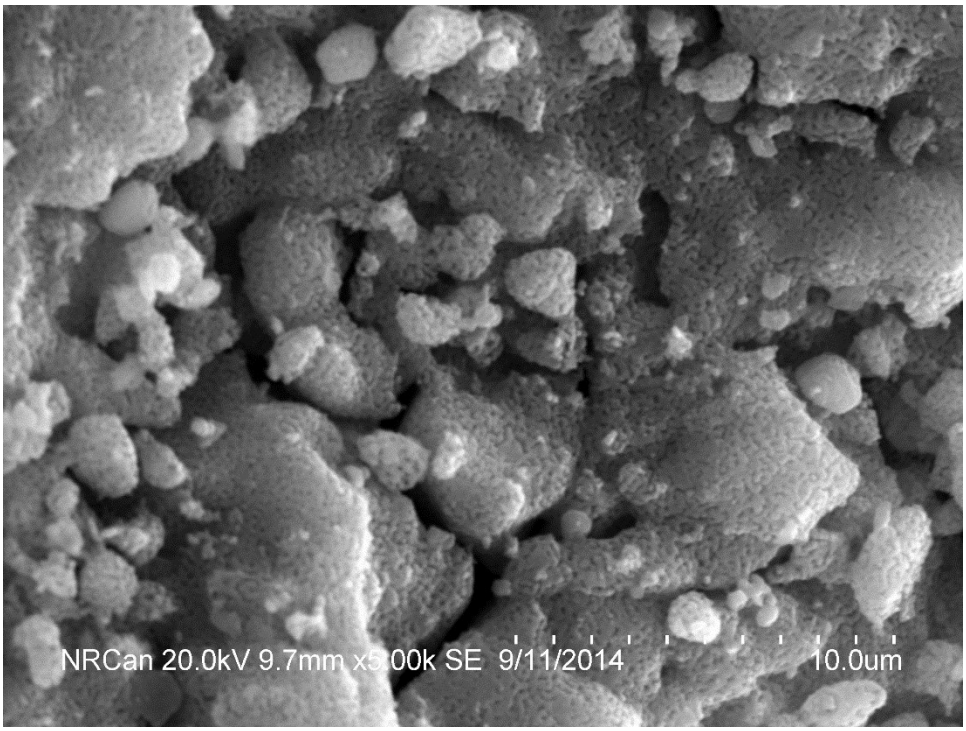

Figure 3.4.11: SEM images of calcined sorbent (Cadomin) particles after 6 fixed bed reactor cycles – (a) Top - carbonation at 650^{o}C (0 ppm HCl, 0 and 15% H_2O, 15% CO_2, balance N_2) (b) Bottom - carbonation at 650^{o}C (2000 ppm HCl, 0 and 15% H_2O, 15% CO_2, balance N_2) both calcinations at 870^{o}C (60% CO_2, 15% H_2O, balance N_2).

3.5 – Conclusions

The effects of HCl injection during carbonation and calcination on the CO_2 carrying capacity of Cadomin limestone (250 to 425μm) have been studied *via* thermogravimetric analysis and fixed bed reactor testing. Preliminary testing under a pure N_2 calcination environment at 870°C showed that the presence of HCl during carbonation led to the irreversible formation of $CaCl_2$, which was supported by phase equilibria analysis. This resulted in lower carbonation conversions over repeated cycles due to a significant quantity of the active portion of the particle surface becoming covered in a layer of $CaCl_2$, increasing the diffusional resistance. After ten calcination / carbonation cycles the carbonation conversion dropped by ~ 3 percentage points in comparison to without HCl present and is expected to continue to decrease as the number of cycles is increased.

The addition of steam during calcination provided very different results than those under pure N_2. The carbonation conversions over repeated cycles were higher with the presence of HCl, which was attributed to the decomposition of $CaCl_2$ to CaO during calcination, supported by phase equilibria analyses. It was hypothesized that the difference in molar volumes between $CaCl_2$ and $CaCO_3$ causes the formation of larger pores at the particle surface during calcination, decreasing the CO_2 diffusional resistance during carbonation. As expected, the addition of steam during carbonation increased the carbonation conversion over repeated cycles. The improvement to carbonation conversion caused by HCl addition was limited when steam was present as sorbent chlorination was suppressed.

Fixed bed test results confirmed that full decomposition of $CaCl_2$ to CaO could be expected under typical oxy-fuel calcination conditions. Additionally, the presence of HCl during carbonation increased both the surface area and pore volume of the sorbent after 6 carbonation /

calcination cycles, which further reinforces the hypothesis that dechlorination during calcination results in a particle structure that increases carbonation reactivity. Fixed bed testing also showed that greater than 99% HCl capture could be achieved without adversely affecting sorbent CO_2 capture performance when steam is present during both carbonation and calcination. Unfortunately, due to $CaCl_2$ decomposition during calcination, HCl concentrations in the concentrated CO_2 product stream could be relatively high. This could lead to potential corrosion and equipment failure issues if not appropriately addressed.

3.6 – Nomenclature

C_{CO_2} outlet concentration of CO_2, vol%

C_{HCl} outlet concentration of HCl, vol%

$F_{CO_2,0}$ inlet flowrate of CO_2, m^3/min

$F_{HCl,0}$ inlet flowrate of HCl, m^3/min

F_{Outlet} total outlet flowrate, m^3/min

m_0 initial sample mass, g

m_{calc} mass of sample after calcination, g

m_{carb} mass of sample after carbonation, g

M_{CaCl_2} molar mass of $CaCl_2$, g/g.mol

M_{CaO} molar mass of CaO, g/g.mol

M_{CO_2} molar mass of CO_2, g/g.mol

M_{HCl} molar mass of HCl, g/g.mol

N cycle number, dimensionless

P_{carb} carbonation period, min

$P_{CO_2,eq}$ equilibrium partial pressure of CO_2, Pa

T temperature, K

$X_{carb,N}$ carbonation conversion at cycle N, %

Greek letters

β initial sample CaO content, dimensionless

ρ_{CO_2} density of CO_2, kg/m^3

ρ_{HCl} density of HCl, kg/m^3

3.7 – References

Abanades, J. C., Grasa, G. S., Alonso, M., Rodriguez, N., Anthony, E. J., & Romeo, L. M. (2007). Cost structure of a postcombustion CO2 capture system using CaO. *Environmental Science & Technology*, 41, 5523-5527.

Abanades, J. C., Rubin, E. S., & Anthony, E. J. (2004). Sorbent costs and performance in CO2 capture systems. *Industrial & Engineering Chemistry Research*, 43, 3462-3466.

Abu-Zahra, M. R., Schneiders, L. H., Niederer, J. P., Feron, P. H., & Versteeg, G. F. (2007). CO2 capture from power plants: part I. A parametric study of the technical performance based on monoethanolamine. *International Journal of Greenhouse Gas Control*, 1(1), 37-46.

Al-Jeboori, M. J., Nguyen, M., Dean, C., & Fennell, P. S. (2013). Improvement of limestone-based CO2 sorbents for Ca looping by HBr and other mineral acids. *Industrial & Engineering Chemistry Research*, 52, 1426-1433.

Arias, B., Abanades, J. C., Grasa, G. S., Manovic, V., & Anthony, E. J. (2012). Effect of steam on the fast carbonation reaction rates of CaO. *Ind. Eng. Chem. Res.*, 51(5), 2478-2482.

Arias, B., Cordero, J. M., Alonso, M., & Abanades, J. C. (2012). Sulfation rates of cycled CaP particles in the carbonator of a Ca-looping cycle for postcombustion CO2 capture. *American Institute of Chemical Engineers*, 58, 2262-2269.

Arias, B., Grasa, G. S., & Abanades, J. C. (2010). Effect of sorbent hydration on the average activity of CaO in a Ca-looping system. *Chemical Engineering Journal*, 163, 324-330.

Arias, B., Grasa, G. S., Alonso, M., & Abanades, J. C. (2012). Post-combustion calcium looping process with a highly stable sorbent activity by recarbonation. *Energy & Environmental Science*, 5, 7353-7359.

Bale, C. W., Pelton, A. D., Thompson, W. T., Eriksson, G., Hack, K., & Chartrand, P. (2014). *FactSage 6.4*. Retrieved from http://www.factsage.com

Ball, R. (2014). Entropy generation analyses of Endex and conventional calcium looping processes for CO2 capture. *Fuel*, 127, 202-211.

Barker, R. (1973). The reversibility of the reaction CaCO3 = CaO + CO2. *J. Appl. Chem. Biotechnol*, 23, 733.

Bie, R., Li, S., & Yang, L. (2005). Reaction mechanism of CaO with HCl in incineration of wastewater in fluidized bed. *Chemical Engineering Science*, 60, 609-16.

Blamey, J., Anthony, E. J., Wang, J., & Fennell, P. (2010). The calcium looping cycle for large-scale CO2 capture. *Progress in Energy and Combustion Science*, 36, 260-279.

Blamey, J., Lu, D. Y., Fennell, P. S., & Anthony, E. J. (2011). Reactivation of CaO-Based Sorbents for CO2 Capture: Mechnism for the Carbonation of Ca(OH)2. *Industrial & Engineering Chemistry Research*, 50, 10329-10334.

Boot-Handford, M. E., Abanades, J. C., Anthony, E. J., Blunt, M. J., Brandani, S., MacDowell, N., . . . Fennell, P. S. (2014). Carbon capture and storage update. *Energy and Environmental Science*.

Borgwardt, R. H. (1970). Kinetics of the reaction of SO2 eith calcined limestone. *Environmental Science & Technology*, 4, 59-63.

Champagne, S., Lu, D. Y., Macchi, A., Symonds, R. T., & Anthony, E. J. (2012). Influence of steam injection during calcination on the reactivity of CaO-based sorbent for carbon capture. *Ind. Eng. Chem. Res.*, 52, 2241-2246.

Champagne, S., Lu, D. Y., Symonds, R. T., Macchi, A., & Anthony, E. J. (2016). The effect of steam addition to the calciner in a calcium looping pilot plant. *Powder Technology*, 290, 114-123.

Chen, H. C., Zhao, C. S., Yang , Y. M., & Zhang, P. P. (2012). CO2 capture and attrition performance of CaO pellets with aluminate cement under pressuirized carbonation. *Applied Energy*, 91, 334-40.

Chin, T., Yan, R., & Liang, D. T. (2005). Study of the reaction of lime with HCl under simulated flue gas conditions using X-ray diffraction characterization and thermodynamic predictions. *Industrial & Engineering Chemistry Research*, 44, 8730-8738.

Chrissafis, K. (2007). Multicyclic study on the carbonation of CaO using different limestones. *J Therm Anal Calorim*, 89, 525-529.

Chyang, C. S., Han, Y. L., & Zhong, Z. C. (2009). Study of HCl absorption by CaO at high temperature. *Energy & Fuels*, 23, 3948-3953.

Davidson, J. F., Clift, R., & Harrision, D. (1985). *Fluidization, 2nd ed.* New York: Academic Press.

Dean, C. C., Blamey, J., Florin, N. H., Al-Jeboori, M. J., & Fennell, P. S. (2011). The calcium looping cycle for CO2 capture form power generation, cement manufacture and hydrogen production. *Chemical Engineering Research and Design*, 89, 836-855.

Dean, C. C., Dugwell, D., & Fennell, P. S. (2011). Investigations into potential synergy between power generation, cement manufacture and CO2 abatement using the calcium looping cycle. *Energy & Environmental Science*, 4, 2050-2053.

Dou, B. L., Song, Y. C., Liu, Y. G., & Feng, C. (2010). High temperature CO2 capture using calcium oxide sorbent in a fixed-bed reactor. *J. Hazard. Mater.*, 183 (1-3), 759-765.

Duo, W., Kirkby, N. F., Seville, J. P., Kiel, J. H., Bos, A., & Den Uil, H. (1996). Kinetics of HCl reactions with calcium and sodium sorbents for IGCC fuel gas cleaning. *Chemical Engineering Science*, 51, 2541-2546.

Elwell, L. C., & Grant, E. S. (2006). Technology options for capturing CO2 - Special reports. *Power*, 150(8).

Fauth, D., Frommell, E. A., Hoffman, J. S., Reasbeck, R. P., & Pennline, H. W. (2005). Eutectic salt promoted lithium zirconate: Novel high temperature sorbent for CO2 capture. *Fuel Process. Technol.*, 86, 1503-1521.

Fennell, P. S., Davidson, J. F., Dennis, J. S., & Hayhurst, A. N. (2007). Regeneration of sintered limestone sorbents for the sequestration of CO2 from combustion and other systems. *Journal of the Energy Institute*, 80, 116-119.

Fennell, P., & Anthony, B. (2015). *Calcium and Chemical Looping Technology for Power Generation and Carbon Dioxide(CO2) Capture.* Cambridge, UK: Elsevier.

Freidina, E. B., & Fray, D. J. (2000). Phase diagram of the system CaCl2-CaCO3. *THermochim Acta*, 351, 107-108.

Garcia-Lablano, F., Abad, A., de Diego, L. F., Gayan, P., & Adanez, J. (2002). Calcination of calcium-based sorbents at pressure in a broad range of CO2 concentrations. *Chemical Engineering Science*, 57, 2381-2393.

Goto, K., Yogo, K., & Higashii, T. (2013). A review of efficiency penalty in a coal-fired power plant with post-combustion CO2 capture. *Applied Energy*, 111, 710-720.

Grasa, G. S., & Abanades, J. C. (2006). CO2 capture capacity of CaO in long series of carbonation/calcination cycles. *Industrial and Engineering Chemistry Research*, 45, 8846-8851.

Grasa, G. S., Abanades, J. C., Alonso, M., & Gonzalez, B. (2008). Reactivity of highly cycled particles of CaO in a carbonation/calcination loop. *Chemical Engineering Journal*, 137, 561-567.

Hack, H., Alvarez, I., Diego, R., Lupion, M., Cortes, V., Hotta, A., . . . Alvarez, J. (2012). Initial operation of the CIUDEN oxy-CFB boiler demonstration project. *The 11th Annual Carbon Capture, Utilization & Sequestration Conference.* Pittsburgh, USA.

Hjornhede, A., Sotkovszki, P., & Nylund, A. (2006). Erosion-corrosion of laser and thermally depsosited coatings exposed in fluidized bed combustion plants. *Materials and Corrosion*, 57 (4), 307-322.

Hughes, R. W., Lu, D., Anthony, E. J., & Wu, Y. (2004). Improved long-tern conversion of limestone-derived sorbents for in situ capture of CO2 in a fluidized bed combustor. *Industrial & Engineering Chemistry Research*, 43, 5529-5539.

IEA. (2010). *Energy technology perspectives 2010: Scenarios and strategies to 2050.* Paris: IEA.

IEA. (2014). *Energy technology perspectives 2014 factsheet - 'Electricty storage as a game changer'.* IEA.

Kierzkowska, A. M., Pacciani, R., & Muller, C. R. (2013). CaO-based CO2 sorbents: from fundamentals to the development of new, highly effective materials. *Chemistry & Sustainability, Energy & Materials*, 6(7), 1130-1148.

Lara, Y., Lisbona, P., Martinez, A., & Romeo, L. M. (2013). Design and analysis of heat exchanger networks for integrated Ca-looping systems. *Applied Energy*, 111, 690-700.

Lawrence, A. D., & Bu, J. (2000). The reactions between Ca-based solids and gases representative of those found in a fluidized-bed incinerator. *Chemical Engineering Science*, 55, 6129-6137.

Lowell, S., Thomas, M. A., & Thommes, M. (2004). *Characterization of porous solids and powders: surface area, pore size, and density.* The Netherlands: Kluwer Academic Publishers.

Lysikov, A. I., Salanov, A. N., & Okunev, A. G. (2007). Change of CO2 carrying capacity of CaO in isothermal recarbonation-decompostion cycles. *Industrial and Engineering Chemistry Research*, 46, 4633-4638.

MacKenzie, A., Granatstein, D. L., Anthony, E. J., & Abanades, J. C. (2007). Economics of CO2 capture using the calcium cycle with a pressurized fluidized bed combustor. *Energy & Fules*, 21, 920-926.

Manovic, V., & Anthony, E. J. (2007). Steam reactivation of spent CaO-based sorbent from multiple CO2 capture cycles. *Environmental Science & Technology*, 41, 1420-1425.

Manovic, V., & Anthony, E. J. (2008). Parametric study on the CO2 capture capacity of CaO-based sorbents in looping cycles. *Energy & Fuels*, 22, 1851-1857.

Manovic, V., & Anthony, E. J. (2008). Thermal activation of CaO-based sorbent and self-reactivation during CO2 capture looping cycles. *Environmental Science & Technology*, 42, 4170-4174.

Manovic, V., & Anthony, E. J. (2010). Carbonation of CaO-Based Sorbents Enhanced by Steam Addition . *INd. Eng. Chem. Res.*, 49, 9105-9110.

Martinez, A., Lara, Y., Lisbona, P., & Romeo, L. M. (2012). Energy penalty reduction in the calcium looping cycle. *International Journal of Greehouse Gas Control*, 7, 74-81.

Pachauri, R. K., & Reisinger, A. (2007). Climate Change 2007: Synthesis Report. Contribution of Working Groups I, II and III to the Fourth Assessment Report of the Intergovernmental Panel on Climate Change. *Intergovernmental Panel on Climate Change (IPCC)*. Geneva, Switzerland.

Partanen, J., Backman, P., Backman, R., & Hupa, M. (2003). Formation of calcium chloride and its interaction with the sand particles during fluidised bed combustion. *17th international conference on FBC.* Jacksonville, FL.

Partanen, J., Backman, P., Backman, R., & Hupa, M. (2005). Absorption of HCl by limestone in hot flue gases. Part III: simultaneous absorption with SO2. *Fuel*, 84, 1685-1694.

Pradyot, P. (2003). *Handbook of Inorganic Chemicals.* New York: The McGraw-Hill Companies Inc.

Resnik, K. P., Yeh, J. T., & Pennline, H. W. (2004). Aqua ammonia process for simultaneous removal of CO2, SO2, and NOx. *Inter. J. Environ. Technol. Management*, 4, 89-104.

Ridha, F. N., Lu, D. Y., Symonds, R. T., & Champagne, S. (2016). Attrition of CaO-based pellets in a 0.1MWth dual fluidized bed pilot plant for post-combustion CO2 capture. *Powder Technology*, 291, 60-65.

Rodriguez, N., Alonso, M., Grasa, G. S., & Abanades, J. C. (2008). Heat requirements in a calciner of CaCO3 integrated in a CO2 capture system using CaO. *Chemical Engineering Journal*, 138, 148-154.

Rodriguez, N., Murillo, R., & Abanades, J. C. (2012). CO2 capture from cement plants using oxyfired precalcination and/or calcium looping. *Environmental Science & Technology*, 46, 2460-2466.

Romeo, L. M., Catalina, D., Lisbona, P., Lara, Y., & Martinez, A. (2011). Reduction of greehouse gas emissions by integration of cement plants, power plants, and CO2 capture systems. *Greenhouse Gases: Science and Technology*, 1, 72-82.

Ryden, M., & Lyngfelt, A. (2006). Using steam reforming to porduce hydrogen with carbon dioxide capture by chemical-looping combustion. *International Journal of Hydrogen Energy*, 31, 1271-1283.

Sanchez-Biezma, A., Paniagua, J., DIaz, L., Lorenzo, M., Alvarez, J., Martinez, D., . . . Abanades, J. C. (2013). Testing postcombustion CO2 capture with CaO ub a 1.7 MWt pilot facility. *Energy Procedia*, 37, 1-8.

Shimizu, T., Hirama, T., Hosoda, H., Kitano, K., Inagaki, M., & Tejima, K. (1999). A twin fluid-bed reactor for removal of CO2 from combustion processes. *Chemical Engineering Research and Design*, 77(A1), 62-68.

Silaban, A., & Harrison, D. P. (1995). High-temperature capture of carbon dioxide: characteristics of the reversible reaction between CaO(s) and CO2(g). *Chem. Eng. Commun*, 137, 177.

Sun, P., Grace, J., Lim, C. J., & Anthony, E. J. (2006). Removal of CO2 by calcium-based sorbents in the presence of SO2. *Energy & Fuels*, 21, 163-170.

Sun, P., Lim, C. J., & Grace, J. R. (2008). Cyclic CO2 capture by limestone-derived sorbent during prolonged calcination/carbonation cycling. *AIChE J*, 54, 1668-1677.

Sun, Z., Yu, F. C., Li, F., Li, S., & Fan, L. S. (2011). Experimental study of HCl capture using CaO sorbents: activation, deactivation, reactivation, and ionic transfer mechanism. *Industrial & Engineering Chemsitry Research*, 50, 6034-6043.

Suraniti, S. L., Nsakala, N. Y., & Darling, S. L. (2009). Alsotn oxyfuel CFB boilers: A promising option for CO2 capture. *Energy Procedia*, 1, 543-548.

Symonds, R. T., Champagne, S., Firas, N., & Lu, D. (2016). CO2 capture performance of CaO-based pellets in a 0.1 MWth pilot-scale calcium looping system. *Powder Technology*, 124-131.

Symonds, R. T., Lu, D. Y., Hughes , R. W., Anthony, E. J., & Macchi, A. (2009). CO2 capture from simulated syngas via cyclic carbonation/calcination for a naturally occuring limestone: pilot-plant testing. *Ind. Eng. Chem. Res.*, 48, 8431-8440.

Symonds, R. T., Lu, D. Y., Macchi, A., Hughes, R. W., & Anthony, E. J. (2009). CO2 capture from syngas via cyclic carbonation/calcination for a naturally occurring limestone: Modelling and bench-scale testing. *Chemical Engineering Science*, 64, 3536-3543.

Tullin, C., & Ljungstrom, E. (1989). Reaction between calcium carbonate and sulphur dioxide. *Energy & Fuels*, 3, 284-287.

Valverde, J. M., Sanchez-Jimenez, P. E., & Perez-Maqueda, L. A. (2014). Calcium-looping for post-combustion CO2 capture. On the adverse effect of sorbent regeneration under CO2. *Applied Energy*, 126, 161-171.

Wall, T., Stanger, R., & Santos, S. (2011). Demonstrations of coal-fired oxy-fuel technology for carbon capture and storage and issues with commercial deployment. *Int. J. Greenhouse Gas Control*, 5, S5-S15.

Wang, J., Manovic, V., Wu, Y., & Anthony, E. J. (2010). A study on the activity of CaO-based sorbents for capturing CO2 in clean energy processes. *Applied Energy*, 87, 1453-1458.

Wang, W., Li, Y., Xie, X., & Sun, R. (2014). Effect of the presence of HCl on cyclic CO2 capture of calcium-based sorbent in calcium looping process. *Applied Energy*, 124, 246-253.

Yang, H., Xu, Z., Fan, M., Gupta, R., Slimane, R. B., Bland, A. E., & Wright, I. (2008). Progress in carbon dioxide separation and capture: a review. *J. Environ. Sci.*, 20(1), 14-27.

Yang, Y., Zhai, R., Duan, L., Kavosh, M., Patchigolla, K., & Oakey, J. (2010). Integration and evaluation of a power plant with a CaO-based CO2 capture system. *International Journal of Greehouse Gas Control*, 4, 603-612.

Chapter 4 – Pilot-Scale Study of CO_2 Capture by CaO-Based Sorbents in the Presence of Steam and SO_2

Robert T. Symonds[a], Dennis Y. Lu[a], Vasilije Manovic[a], Edward J. Anthony[a]

[a]Natural Resources Canada, CanmetENERGY

1 Haanel Drive, Ottawa, Ontario K1A 1M1, Canada

Article published in *Industrial & Engineering Chemistry Research* **2012** *51*, 7177-7184.

4.1 – Abstract

Calcium looping cycles require an oxy-fired calciner burning coal for sorbent regeneration. Thus, besides O_2 and CO_2, the flue gases will include both steam and SO_2 and similarly carbonation of real flue gases will occur in the presence of steam. However; to date most research has been done without either of these two gaseous components present. Here, batch pilot-scale fluidized bed reactor combustion (FBC) experiments were performed on the effect of steam and SO_2 addition on CO_2 capture by limestone-based sorbents calcined under oxygen-enriched air and oxy-fuel conditions. The initial fast kinetically-controlled CO_2 capture stage was drastically reduced when the sorbent was calcined at realistic temperatures in the presence of SO_2. This is attributed to greater sintering due to higher local calcination temperatures required by high CO_2 concentrations and to $CaSO_4$ formation. By contrast, steam in the synthetic flue gas during carbonation extended the initial, high-efficiency CO_2 capture period compared with carbonation with dry synthetic flue gases. A comparison between pilot-scale fluidized bed combustion (FBC) and thermogravimetric analysis (TGA) results showed that sorbent reactivity was considerably lower during pilot-scale FBC testing as anticipated given the higher calcination temperatures employed in the FBC reactor and to the presence of the other feed gases. The enhanced CO_2 capture efficiency in FBC reactors with steam present was also confirmed by TGA tests. These results are important because they demonstrate how sorbent deactivation effects seen in realistic FBC calcium looping operation can be successfully mitigated by the presence of steam in the carbonator.

4.2 – Introduction

CO_2 emissions from coal-fired power plants are believed to be a major contributor to global warming and climate change (IPCC, 2007). A promising solution to reduce such CO_2

emissions is post-combustion capture from flue gas with subsequent compression, transportation, and sequestration in the deep oceans or in underground geological formations (Bachu, 2008) (Beer, 2000) (Metz, et al., 2005). Of the many developing capture technologies, CO_2 absorption processes such as calcium looping appear to be promising. Calcium looping is considered technically feasible at an industrial scale, economically competitive (Mackenzie, et al., 2007) (Abanades, et al., 2007) and environmentally benign due to the relatively inert nature of the solid residues produced from the process. Moreover, the spent residues could also be used for instance in cement manufacture (Harrison, 2004) (Yang, et al., 2008) (Blamey, et al., 2010)

Much research has demonstrated the potential of fluidized bed combustion (FBC), as a technology to carry out calcium looping cycles (Blamey, et al., 2010). Circulating fluidized bed combustion (CFBC) systems are particularly suitable for processing large amounts of solids (Davidson, et al., 1985), and reactions between gas and solid streams are significantly enhanced by superior mixing which maximizes mass/heat transfer along with reaction rates. Therefore, at appropriate temperatures and pressures, a flue gas stream can be decarbonized by passing it through a fluidized bed of calcined limestone to form $CaCO_3$ (carbonation, forward reaction of Equation 4.1). This carbonated material can then be transferred to a second fluidized bed or calciner where, at higher temperatures and/or lower pressures, the calcination reaction occurs (reverse reaction of Equation 4.1). The resulting gas stream is concentrated CO_2 (>90%), which is then suitable for liquefaction and ultimate sequestration.

$$CaO_{(s)} + CO_{2(g)} = CaCO_{3(s)} \quad (4.1)$$

FBCs are also used for SO_2 removal using calcium-based sorbents *via* either indirect (Equation 4.2) or direct (Equation 4.3) sulphation (Anthony & Granatstein, 2001).

$$CaO_{(s)} + SO_{2(g)} + 1/2O_{2(g)} = CaSO_{4(s)} \quad (4.2)$$

$$CaCO_{3(s)} + SO_{2(g)} + 1/2O_{2(g)} = CaSO_{4(s)} + CO_{2(g)} \quad (4.3)$$

Unfortunately, SO_2 in calcium looping systems decreases sorbent activity, as the SO_2 irreversibly forms $CaSO_4$ (Borgwardt, 1970) (Tullin & Ljungstrom, 1989) (Sun, et al., 2006) (Arias, et al., 2011). This requires the use of additional sorbent, which reduces the environmental and economic benefits of the calcium looping process (Mackenzie, et al., 2007) (Abanades, et al., 2007). One solution to this problem is to desulphurize the flue gases in a separate reactor (Hughes, et al., 2005). However, there is evidence that partial sulphation reduces the loss of material due to elutriation from the FBC reactor (Jia, et al., 2007), and the use of a separate SO_2 removal step would increase both the complexity and cost of a Ca looping system. It appears that steam might mitigate the effects of SO_2, as TGA studies have shown that steam enhances sorbent performance during CO_2 capture cycles (Manovic & Anthony, 2010) (Arias, et al., 2010) (Donat, et al., 2012), but those tests did not include the deactivation effects due to the presence of SO_2. Moreover, the effect of the simultaneous presence of SO_2 and steam has still not been explored in pilot-plant studies (Wang, et al., 2010) (Charitos, et al., 2011) (Galloy et al., 2011) (Fang et al., 2009). Therefore, the primary aim of this work is to examine the effect of steam on the CO_2 capture efficiency and utilization of sorbent calcined under more realistic operation conditions (higher temperatures and CO_2 concentrations) and with SO_2 present during calcination in a pilot-scale FBC reactor.

4.3 – Experimental Section

4.3.1 – Pilot-Scale FBC Reactor

The pilot-scale dual fluidized bed system is described in detail elsewhere (Lu, et al., 2008) (see Chapter 5). The system comprises two separate FBC reactors (calciner and

carbonator), but only one reactor was used for the batch experiments performed here and it was operated in bubbling bed mode during both calcination and carbonation. CO_2 capture cycles were achieved by altering both temperature and gas compositions. As well, the reactor is designed to allow the introduction of superheated steam together with fluidization gas. The reactor's internal diameter is 0.1 m, and it is surrounded by three 4.5 kW electric heaters which provide supplemental heating during start-up/system pre-heat. Instrumentation ports are situated at approximately 0.3 m intervals over the reactor's total length and are used for both temperature and pressure measurements. The gas analysis sampling port is located on the top of the reactor cyclone, and during tests the data on gas outlet concentrations were continuously monitored. The system control and data acquisition were operated using Labview (National Instruments) *via* a FieldPoint instrument interface.

4.3.2 – Experimental Conditions

4.3.2.1 – Sorbents

Two natural limestones were used for experimental testing (Table 4.3.1), Cadomin (Canadian) and Piasek Wapieny (Polish) which have purities of 90.0 and 95.6%, and mean surface-to-volume diameter of 612 and 512 μm, respectively. For convenience the Piasek Wapieny limestone will be referred to hereafter as Polish limestone.

Table 4.3.1: XRF Elemental Analyses of Cadomin and Piasek Wapieny Limestones (wt%)

Sorbent	SiO_2	Al_2O_3	Fe_2O_3	TiO_2	P_2O_5	CaO	MgO	SO_3	Na_2O	K_2O	LOF
Polish Limestone	0.85	0.24	0.09	<0.03	<0.03	54.10	0.89	<0.1	<0.2	0.06	43.64
Cadomin Limestone	1.30	0.40	0.11	0.04	<0.03	50.64	3.28	<0.1	<0.2	0.14	43.99

LOF – Loss on fusion

4.3.2.2 – Calcination conditions

Sorbents were calcined under two different regimes: oxygen-enriched air or oxy-fuel combustion, which in both cases implied elevated CO_2 concentrations compared with air firing. Before each cyclic test of CO_2 capture, a fresh amount of sorbent (~6.0 kg) was loaded into the

reactor at room temperature. The reactor was heated up, and fluidization and feed of biomass fuel started at ~600 °C. The temperatures during oxy-fuel and oxygen-enriched combustion were approximately 910-920 ^{o}C and 860-870 ^{o}C, respectively. These temperatures are ~30 ^{o}C higher than those thermodynamically required under given CO_2 partial pressures (Baker, 1962), and they were chosen to ensure a practical calcination rate.

The fuel used for calcination was low-ash biomass (wood pellets) and its proximate and ultimate analyses are given in Table 4.3.2. The average flue gas compositions, fuel feed rates, and oxygen flow rates under the two calcination conditions are given in Table 4.3.3. For experiments with SO_2 addition, inlet SO_2 concentrations were 2000 ppm, but only ~20 ppm was measured during the entire calcination period in the outlet flue gas. The total calcination time was ~60 min which also means that in experiments with SO_2 present the sorbent was sulphated for that period.

Table 4.3.2: Proximate and Ultimate Analyses of Biomass (Wood Pellets) Used in Calciner

Wood Pellet (Biomass)	Proximate Analysis (wt%)				Ultimate Analysis (wt%)				
	Moisture	Ash	Volatiles	FC	C	H	N	S	O
Pure Fiber Hardwood Blend	7.81	0.68	75.54	15.97	45.80	5.52	<0.10	<0.05	40.04

FC – Fixed carbon

Table 4.3.3: Gas Flow and Fuel Feed Rates and Average Gas Composition at the FBC Reactor Outlet during Limestone Calcination

Calcination Conditions	Temperature (^{o}C)	Feed/Flow Rate					Outlet Gas Composition (dry basis)			
		Fuel (kg/h)	Oxygen (SLPM)	Air (kg/h)	Recycle (kg/h)	SO_2 (SLPM)	O_2 (vol%)	CO_2 (vol%)	CO (vol%)	SO_2 (ppm)
O_2 Enriched Air	860	1.4	40	9.0	-	0.25	7.5	35	1.0	20
Oxy-Fuel	910	1.7	65	-	9.0	0.25	6.5	80	1.0	20

Table 4.3.4: Gas Flow Rates and Inlet Gas Composition during CO_2 Capture Steps

Carbonation Conditions	Temperature (°C)	Flow Rate			Inlet Gas Composition			
		Air (SLPM)	CO_2 (SLPM)	Steam (kg/h)	N_2 (vol%)	O_2 (vol%)	CO_2 (vol%)	Steam (vol%)
No Steam	600	65	5.7	0	72.7	19.3	8.0	0
Steam Present	600	56	5.7	0.48	59.3	15.7	8.0	17.0

4.3.2.3 – Carbonation conditions

When calcination was finished the reactor was cooled down to ~600 °C and gas flows were switched to enable carbonation. The amount of calcined material at the beginning of carbonation step was ~3.5 kg. The gas flow rates and gas composition at the inlet in the reactor are listed in Table 4.3.4. The carbonation step was for 70 min, and during that period gas composition at the outlet was continuously measured. To observe the effect of steam on the performance of the limestone sorbents, carbonation was performed with and without steam added and a heated line was used to introduce the steam to ensure condensation did not occur. During several runs, after CO_2 concentration in the outlet gas rapidly increased, approaching CO_2 inlet concentration (CO_2 breakthrough), the temperature was subsequently raised to ~700 °C, which resulted in a rapid decrease in CO_2 concentration. These tests showed that the sorbent performance, *i.e*., its capture efficiency, was very sensitive to the temperature changes after CO_2 breakthrough (see Figure 4.4.1below). Therefore, to compare the effects of steam on CO_2 capture performance of different sorbents, calcined with or without SO_2, only the results obtained during the initial period including the CO_2 breakthrough are presented here.

4.3.2.4 – TGA Tests

Steam effects on CO_2 capture efficiency by sorbent partially sulphated during calcination were also compared by performing tests using a Perkin Elmer TGA-7 thermogravimetric analyzer. The sorbent sample (~5 mg) was suspended in a quartz tube (ID 20 mm) on a platinum

pan (ID 5 mm). The gas flow rate was controlled by a flowmeter, at 0.04 dm^3/min. The temperature and gas used were controlled by Pyris software. Sample mass data during the experiments were monitored and the degree of both sulphation and carbonation were calculated on the basis of mass change, assuming that mass change occurs only due to the irreversible formation of $CaSO_4$ and the reversible formation/decomposition of $CaCO_3$.

The samples were calcined in an atmosphere containing 50% CO_2, and 2250 ppm SO_2 (N_2 balance). The temperature program for the first calcination included heating to 870 °C, followed by an isothermal step at 870 °C for 10 min. At the beginning of the cooling step the gas mixture was switched to N_2 to avoid sulphation and carbonation before the desired carbonation temperature was reached. A gas mixture containing 10% CO_2 in nitrogen was introduced when a temperature of 600 °C was reached, and carbonation was continued for 20 min isothermally at 600 °C. Here, 20% steam was introduced in the gas mixture for the tests of CO_2 capture in the presence of steam. Steam was produced using a syringe pump and steam generator. Feed lines containing both steam and the mixed gas were insulated and electrically heat-traced to ensure no steam condensation. Both heating and cooling rates were 50 °C/min. In all, five carbonation/calcination cycles were performed, and SO_2 was present during each calcination step, while steam was only present during carbonation tests exploring the effect of steam addition.

4.4 Results and Discussion

4.4.1 – Effect of Calcination Conditions

The calcination of sorbents was performed under both oxygen-enriched air and oxy-fuel conditions, with and without SO_2 present. Under such conditions one must examine the effect of high CO_2 concentrations as well as the presence of SO_2 during calcination, on the effectiveness

of subsequent CO_2 capture. Namely, high CO_2 concentrations during calcination under realistic Ca looping conditions are required to produce concentrated CO_2 streams, while SO_2 is always present if solid fossil fuels are used to generate heat for sorbent regeneration in the calciner.

4.4.1.1 – Effect of CO_2 Partial Pressure and Temperature

Figure 4.4.1 shows the carbonator outlet CO_2 concentration during the first cycle of CO_2 capture from simulated flue gas (8% CO_2, balance air) for tests with both oxygen-enriched and oxy-fuel calcined Cadomin limestone. CO_2 capture by CaO-based sorbents takes place in two distinct stages (Blamey, et al., 2010): a fast kinetically-controlled stage, followed by a significantly slower diffusion controlled stage. In practice, only the fast reaction stage is important for CO_2 capture in the FBC reactors and Figure 4.4.1 shows that, during the initial period of CO_2 capture, CO_2 concentration is <0.5% and is mainly determined by the equilibrium CO_2 partial pressure. That means that the reaction is under the fast kinetically-controlled stage. However, when the level of sorbent carbonation reaches some critical value the fast stage shifts to a slow diffusion-controlled stage, at which point the activity of sorbent is insufficient to prevent CO_2 breakthrough and CO_2 concentration immediately increases at the carbonator outlet. The duration of the period before CO_2 breakthrough depends on sorbent activity, and is a useful parameter to compare the activities of sorbents calcined here under different conditions as well as to evaluate the effects of steam addition.

The CO_2 concentration profiles in Figure 4.4.1 show that for the sorbent calcined under oxygen-enriched air calcination conditions the fast CO_2 capture period is ~35 min, which is seven times longer than for the sorbent calcined under oxy-fuel conditions. These results are similar to those reported earlier by Symonds *et al*. (2009) and are explained by sorbent sintering (Abanades & Alvarez, 2003), which is more prominent during calcination under high CO_2

concentrations/temperatures (Dobner, et al., 1977) (Borgwardt, 1989). Although not presented here for reasons of space, the same phenomenon was also observed for the Polish limestone.

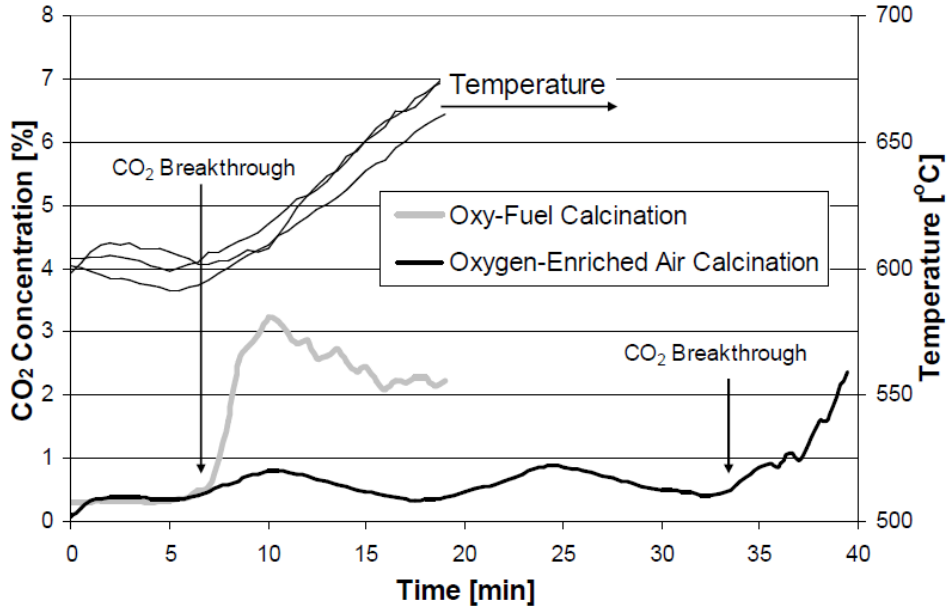

Figure 4.4.1: CO_2 concentration at the FBC carbonator outlet during the CO_2 capture (batch test) from simulated flue gas (8 vol% CO_2, air balance) at 600 °C by Cadomin limestone calcined at 860 °C under oxygen-enriched air and at 910 °C under oxy-fuel combustion conditions. Temperature measured at three different positions in the bed is presented for the oxy-fuel calcination run.

These results show that the effect of high CO_2 concentrations is quite dramatic in comparison to that of previous work performed using a TGA (Manovic & Anthony, 2010) (Lu, et al., 2009). As an example, Table 4.4.1 lists the carbonation conversions over the first two cycles for Cadomin limestone for experiments performed in both a TGA and a pilot-scale FBC (this work), at similar temperatures and carbonation conditions. As previously reported (Lu, et al., 2009), the addition of CO_2 during the first calcination caused a decrease in the subsequent carbonation conversion to a level typically achieved after 5-6 cycles for the same sorbent calcined in a pure N_2 atmosphere. However, in the case of the pilot-scale FBC tests presented here (Table 4.4.1), for calcination in a CO_2-rich atmosphere, the carbonation conversion in the first cycle falls to levels typically seen after 15-20 cycles with calcinations in a pure N_2

atmosphere, or after 5-6 cycles with calcinations in a high-CO_2 (90%) atmosphere when similar experiments were performed in a TGA.

Table 4.4.1: Comparison of Carbonation Conversions in TGA (Lu, et al., 2009) and in Pilot-Scale FBC (this work) for Cadomin Limestone over Two Cycles

Reactor	Conditions		Cycle	Carbonation Conversion
	Carbonation	Calcination		
TGA	15% CO_2 (N_2 balance), 700 °C, 30 min	100% N_2, 700 °C, 60 min	1	0.75
			2	0.68
		90% CO_2 (N_2 balance), 925 °C, 30 min	1	0.54
			2	0.31
Pilot-Scale FBC	O_2-Enriched Air		1	0.26
			2	0.24
	Oxy-Fuel		1	0.27
			2	0.11

This significant decrease in sorbent activity over repeated cycles can also be explored in terms of CO_2 concentration at the outlet of the carbonator for the first two cycles (Figure 4.4.2). As expected, the high-CO_2-capture-efficiency period is shorter and the CO_2 capture during the diffusion-limited period is reduced during the second cycle. These results agree with those of similar FBC tests, using simulated gasification syngas streams (Symonds et al., 2009), for both oxygen-enriched air and oxy-fuel calcination conditions.

The large disparity in carbonation conversions obtained in TGA and in pilot-scale experiments is believed to be related to pore sintering associated with the calcination process, which depends mainly on the gas composition, final calcination temperature, heating rate, and duration. First, an increase in temperature tends to increase pore sizes, which reduces the surface area (Borgwardt, et al., 1986) (Borgwardt, 1989). Second, high CO_2 concentrations enhance

sintering, and moreover, other gases such as steam (typically present in a calcium looping operation) can also promote sintering (Dobner, et al., 1977). Finally, it should also be pointed out that the combined effect of CO_2 and steam on sorbent sintering is believed to be even more severe (Borgwardt, 1989).

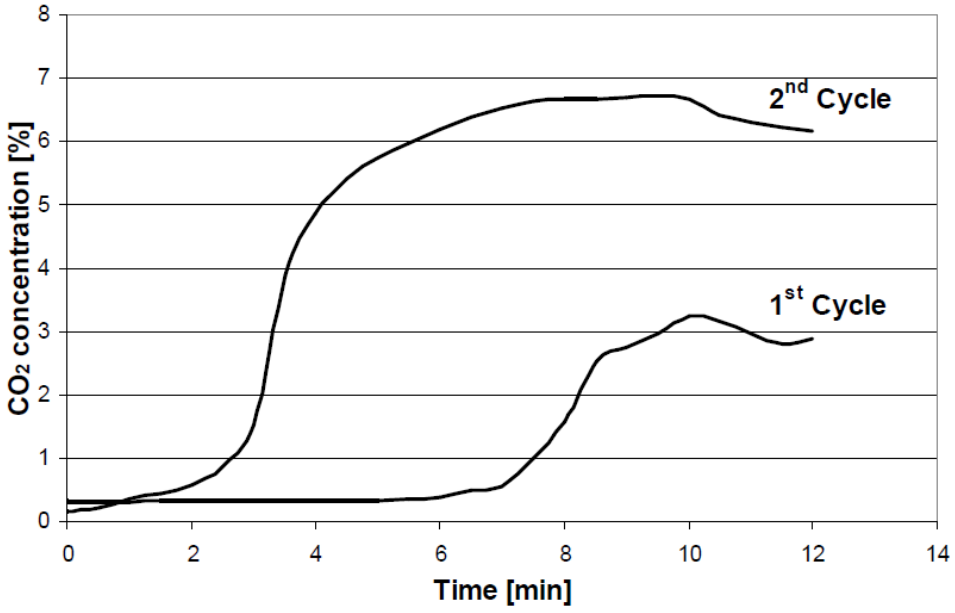

Figure 4.4.2: CO_2 concentration at the FBC carbonator outlet during the first two CO_2 capture cycles (batch test) from simulated flue gas (8 vol% CO_2, air balance) at 600 °C by Cadomin limestone calcined at 910 °C under oxy-fuel combustion conditions.

These factors that enhance sintering are simultaneously present and even more pronounced during pilot-scale FBC testing. Namely, it is reasonable to suppose that during calcination in FBC the CO_2 will be released to the emulsion phase, causing significantly higher CO_2 concentrations around the sorbent particles than in the bulk gas phase. In other words, the CO_2 concentrations measured at the calciner outlet are lower than those around calcining sorbent particles. Thus, in order to complete calcination, the temperatures required to achieve a practical calcination rate are appreciably higher than those predicted based on the measured CO_2 concentration at the outlet of the reactor. For example, based on results in Table 4.3.3, the measured CO_2 concentration during calcination under oxy-fuel condition was approximately 80

vol%. The equilibrium temperature at this CO_2 partial pressure is approximately 880 ^oC, whereas the actual required temperature for reasonably rapid calcination was about 910^oC. This increased temperature enhances sintering observed during pilot-scale testing presented in this work. Other important factors affecting sorbent sintering during pilot-scale FBC testing involve the effect of char particle temperatures which are significantly higher during burning than the bulk temperature of the fluidized bed, and the presence of low-melting-point compounds in the ash from of solid fuels. Namely, it has been shown that the average particle temperature of a series of coals and coal chars was 87-191^oC above the average bed temperature during combustion (Joutsenoja, et al., 1999). Moreover, during oxy-fuel or oxygen-enriched air combustion even higher local temperatures due to burning particles can be expected, especially for more reactive fuels such as biomass (higher porosity and pore surface area of wood char), as confirmed by modeling studies of combustion with elevated O_2 concentrations (Manovic, et al., 2008). These high char particle burning temperatures can cause local superheating of sorbent particles during any physical particle-particle contacts. Moreover, ash can build up on the surface of the sorbent particles resulting in local melts on the sorbent particle surface, which additionally enhances sorbent sintering and deactivation (Hughes, et al., 2009). Although the ash content in the feed fuel was relatively low (0.68 wt%), it still seems plausible that ash melts on the sorbent surface were a significant factor affecting sintering. Moreover, it should also be noted that, during each calcination, up to ~1% sorbent can be sulphated (under the conditions in this study), which can additionally contribute to the sintering. Namely, there is potential for low-temperature eutectic melts with $CaSO_4$ (Paterson, et al., 2001), which could promote sintering.

Another important difference between TGA and pilot-scale FBC experiments, which can affect CO_2 capture efficiency, is the presence of steam during calcination, as all fuels that might

reasonably be used in the calciner contain moisture and hydrogen. In this particular case, the respective values are 7.91 wt% and 5.52 wt%, (wood pellets, Table 4.3.2). Hence, the resulting steam presence in the calciner must affect sorbent sintering during calcination and its subsequent performance during CO_2 capture. Also, as noted above, the simultaneous presence of both CO_2 and steam has a combined effect on sintering, and these results show that it is critical to include steam during calcination of calcium-based sorbents in TGA experiments to accurately simulate pilot-scale FBC conditions.

4.4.1.2 – Effect of SO_2 Addition

Figure 4.4.3 shows the CO_2 concentration at the outlet of the carbonator during the first cycle of CO_2 capture from a simulated flue gas (8% CO_2, balance air), with both limestones calcined under oxygen-enriched air conditions with and without SO_2 present. It can be seen that the initial kinetically-controlled CO_2 capture stage is drastically reduced from ~35 min to only ~4 min. Moreover, during the diffusion-controlled capture stage the CO_2 outlet concentration is significantly higher than seen without SO_2 addition during sorbent calcination. Similar, if less pronounced, effects are seen for the Polish limestone.

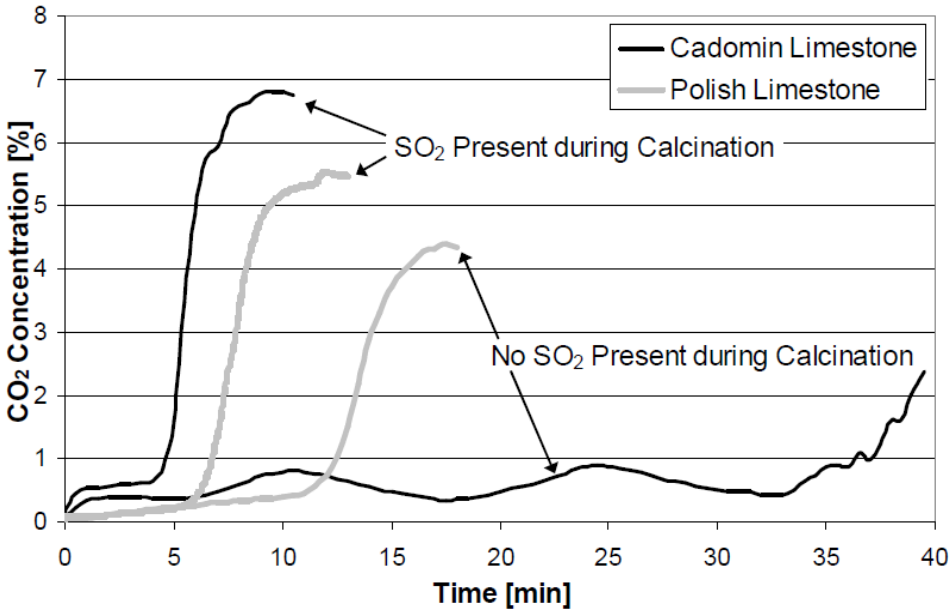

Figure 4.4.3: CO_2 concentration at the FBC carbonator outlet during CO_2 capture (batch test) from simulated flue gas (8 vol% CO_2, air balance) at 600 °C for the two limestones tested, calcined at 860 °C under oxygen-enriched air combustion conditions with (2000 ppm) and without SO_2.

Based on these observations it is plausible to argue that the surface of the particles partially sulphated during calcination is less porous, significantly increasing the diffusion resistance. Moreover, during carbonation remaining pores at the surface of sorbent particles are also plugged by the carbonation product ($CaCO_3$). This phenomenon is consistent with the fact that a $CaSO_4$ shell at the particle surface is formed during sulphation of most limestones (Laursen, et al., 2000), and this has also been recently demonstrated for the simultaneous sulphation and carbonation tests (Manovic & Anthony, 2010).

Even greater sorbent deactivation can be expected over repeated CO_2 capture cycles because $CaSO_4$ is continually produced during each cycle. Figure 4.4.4 illustrates the CO_2 concentration at the outlet for the first three cycles of CO_2 capture by the Polish limestone. These results show that the high-CO_2-capture-efficiency period is reduced from ~6 min during the first cycle to <1 min during the third cycle. From this result it appears that after calcination in the

presence of SO_2 over three cycles, the build-up of $CaSO_4$ on the particle surface is such that the only available CaO for carbonation is found in the interior of the partially sulphated sorbent particles. As the $CaSO_4$ does not decompose under calcium looping cycle conditions, the $CaSO_4$ product shell must gradually increase over repeated cycles, leading to greater diffusion resistance (Anthony & Granatstein, 2001). Finally, after only three cycles the fast carbonation period has almost disappeared and from the very beginning the reaction is controlled by CO_2 diffusion through the sulphate shell.

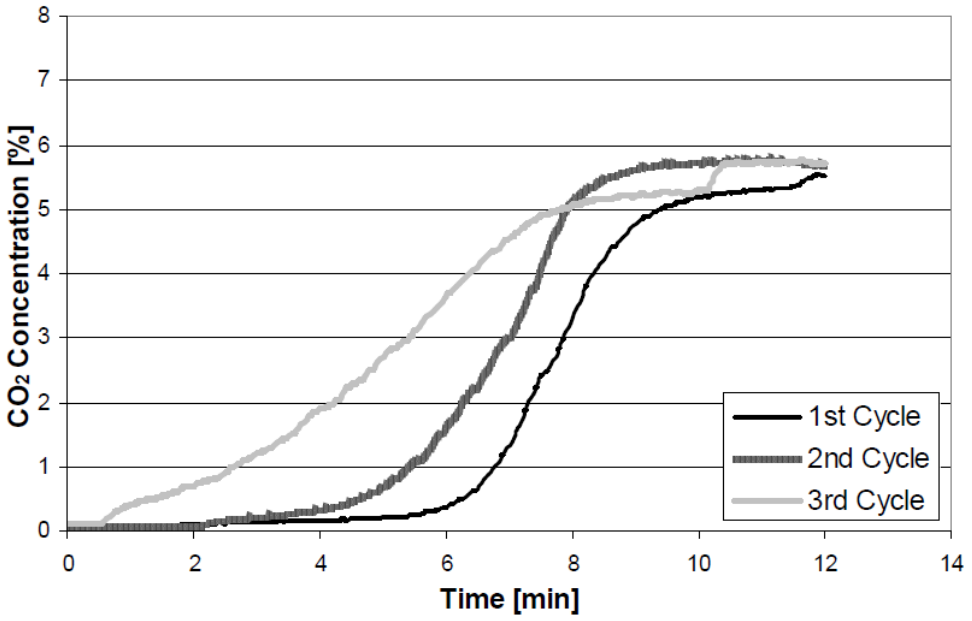

Figure 4.4.4: CO_2 concentration at the FBC carbonator outlet during the first three CO_2 capture cycles (batch test) from simulated flue gas (8 vol% CO_2, air balance) at 600 °C by Polish limestone calcined at 860 °C under oxygen-enriched air combustion conditions with 2000 ppm SO_2 present.

These results suggest that CO_2 capture by calcium-based sorbents employing realistic calcination conditions poses significant challenges. The combination of higher calcination temperatures and CO_2 concentrations, along with the presence of steam and SO_2, can be expected to lead to drastically reduced sorbent performance and CO_2 capture efficiency. Thus, in order to avoid large amounts of fresh sorbent make-up, which negatively affect the overall economics of

the calcium looping cycle process, other methods to improve sorbent activity should be considered if the use of makeup sorbent is to be kept to low levels (Blamey, et al., 2010) (Manovic, et al., 2008).

4.4.2 – Effect of Steam during Carbonation

It is known that the presence of gaseous species such as steam significantly impacts solid state diffusion (Borgwardt, 1989). Until recently, there was little evidence in the literature suggesting that the presence of steam in flue gas would enhance sulphation or carbonation. Therefore, experimentation performed by TGA typically did not include steam during sulphation/carbonation. However, steam is present in a real flue gas originating from both the moisture and hydrogen in coal or other carbonaceous feed stocks and could be added if it were desirable. A study by Symonds *et al*. (2009) on CO_2 capture from syngas showed a significant improvement in the overall sorbent conversion with the addition of steam, which was also observed by Manovic and Anthony (2010) over a larger temperature range (350-800^{o}C) for several different calcium-based sorbents. Recent studies by Wang *et al*. (2010) and Stewart *et al*. (2010) have also clearly shown a strong positive influence of steam on sulphation. Therefore, the effect of the presence of steam in flue gas during carbonation was examined in order to evaluate the performance of the sorbent (partially sulphated) which was subjected to more realistic conditions.

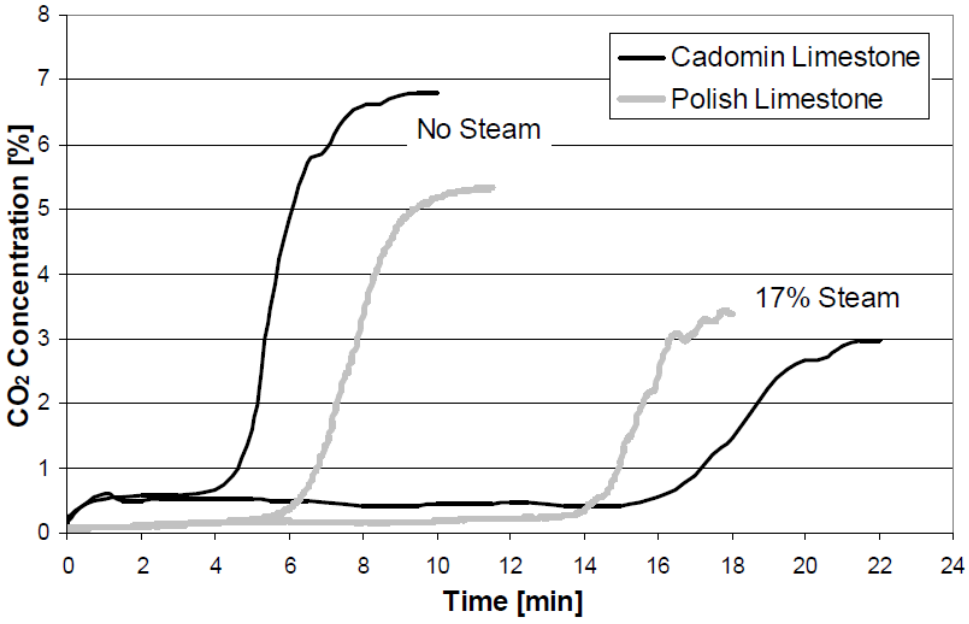

Figure 4.4.5: The effect of steam presence in the FBC carbonator on CO_2 concentration (dry basis) at the outlet during CO_2 capture (batch test) from simulated flue gas (8 vol% CO_2, air balance) at 600 °C by two tested limestones calcined at 860 °C under oxygen-enriched air combustion conditions with (2000 ppm) SO_2.

Figure 4.4.5 shows the effect of steam addition on CO_2 concentration at the outlet of carbonator during the CO_2 capture from synthetic flue gas (8% CO_2, balance air) by limestones partially sulphated during calcination under oxygen-enriched air combustion conditions. It can be clearly observed that the CO_2 capture efficiency is superior in the presence of 17% steam, *i.e.*, the duration of the high-CO_2-capture-efficiency period is now considerably longer. The rapid kinetically-controlled stage of CO_2 capture by the Polish limestone increases from ~5 min to ~14 min, an increase of nearly three times, with an average CO_2 capture of 98% over this period. A similar but even better result can be seen for Cadomin limestone, and the high-CO_2-capture-efficiency period was even longer in this case. These results are in agreement with the work of Manovic and Anthony (2010), which showed that steam addition reduces diffusion resistance during carbonation in the TGA, and the onset of the diffusion-controlled stage is consequently delayed by the presence of steam.

The effect of steam on CO_2 capture efficiency is further illustrated by the results presented in Figure 4.4.6. In this experiment Cadomin limestone, partially sulphated during calcination under FBC oxygen-enriched air-fired conditions with 2000 ppm of SO_2 present, is employed for CO_2 capture from a dry synthetic flue gas mixture. During the 2nd capture cycle (presented in Figure 4.4.6), the carbonator outlet CO_2 concentration rapidly increased after a few minutes and, despite some instability due to temperature fluctuations, stayed above 6 vol% for 35 min. When steam at 17 vol% was introduced with the flue gas into the carbonator the outlet CO_2 concentration instantly decreased to ~2.5%. After ~12 min of CO_2 capture from the steam-containing gas mixture, steam was cut, causing the outlet CO_2 concentration to increase sharply to a level seen for CO_2 capture with no steam (>6 vol%). These results support a hypothesis that steam enhances diffusion through the product layer/shell (in this case both $CaCO_3$ and $CaSO_4$).

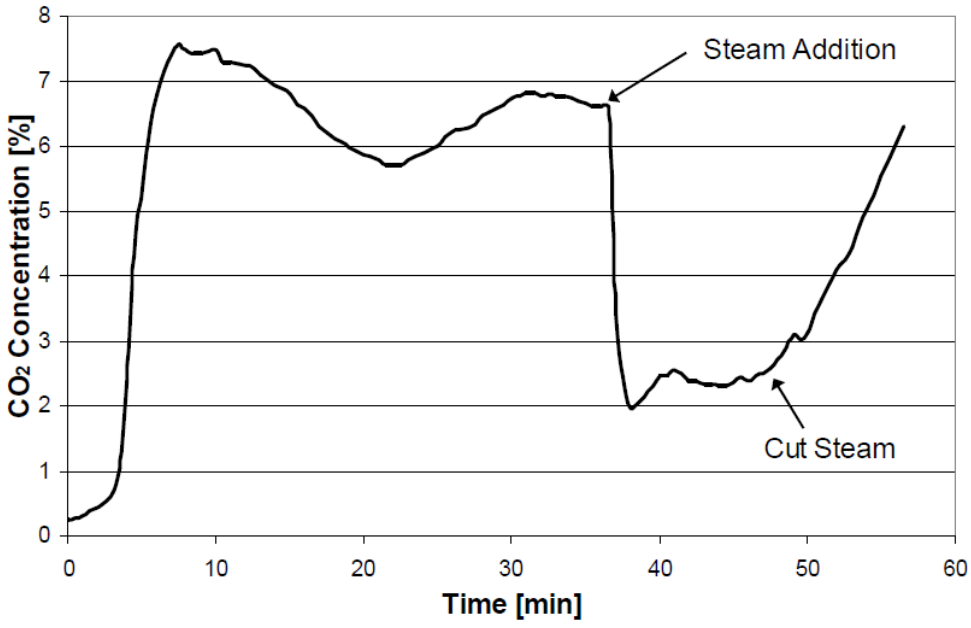

Figure 4.4.6: The effect of steam addition/cut into the FBC carbonator on CO_2 capture efficiency by Cadomin limestone during the 2nd CO_2 capture cycle (1st carbonation is presented in Figure 4.4.6).

Table 4.4.2: Summary of Carbonation Conversion of Tested Limestones Calcined with SO_2 Addition

Sorbent	Calcination Condition	Carbonation Feed Gas	Cycle	Carbonation Conversion
Cadomin Limestone	O_2-Enriched Air	8 % CO_2 Balance Air	1	0.166
			2	0.168
		8% CO_2 , 17% H_2O Balance Air	1	0.359
			2	0.388
	Oxy-Fuel	8 % CO_2 Balance Air	1	0.131
			2	0.133
		8% CO_2 , 17% H_2O Balance Air	1	0.179
			2	0.156
			3	0.218
Polish Limestone	O_2-Enriched Air	8 % CO_2 Balance Air	1	0.222
			2	0.192
			3	0.178
		8% CO_2 , 17% H_2O Balance Air	1	0.315
			2	0.182
	Oxy-Fuel	8 % CO_2 Balance Air	1	0.143
			2	0.110
			3	0.100
		8% CO_2 , 17% H_2O Balance Air	1	0.312
			2	0.133
			3	0.126

Table 4.4.2 summarizes the carbonation conversions for the two limestones partially sulphated during calcination. These conversions were determined by heating samples in a muffle furnace. For tests performed with no steam addition during carbonation, there was a decrease in carbonation conversion of sorbents calcined under oxy-fired combustion conditions compared to that of oxygen-enriched air calcination, 21.0% and 40.5% for Cadomin and Polish limestone, respectively. In the case of the Cadomin limestone, the addition of steam during carbonation resulted in an increased conversion of roughly 124% and 40% (relative) for oxygen-enriched air and oxy-fuel calcination conditions, respectively. Similar improvements were observed for the Polish limestone, with carbonation conversion increases of approximately 26% and 62% for oxygen-enriched air and oxy-fuel calcination conditions, respectively.

Although there are some differences in the behavior of the two limestones, in both cases the presence of steam during carbonation significantly increases the carbonation conversion over

repeated cycles. An important result from this work is that steam can mitigate the effects of SO_2 on sorbent performance during CO_2 capture cycles as is clearly confirmed by supporting TGA experiments. The results presented in Figure 4.4.7 show that during the first calcination of Cadomin limestone ~15% of the sorbent is converted to $CaSO_4$. Moreover, sulphation conversion increased with subsequent CO_2 capture cycles and it is clearly greater when steam was present during carbonation. These results indicate that the presence of steam during carbonation changes sorbent morphology, and that sulphation is enhanced during calcination regardless of the fact that steam was not present during this stage.

It is evident that carbonation is hindered due to sulphation, resulting in only ~12% carbonation conversion after five cycles. However, despite higher sulphation conversions with steam present during calcination the subsequent carbonation conversions are also higher (here ~19% after five cycles). This encouraging finding supports the results obtained in the FBC reactor (Figure 4.4.5 and Figure 4.4.6), and shows that the presence of steam during carbonation reduces the negative effects of SO_2 on the CO_2 capture activity of CaO-based sorbents.

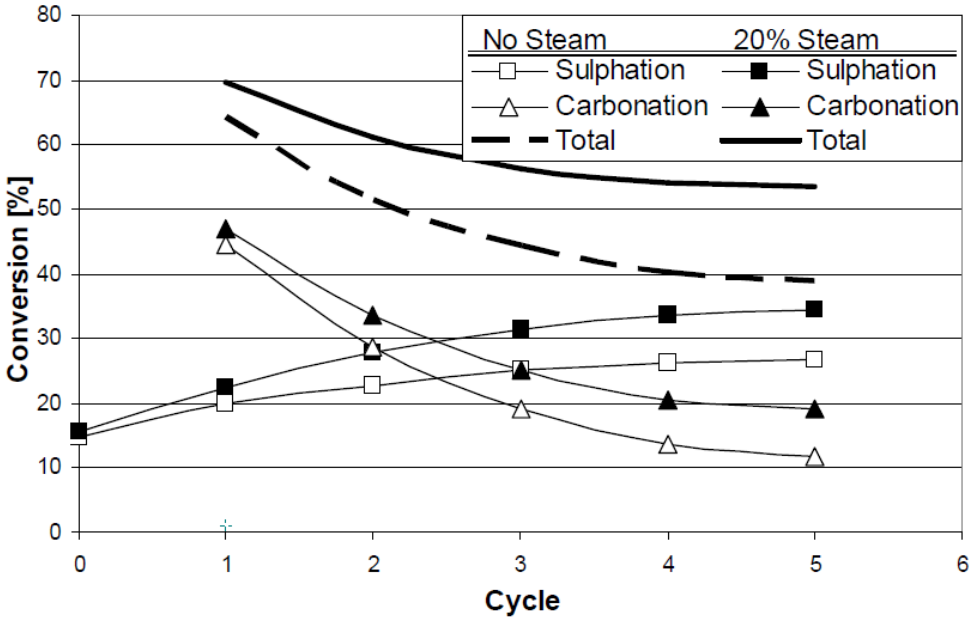

Figure 4.4.7: Sulphation and carbonation conversions during CO_2 capture cycles in TGA by Cadomin limestone. Conditions: calcination in 50% CO_2 (N_2 balance) in the presence 2250 ppm SO_2 at 870 °C for 10 min; carbonation in 10% CO_2 (N_2 balance) at 600 °C for 20 min.

4.5 – Conclusions

Calcium looping tests were performed using a pilot-scale FBC reactor, operated in batch mode, to explore the effect of high CO_2 concentrations and the presence of SO_2 during calcination on CO_2 capture efficiency. Under these conditions the initial rapid kinetically-controlled CO_2 capture stage was drastically reduced. Moreover, CO_2 capture efficiency was substantially reduced during the diffusion-controlled stage. This was attributed to both enhanced sorbent sintering and the formation of a solid $CaSO_4$ layer/shell which increases the diffusion resistance. With steam present in the feed gas during carbonation: the fast CO_2 capture period was significantly extended with enhanced CO_2 capture efficiency compared to carbonation with only CO_2 present. These findings were confirmed by TGA experiments which also included both SO_2 and steam addition. These results suggest that CO_2 capture cycles in TGA should encompass as many of the factors present during FBC operation as possible (*i.e.*, higher calcination

temperatures/CO_2 concentrations and the presence of steam and other gases such as SO_2), to avoid somewhat misleading results and conclusions related to sorbent performance.

4.6 – References

Abanades, J. C., Alvarez, D. (2003). Conversion Limits in the Reaction of CO2 with Lime. *Energy Fuels*, 17, 308-315.

Abanades, J. C., Grasa, G., Alonso, M., Rodriguez, N., Anthony, E. J., Romeo, L. M. (2007). Cost Structure of a Postcombustion CO2 Capture System using CaO. *Environ. Sci. Technol*., 41, 5523-5527.

Anthony, E. J., Granatstein, D. L., (2001). Sulphation Phenomena in Fluidized Bed Combustion Systems. *Prog. Energy. Combust. Sci*., 27, 215-236.

Arias, B., Cordero, J. M., Alonso, M., Abanades, J. C. (2011). Sulfation Rates of Cycled CaO Particles in the Carbonator of a Ca-Looping Cycle for Postcombustion CO2 capture. *AIChE J*., 58 (7), 2262-2269.

Arias, B., Grasa, G. S., Abanades, J. C. (2010). Effect of Sorbent Hydration on the Average Activity of CaO in a Ca-looping System. *Chem. Eng. J*., 163, 324-330.

Bachu, S. (2008). CO2 Storage in Geological Media: Role, Means, Status, and Barriers to Deployment. *Prog. Energy Combust. Sci*., 34, 254-273.

Baker, E. H. (1962). The Calcium Oxide-Carbon Dioxide System in the Pressure Range 1-300 Atmospheres. *J. Chem. Soc*., 87, 464-470.

Beer, J. M. (2000). Combustion Technology Developments in Power Generation in Response to Environment Challenges. *Prog. Energy Combust. Sci*., 26, 301-327.

Blamey, J., Anthony, E. J., Wang, J., Fennell, P. (2010). The Use of the Calcium Looping Cycle for Post-combustion CO2 Capture. *Prog. Energy Combust. Sci*., 36, 260-279.

Borgwardt, R. H. (1989). Calcium Oxide Sintering in Atmospheres Containing Water and Carbon Dioxide. *Ind. Eng. Chem. Res*., 28, 493-500.

Borgwardt, R. H. (1970). Kinetics of the Reaction of SO2 with Calcined Limestone. *Environ. Sci. Technol*., 4, 59-63.

Borgwardt, R. H. (1989). Sintering of Nascent Calcium Oxide. *Chem. Eng. Sci*., 44, 53-60.

Borgwardt, R. H., Roache, N. F., Bruce, K. R. (1986). Method for Variation of Grain Size in Studies of Gas-Solid Reactions Involving Calcium Oxide. *Ind. Eng. Chem. Fundam*., 25, 165-169.

Charitos, A., Rodriguez, N., Hawthorne, C., Alonso, M., Zieba, M., Arias, B., Kopanakis, G., Scheffknecht, G., Abanades, J. C. (2011). Experimental Validation of the Calcium Looping CO2 Capture Process with Two Circulating Fluidized Bed Carbonator Reactors. *Ind. Eng. Chem. Res*., 50, 9685-9695.

Davidson, J. F., Clift, R., Harrison, D. (1985). *Fluidization, 2nd Edition*, Academic Press.

Dobner, S., Sterns, L., Graff, R. A., Squires, A. M. (1977). Cyclic Calcination and Recarbonation of Calcined Dolomite. *Ind. Eng. Chem. Process Des. Dev*., 16, 479-486.

Donat, F., Florin, N. H., Anthony, E. J., Fennell, P. S. (2012). The Influence of High-temperature Steam on the Reactivity of CaO Sorbent for CO2 Capture. *Environ. Sci. Technol*., 46, 1262–1269.

Fang, F., Li, Z.-S., Cai, N.-S. (2009). Continuous CO2 Capture from Flue Gases using a Dual Fluidized Bed Reactor with Calcium-Based Sorbent. *Ind. Eng. Chem. Res*., 48, 11140-11147.

Galloy, A., Strohle, J., Epple, B. (2011). Design and Operation of a 1 MWth Carbonate and Chemical Looping CCS Test Rig. *VGB PowerTech*, 91, 64-68.

Harrison, D. P. (2004). The Role of Solids in CO2 Capture: A Mini Review. In: *Proceedings of the Seventh International Conference on Greenhouse Gas Control Technologies*, Vancouver, Canada, September 5-9, 2004.

Hughes, R., Lu, D., Anthony, E. J., Macchi, A. (2005). Design, Process Simulation and Construction of an Atmospheric Dual Fluidized Bed Combustion System for in situ CO2 Capture using High-Temperature Sorbents. *Fuel Process. Technol*., 86, 1523-1531.

Hughes, R. W., Macchi, A., Lu, D. Y., Anthony, E. J. (2009). Changes in Limestone Sorbent Morphology during CaO-CaCO3 Looping at Pilot Scale. *Chem. Eng. Technol*., 32, 425-434.

Intergovernmental Panel on Climate Change (IPCC), (2007). Climate Change 2007: Synthesis Report. *Contribution of Working Groups I, II, III, to Fourth Assessment Report of the Intergovernmental Panel on Climate Change*, Geneva, Switzerland.

Joutsenoja, T., Heino, P., Hernberg, R., Bonn, B. (1999). Pyrometric Temperature and Size Measurements of Burning Coal Particles in a Fluidized Bed Combustion Reactor. *Combust. Flame*, 118, 707-717.

Laursen, K., Duo, W., Grace, J. R., Lim, J. (2000). Sulfation and Reactivation Characteristics of Nine Limestones. *Fuel*, 79, 153-163.

Laursen, K.; Grace, J. R.; Lim, C. J. (2001). Enhancement of the Sulfur Capture Capacity of Limestones by the Addition of Na2CO3 and NaCl. *Environ. Sci. Technol*., 35, 4384-4389.

Lu, D. Y., Hughes, R. W., Anthony, E. J. (2008). Ca-based Sorbent Looping Combustion for CO2 Capture in Pilot-Scale Dual Fluidized Beds. *Fuel Process. Technol*., 89, 1386-1395.

Lu, D. Y., Hughes, R. W., Anthony, E. J., Manovic, V. (2009). Sintering and Reactivity of CaCO3-Based Sorbents for in situ CO2 Capture in Fluidized Beds under Realistic Calcination Conditions. *J. Environ. Eng*., 135, 404-410.

Jia, L., Hughes, R., Lu, D., Anthony, E. J. (2007). Lau, I. Attrition of Calcined Limestones in Circulating Fluidized Bed Systems. *Ind. Eng. Chem. Res.*, *46*, 5199-5209.

MacKenzie, A., Granatstein, D. L., Anthony, E. J. (2007). Economics of CO2 Capture using the Calcium Cycle with a Pressurized Fluidized Bed Combustor. *Energy Fuels*, 21, 920-926.

Manovic, V., Anthony, E. J. (2010). Carbonation of CaO-Based Sorbents Enhanced by Steam Addition. *Ind. Eng. Chem. Res*., 49, 9105-9110.

Manovic, V., Anthony, E. J. (2010). Competition of Sulphation and Carbonation Reactions during Looping Cycles for CO2 Capture by CaO-Based Sorbents. *J. Phys. Chem*. *A*, 114, 3997-4002.

Manovic, V., Anthony, E. J., Grasa, G., Abanades, J. C. (2008). CO2 Looping Cycle Performance of a High-Purity Limestone after Thermal Activation/Doping. *Energy Fuels*, 22, 3258-3264.

Manovic, V., Komatina, M., Oka, S. (2008). Modeling the Temperature in Coal Char Particle during Fluidized Bed Combustion. *Fuel*, 87, 905-914.

Metz, B., Davidson, O., de Conninck, H., Loos, M., Meyer, L. (2005). Special Report on Carbon Dioxide Capture and Storage. *Intergovernmental Panel on Climate Change*, Cambridge Univ. Press, 2005.

Paterson, N., Elphick, S., Dugwell, D. R., Kandiyoti, R. (2001). Calcium-Based Liquid Phase Formation in Pressurized Gasifier Environments. *Energy Fuels*, 15, 894-902.

Sun, P., Grace, J. R., Lim, C. J., Anthony, E. J. (2006). Removal of CO2 by Calcium-based Sorbents in the Presence of SO2. *Energy Fuels*, 21, 163-170.

Stewart, M. C., Manovic, V., Anthony, E. J., Macchi, A. (2010). Enhancement of Indirect Sulphation of Limestone by Steam Addition. *Environ. Sci. Technol*., 44, 8781-8786.

Symonds, R. T., Lu, D. Y., Hughes, R. W., Anthony, E. J., Macchi, A. (2009). CO2 Capture from Simulated Syngas via Cyclic Carbonation/Calcination for a Naturally Occurring Limestone: Pilot-Plant Testing. *Ind. Eng. Chem. Res*., 48, 8431-8440.

Symonds, R., Lu, D., Macchi, A., Hughes, R., Anthony, E. J. (2009). CO2 Capture from Syngas via Carbonation/Calcination for a Naturally Occurring Limestone: Modelling and Bench-scale Testing. *Chem. Eng. Sci*., 64, 3536-3543.

Tullin, C., Ljungstrom, E. (1989). Reaction between Calcium Carbonate and Sulphur Dioxide. *Energy Fuels*, 3, 284-287.

Wang, C., Jia, L., Tan, Y., Anthony, E. J. (2010). The Effect of Water on the Sulphation of Limestone. *Fuel*, 89, 2628-2632.

Wang, W., Ramkumar, S., Li, S., Wong, D., Iyer, M., Sakadjian, B. B., Statnick, R. M., Fan, L.-S. (2010). Subpilot Demonstration of the Carbonation-Calcination Reaction (CCR) Process: High-Temperature CO2 and Sulfur Capture from Coal-Fired Power Plants. *Ind. Eng. Chem. Res*., 49, 5094-5101.

Yang, H., Xu, Z., Fan, M., Gupta, R., Slimane, R. B., Bland, A. E., Wright, I. (2008) Progress in Carbon Dioxide Separation and Capture: A Review. *J. Environ. Sci*., 20, 14-27.

Chapter 5 – System Design, Construction, and Commissioning of a Dual Fluidized Bed System for Calcium Looping

Robert T. Symonds[a], Dennis Y. Lu[a], Scott Champagne[a], Arturo Macchi[b], Edward J. Anthony[c]

[a]Natural Resources Canada, CanmetENERGY

1 Haanel Drive, Ottawa, Ontario K1A 1M1, Canada

[b]Department of Chemical and Biological Engineering, University of Ottawa

161 Louis Pasteur Street, Ottawa, Ontario K1N 6N5, Canada

[c]School of Applied Science, Cranfield University

Cranfield, Bedfordshire MK43 0AL, United Kingdom

Manuscript prepared for publication in an academic journal.

5.1 – Abstract

Calcium looping (CaL) is a promising, economically competitive post-combustion CO_2 capture technology that is actively being tested at the larger pilot-scale (up to 1.7 MWth). Information about sorbent performance, the fate of trace pollutant emissions, dual fluidized bed operating configurations, and effect of realistic operating conditions still needs to be addressed. Unfortunately to date, most such data is generated at the bench-scale and cannot accurately represent what is observed at the pilot-scale and beyond.

This paper delineates the design, construction, and commissioning of an atmospheric dual fluidized bed system for continuous CO_2 capture and provides an overview of the main process components. The research group at Natural Resources Canada, CanmetENERGY – Ottawa initiated this effort with the main focus on bridging the gap between bench-scale testing and what can be expected at the commercial scale. The 100 kW_{th} pilot-scale system is capable of operating over a wide range of conditions, system configurations, fuel feedstocks, and sorbents without major modifications to the overall system, as would be the case for larger-scale facilities. Along with a successful commissioning campaign, preliminary continuous CO_2 capture testing has yielded promising results, with CO_2 capture efficiencies greater than 90% and CO_2 levels of over 90 vol.% during oxy-fired combustion sorbent regeneration with flue gas recycle.

5.2 – Introduction

CO_2 emissions from fossil-fuelled power stations are believed to be a major contributor to global warming and climate change (Pachauri & Reisinger, 2007). One method for reducing CO_2 emissions would be *via* a carbon capture and storage (CCS) technology. The rationale for the use of CCS on fossil-fuelled power plants is that, when deployed with other technologies

(e.g., renewables), the overall cost of electricity would be minimized. Since the use of renewable sources of electricity (e.g., wind, solar, etc.) are intermittent, the implementation of CCS to coal-fired power plants would reduce the need for large-scale energy storage systems. At this time, CCS has been proposed for fossil-fuel combustion (related to power generation), where the CO_2 is captured at a particular point within the overall process. Other industries such as cement production, iron / steel making, and natural gas treatment could also be adapted with CO_2 capture technologies. After the CO_2 has been captured, it is then compressed to 80 bar or more to facilitate transportation to a storage site. Once at one of the many types of stable geological sites, the CO_2 is injected underground trapping it and preventing its subsequent emission into the atmosphere (Bachu, 2008) (Beer, 2000) (Metz, Davidson, de Conninck, Loos, & Meyer, 2005). To date, all of the individual elements of the CCS chain including capture, compression, transportation, and sequestration have been demonstrated at or close to the commercial scale (Krebs, 2012).

Several processes aimed at reducing CO_2 emissions from fossil-fuelled power plants are currently being investigated. First generation processes such as oxy-fuel combustion and amine scrubbing are being applied at the demonstration level (Global CCS Institute, 2014) (Vattenfall, 2010) (Ademe, 2010), whereas the Integrated Gasification Combined Cycle (IGCC) CSS technology is moving towards demonstration also (Global CCS Institute, 2014) (Dietmar, 2010). Unfortunately, all of these technologies result in a fairly high efficiency penalty, which increases the demand for a more economically competitive alternative. This paper describes the design, construction, and commissioning of a 100 kW_{th} dual fluidized bed system, utilizing calcium looping technology as a method for CO_2 capture from fossil-fuelled power plants.

5.3 – Calcium Looping for Post-Combustion CO_2 Capture

Of the many developing capture technologies, CO_2 sorption processes such as calcium looping (CaL) appear to be promising. The process was first proposed by (Shimizu, Hirama, Hosoda, Kitano, Inagaki, & Tejima, 1999) for the goal of carbon capture and storage, with several configurations existing to maximize net electrical efficiency (Abanades, Anthony, & Oakey, 2005). The capture technology is based on the reversible, exothermic reaction between calcined limestone (CaO) and CO_2 (Equation 5.1):

$$CaO_{(s)} + CO_{2(g)} \leftrightarrow CaCO_{3(s)} \qquad \Delta H^0_{298\,K} = -179\ kJ\ mol^{-1} \tag{5.1}$$

Figure 5.3.1 shows the principle of the calcium looping process. In the first reactor (carbonator), CO_2 is captured from flue gas *via* Reaction 1 leaving a CO_2 depleted stream containing mostly N_2 and other trace species not captured by the system. In the second reactor, the CO_2 is released *via* the calcination reaction (reverse of Reaction 1) resulting in an effluent gas of concentrated CO_2 (>90 vol.%) which, after drying and oxygen removal, is suitable for liquefaction and ultimate sequestration. Since the calcination reaction is endothermic, heat is supplied by the oxy-combustion of a fuel, such as coal, with high purity O_2 and a diluent; recycled flue gas or steam. Based on chemical equilibrium considerations (Baker, 1962), operation temperatures for the two reactors are 600-650^{o}C and 900-950^{o}C, respectively at atmospheric pressure.

The solids (CaO and $CaCO_3$) are looped between the reactors to establish a closed loop and take advantage of the reversible nature of Equation 5.1. Unfortunately, it is well known that the sorbent CO_2 conversion reactivity decreases over repeated cycles down to a minimum value (typically between 8 and 12%) due to chemical and high temperature sintering (Lu, Hughes,

Anthony, & Manovic, 2009). To maintain a particular capture efficiency, a make-up flow must be introduced into the system while simultaneously removing a fraction of the spent sorbent, which includes ash generated during the oxy-combustion of solid fuels (Abanades J. C., Anthony, Lu, Salvador, & Alvarez, 2004). It should be mentioned at this point that several techniques have been demonstrated at the bench-scale to enhance the mechanical (particle attrition resistance) and chemical behaviour of the sorbents to improve performance. Some of these techniques include chemical doping, steam reactivation, thermal pre-treatment, and pelletization (Manovic, Anthony, & Loncarevic, 2009) (Manovic & Anthony, 2007), but none have been tested at the pilot-scale to date.

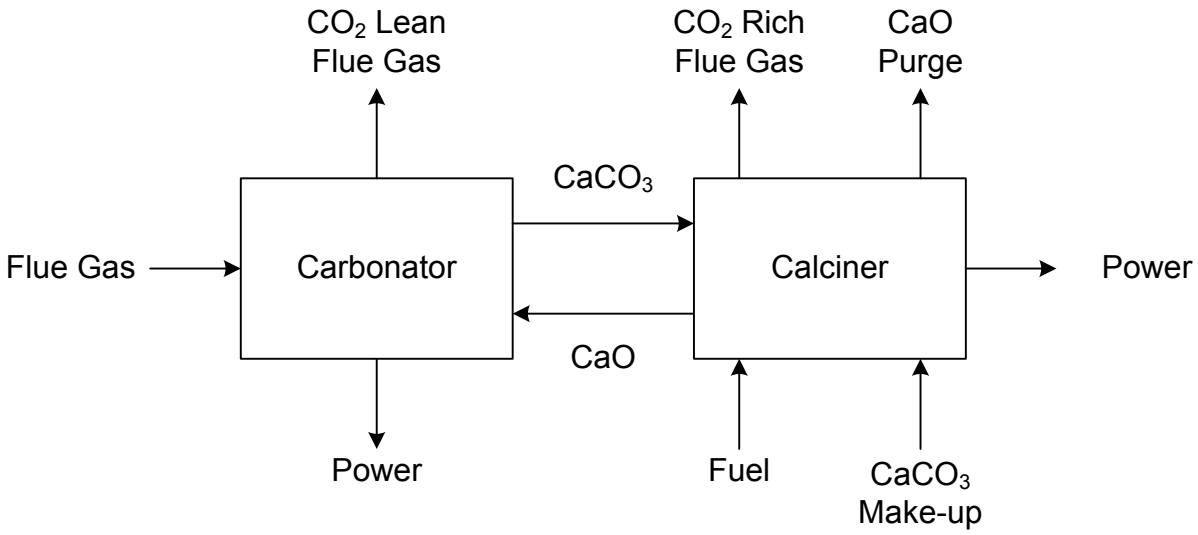

Figure 5.3.1: Simplified process flow diagram for calcium looping (CaL).

The largest pilots globally for post-combustion CaL testing are the 1.9 MW_{th} unit in Taiwan (Chang, et al., 2013) and the 1.7 MW_{th} La Pereda system in Spain, which has been able to treat up to 2400 kg/h of flue gas from an existing 50 MW_e CFBC power plant (Arias, et al., 2013). Also successfully commissioned is a 1 MW_{th} test facility located at Darmstadt University. Experimental campaigns using propane and pulverized coal as fuels to supply the

heat for sorbent calcination provided CO_2 capture efficiencies above 90% (Galloy, Strohle, & Epple, 2011). Several smaller units also exist such as the 200 kW_{th} pilot plant at IFK (Hawthorne, et al., 2011) and the 30 kW_{th} pilot plant at CSIC (Rodriguez, Alonso, & Abanades, Experimental Investigation of a Circulating Fluidized-Bed Reactor to Capture CO2 with CaO, 2011).

Even though CaL technologies have now been demonstrated at larger scale, there is still a significant quantity of information about sorbent performance, the fate of trace pollutant emissions (for example SO_2 and HCl), dual fluidized bed operating configurations, and the effect of realistic operating conditions that still needs to be determined. To date, there is a considerable amount of data on CaL technologies that have been performed at the bench-scale but, unfortunately, this information cannot always represent what is observed at the pilot-scale (Symonds, Lu, Manovic, & Anthony, 2012). Thus, the main focus of this work is to bridge the gap between bench-scale testing and what can be expected at the commercial scale (i.e., proper gas-solid contacting, heating rates, reactive environments, and attrition), where the data generated can better facilitate process modelling and scale-up engineering. This will be done *via* the use of a 100 kW_{th} pilot-scale dual fluidized bed system where a wide range of operating conditions, systems setups, feedstocks, and sorbents can be examined without major modifications to the overall system, as would be the case for larger-scale demonstration plants.

5.4 – Dual Fluidized Bed System Design

5.4.1 – Objectives

CanmetENERGY developed its first dual fluidized bed system for calcium looping technology in 2004 (Hughes, Lu, Anthony, & Macchi, 2005). The dual fluidized bed system

described here addresses the need for extended piloting capabilities to evaluate calcium looping technology enhancements over the last decade. The design of the 100 kW_{th} dual fluidized bed calcium looping system has the following objectives: (1) prove the capabilities of several different reactor configurations such as circulating fluidized bed (CFB) vs. bubbling fluidized bed (BFB) operation and pneumatic vs. mechanical sorbent transfer system; (2) determine acceptable operating conditions and practical operational limits for all of the configurations; (3) determine practical start-up and shut-down procedure for each of the configurations; and (4) demonstrate continuous CO_2 capture (>90%) using calcium based sorbents under realistic operating conditions including: oxy-fuel combustion with flue gas recycle (dry and wet), CO_2 capture from real flue gas generated from natural gas and solid fuel combustion, and simultaneous sorbent make-up and removal. It is a further objective of this paper to provide a detailed description of the research facility for use by the calcium looping research community.

5.4.2 – Design Methodology

Calciner

As mentioned in the previous sections, it is imperative that the calciner operate under oxy-fuel combustion mode, as this is the only economic method in which to produce a concentrated stream of CO_2 suitable for compression. It was desired to have a recycled flue gas system that could be operated at elevated temperatures in order to permit wet flue gas recycle as a means of lowering the overall CO_2 partial pressure in the calciner. Recent bench-scale experimentation has shown significant benefits in terms of limiting sorbent decay over repeated cycles *via* steam addition during calcination (Champagne S. , Lu, Macchi, Symonds, & Anthony, 2013). Furthermore, the feed gas system to the calciner was to be connected to an auxiliary

steam boiler to increase the steam partial pressure to examine any additional benefits above those expected with wet flue gas recycle.

The calciner was to be designed to handle a variety of solid feedstocks for sorbent regeneration including coals, cokes, and biomasses in order to study potential sorbent / ash interactions (Hughes, Macchi, Lu, & Anthony, 2009). It was essential that the calciner could be pre-heated within a relatively short duration, and that the entire reactor (both bed and riser) temperature profile could be controlled and maintained at a given temperature, while minimizing heat loss to the surroundings.

As it was of particular interest to study a variety of sorbent types (natural, modified, pelletized, etc.) (Manovic, Wu, He, & Anthony, 2012) and particle sizes (<1000 micron), the calciner required the capability of operating in either circulating or bubbling fluidized bed modes, due to practical limitations on reactor superficial gas velocities. Therefore, the calciner was required to incorporate both an overflow discharge and a loop-seal (in the return-leg) as a method to remove material and minimize gas bypass, which could cause unwanted sorbent re-carbonation. A controlled discharge method was required to purge the system of ash and spent sorbent.

Carbonator

Similar to the calciner, the carbonator required a pre-heat method along with temperature profile control, as this temperature will ultimately govern the maximum CO_2 capture efficiency. The necessity for steam addition during carbonation was required based on two important factors. Firstly, flue gas generated from a real fossil-fuelled power plant will contain a certain amount of moisture (assuming it wasn't condensed prior to entering the carbonator) and

secondly, it has been reported by several authors that there exists a considerable improvement in sorbent CO_2 capture carrying capacity *via* the addition of steam during carbonation (Symonds, Lu, Macchi, Hughes, & Anthony, 2009) (Symonds, Lu, Hughes, J, & Macchi, 2009) (Li, Liu, & Cai, 2014). Consequently, the fluidizing gas entering the carbonator should contain steam either from an auxiliary steam boiler and / or from the combustion of a carbonaceous fuel such as natural gas or solid fuels. The latter has the added benefit of flexibility to study the effect of trace species, such as SO_2, on sorbent performance, which is well known to be detrimental to the calcium looping technology (Sun, Grace, Lim, & Anthony, 2006) (Arias B. , Cordero, Alonso, & Abanades, 2012). Several investigations of the chemical reaction rates and CO_2 capture capacities for many sorbents have been conducted (Abanades J. C., Anthony, Lu, Salvador, & Alvarez, 2004) (Bhatia & Perlmutter, 1983) and concluded that there is only a relatively short fast reaction kinetic-controlled regime suitable for large-scale CO_2 capture facilities. Based on this fact, the optimum solids residence time and bed inventory can be determined for a particular sorbent, leading to the determination of an appropriate reactor size, superficial fluidizing gas velocity (if operating in circulating mode), and overflow discharge height (if operating in bubbling mode).

Solids Transfer

Depending on the mode of operation of both reactors, several options exist for transferring the solids from the calciner to the carbonator, and *vice versa*. Given that the solids transfer essentially dictates the overall reliability of the calcium looping process (Lu, Hughes, & Anthony, 2008) (Alonso, Rodriguez, Gonzalez, Grasa, Murillo, & Abanades, 2010) (Hawthorne, et al., 2011), special attention should be given to this particular portion of the system. The following criteria were established as a metric in designing the solids transfer system: (1) the

solids flow must be able to be accurately controlled / maintained at any particular value and allow for the adjustment of bed inventories; (2) the system should try to minimize any particle attrition or fragmentation; (3) allow for solids sampling whilst minimizing system disruptions; (4) minimize possible sorbent re-carbonation; and (5) minimize or eliminate any gas bypass into, out of, or between the carbonator and calciner.

5.5 – Dual Fluidized Bed System Engineering and Construction

The dual fluidized bed reactor system is shown in Figure 5.5.1. In addition to the two fluidized bed reactors, acting as the carbonator and calciner, the facility is comprised of two feed hoppers (fuel and limestone), a flue gas treatment train, recycle gas loop, solids transfer system, fluidizing gas supply system, gas sampling train, and electric boiler. All solids transfer and flue gas lines are constructed of high temperature stainless steel and are externally insulated to minimize heat loss to the surroundings (insulation not shown in Figure 5.5.2 and Figure 5.5.3).

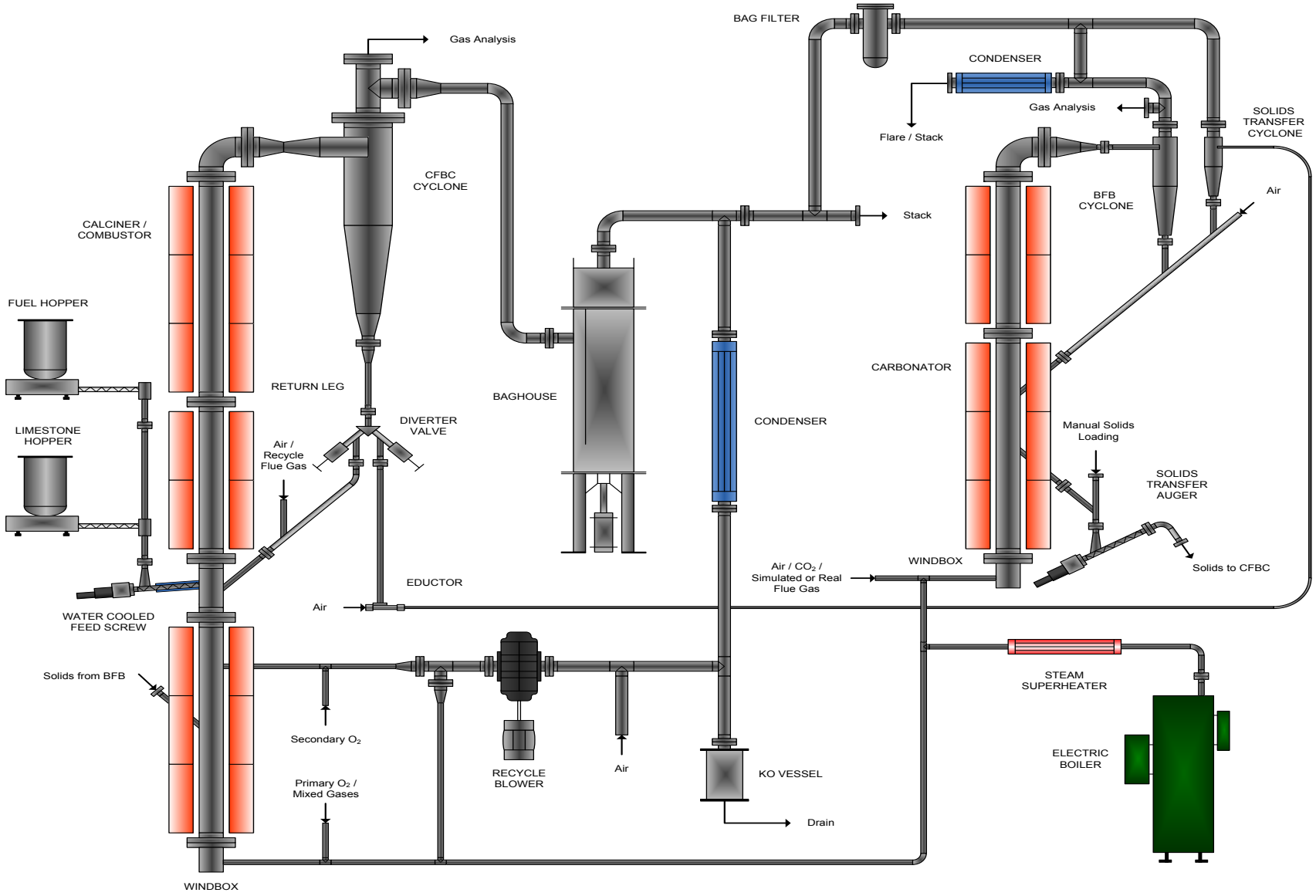

Figure 5.5.1: Schematic of the CanmetENERGY dual fluidized bed reactor system.

Oxy-fuel Combustor / Calciner and Carbonator

Both the oxy-fuel combustor / calciner (Figure 5.5.2: A) and carbonator (Figure 5.5.2: B) have an internal diameter of 0.1 m and are constructed out of SS310. The total heights of each reactor are 5.1 and 3.0 m, respectively, and are outfitted with high temperature electric heaters (C) capable of operating at up to 1100^{o}C. Each heater section (hemi-cylindrical) can supply up to 2.5kW of heat and is constructed of high temperature alumina-silica insulation to minimize heat loss. The calciner is surrounded by 16 heater sections which are used to pre-heat the system before the addition of solid fuel, and can be used throughout experimentation to ensure a uniform temperature profile along the entire reactor height. Similarly, the carbonator is enclosed with 10 heater sections which control the reactor temperature over the entire duration of experimentation. Currently, temperature can be controlled within +/- 1^{o}C.

The calciner and carbonator have been constructed with several inlet and discharge ports, which allow for fuel / limestone feeding (D), cyclone return (E), solids sampling (F), spent sorbent / ash discharge (G), and solids transfer (H). Each reactor has been fabricated with high efficiency cyclones (I) to re-entrain the sorbent during circulating fluidized bed operation, minimizing sorbent elutriation.

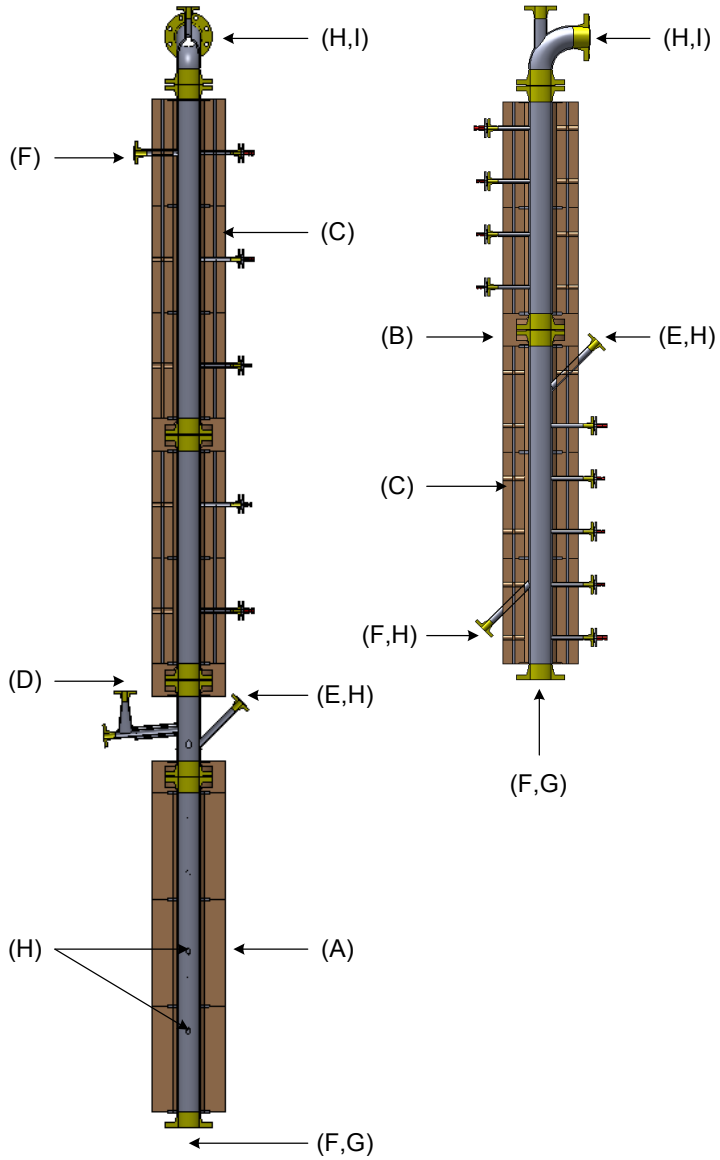

Figure 5.5.2: CanmetENERGY oxy-fuel combustor / calciner and carbonator (section view).

Flue Gas Generator

As mentioned above, one of the main objectives of this facility was to have the flexibility to operate the carbonator under real flue conditions. Therefore, a small combustor was constructed that can produce flue gas from the combustion of both natural gas and solid fuels (Figure 5.5.3: A). The vessel is constructed from SS316 and is lined with high temperature refractory (alumina-silica). The combustion flue gas exits the vessel where it is then pumped

into the carbonator windbox (B) using a heated-head pump, avoiding any unwanted steam condensation. All process lines are heat traced in order to avoid steam condensation and a solids discharge port (C) is located at the bottom of the vessel to remove any ash build-up during solid fuel combustion.

Solids Transfer System

The solids transfer system is comprised of two main components: (1) transfer of solids from the calciner to the carbonator and (2) transfer of solids from carbonator to the calciner. As previously stated, the material leaving the calciner would either be from an overflow port or from the loop-seal, depending on the fluidizing regime in the reactor (Figure 5.5.2: H). The overflow ports (45 degree decline) are located approximately 0.46m and 0.84 m above the windbox and discharge the material through a 0.0266 m internal diameter line directly into a pneumatic eductor (Figure 5.5.3: D). The slope of the discharge line has been specifically designed to ensure a seal (*via* the use of solids) between the calciner and eductor to minimize gas by-pass, which could cause unwanted re-carbonation or dilution of the concentrated CO_2 effluent stream. During circulating fluidized bed operation, the solids collected from the calciner cyclone (E) are directed downwards into a specialized high temperature diverter valve (F). This valve can be positioned to either allow solids flow to the return-leg (i.e., back to the calciner) or any required solid flux split down to the transfer system. This flexibility is particularly useful during start-up when solids transfer to the carbonator is not required. Material then drops down through a 0.0254 m line into a U-shaped loop-seal (G) and eventually into the pneumatic eductor. It should be mentioned at this point, that both the overflow and loop-seal systems can be operated independently or simultaneously in tests with large particle size distributions.

The pneumatic eductor uses compressed air to transfer the solids vertically through a 0.0191 m line to a high-efficiency cyclone (H), which discharges into a return-leg (I), and is gravity fed into the carbonator. The transfer rate can be adjusted by changing the flowrate of compressed air to the eductor and is calibrated prior to testing *via* the use of a solids sampling port. Additional compressed air is used to ensure the material exiting the transfer cyclone flows smoothly into the carbonator.

Unlike the calciner, overflow discharge is the only means of removing material from the carbonator, although the system does have a cyclone (J). The overflow port is located 0.47 m above the carbonator windbox, on a 45 degree decline, and drops the material down into a specially designed 0.0254 m mechanical auger system (K). The auger transfers the solids up a 45 degree pipe section and drops them into the calciner. This angle was specifically chosen to provide a solids seal between both reactors, eliminating any gas by-pass. Other benefits of this mechanical transfer method includes (1) the auger can be calibrated for any material (different particle size and density); (2) the solids transfer rate is known and can be easily adjusted; (3) ensures a minimum bed loading in the carbonator; and (4) during solids loading to the system, the bed inventory in each reactor can be effortlessly adjusted to suit any type of operation. It should be noted that independent calibrations of both pneumatic and mechanical transfer systems show excellent agreement, and transfer rates between 20 and 50 kg/h can be readily achieved.

Gas Supply

The main gas supply to the calciner, either ambient air or recycled flue gas, is provided by a lobe style blower. Before the gas enters the calciner windbox (Figure 5.5.3: L), it is first mixed with a pure oxygen stream within a gas diffuser to ensure proper mixing. Up to four

additional bottled gases can be added, such as SO_2, as necessary. The fluidizing gas is fed through a SS316 windbox outfitted with a sintered metal distributor, to minimize jetting effects and ensure uniform flow distribution, before entering the calciner. It should be mentioned that prolonged exposure to high temperature (> 900^{o}C) environments can cause increased pressure drop over the plate due to enhanced sintering. The fluidizing gas can be split prior to the windbox to allow for injection at various levels along the reactor bed height. Typical operating superficial velocities in the calciner range from approximately 1 to 4 m/s.

The carbonator has been constructed with a windbox containing a sintered metal distributor. The fluidizing gas is provided either by (1) bottled gas / compressed air during simulated flue gas operation or (2) from the flue gas generator during real flue gas operation. Operating superficial velocities range between 0.5 and 2 m/s. Additionally, both reactors feed gas lines are connected to an electric boiler (see Figure 5.5.1), permitting steam addition during experimental testing.

A slip stream is removed after the recycle flue gas blower for use in various parts of the calciner system. This includes solids feed purging and solids entrainment back to the calciner through the return-leg. Other gas supplies, such as those required for the eductor and solids transfer to the carbonator, are provided *via* a building air compressor and are controlled either by the use of mass flow controllers (MFC's) or rotameters. Table 5.5.1 lists each process gas supply stream with approximate flow ranges:

Table 5.5.1: Summary of gas supplies to the CanmetENERGY dual fluidized bed system (SLPM).

Gas Supply	Flow Range
Calciner Primary Fluidizing Gas	100 – 400
Calciner Secondary Fluidizing Gas	0 – 140

Primary Oxygen	0 – 200
Secondary Oxygen	0 – 27
Calciner Bottled Gases	0 – 50
Solids Feed Purging	0 – 10
Return-leg Entrainment	5 – 15
Carbonator Primary Fluidizing Gas	50 – 200
Carbonator Bottled Gases	0 – 50
Steam	0 – 600
Eductor	15 – 22
Solids Transfer to Carbonator	12 – 18

Solid Fuel and Limestone (Sorbent) Supply

The accurate and controlled supply of fuel to the calciner (and flue gas generator), as well as limestone make-up, is important for the overall process goal of achieving consistent experimental conditions. Therefore, loss-in-weight feeders are used to generate a controlled, constant mass flow of solid fuel and limestone into the system (M). Since one of the facility objectives is to operate with several different fuel types, including coals, cokes, and biomasses, the fuel feeder has been designed to handle different particle shapes, sizes, and densities *via* the use of several different feed augers. Feed rates of up 30 kg/h solid fuel and 10 kg/h of sorbent are achievable with the current arrangement. Both the calciner and flue gas generator are fabricated with a water-cooled incline auger (5 degree incline) which meter the solids into the reactors (N). They have been specifically designed to operate in parallel with the loss-in-weight feeders to make certain a plug-flow of solids enter the combustion chambers. This minimizes gas by-pass and reduces the risk of pre-mature combustion in the feed lines and air ingress.

Flue Gas Train

Since the flue gas leaving the calciner and carbonator cyclones are at high temperature, and typically contain some fraction of solids, flue gas treatment is required. The flue gas is first cooled down to approximately 200^{o}C; either by natural heat loss to the surrounding environment or by a water cooled heat exchanger (O). In the case where steam is added to the system, a condenser (P) is used to knock-out the moisture before entering the baghouse. The bag house (Q) is constructed of SS316 and uses high temperature Nomex bags to remove any solids contained in the flue gas. After exiting the baghouse, a portion of the flue gas is sent to an additional condenser to remove any remaining moisture (if operating in dry recycle mode), before being re-circulated back into the calciner. The remainder of the flue gas, including that from the carbonator and solids transfer cyclone, is removed from the system by an induced draft (ID) fan. The pressure of both trains can be independently controlled by means of pressure control valves situated before the ID fan.

Instrumentation, Control, and Gas Analysis

The dual fluidized bed system is fully automated with safety interlocks and contains many sensors and control loops. Both pressure and temperature can be measured at one second intervals over the entire height of both reactors (see Figure 5.5.2). Furthermore, all inlet gas flow rates are measured and controlled using MFC's or vortex flow meters in order to close the CO_2 mass balance and accurately calculate the CO_2 capture efficiency. The effluents from the calciner, carbonator, and flue gas generator are connected to gas conditioning and analysis trains (O_2, CO_2, CO, SO_2, and NO_x). A moisture probe can also be connected to any of the various ports in the system to accurately measure the moisture content of the sample gas. The product gas concentration profiles can be used to validate existing carbonator models (Alonso,

Rodriguez, & Abanades, 2009) (Hawthorne, Charitos, Perez-Pulido, Bing, & Scheffknecht, 2008).

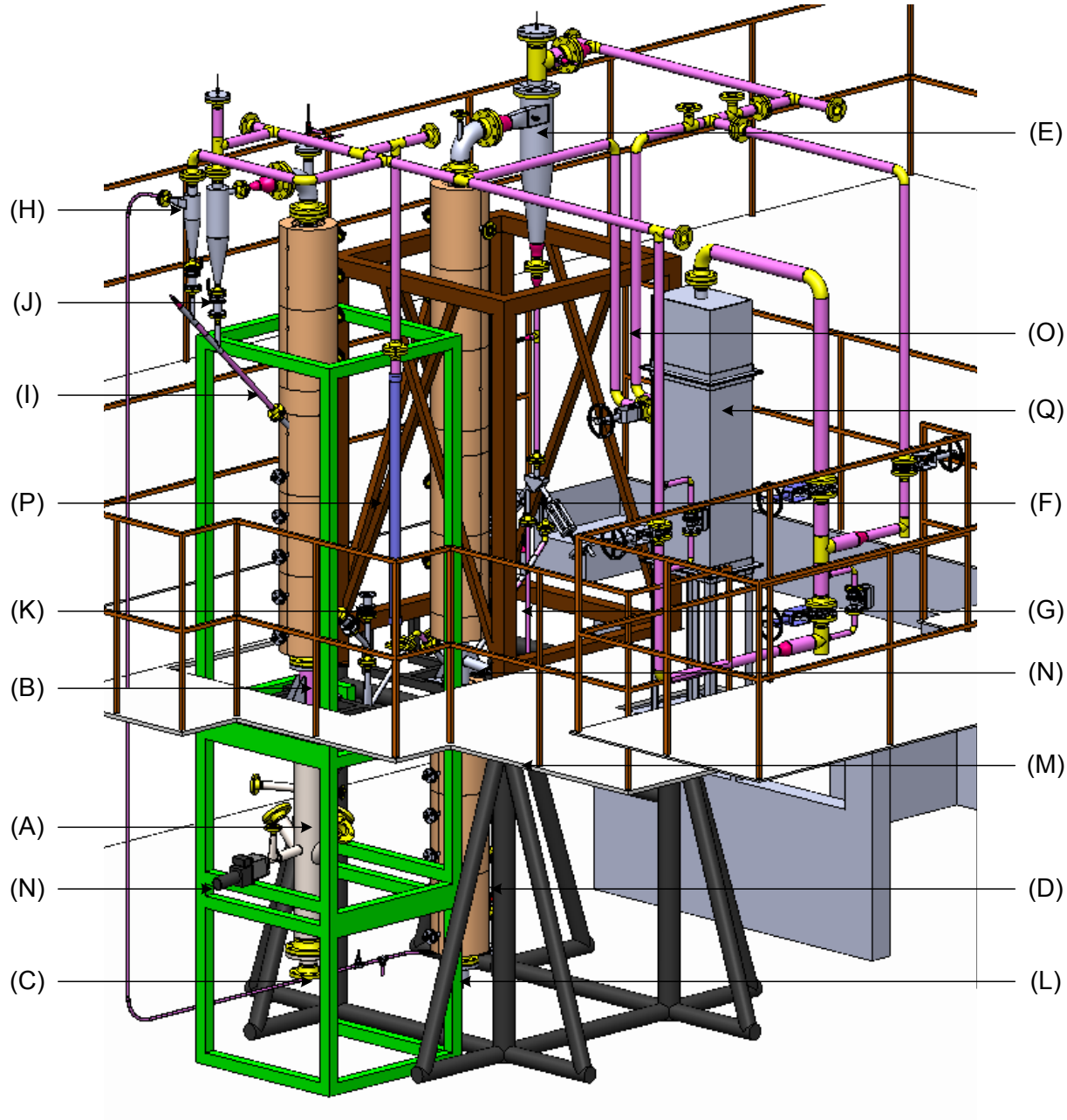

Figure 5.5.3: General arrangement of the CanmetENERGY dual fluidized bed reactor system.

5.6 – Commissioning and Preliminary Experimental Results

Commissioning

During the initial commissioning test trials of the dual fluidized bed reactor system, it was shown that the calciner can operate in both air and oxy-fuel fired modes with several feedstocks (including biomass and coal). Figure 5.6.1 illustrates the period of switch-over from air-fired to oxy-fired combustion. The switch-over period took approximately 45 minutes, which is a similar duration as the 0.8 MW_{th} oxy-CFBC facility located at CanmetENERGY (Jia, et al., 2012). CO_2 levels of over 90% were achieved during oxy-fuel combustion (see Figure 5.6.2), and it was determined that both the overflow discharge and loop-seal system solids transfer methods functioned as designed. Furthermore, the system has been tested in fully continuous CO_2 capture mode, using both the solids discharge methods. In both cases, a CO_2 capture efficiency of greater than 90% was achieved using particles in the size range of 250 to 810 micron. Other design objectives were also attained such as: stable temperature profiles in the calciner and carbonator (Figure 5.6.2 and Figure 5.6.3, respectively), controllable solids transfer rates between reactors (Figure 5.6.4), and solids sampling without system disruptions.

Based on results for the commissioning tests, the system has been shown to be flexible to a multitude of operating conditions, while also being reliable over long duration testing. By allowing for different solids transfer methods, a variety of sorbents with varying physical characteristics (i.e., particle size, density, etc.) can be tested without the risk of affecting particle attrition. With the combination of full oxy-fuel combustion and CO_2 capture from real flue gas, the dual fluidized bed system can closely mimic what can be expected in a demonstration or fully commercialized plant.

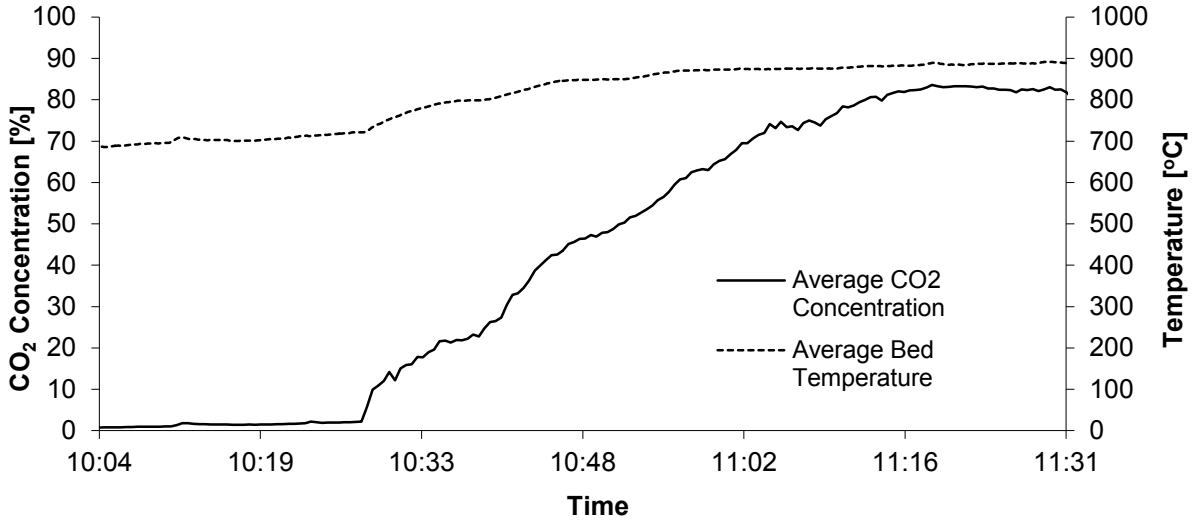

Figure 5.6.1: Average CO_2 concentration and bed temperature versus time in the calciner during switch-over from air-fired to oxy-fired operation (air-fired operation initiated at ~10:30).

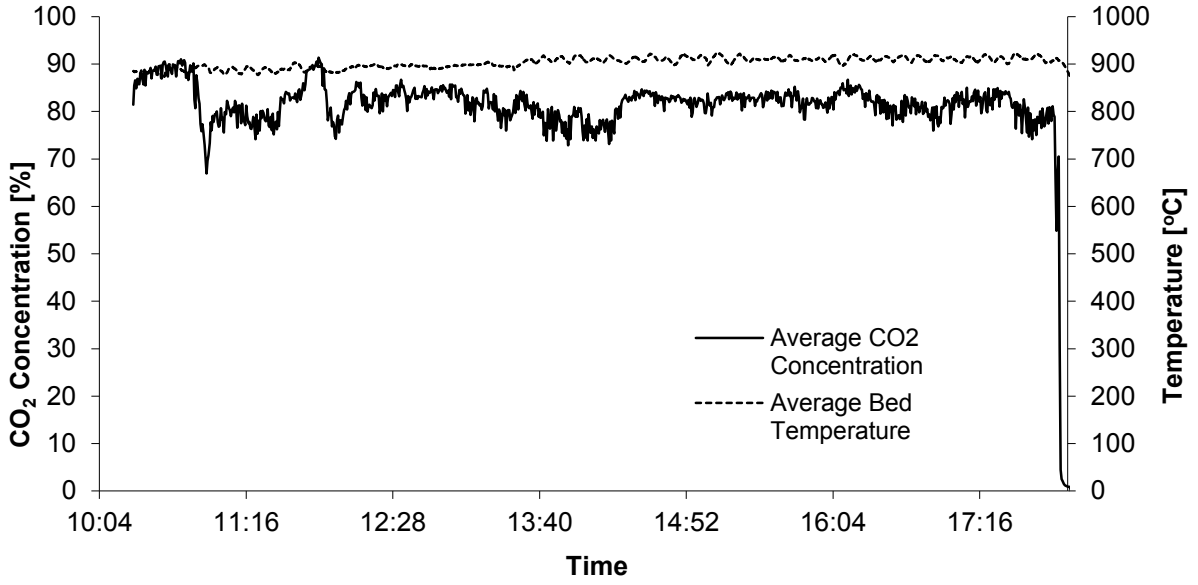

Figure 5.6.2: Average CO_2 concentration and bed temperature versus time in the calciner during oxy-fired operation.

Preliminary Experimental Results

The pilot-scale calcium-looping facility was used to evaluate CO_2 capture from flue gas in continuous operation for several hours. Each experimental trial consisted of three periods: (1) simulated flue gas (15 vol.% CO_2) was fed into the carbonator while simultaneously an initial batch of sorbent was introduced into the looping system; (2) once the initial batch of sorbent could no longer maintain the desired CO_2 capture level (>90%), additional fresh sorbent was periodically added until the previous CO_2 capture level was achieved; and (3) the system was maintained under stable operating conditions (i.e., no addition of fresh sorbent) until the CO_2 capture level diminished to less than 50% (Figure 5.6.3). A total of approximately 30 hours of preliminary CO_2 capture testing has been achieved without any major operational issues, indicating good system reliability in terms of oxy-fuel sorbent regeneration, solids transfer, and fuel/sorbent feed system control.

Figure 5.6.4 shows the bed differential pressure profile for both the calciner and carbonator during continuous CO_2 capture experimentation. These results indicate that the solids transfer rate from the calciner to carbonator, and vice versa, can be accurately controlled and equalized to maintain a given bed inventory in both reactors. Several solids samples were taken from the transfer system during continuous CO_2 capture operation without affecting the overall process (i.e., solids transfer stability, bed inventories, temperature profiles, etc.).

It was found that oxy-fuel combustion, under high CO_2 partial pressures, is reliable for sorbent regeneration within the right temperature window (typically >900°C). The CO_2 content of the solid samples taken from the calciner, either at the loop-seal or at the overflow discharge at the dense bed, are low (<0.5%) at these conditions. In terms of CO_2 content in the solid samples from the carbonator, the carbonation conversions range between 8 and 13% and indicate

that carbonation has mainly occurred on the particle surface under realistic operation conditions (~650^{o}C and 15 vol.% inlet CO_2 concentration). It was observed that there was a conversion drop with increasing cyclic time (Figure 5.6.3), but the decline was not significant and could be easily compensated for by adding a suitable amount of sorbent makeup.

Steam was added to the carbonator during one of the preliminary experimental trials while maintaining similar operating conditions as previously discussed. Initial results signify an improvement in sorbent performance by extending the initial, high-efficiency CO_2 capture period, and lowering the negative effect of sintering caused during repeated calcination / carbonation cycles, as compared with carbonation with dry synthetic flue gases. The analyses of the sorbent samples from carbonation with steam addition also show a higher overall CO_2 conversion, indicating the capability of steam in helping the diffusion of CO_2 into the deeper pores of the sorbent particles. This is further evidence of the importance of steam and its remarkable role in enhancing CO_2 capture *via* high-temperature solid sorbents.

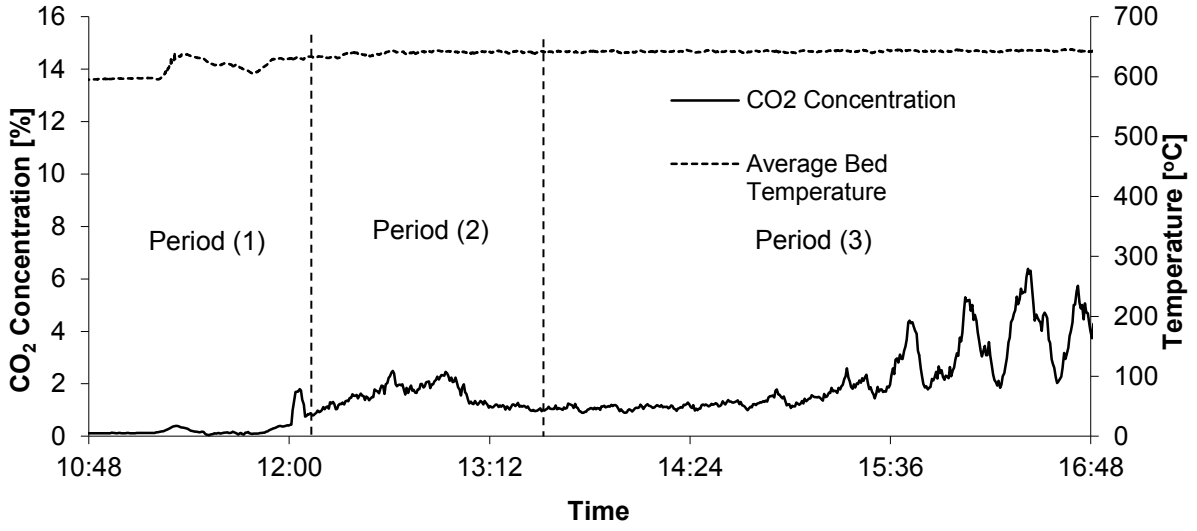

Figure 5.6.3: CO_2 concentration and bed temperature versus time in the carbonator during simulated flue gas CO_2 capture.

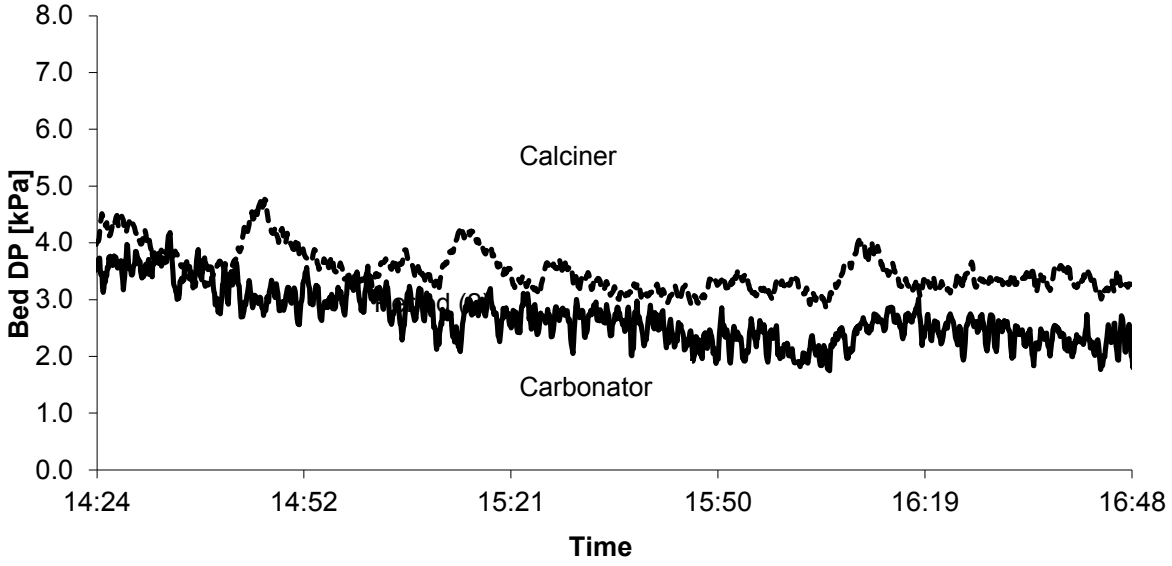

Figure 5.6.4: Bed differential pressure versus time in the calciner and carbonator during simulated flue gas CO_2 capture.

5.7 – Conclusions and Future Work

An atmospheric dual fluidized bed system for continuous CO_2 capture has been designed, constructed, and commissioned by the research group at CanmetENERGY – Ottawa. Preliminary testing has shown that the system can handle a variety of solid feedstocks for sorbent regeneration in oxy-fired combustion mode, CO_2 capture efficiencies greater than 90% can be achieved with simulated flue gas, and CO_2 levels of over 90 vol.% can be achieved during oxy-fired combustion. Other design objectives were also attained such as: stable temperature profiles in both reactors, controllable solids transfer rates between reactors, and solids sampling without system disruptions.

Future work now focuses on the use of different sorbents (natural, modified, and pelletized) and fuel sources for CO_2 capture, examining the effects of steam addition during both calcination and carbonation, and quantifying changes in particle morphology over long duration

testing. It is believed that, with this particular experimental facility, experimental results can closely mimic that of what can be expected in a large scale demonstration plant.

5.8 – Acknowledgements

The design, construction, and operation of the dual fluidized bed system for calcium looping at CanmetENERGY was funded by Natural Resources Canada, through the Program of Energy Research and Development (PERD).

5.9 – References

Abanades, J. C., Anthony, E. J., & Oakey, J. E. (2005). Fluidized Bed Combustion Systems Integrating CO_2 Capture with CaO. *Env. Sci. and Tech.*, 39, 2861-2866.

Abanades, J. C., Anthony, E. J., Lu, D. Y., Salvador, C., & Alvarez, D. (2004). Capture of CO_2 from Combustion Gases in a Fluidized Bed of CaO. *AIChE Journal*, 50, 1614-1622.

Ademe. (2010). Abtrennung und -Speicherung - ADEME mit vier Projekten. *VGB PowerTech*, 90, 24.

Alonso, M., Rodriguez, N., & Abanades, J. C. (2009). Modelling of a Fluidized Bed Carbonator to Capture CO_2 for a Combustion Flue Gas. *CES*, 64, 883-891.

Alonso, M., Rodriguez, N., Gonzalez, B., Grasa, G., Murillo, R., Abanades, J. C. (2010). Carbon Dioxide Capture from COmbustion Flue Gases with Calcium Oxide Chemical Loop. Experimental Results and Process Development. *Int. J. Greenhouse Gas Control*, 4, 167-173.

Arias, B., Cordero, J. K., Alonso, M., & Abanades, J. C. (2012). Sulfation Rates of Cycled CaO Particles in the Carbonator of a Ca-Looping Cycle for Postcombustion CO2 Capture. *AIChE*, 58, 2262-2269.

Arias, B., Diego, M. E., Abanades, J. C., Lorenzo, M., Diaz, L., Martinez, D. Alvarez, J., Sanchez-Biezma, A. (2013). Demonstration of Steady State CO_2 Capture in a 1.7 MWth Calcium Looping Pilot. *Int. J. Greenhouse Gas Control*, 18, 237-245.

Bachu, S. (2008). CO_2 Storage in Geological Media: Role, Means, Status, and Barriers to Deployment. *Prog. Energy Combust. Sci.*, 34, 254-273.

Baker, E. H. (1962). The Calcium Oxide-Carbon Dioxide System in the Pressure Range 1-300 Atmospheres. *J. Chem. Soc.*, 87, 464-470.

Beer, J. M. (2000). Combustion Technology in Power Generation in Response to Environment Challenges. *Prog. Energy Combust. Sci.*, 25, 301-327.

Bhatia, S. K., & Perlmutter, D. D. (1983). Effect of the Product Layer on the Kinetics of the CO_2-lime Reaction. *AIChE Journal*, 29, 79-86.

Champagne, S., Lu, D. Y., Macchi, A., Symonds, R. T., & Anthony, E. J. (2013). Influence of Steam Injecttion during Calcination on the Reactivity of CaO-Based Sorbent for Carbon Capture. *Ind. Eng. Chem. Res.*, 52, 2241-2246.

Chang, M. H., Huang, C. M., Liu, W. H., Chen, W. C., Cheng, J. Y., Chen, W., et al. (2013). Design and Experimental Investigation of the Calcium Looping Process for 3-kWth and 1.9-MWth Facilities. *Chem. Eng. Technol.*, 36, 1525-1532.

Dietmar, K. (2010). Development Perspectives of Lignite-basaed IGCC Plants with CCS. *VGB PowerTech*, 90, 30-34.

Galloy, A., Strohle, A. J., & Epple, B. (2011). Design and Operation of a 1 MWth Carbonate and Chemical Looping CCS Test Rig. *VGB PowerTech*, 6, 64-68.

Global CCS Institute. (2014, July 08). *Boundary Dam Integrated Carbon Capture and Sequestration Demostration Project.* Retrieved Jul7 21, 2014, from Global CCS Institute: http://www.globalccsinstitute.com/project/boundary-dam-integrated-carbon-capture-and-sequestration-demonstration-project

Global CCS Institute. (2014, July 8). *Kemper County Energy Facility (formerly Kemper County IGCC Project).* Retrieved July 21, 2014, from Global CCS Institute: http://www.globalccsinstitute.com/project/kemper-county-energy-facility

Hawthorne, C., Charitos, A., Perez-Pulido, C., Bing, Z., & Scheffknecht, G. (2008). Design of a Dual Fluidized Bed System for the Post-combustion Removal of CO_2 using CaO. Part I: CFB Carbonator Reactor Model. *9th International Conference on Circulating Fluidized Beds*. Hamburg, Germany.

Hawthorne, C., Dieter, H., Bidwe, A., Schuster, A., Scheffknecht, G., Unterberger, S., et al. (2011). CO_2 Capture with CaO in a 200 kWth Dual Fluidized Bed Pilot Plant. *Energy Procedia*, 4, 441-448.

Hughes, R. W., Macchi, A., Lu, D. Y., & Anthony, E. J. (2009). Changes in Limestone Sorbent Morphology during CaO-CaCO3 Looping at Pilot Scale. *Chem. Eng. & Tech.*, 32, 425-434.

Hughes, R., Lu, D., Anthony, E. J., & Macchi, A. (2005). Design, process simulation and construction of an atmospheric dual fluidized bed combustion system for in situ CO_2 capture using high-temperature sorbents. *Fuel Processing Technology*, 86, 1523-1531.

Jia, L., Tan, Y., McCalden, D., Wu, Y., I, H., Symonds, R., et al. (2012). Commissioning of a 0.8 MWth CFBC for Oxy-fuel Combustion. *Int. J. Greenhouse Gas Control*, 7, 240-243.

Krebs, F. (2012). Carbon Dioxide - A Themed Issue. *Energy Environ. Sci.*, 5, 7238-7239.

Li, Z., Liu, Y., & Cai, N. (2014). Understanding the Enhancement Effect of High-Temperature Steam on the Carbonation reaction of CaO with CO_2. *Fuel*, 127, 88-93.

Lu, D. Y., Hughes, R. W., & Anthony, E. J. (2008). Ca-Based Sorbent Looping Combustion for CO_2 Capture in Pilot-Scale Dual Fluidized Beds. *Fuel Processing Technology*, 89, 1386-1395.

Lu, D. Y., Hughes, R. W., Anthony, E. J., & Manovic, V. (2009). Sintering and Reactivity of CaCO3-based Sorbents for In Situ CO_2 Capture in Fluidized Beds under Realistic Calcination Conditions. *Journal of Environmental Engineering*, 6, 404-410.

Manovic, V., & Anthony, E. J. (2007). Steam Reactivation of Spent CaO-based Sorbent for Multiple CO_2 Capture Cycles. *Envi. Sci. & Tech.*, 41, 1420-1425.

Manovic, V., Anthony, E. J., & Loncarevic, D. (2009). CO_2 Looping Cycles with CaO-based Sorbent Pretreated in CO_2 at High Temperature. *CES*, 64, 3236-3245.

Manovic, V., Wu, Y., He, I., & Anthony, E. J. (2012). Spray Water Reactivation/Pelletization of Spent CaO-based Sorbent from Calcium Looping Cycles. *Envi. Sci. and tech.*, 46, 12720-12725.

Metz, B., Davidson, O., de Conninck, H., Loos, M., & Meyer, L. (2005). *IPCC Special Report on Carbon Dioxide Capture and Storage.* New York: Cambridge University Press.

Pachauri, R. K., & Reisinger, A. (2007). *Climate Change 2007: Synthesis Report. Contribution of Working Groups I, II and III to the Fourth Assessment Report of the Intergovernmental Panel on Climate Change.* Geneva, Switzerland: Intergovernmental Panel on Climate Change (IPCC).

Rodriguez, N., Alonso, M., & Abanades, J. C. (2011). Experimental Investigation of a Circulating Fluidized-Bed Reactor to Capture CO_2 with CaO. *AIChE Journal*, 57, 1356-1366.

Shimizu, T., Hirama, T., Hosoda, H., Kitano, K., Inagaki, M., & Tejima, K. (1999). A Twin Fluid-bed Reactor for Removal of CO_2 from Combustion Processes. *Chem. Eng. Res. & Design*, 77, 62-68.

Sun, P., Grace, J., Lim, C. J., & Anthony, E. J. (2006). Removal of CO_2 by Calcium-based Sorbents in the Presence of SO2. *Energy Fuels*, 21, 163-170.

Symonds, R. T., Lu, D. Y., Hughes, R. W., J, A. E., & Macchi, A. (2009). CO_2 Capture from Simulated Syngas via Cyclic Carbonation/Calcination for a Naturally Occurring Limestone: Pilot-Plant Testing. *Ind. Eng. Chem. Res.*, 48, 8431-8440.

Symonds, R. T., Lu, D. Y., Macchi, A., Hughes, R. W., & Anthony, E. J. (2009). CO_2 Capture from Syngas via Cyclic Carbonation/Calcination for a Naturally Occurring Limestone: Modelling and Bench-Scale Testing. *Chemical Engineering Science*, 64, 3536-3543.

Symonds, R. T., Lu, D. Y., Manovic, V., & Anthony, E. J. (2012). Pilot-Scale Study of CO_2 Capture by CaO-Based Sorbents in the Presence of Steam and SO2. *Ind. & Eng. Chem. Res.*, 51, 7177-7184.

Vattenfall. (2010). CCS-Pilotanlage liefert ausgezeichnete Ergebnisse. *VGB PowerTech*, 90, 16-17.

Chapter 6 – CO_2 Capture Performance of CaO-based Pellets in a 0.1 MW_{th} Pilot-scale Calcium Looping System

Robert T. Symonds[a], Scott Champagne[a], Firas N. Ridha[a], Dennis Lu[a]

[a]Natural Resources Canada, CanmetENERGY

1 Haanel Drive, Ottawa, Ontario K1A 1M1, Canada

Article published in *Powder Technology* **2016** *290*, 124-131.

6.1 – Abstract

Post-combustion CO_2 capture performance of CaO-based pellets tested in a pilot-scale calcium looping system is investigated. The pellets were prepared from two natural limestones with 10 wt% cement as a binder. The pilot-scale system setup consists of a circulating fluidized bed calciner operating at 900 °C and a bubbling bed carbonator operating at 650 °C. The flue gas was supplied to the carbonator from a natural gas-fired combustor, while the oxy-fuel combustion condition was established in the calciner using wood pellets as the fuel source. The test campaign results showed that CO_2 capture efficiencies in the range of 80-90% can be achieved for each sorbent. The carbonation efficiency with limestone was steady throughout the ~5 h steady-state operation period, whereas efficiencies obtained with pellets exhibited a gradual decline over the duration of the test. An average carbonation conversion over the steady-state duration indicated the superiority of limestone with a conversion of 7.8%, compared to that of 6.0-6.8% achieved by pellets. Neither the limestone type nor the make-up mode showed any significant effect on the performance of the pellets. The inferior performance of pellets compared to that of limestone was attributed to the rapid and sever sintering of the pellets at the early stages of the test. It was concluded that, under the test conditions tested here, the use of CaO-based pellets in a pilot-scale calcium looping system does not seem to be a promising approach due to the significantly higher cost of production with comparable CO_2 capture performance to that of limestone. Nonetheless, the test campaign provided important insights into the behaviour of synthetic/modified sorbents under pilot-scale calcium looping conditions, which has never been reported elsewhere.

6.2 – Introduction

Environmental issues associated with CO_2 emissions and global warming have attracted an increased attention in recent years. Carbon capture and storage (CCS) has been considered as a means of reducing CO_2 emissions to atmosphere (Bernstein, et al., 2005) (Boot-Handford, et al., 2014). In the CCS approach, capturing CO_2 is the most challenging and costly stage (Herzog, 2011). There have been numerous efforts focusing on developing new technologies for CO_2 capture from fossil fuel-fired power plants and other industrial facilities. Calcium looping (CaL) is a promising technology whereby CO_2 is captured by a CaO-based sorbent during carbonation at 600-700 $^{\circ}$C, and released by subsequent calcination at 850-950 $^{\circ}$C according to Equation (6.1), to produce a high purity CO_2 stream for sequestration after purification (Masnadi, et al., 2015) (Blamey, et al., 2010). The CaL process utilizes a dual-fluidized bed (DFB) system which represents an optimal configuration for such a process, since they permit large amounts of solids to be transferred easily from the carbonator to the calciner (Shimizu et al., 1999; Abanades et al., 2004; Hughes et al., 2005).

$$CaO_{(s)} + CO_{2(g)} \longleftrightarrow CaCO_{3(s)} \qquad \Delta H_r^0 = -178.2 \text{ kJ/mol} \qquad (6.1)$$

Economic analyses (Romeo, et al., 2009a and 2009b) showed that when an inexpensive CaO-based material such as limestone is used, CaL processes can be a cost-effective method for large-scale CO_2 mitigation, with a 5% (absolute) lower energy penalty when compared to current, more developed technologies such as amine scrubbing (Wang, et al., 2013). The higher return on energy investment is due to the extra power produced from the high temperature processes required for both calcination and carbonation. However, CaL has two major limitations that must be overcome in order to fully reap its rewards in commercial-scale applications: (1) decay in CO_2 capture capacity of CaO-based sorbent with increasing number of cycles (Grasa

and Abanades, 2006) (Fennell, et al., 2007) (Chen, et al., 2009), and (2) attrition of sorbent and elutriation from the fluidized-bed system (Lu, et al., 2008) (Lu, et al., 2009) (Symonds, et al., 2009) (Charitos, et al., 2010) (Scala and Salatino, 2010). The make-up stream to account for elutriated sorbent can influence the economics, and thus the competitiveness of CaL (Romeo, et al., 2009b).

In an attempt to improve the performance of CaO-based sorbents for CaL cycles, several approaches have been applied including the development of synthetic CaO-based sorbents (Dennis and Pacciani, 2009) (Florin, et al., 2010) (Qin, et al., 2012) (Broda and Müller, 2012) (Kierzkowska, et al., 2013) (Li, et al., 2005), modification of limestone by organic acids (Li, et al., 2011) (Ridha, et al., 2013), doping (Reddy and Smirniotis, 2004) (Albrecht, et al., 2008) (Sun, et al., 2009) (Al-Jeboori, et al., 2012) (Manovic, et al., 2013), and thermal pre-treatment (Manovic and Anthony, 2008) (Ozcan, et al., 2011). It should be noted that the use of synthetic CaO-based sorbents will increase the cost of the CaL process significantly. On the other hand, modified natural sorbents exhibited a marginal improvement in the CO_2 capture capacity, with additional costs due to the modification treatment.

A series of work conducted at CanmetENERGY attempted to investigate the possibility of pelletizing CaO-based sorbents to enhance their mechanical strength, thus reducing sorbent losses due to attrition. Moreover, if an appropriate binder is chosen, the pelletized sorbents can have an enhanced CO_2 capture performance. A previous work on binder screening (Manovic and Anthony, 2009a) identified Calcium aluminate cements (Ca cements) as a promising class of binders. Also work by Manovic and Anthony (2009b) showed that ~1 mm pellets made from Cadomin limestone with 10 wt% Ca cement outperformed Cadomin powder, maintaining a conversion of ~60% compared to ~40% for the latter after 30 isothermal cycles at 850 $^{\circ}$C. While

a residual conversion of 28% was reported for pellets after 1000 cycles, compared to 17% for original limestone cycled isothermally at 800 °C (Manovic and Anthony, 2009c). The improved performance of pelletized sorbent with Ca cement is attributed to the reaction between Al_2O_3 and CaO to form mayenite ($Ca_{12}Al_{14}O_{33}$) which assists in forming a stable inert matrix dispersed uniformly within the structure of the sorbent. The stable matrix enhances the sintering resistance of the sorbent during multiple cycles (Martavaltzi and Lemonidou, 2008). Manovic and Anthony (2011) suggested the possibility of re-activating the spent pellets (made with Ca cement as a binder) and re-charging them to the system. However, although this may appear a cost-effective approach with respect to the fresh sorbent required, it claims an additional cost for re-pelletizing the material.

Despite the promising CO_2 capture performance of pelletized sorbents, all previous studies were carried out at the bench-scale, which does not reflect the performance under realistic conditions expected at the industrial scale. Thus, the aim of this work is to investigate the CO_2 capture performance of different pelletized Ca-based sorbents in a pilot-scale CaL system. The CaL tests were conducted in a dual-fluidized bed pilot-plant under continuous operation with and without continuous sorbent make-up. Results for natural Cadomin limestone test are also presented for comparison and assessment purposes.

6.3 – Experimental

6.3.1 – Materials

Single batches of Cadomin and Spanish limestones were the source for all CaO-based sorbents in this work. Elemental analyses of the powdered limestones were carried out using X-ray fluorescence (XRF) spectroscopy. The contents of the major elements in these limestones are

shown in Table 6.3.1. The binder was commercial calcium aluminate cement (CA-14) with composition (in wt%) of 72.7% Al_2O_3, 27.2% CaO, and 0.1% impurities.

Table 6.3.1: XRF analysis of major elements in limestone (in wt%).

Component	Cadomin	Spanish
SiO_2	1.30	<0.10
Al_2O_3	0.40	<0.10
Fe_2O_3	0.11	0.03
CaO	50.64	55.71
MgO	3.12	0.39
K_2O	0.14	<0.02
LOF*	43.99	43.83
Sum	99.86	99.96

*LOF – Loss on fusion

Powdered Cadomin and Spanish limestones (<75 μm) were used for the production of pellets. The pelletization work was carried out in a mechanical pelletizer in batch mode. The starting materials for pelletization were calcined limestone (lime) and Ca cement (CA-14) with lime/cement mixing mass ratio of 90/10. Further details on the pelletization techniques are available elsewhere (Manovic, et al., 2011). The pellets are designated according to their starting limestone, i.e. CD pellets and SP pellets. All sorbents in this work were sieved to a particle size in the range of 250-600 μm (surface-to-volume mean diameter of 342, 350, and 340 μm for Cadomin limestone, Cadomin pellets, and Spanish pellets, respectively) to enable a consistent comparison of results. Cadomin limestone is designated with the letters "CD", while the limestone from Spain is designated as "SP". The biomass fuel pellets were pure fiber hardwood blend with proximate and ultimate composition as shown in Table 6.3.2.

Table 6.3.2: Proximate and ultimate analyses of biomass fuel pellets.

Proximate Analysis (wt%)				Ultimate Analysis (wt%)				
Moisture	Ash	Volatiles	Fixed C	C	H	N	S	O
7.81	0.68	75.54	15.97	45.80	5.52	<0.10	<0.05	40.04

6.3.2 – Pilot-plant setup

The tests were carried out in an atmospheric 0.1 MW_{th} pilot-plant designed and constructed at Natural Resources Canada – CanmetENERGY. A schematic of the facility is shown in Figure 6.3.1. A more detailed description of the setup is provided in Chapter 5. The system consists of two interconnected fluidized bed reactors; a calciner which operates as a circulating fluidized bed (CFB) and a carbonator which operates as a bubbling fluidized bed (BFB). Both the calciner and carbonator are constructed out of stainless steel, have an internal diameter of 0.1 m, and have heights of 5.1 and 3.0 m, respectively. In addition, the reactors are outfitted with electric heaters capable of operating at temperatures of <1100°C and are utilized during system pre-heat and for temperature control along the entire length of the reactors.

Each reactor is fabricated with high efficiency cyclones to re-entrain the sorbent during circulating fluidized bed operation, thus minimizing sorbent elutriation. The feeding system is comprised of two feed hoppers (one fuel and one sorbent), with the capability to operate in batch or continuous mode. This feature enables investigation of sorbents addition mode on the CO_2 capture performance of the system.

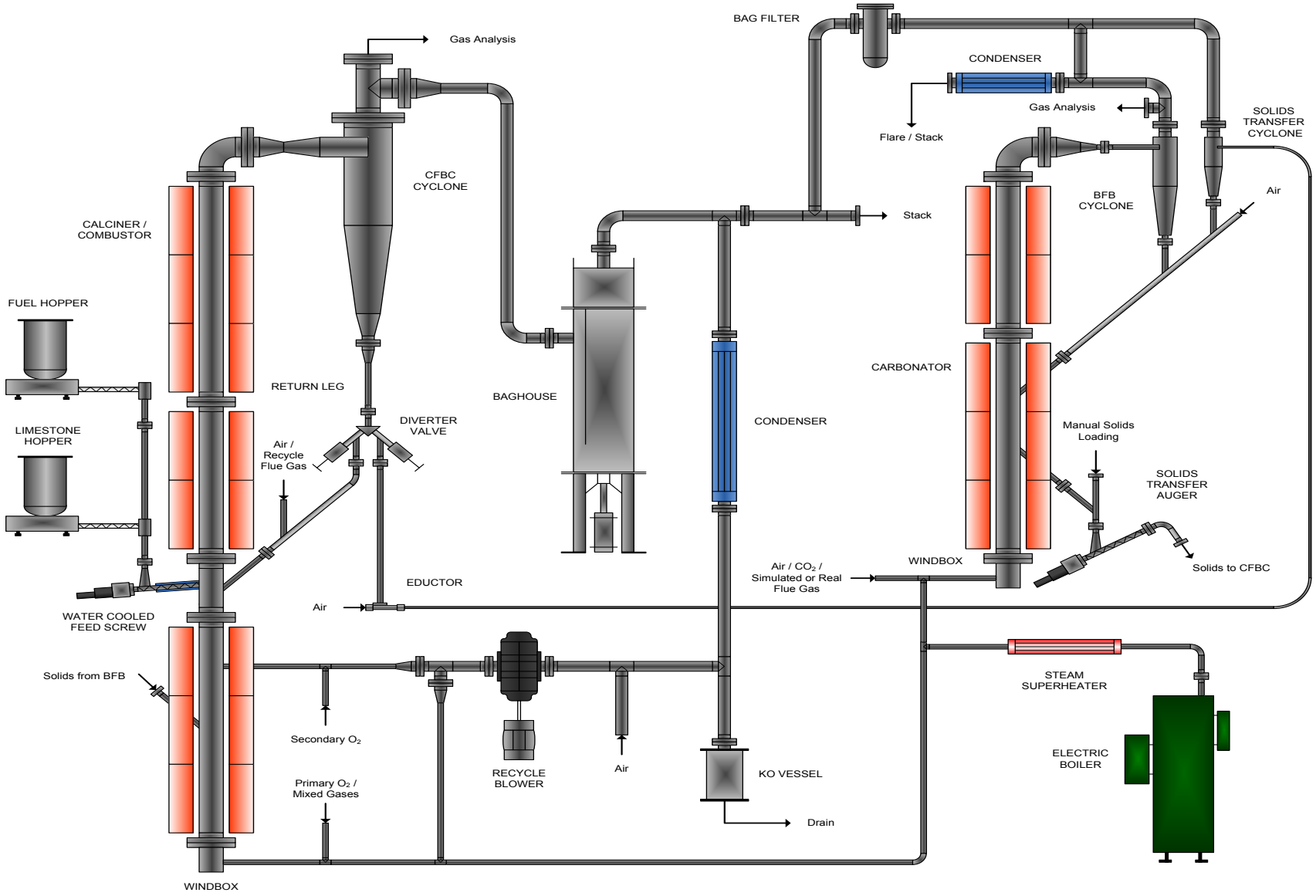

Figure 6.3.1: A schematic of the CaL pilot-plant at Natural Resources Canada – CanmetENERGY

6.3.3 – Methods

Prior to the test, the calciner was charged with 4.5 kg olivine sand with a particle size in the range of 525-1180 μm to help distribute heat while heating the system *via* the electric heaters. Similarly, 5.5 kg of CD limestone, 4.9 kg of CD pellets, or 4.7 kg of SP pellets (this quantity varied according to the CaO content in the sorbent) was loaded to the BFB before pre-heating up to ~650°C. After the calciner reached a temperature of above 850°C, fuel feeding was initiated and the calciner was subsequently switched over to oxy-fired operation. Once the desired operating temperature was achieved, sorbent looping was started. Table 6.3.3 shows the operating conditions of tests performed in this work. The calcination temperature in Table 6.3.3 was calculated according to Equation (6.2), which describes the equilibrium CO_2 partial pressure, P_{eq}, at a particular reaction temperature, T (Gracia-Labiano et al., 2002):

$$P_{eq} = 4.137 \text{ x } 1012 \exp\left(-\frac{20474}{T}\right) \tag{6.2}$$

It was decided to run the calciner approximately 20°C above equilibrium to allow for calcination to proceed rapidly due to the relatively short solids residence time in the CFB calciner. It should be noted that all test were performed at atmospheric pressure.

During sorbent looping operation, the calcined sorbent was diverted from the calciner return-leg through a pneumatic transfer system to a cyclone and into the carbonator. After carbonation, the sorbent exited the carbonator *via* an overflow port and was transferred back to the calciner using a mechanical auger system (see Chapter 5).

The flue gas supplied to the carbonator was generated using an air-fired natural gas burner with a composition as shown in Table 6.3.4. The flue gas was sent to the carbonator *via* a heated diaphragm pump and entered the windbox at 175°C.

On-line gas analyzers continually monitored O_2 (Siemens Oxymat 61), CO_2 (Horiba VIA-510), CO (Horiba VIA-510), SO_2 (Amatek 921), and NO_2 (Thermo 32C) concentrations from the calciner exhaust and O_2 (Siemens Oxymat 61), CO_2 (Horiba VIA-510), CO (Horiba VIA-510), and SO_2 (Horiba VIA-510) concentrations from the carbonator exhaust. The measured gas concentrations were then used to calculate the carbonation efficiency, E_{carb}, according to the following equation:

$$E_{carb} = \frac{F_{CO_2} - F_{carb}}{F_{CO_2}} \tag{6.3}$$

where F_{CO_2} represents the molar flow rate of CO_2 entering the carbonator and F_{carb} represents the molar flow rate of CO_2 leaving the carbonator.

In the batch addition test, 1 kg of sorbent was added to the system when the carbonator outlet CO_2 concentration reached 1.5 vol% (dry basis), which represents the objective of 90% capture. This amount was translated to an input make-up flow rate in the continuous addition test. Solids were also removed from the system, through a bed discharge valve, to keep the total inventory in the system constant and to avoid the accumulation of solids, such as ash and spent sorbent. In general, all tests were run for a minimum of ~5 h under continuous steady-state operation (i.e., at steady CO_2 capture performance). Solid samples (~0.1 kg) were taken from the carbonator and the calciner each hour for analysis purposes.

Table 6.3.3: Experimental test campaign operating conditions.

Sorbent	Sorbent/addition	Calciner				Carbonator		
		Temp. (°C)	CO_2 (vol% dry at outlet)	Fuel feed rate (kg/h)	Fluidization velocity (m/s)	Temp. (°C)	Average calcium looping ratio (F_{CaO}/F_{CO_2})	Fluidization velocity (m/s)
CD	Limestone/batch	900	>80	5-7	2.0-2.6	650	9.22	0.5-0.8
CD-B	Pellets/batch	900	>80	5-7	2.0-2.6	650	12.26	0.5-0.8
CD-C	Pellets/continuous	900	>80	5-7	2.0-2.6	650	9.77	0.5-0.8
SP-C	Pellets/continuous	900	>80	5-7	2.0-2.6	650	10.72	0.5-0.8

Table 6.3.4: Natural gas burner flue gas composition.

Composition (vol% wet)		
CO_2	H_2O	O_2
8.59	15.80	2.04

6.3.4 – Characterization

The physical properties of the sorbents (calcined at 850°C in air then degassed at 250°C under a blanket of N_2 overnight) were obtained from N_2 adsorption isotherms measurement at -196 °C (Micromeritics TriStar II-3020). These properties include Brunauer-Emmett-Teller (BET) specific surface area, Barrett-Joyner-Halenda (BJH) specific pore volume and pore size distribution (Lowell et al., 2004). BJH surface area distribution was derived from adsorption data, while BJH pore volume distribution was derived from the corresponding desorption data. The surface morphology was examined by scanning electron microscopy, SEM (Hitachi S-3400N), where the sample was coated with a thin layer of molybdenum (~2 nm). Carbonation and calcination conversions were obtained from thermogravimetric analysis (TGA) (Mettler Toledo SDTA851), where samples were heated from room temperature to 900°C at a heating rate of 50°C/min in N_2.

6.4 – Results

A low sulphur/low ash biomass was used in the calciner, while natural gas (low sulphur-content) was used to generate the required flue gas for the carbonator. Accordingly, the effects of sulphation and ash are considered to be insignificant and; thus, will not be discussed in this work. Prior to presenting the test campaign results with the pelletized sorbents, it is important to describe the results of a reference test to establish a base line for performance comparisons with the pellets.

Figure 6.4.1 presents the temperature profiles (bed and riser sections) in the calciner and the carbonator, and CO_2 capture performance (dry basis) of the reference case performed with limestone, CD. The start-up occurred during the first 2 h of the test, while flue gas recirculation in the calciner was started 1.5 h into the test. The CO_2 level in the calciner reached 90%

approximately 0.5 h after the start of flue gas circulation, indicating a suitable oxy-fired condition was attained. After the two beds reached the desired temperatures (900 and 650°C in the calciner and carbonator, respectively), solid circulation was started which was ~2 h into the test. Shortly after the start of solids circulation, an auger failure (point 2), which prevented solids transfer between both beds, resulted in a sharp decline in CO_2 capture in the carbonator as the sorbent in the system was no longer being calcined. This event led to the distinct peak on the carbonator CO_2 concentration profile shown in the figure. The auger was fixed shortly after this, and the system ran at steady state for ~5 h.

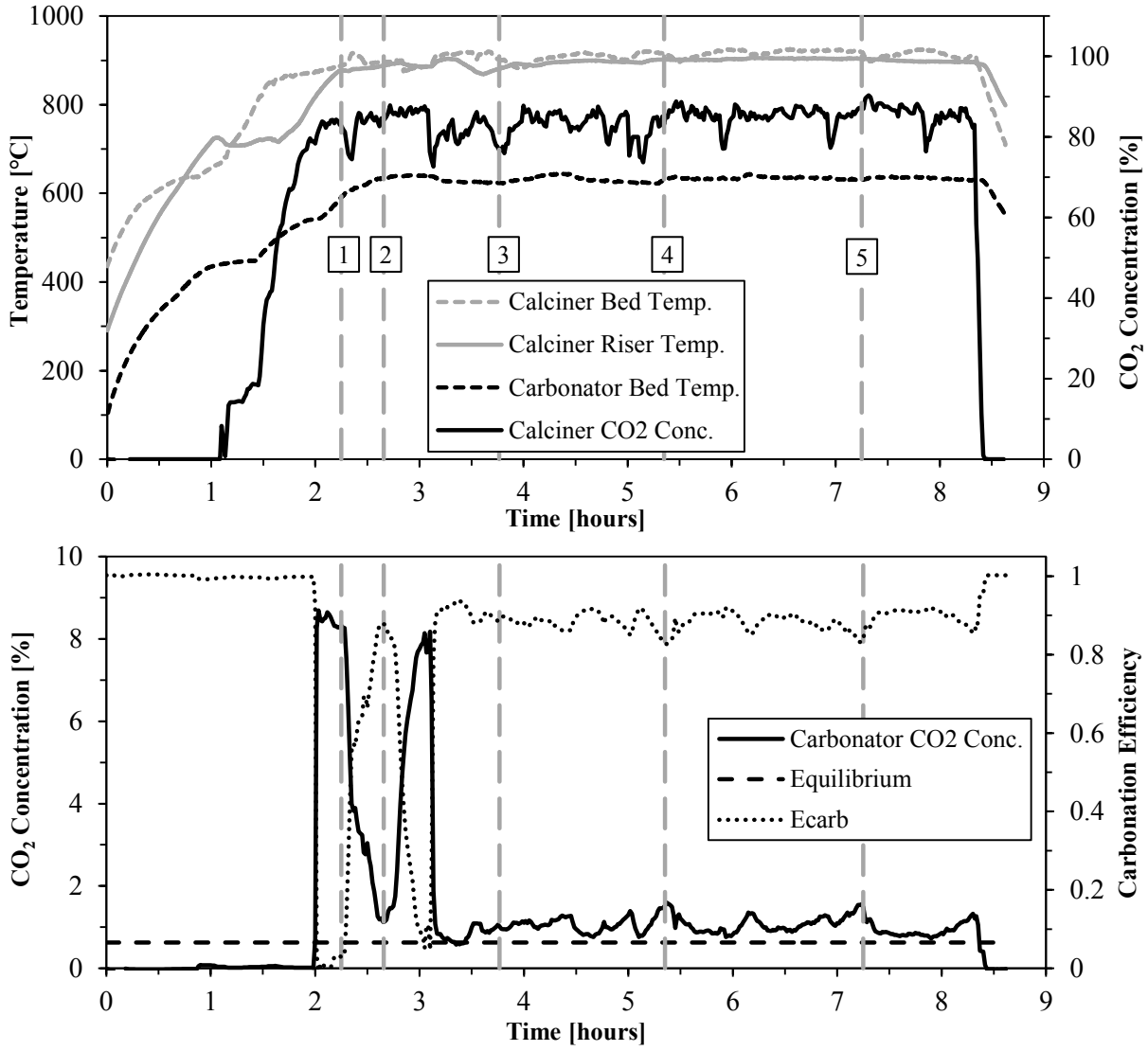

Event	Description
1	Starting solids circulation
2	Auger failure
3	Limestone make-up (1 kg)
4	Limestone make-up (1 kg)
5	Limestone make-up (1 kg)

Figure 6.4.1: Calciner and carbonator bed temperatures, CO_2 concentrations (dry basis), and carbonation efficiency profiles for the CD test.

Batches of fresh limestone were added to maintain CO_2 capture level. An average bed inventory of 3.8 kg was maintained in the carbonator (similar bed inventory was established in all tests for consistency), resulting in an average solids residence time of ~10 min. The relatively long residence time is due to the fact that the CanmetENERGY CaL pilot-plant utilizes a bubbling bed carbonator, which has a longer residence time than circulated fluidized bed in most pilot-scale CaL systems (Charitos et al., 2011). The longer residence time will result in a higher sorbent utilization.

A closer examination of the CO_2 capture profile in the carbonator reveals that the CO_2 outlet concentration reached 1.5 vol% every ~1.75 h throughout the test, thus allowing for the determination of the required sorbent make-up rate, which was estimated to be ~0.93 kg/h. The carbonator CO_2 outlet concentration was maintained near equilibrium (at an average temperature of ~633°C) for the duration of the test, resulting in carbonator efficiencies between 80% and 90%. Minor interruptions can be seen on CO_2 profiles of both beds, which are attributed to different circumstances, e.g., solids removal, sampling, solids addition, etc. However, their effect was negligible on the overall performance, which indicates the high reliability of the system.

The first test in the experimental campaign with pellets was performed with batch make-up of Cadomin pellets (CD-B). Figure 6.4.2 presents the temperature profiles and CO_2 capture performance of the test performed with CD-B. The introduction of the flue gas to the carbonator and solids circulation between the two beds occurred ~2.5 h into the test where a steady-state operation for ~5 h followed. Unlike in the reference test, only two batch make-up additions (1 kg each) were required to maintain the desired CO_2 capture level throughout the test, with a

F_{CaO}/F_{CO_2} ratio of 12.26, which was higher than that used in the CD test, as shown in Table 6.3.3. However, it can be observed that the carbonator exhibited a steady decline in its carbonation efficiency; from ~93% achieved shortly after starting solids circulation to ~80% at the end of the 5 h steady-state operation duration. The drop in the carbonation efficiency resulted in the gradual increase of CO_2 concentration in the outlet of the carbonator with the progress of the test. This was not observed in the CD test.

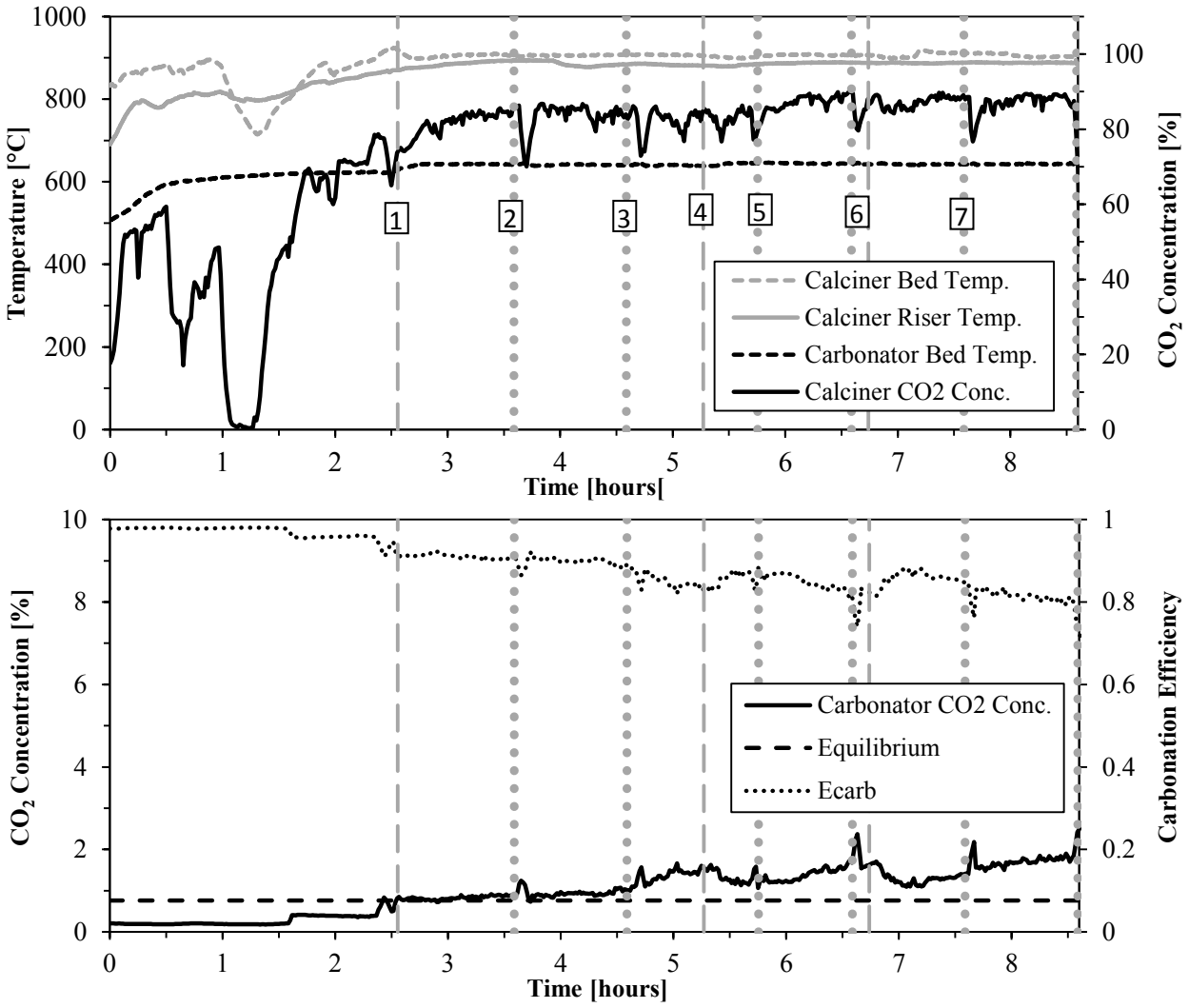

Event	Description
1	Starting solids circulation
2	Sampling
3	Sampling
4	Pellets make-up (1 kg)
5	Sampling
6	Sampling, pellets make up (1 kg)
7	Sampling

Figure 6.4.2: Calciner and carbonator bed temperatures, CO_2 concentrations (dry basis), and carbonation efficiency profiles for the CD-B test.

The batch make-up of pellets was translated to a continuous make-up in the CD-C test, the results showing the temperature profiles and CO_2 capture performance are shown in Figure 6.4.3. The pilot-plant start-up procedure was similar to that used in the previous test. Changing the make-up rate of Cadomin pellets (between 0.71 and 0.5 kg/h) helped in counter balancing the increase in the carbonator CO_2 concentration, and maintaining the carbonation efficiency between 80% and 90%. The carbonation efficiency in this test declined gradually from ~89% at point 4 to ~81% at the end of the test (over a duration of ~3.5 h of steady-state operation), despite the continuous make-up of pellets, maintaining an average F_{CaO}/F_{CO_2} ratio of 9.77, which is slightly higher than that for the CD test. The drop in the calciner CO_2 concentration between points 1 and 2 until the end of the test is attributed to air entering the process through the pneumatic transport line after switching on the solid circulation. This in turn resulted in diluting the true CO_2 output concentration in the calciner to ~80%. It can be realized from these results that the carbonation efficiency profile of CD-C test resembled to a large extent that of CD-B test.

The final test was performed with Spanish pellets in a continuous make-up mode (SP-C) to determine whether or not pellets prepared with different limestone perform differently. Temperature profiles and CO_2 capture performance are shown in Figure 6.4.4. Solid circulation between the two beds and the introduction of the flue gas to the carbonator started after ~1.5 h into the test. The make-up rate was adjusted between 0.62 and 0.71 kg/h to maintain the carbonator CO_2 outlet concentration in the range of 0.95-1.5 vol% (dry basis). An oxy-fired condition with 90% CO_2 (dry basis) was attained ~2.5 h into the test. Despite the slight gradual decline in the carbonation efficiency throughout the test, SP-C exhibited an average efficiency of ~91% at an average F_{CaO}/F_{CO_2} ratio of 10.72.

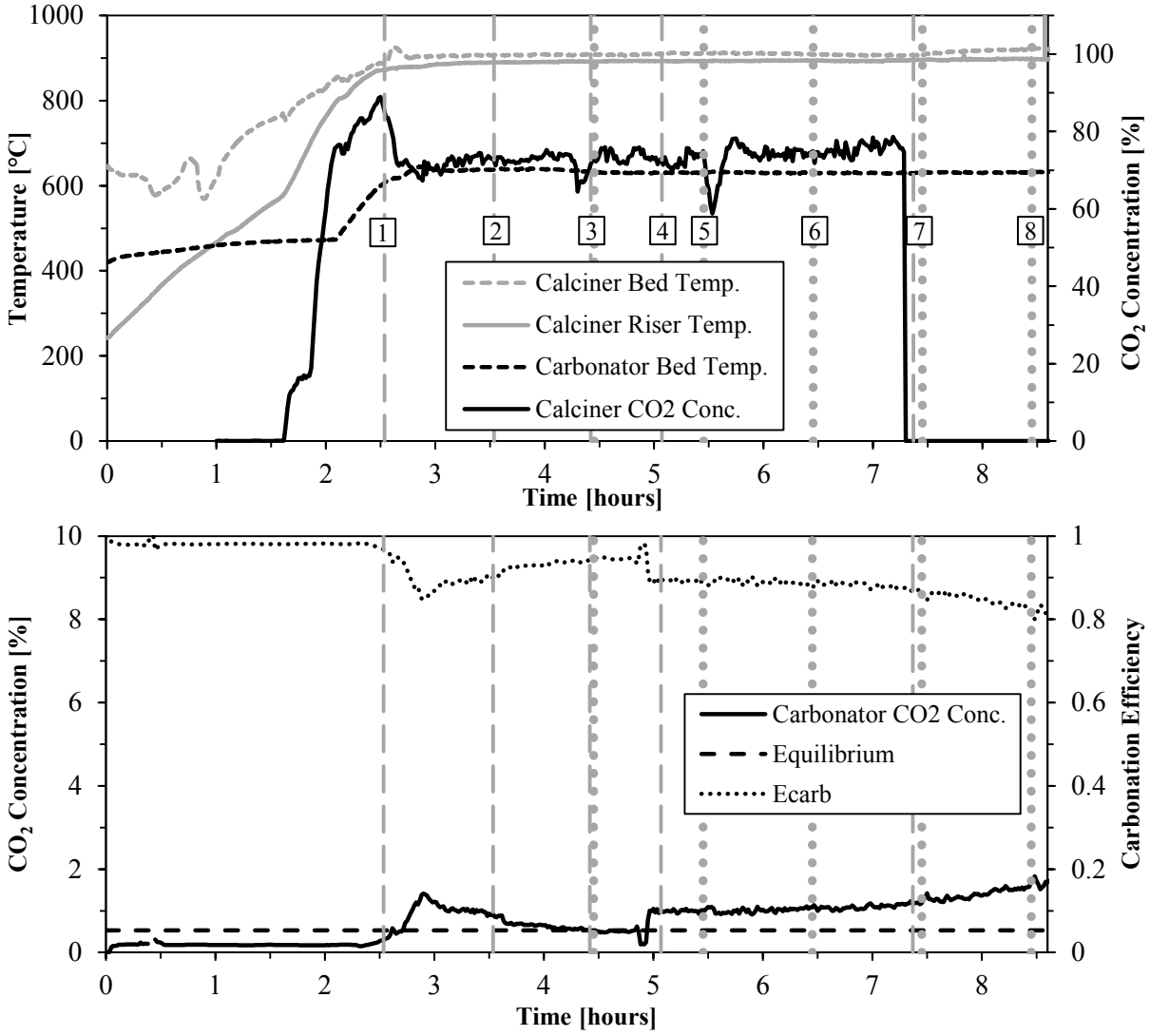

Event	Description
1	Starting solids circulation
2	Starting pellets make-up (0.71 kg/h)
3	Sampling, decreasing pellets make-up (0.5 kg/h)
4	Increasing pellets make-up (0.71 kg/h)
5	Sampling
6	Sampling
7	Sampling, end of make-up
8	Sampling

Figure 6.4.3: Calciner and carbonator bed temperatures, CO_2 concentrations (dry basis), and carbonation efficiency profiles for the CD-C test.

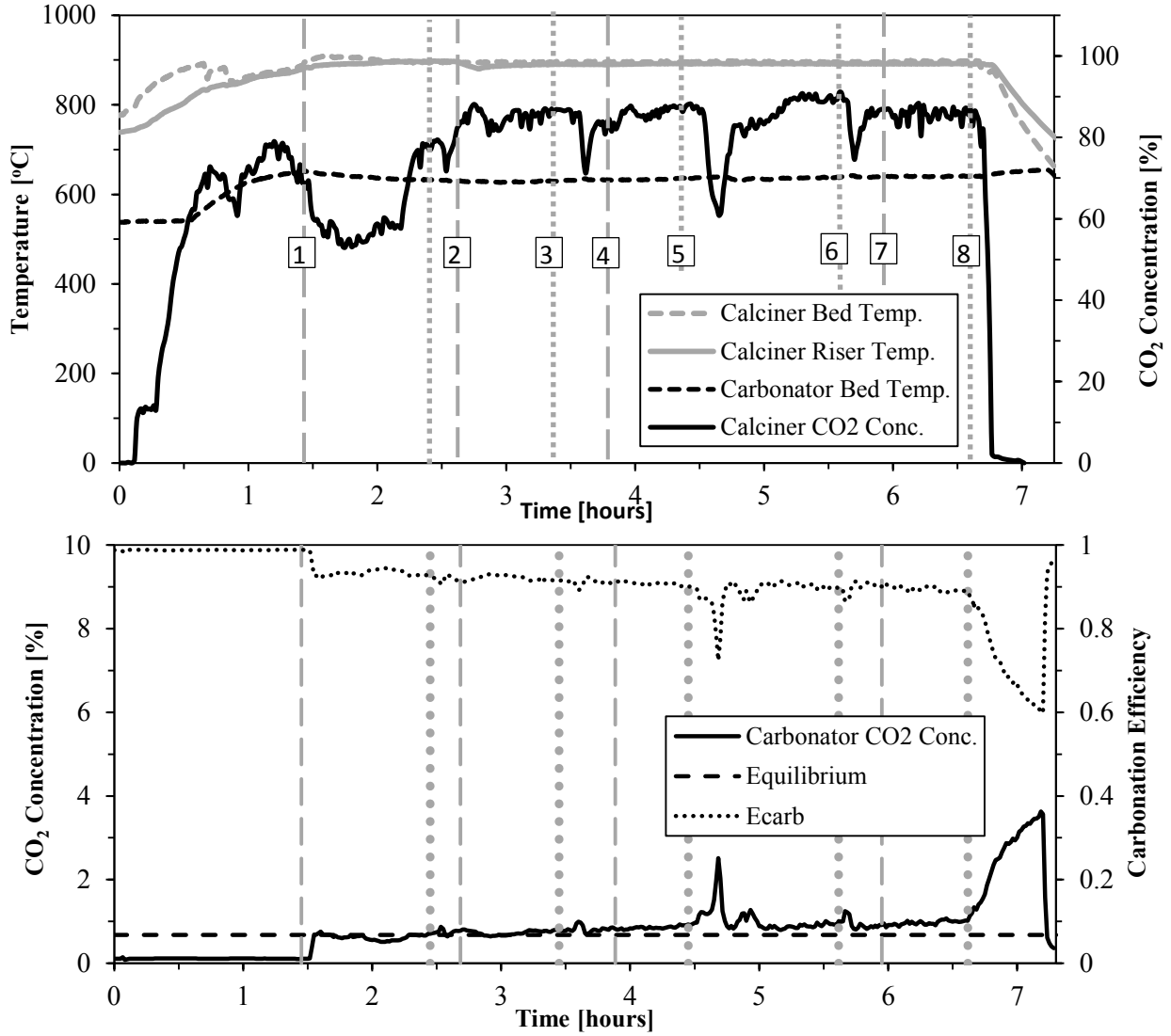

Event	Description
1	Starting solids circulation
2	Sampling, starting pellets make-up (0.62 kg/h)
3	Sampling
4	Increasing pellets make-up (0.71 kg/h)
5	Sampling
6	Sampling
7	End of make-up
8	Sampling, end of solids looping

Figure 6.4.4: Calciner and carbonator bed temperatures, CO_2 concentrations (dry basis), and carbonation efficiency profiles for the SP-C test.

6.5 – Discussion

As sorbent make-up strongly influences the cost of CaL technologies, modified or synthesized CaO-based sorbents must demonstrate a significant improvement in their capture performance and durability compared to that of natural limestones in order to justify the cost of manufacturing. The current pilot-scale test campaign aimed at examining the CO_2 capture performance of two types of CaO-based pellets prepared from different naturally occurring limestones. A comparison with a non-modified naturally occurring limestone was necessary in order for proper assessment.

As indicated above, the same start-up procedure was followed for all tests in order to minimize the effect of the operating procedure on the performance of the sorbents. Figure 6.5.1 shows the performance of each sorbent through an overall comparison of carbonation conversions over the steady-state operation period. These results were obtained from TGA for samples withdrawn from the carbonator. It should be noted that these carbonation conversions have been corrected for re-carbonation within the transfer lines and should allow for an accurate comparison between sorbents. The results are consistent with CO_2 capture profiles shown in Figure 6.4.1 through Figure 6.4.4. It can be seen that Cadomin pellets in the CD-B test exhibited an average conversion 14.7% lower (relative) than that for limestone achieved in the CD test. Initially, it was believed that the difference between active CaO content in limestone and Cadomin pellets was responsible for the difference in performance (90.6% in calcined limestone and 81.6% in calcined Cadomin pellets). However, as the F_{CaO}/F_{CO_2} ratio in the CD-B test was 33% higher than that used in the CD test (Table 6.3.3), a higher CO_2 capture efficiency was expected to be achieved with the pellets, but the results demonstrated the opposite. Changing the make-up of Cadomin pellets to continuous mode (CD-C test), resulted in a similar average

conversion, suggesting the insignificant effect of sorbent make-up mode on the carbonation behaviour of the sorbent. However, the F_{CaO}/F_{CO_2}ratio in the CD-B test was 25.5% higher than that applied in the CD-C test. It must be noted that in the CD-B test, where batch make-ups were made, a sample withdrawn for analysis could exhibit a higher conversion as the new batch of sorbent (1 kg) had not yet sintered significantly.

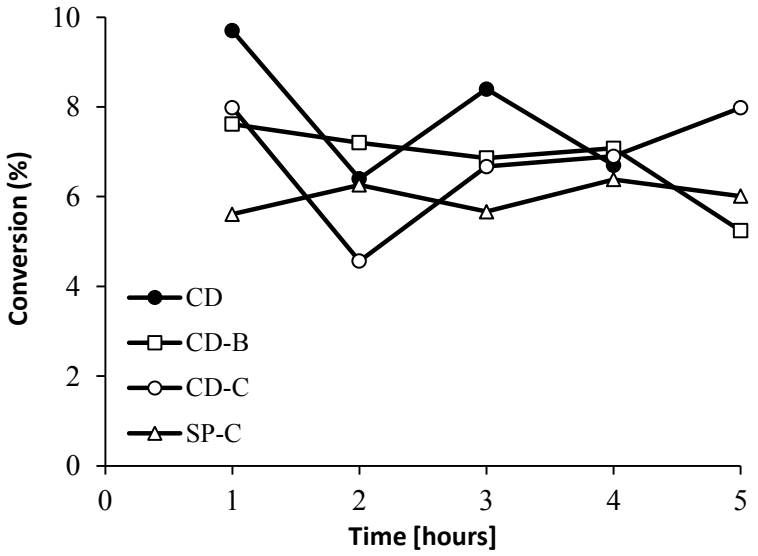

Figure 6.5.1: Carbonation conversion of limestone and pellets from the carbonator.

In the case of SP-C test, it was shown earlier that a particularly high carbonation efficiency (~91%) was achieved, suggesting that Spanish pellets performed better than Cadomin pellets in the pilot test with continuous make-up. This outcome can be attributed to two possible reasons: (1) the 9.7% higher F_{CaO}/F_{CO_2}ratio used in SP-C test than in CD-C test, or (2) the higher CaO content in Spanish pellets (i.e., 86.5%). However, despite the fact that the F_{CaO}/F_{CO_2}ratio used in the SP-C test was 16.3% higher than that of the CD test, the non-modified limestone still exhibited better carbonation conversion, being 30.3% (relative) higher than that of Spanish pellets.

According to the results obtained from the pilot-plant test campaign, it is now possible to make a few conclusions on the performance of these sorbents. Limestone tested in the current pilot-scale CaL system under the specified operating conditions outperformed both Cadomin and Spanish pellets regardless of the make-up mode of sorbent. The Spanish pellets performed slightly better than Cadomin pellets in the pilot test, likely due to the higher CaO content. It is worth noting that, according to a previous study (Manovic and Anthony, 2010), CO_2 capture capacity of CaO-based pellets can be improved by steam addition to the carbonation environment (e.g., up to 20%). However, this is significantly higher than what was observed in the current tests (steam generated through natural has combustion) and could most likely be explained *via* more severe calcination conditions.

A mass balance was performed in order to verify the accuracy of the results. This was realized by comparing the amount of CO_2 removed from the flue gas stream entering the carbonator to that of $CaCO_3$ formed. The gas-solid mass balance is shown in Equations 6.4a and 6.4b:

CO_2 removed from gas = $CaCO_3$ formed in solids (6.4a)

$$F_{CO_2} E_{carb} = F_{CaO}(X_{carb} - X_{calc}) \quad (6.4b)$$

where X_{carb} is the carbonation conversion of the sorbent at the outlet of the carbonator determined by TGA, X_{calc} is the carbonation conversion of the sorbent after exiting the calciner, and F_{CaO} is the molar flow rate (or solid circulation rate) determined *via* auger calibration performed for each sorbent tested. Accordingly, it was possible to determine the amount of CO_2 removed from the flue gas *via* the inlet and outlet carbonator gas compositions. All parameters in Equation 4b were measured intermittently with the assumption that each sample taken during the

tests was a depiction of the bulk bed inventory. Although this assumption might be too idealistic, it is still a reasonable approach considering the efficient mixing and circulation of solids in the system. To reduce the effect of errors in the experimental measurement of these parameters, a mass balance at each point where the samples were taken was performed. The results of these mass balances are illustrated in Figure 6.5.2. Good closure of the CO_2 balance is shown with each point being relatively close to the 45^o line, which represents perfect closure. It is believed that changes in particle density and size distribution over the duration of the tests contributed to some uncertainties in the F_{CaO} measurement.

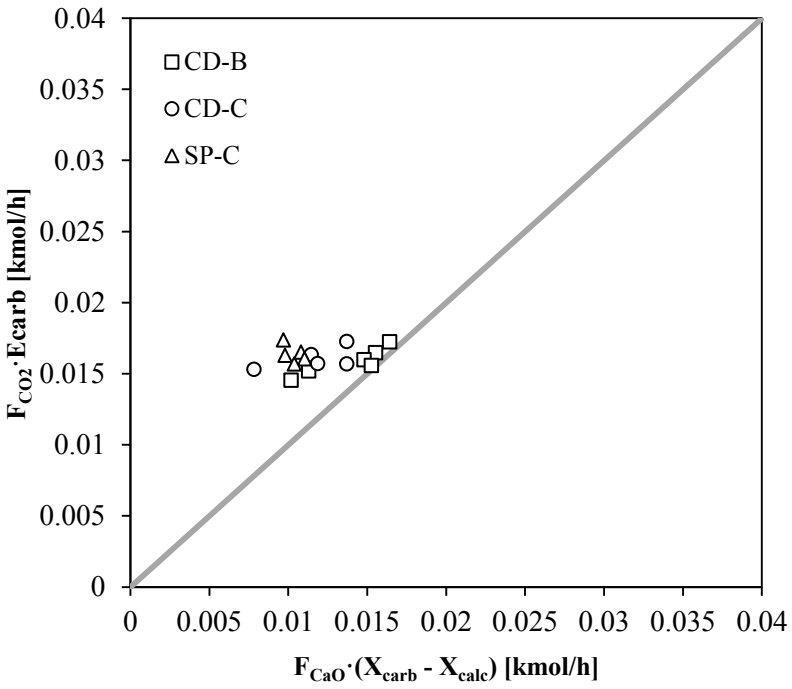

Figure 6.5.2: CO_2 balance comparison over the carbonator (gas and solid).

The results indicate a clear trend where the performance of sorbents can be assessed. The carbonation efficiencies and conversions of pellets are inferior to those of natural limestone despite the higher F_{CaO}/F_{CO_2} ratio in the system in all tests performed with pellets (Table 6.3.3). In addition, the limestone type does not appear to play a significant role in governing the

performance of the resultant pellets. However, to fully understand the performance of these pellets, it is important to discuss the effect of the operating conditions in the pilot-scale system on the morphology of the pellets, and the subsequent sintering and decay in their CO_2 capture capacity over the duration of the test. Pore size distributions of pellets taken from the system at different intervals are shown in Figure 6.5.3. The results are also compared to reference sorbents (CD-R and SP-R pellets calcined once at 850 $^{\circ}$C for 2 h in air) for assessment. The results of both groups of pellets show the dramatic decline in pore surface area and the shift in pore size distribution to a wider pore size, indicating a loss of microporosity in these pellets with the progress of the test. These changes eventually reached to a level where no further significant change occurred in the morphology of these pellets. The severe morphological changes appeared to occur sometime before ~1 h into the steady-state operation, suggesting that the pellets experienced an intense sintering at the early stages of the test. The major reason for sintering of these pellets is the exposure of sorbent to high temperatures during the regeneration in the calciner (Borgwardt, 1989a) (Rodriguez-Navarro, et al., 2009). In addition, as the calciner operates in oxy-fired condition, the high CO_2 concentration accelerated the sintering process (Borgwardt, 1989b). Since both CD-C and SP-C tests were performed at fairly similar conditions (temperatures and oxy-fired CO_2 concentrations), both groups of pellets sintered in a similar fashion.

This rapid sintering explains the inferior CO_2 capture capacity of pellets despite their high F_{CaO}/F_{CO_2} ratios maintained in the system compared to that of limestone. This also implies that the only possible approach to improve the performance of pellets is by applying a higher make-up rate and removing more spent materials from the system to maintain the F_{CaO}/F_{CO_2} ratio while achieving higher CO_2 capture. However, with an average make-up rate of

0.64 kg/h in the CD-C and SP-C tests, compared to 0.93 kg/h in the CD test, increasing the make-up rate of pellets does not appear to favour the utilization of pellets due to the additional costs involved for preparation. It should be noted that a full qualitative analysis of the sorbents was performed using SEM and all results are in alignment with the quantitative sintering findings shown in Figure 6.5.3.

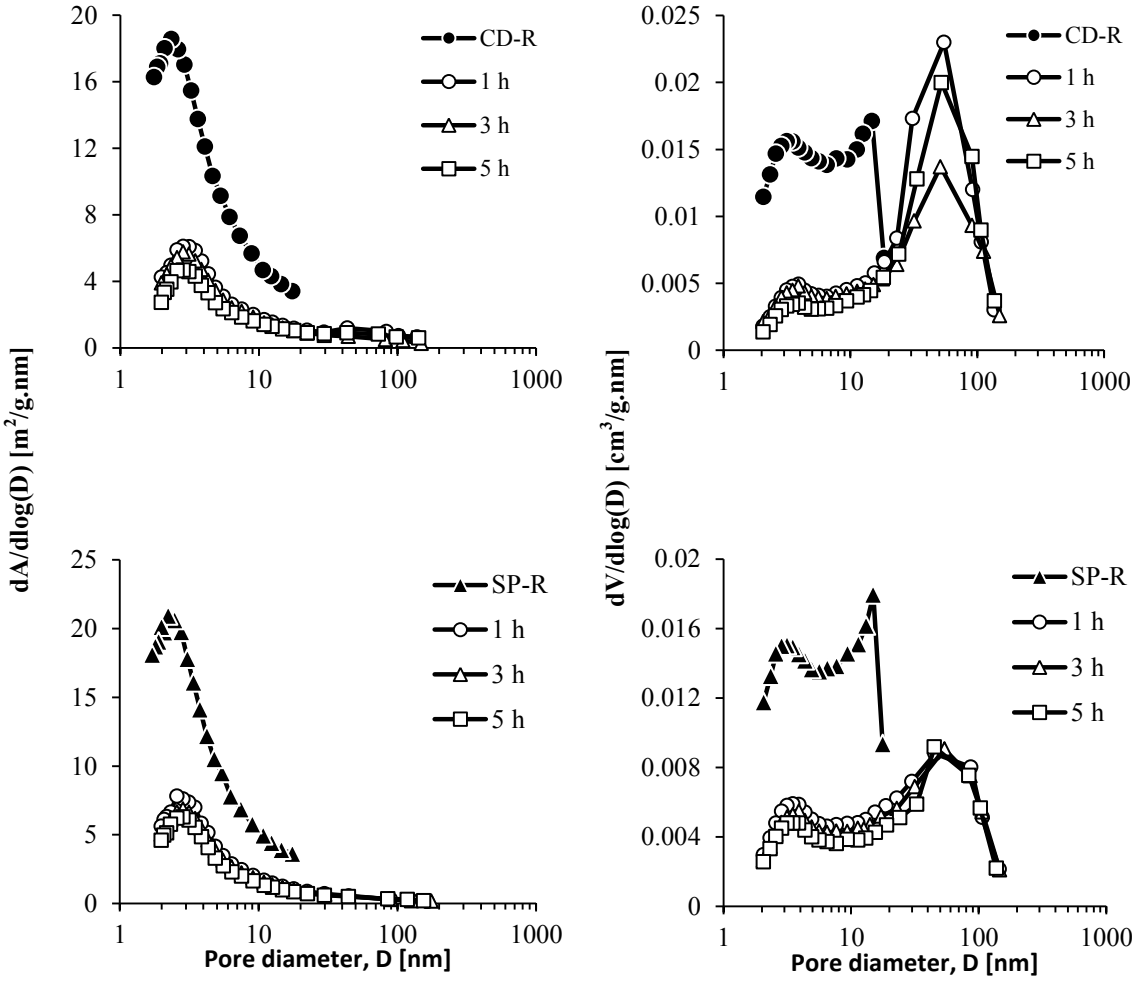

Figure 6.5.3: Effect of operation time on the pore size distribution of CD-C and SP-C sorbents (Area left – Volume right).

6.6 – Conclusions

This work investigated the CO_2 capture performance of CaO-based pellets in pilot-scale CaL cycles. The pellets were prepared from two limestone powders with 10 wt% cement as a binder. The tests were operated following the same procedure, establishing a steady-state operation period of ~5 h. The results showed that Cadomin limestone appeared to perform better than pellets with a stable carbonation efficiency between 85% and 90%, while it decreased gradually with pellets reaching ~80% at the end of the test. Furthermore, despite the higher calcium looping ratio for the pellets (F_{CaO}/F_{CO_2}), the average carbonation conversion of pellets over the steady-state period was 6.0-6.8% compared to 7.8% achieved by limestone. Analysis of the physical properties showed a significant loss of surface area and shift of pore size distribution to a wider range of pore size. These morphological changes occurred shortly after injecting the pellets into the system, suggesting a rapid sintering of pellets that reduced their CO_2 capture capacity. It was concluded that pelletization of CaO-based sorbents for CaL processes does not appear to be a practical approach, due to the high production cost of such pellets and the marginal improvement in CO_2 capture performance compared to natural non-modified limestones.

In conjunction with published works on CO_2 capture performance of synthetic/modified CaO-based sorbents at the bench-scale, this work highlighted the fact that such sorbents could have a significantly different performance when tested in a pilot-scale system. This suggests that the assessment of such relatively expensive sorbents should be performed at a pilot-scale testing condition to evaluate their performance against their production cost. Finally, this work demonstrated the reliability of Natural Resources Canada – CanmetENERGY's pilot-scale facility for carrying out a systematic test campaign to evaluate the performance of

synthetic/modified CaO-based sorbents and to gain experience and insight into the potential of such sorbents under realistic operating conditions, closely mimicking what is expected at the commercial scale.

6.7 – Acknowledgements

This research and experimental test campaign was funded by Natural Resources Canada, through the Program of Energy Research and Development (PERD).

6.8 – Nomenclature

E_{carb} carbonator efficiency

T temperature, K

F_{CaO} molar flow rate of CaO from the calciner to the carbonator, kmol/h

F_{CO_2} molar flow rate of CO_2 to the inlet of the carbonator, kmol/h

F_{carb} molar flow rate of CO_2 leaving the carbonator, kmol/h

P_{eq} equilibrium partial pressure of CO_2, Pa

X_{carb} carbonation conversion

X_{calc} carbonation conversion of sorbent at the outlet of the calciner

6.9 – References

Abanades, J. C., Anthony, E. J., Alvarez, D., Lu, D., Salvador, C. (2004). Capture of CO_2 from Combustion Gases in a Fluidized Bed of CaO. *AIChE J.*, 50, 1614–1622.

Albrecht, K.O., Wagenbach, K.S. Satrio, J.A., Shanks, B.H., Wheelock, T.D. (2008). Development of a CaO-based CO_2 sorbent with improved cyclic stability. *Ind. Eng. Chem. Res.*, 47, 7841-7848.

Al-Jeboori, M.J., Fennell, P.S., Nguyen, M., Feng, K. (2012) Effects of Different Dopants and Doping Procedures on the Reactivity of CaO-based Sorbents for CO2 Capture. *Energy Fuels,* 26, 6584−6594.

Bernstein, L. , Lee, A., Crookshank, S. (2006) Carbon dioxide capture and storage: A status report. *Climate Policy,* 6, 241-246.

Blamey, J., Anthony, E.J., Wang, J., Fennell, P.S. (2010) The calcium looping cycle for large-scale CO2 capture. *Progress in Energy and Combustion Science,* 36, 260–279.

Boot-Handford, M.E, Abanades, J.C., Anthony, E.J., Blunt, M.J., Brandani, S., Mac Dowell, N., Fernández, J.R., Ferrari, M.-C., Gross, R., Hallett, J.P., Haszeldine, R.S., Heptonstall, P., Lyngfelt, A., Makuch, Z., Mangano, E., Porter, R.T.J., Pourkashanian, M., Rochelle, G.T., Shah, N., Yao, J.G. (2014). Carbon capture and storage update. *Energy and Environmental Science,* 7, 130-189.

Borgwardt, R.H., (1989a). Sintering of nascent calcium oxide. *Chemical Engineering Science*, 44, 53-60.

Borgwardt, R.H. (1989b). Calcium Oxide Sintering in Atmospheres Containing Water and Carbon Dioxide. *Ind. Eng. Chem. Res*, 28, 493-500.

Broda, M., Muller, C.R. (2012). Synthesis of highly efficient, Ca-based, Al2O3-stabilized, carbon gel-templated CO2 sorbents. *Adv. Mat*, 24, 3059-3064.

Charitos, A., Hawthorne, C., Bidwe, A.R., Sivalingam, S., Schuster A., Spliethoff, H., Scheffknecht, G. (2010). Parametric investigation of the calcium looping process for CO2 capture in a 10kWth dual fluidized bed. *International Journal of Greenhouse Gas Control,* 4, 776–784.

Charitos, A., Rodriguez, N., Hawthorne, C., Alonso, M., Zieba, M., Arias, B., Kopanakis, G., Scheffknecht, G., Abanades, J. C. (2011). Experimental Validation of the Calcium Looping CO_2 Capture Process with Two Circualtion Fluidized Bed Carbonator Reactors. *Ind. Eng. Chem. Re,* 50, 9685-9695.

Chen, Z., Song, H.S., Portillo, M., C. Lim, J., Grace, J.R., Anthony, E.J. (2009). Long-Term Calcination/Carbonation Cycling and Thermal Pretreatment for CO_2 Capture by Limestone and Dolomite. *Energy & Fuels*, 23, 1437–1444.

Dennis, J.S., Pacciani, R. (2009) The rate and extent of uptake of CO_2 by a synthetic, CaO-containing sorbent. *Chemical Engineering Science,* 64, 2147 – 2157.

Fennell, P.S., Pacciani, R., Dennis, J.S., Davidson, J.F., Hayhurst, A.N. (2007). The Effects of Repeated Cycles of Calcination and Carbonation on a Variety of Different Limestones, as Measured in a Hot Fluidized Bed of Sand. *Energy & Fuels*, 21, 2072-2081.

Florin, N.H., Blamey, J., Fennell, P.S. (2010). Synthesis CaO-based sorbent for CO_2 capture from large-point sources. *Energy Fuels*, 24, 4598-4604.

Gracia-Labiano, F., Abad, A., de Diego, L.F., Gayan, P., Adanez, J. (2002). Calcination of calcium-based sorbents at pressure in a board range of CO_2 concentrations. *Chem. Eng. Sci*, 57, 2381-2393.

Grasa, G.S., Abanades, J.C. (2006). CO_2 Capture Capacity of CaO in Long Series of Carbonation/Calcination Cycles. *Ind. Eng. Chem. Res*, 4, 8846-8851.

Herzog, H. J. (2011). Scaling up carbon dioxide capture and storage: From megatons to gigatons. *Energy Economics,* 33, 597–604.

Hughes, R. W., Lu, D. Y., Anthony, E. J., Macchi, A. (2005). Design, Process Simulation and Construction of an Atmospheric Dual Fluidized Bed Combustion System for in situ CO_2 Capture using High-Temperature Sorbents. *Fuel Process. Technol*, 14-15, 1523–1531.

Kierzkowska, A.M., Poulikakos, L. V., Broda, M., Müller, C. R. (2013). Synthesis of calcium-based, Al2O3-stabilized sorbents for CO_2 capture using a co-precipitation technique, *International Journal of Greenhouse Gas Control,* 15, 48–54.

Li, Z.S., Cai, N.S., Huang, Y.Y., Han H.J. (2005). Synthesis, experimental studies, and analysis of a new calcium-based carbon dioxide adsorbent. *Energy Fuels,* 19, 1447-1452.

Li, Y., Sun, R., Liu, H., Lu, C., Cyclic CO_2 Capture Behavior of Limestone Modified with Pyroligneous Acid (PA) during Calcium Looping Cycles. *Ind. Eng. Chem. Res*., 50, 10222–10228.

Lowell, S., Shields, J.E., Thomas, M.A., Thommes, M. (2004). Surface area analysis from the Langmuir and BET theories. *Characterization of Porous Solids and Powders: Surface Area, Pore Size and Density*, 16, 58-81.

Lu, D.Y, Hughes, R.W, Anthony, E.J. (2008). Ca-based sorbent looping combustion for CO_2 capture in pilot-scale dual fluidized beds. *Fuel Processing Technology,* 89, 1386 –1395.

Lu, D. Y., Hughes, R. W., Anthony, E. J. (2009). Sintering and Reactivity of $CaCO_3$-Based Sorbents for In Situ CO_2 Capture in Fluidized Beds under Realistic Conditions. *J. Environ. Eng*., 135, 404-410.

Manovic, V., Anthony, E.J. (2008). Thermal Activation of CaO-Based Sorbent and Self-Reactivation during CO_2 Capture Looping Cycles. *Environ. Sci. Technol*., 42, 4170–4174.

Manovic, V., Anthony, E.J. (2009a). Screening of binders for pelletization of CaO-based sorbents for CO_2 capture. *Energy and Fuels,* 23, 4797-4804.

Manovic, V., Anthony, E.J. (2009b). CaO-based pellets supported by calcium aluminate cements for high-temperature CO_2 capture. *Environ. Sci. Technol*., 43, 7117-7122.

Manovic, V., Fennell, P.S., Al-Jeboori, M.J., Anthony, E.J. (2013). Steam-Enhanced Calcium Looping Cycles with Calcium Aluminate Pellets Doped with Bromides. *Ind. Eng. Chem. Res*., 52, 7677−7683.

Manovic, V., Anthony, E.J. (2009c). Long-Term Behavior of CaO-Based Pellets Supported by Calcium Aluminate Cements in a Long Series of CO_2 Capture Cycles. *Ind. Eng. Chem. Res*., 48, 8906–8912.

Manovic, V., Anthony, E.J. (2010). Carbonation of CaO-Based Sorbents Enhanced by Steam Addition. *Ind. Eng. Chem. Res*., 49, 9105–9110.

Manovic, V., Anthony, E.J. (2011). Reactivation and remaking of calcium aluminate pellets for CO_2 capture. *Fuel,* 90, 233-239.

Manovic, V., Wu, Y., He, I., Anthony E.J. (2011). Core-in-Shell CaO/CuO-Based Composite for CO_2 Capture. *Ind. Eng. Chem. Res.,* 50, 12384–91.

Martavaltzi, C.S., Lemonidou, A.A. (2008). Parametric study of the CaO-$Ca_{12}Al_{14}O_{33}$ synthesis with respect to high CO_2 sorption capacity and stability of multicycle operation. *Ind. Eng. Chem. Res.,* 47, 9537-9543.

Masnadi, M.S., Grace, J.R., Bi, X.T., Ellis, N., Lim, C.J., Butler, J.W. (2015). Biomass/coal steam co-gasification integrated with in-situ CO_2 capture. *Energy,* 83, 326-336.

Ozcan, D. C., Shanks, B. H., Wheelock, T. D. (2011). Improving the Stability of a CaO-Based Sorbent for CO_2 by Thermal Pretreatment. *Ind. Eng. Chem. Res*., 50, 6933-6942.

Qin, C., Liu, W., An, H., Yin, J., Feng, B. (2012). Fabrication of CaO-Based Sorbents for CO_2 Capture by a Mixing Method. *Environ. Sci. Technol*., 46, 1932−1939.

Reddy, E. P., Smirniotis, P. G. (2004). High-Temperature Sorbents for CO_2 Made of Alkali Metals Doped on CaO Supports. *J. Phys. Chem. B.,* 108, 7794-7800.

Ridha, F., Manovic, V., Macchi, A., Anthony, M., & Anthony, E. (2013). Assessment of limestone treatment with organic acids for CO_2 capture in Ca-looping cycles. *Fuel Process Technol*., 116, 284-291.

Rodriguez-Navarro, C., Ruiz-Agudo, E., Luque, A., Rodriguez-Navarro, A. B., Ortega-Huertas, M. (2009). Thermal decomposition of calcite: Mechanisms of formation and textural evolution of CaO nanocrystals. *Am. Mineral*., 94, 578-593.

Romeo, L.M., Lara, Y, Lisbona, P., Martínez, A. (2009a). Economical assessment of competitive enhanced limestones for CO_2 capture cycles in power plants. *Fuel Processing Technology*, 90, 803–811.

Romeo, L.M., Lara, Y., Lisbona, P., Escosa, J.M. (2000b). Optimizing make-up flow in a CO_2 capture system using CaO. *Chemical Engineering Journal*, 147, 252–258.

Scala, F., Salatino, P. (2010). Limestone fragmentation and attrition during fluidized bed oxyfiring. *Fuel*, 89, 827–832.

Shimizu, T., Hirama, T., Hosoda, H., Kitano, K., Inagaki, M., Tejima, K. (1999). A Twin Fluid-Bed Reactor for Removal of CO_2 from Combustion Processes. *Chem. Eng. Res. Des*., 77, 62–68.

Sun, P., Grace, J.R., Lim, C.J., Anthony, E.J. (2009). Investigation of attempts to improve cyclic CO_2 capture by sorbent hydration and modification. *Ind. Eng. Chem. Res*., 47, 2024-2032.

Sun, P., Grace, J.R., Lim, C.J., Anthony, E.J. (2007). The effect of CaO sintering on cyclic CO_2 capture in energy systems. *AIChE J*., 53, 2432-2442.

Symonds, R.T., Lu, D.Y., Macchi, A., Hughes, R.W., Anthony E.J. (2009). CO_2 capture from syngas via cyclic carbonation/calcination for a naturally occurring limestone: Modelling and bench-scale testing. *Chemical Engineering Science*, 64, 3536 – 3543.

Wang, W., Ramjumar, S., Fan, L. (2013). Energy penalty of CO_2 capture for the Carbonation-Calcination Reaction (CCR) Process: Parametric effects and comparisons with alternative processes. *Fuel*, 103, 561-574.

Chapter 7 – Attrition of CaO-based Pellets in a 0.1 MW_{th} Dual Fluidized Bed Pilot Plant for Post-combustion CO_2 Capture

Firas N. Ridha[a], Dennis Lu[a], Robert T. Symonds[a], Scott Champagne[a]

[a]Natural Resources Canada, CanmetENERGY

1 Haanel Drive, Ottawa, Ontario K1A 1M1, Canada

Article published in *Powder Technology* **2016** *291*, 60-65.

7.1 – Abstract

This work investigates the attrition of CaO-based pellets in pilot-scale calcium looping cycles for post-combustion CO_2 capture. Two groups of pellets with size 250-600 μm were prepared from Canadian and Spanish limestones using 10% calcium aluminate cement as a binder. The results showed that all groups of pellets experienced a significant extent of attrition, as ~50% of the sorbent fed to the system was collected as fragments with particle size smaller than 250 μm. The attrition of pellets was found to be comparable to that of limestone tested under similar conditions. The results also indicated the same tendency of attrition for all groups of pellets, with attrition extent being relatively insensitive to limestone type used for pelletization or injection method of sorbent to the system. The attrition trends suggest that the improvement in mechanical strength of the pellets was marginal compared to that of limestone.

7.2 – Introduction

It has been widely accepted that the increasing concentration of CO_2 in the atmosphere is a major contributor to climate change. Fossil-fuel combustion facilities, e.g., power plants, cement manufacture, hydrogen production, etc., are major stationary sources of CO_2 emissions. Carbon capture and storage (CCS) has been proposed as a promising technology for controlling CO_2 emissions and reducing the effect of CO_2 on the climate (Bernstein and Crookshank, 2006) (Boot-Handford, et al., 2014). In the CCS approach, capturing CO_2 is the most challenging and costly stage. There have been numerous efforts to develop new technologies for capturing CO_2 from such large-point sources in order to control CO_2 emissions. One of these emerged technologies is calcium looping (CaL) cycles. This technology is designed to operate in a dual fluidized bed (DFB) system consisting of a carbonator and calciner (Blamey, et al., 2010a). CO_2 is captured in the carbonator by a CaO-based sorbent during carbonation at 600-700°C, and

released in the calciner by subsequent calcination at 850-950°C, thus producing a high purity CO_2 stream ready for sequestration. Limestone as a CaO-based material is an attractive sorbent and has been proposed for CaL because it is abundant and relatively inexpensive when used at the industrial scale. Economic studies (MacKenzie, et al., 2007) (Romeo, et al., 2009) showed that when limestone is used, CaL technology emerges as a competitive option to the currently deployed technology for large-scale CO_2 capture, which involves scrubbing the gas with amine-based chemical solutions (Giuffrida, et al., 2013) (Nittaya, et al., 2014).

During fluidization, particles are subjected to mechanical stress (compression, impact, and shear), where impact-based stress has been acknowledged to be the main cause of attrition (Materic, et al., 2014). Under the typical operating conditions of CaL, sorbent particles will experience thermal stress in addition to mechanical stress, which will increase the severity of fragmentation and attrition. Prior research on the attrition of limestone noted that higher calcination temperature (Hu and Scaroni, 1995) (Blamey, et al., 2010b) and higher impact velocity (Chen, et al., 2007) (Scala, et al., 2007) result in more attrition. Blamey et al. (2010b) reported a significant increase in limestone attrition after reactivation of sorbent by hydration in a bench-scale fluidized bed. The mass loss was found to occur mainly in the first few cycles after hydration, which was attributed to the increased friability of the hydrated sorbent. A recent study in a pilot DFB system (Arias, et al., 2013) argued that the high attrition rate of limestone occurred in the first calcination, followed by a drastic drop in attrition rate where the sorbent reached a steady-state attrition condition. The steady-state attrition pattern was noted to continue with a lower rate over an extended period of operation, e.g., 140 h (Gonzalez, et al., 2010). However, different attrition behaviour was also observed where attrition of limestone in a pilot

DFB system appeared to continue at a relatively high level with increasing number of cycles (Lu, et al., 2008).

Prior research showed that the different environments in the carbonator and calciner will result in different attrition behaviour. Scala et al. (2010) observed that calcined sorbent tends to suffer more attrition than carbonated sorbent in fluidized bed systems, which confirms earlier results by Lu et al. (2008) who noted that most fines were collected from the cyclone of the calciner. This indicated that attrition is occurring at a higher rate in the calciner than in the carbonator. This occurrence is attributed to the fact that calcined particles are lighter and more fragile than carbonated ones, which are denser and more compact. Fine particles generated due to attrition tend to elutriate from the fluidization beds, causing loss of materials. Accordingly, a make-up sorbent flow is essential to maintain a desirable CO_2 capture performance. However, a subsequent study found that maintaining a high make-up flow to replace the spent sorbent and elutriated materials significantly influences the economics of the process (Romeo, et al., 2009). Therefore, it is important for CaL processes to minimize sorbent attrition rates.

One approach for improving the mechanical strength of sorbent particles is through pelletization. A variety of binders were tested for pelletization; an early study on the pelletization of CaO-based sorbent showed that Ca- and Na-bentonites were inadequate as binders for the preparation of CaO-based pellets due to the high SiO_2 content (~60 wt%) (Manovic and Anthony, 2009a). At high temperatures, SiO_2 was found to form eutectic mixtures, which enhance sorbent sintering (Manovic, et al., 2009). Similarly, kaolin binder was also found to accelerate sintering of CaO-based pellets due to its high SiO_2 content (~46 wt%), whereas Al_2O_3 was found to be a weak binder (Ridha, et al., 2012). On the other hand, a series of studies (Manovic and Anthony, 2009b) (Manovic and Anthony, 2009c) (Manovic and Anthony, 2010)

showed that pellets made from Cadomin limestone and calcium aluminate cement as a binder outperformed limestone exhibiting an enhanced carbonation conversion over multiple cycles in a thermogravimetric analyzer (TGA). Furthermore, it was realized that spent pellets prepared with cement can be reactivated, remade and recharged to the system without any major obstacles (Manovic and Anthony, 2011). Despite the fact that prior studies on pelletization of sorbents with cement demonstrated the superiority of these pellets compared to natural material with regards to CO_2 capture capacity, these studies were conducted in TGA under relatively mild conditions (e.g., calcination in N_2 at 800°C) with complete absence of mechanical challenges. Accordingly, the mechanical strength of these pellets has never been examined under typical CaL conditions. A survey on literatures shows that there has been no prior research on the attrition of pelletized CaO-based sorbents in pilot fluidized bed systems under realistic conditions. Therefore, studying the fragmentation/attrition behaviour of pelletized CaO-based sorbents in pilot-scale FBC system is essential for their successful deployment in CaL processes.

This work investigates the fragmentation and attrition of CaO-based pellets in a pilot-scale dual FBC system. The pellets were prepared from limestone and calcium aluminate cement as a binder. Operating conditions were chosen to be as close as possible to the real conditions of CaL cycles to obtain more realistic results. Attrition of Cadomin limestone was also examined for comparison purposes.

7.3 – Experimental

7.3.1 – Sorbents

Single batches of Cadomin and Spanish limestones were the source of all CaO-based sorbents in this work. Elemental analysis of the powdered limestones was carried out using X-ray fluorescence (XRF) spectroscopy. The content of the major elements in these limestones is

shown in Table 7.3.1. The binder was commercial calcium aluminate cement (CA-14) with composition (in wt%) of 72.7% Al_2O_3, 27.2% CaO, and 0.1% impurities, respectively.

Table 7.3.1: XRF elemental analysis of limestone (wt%).

Component	Cadomin	Spanish
SiO_2	1.30	<0.10
Al_2O_3	0.40	<0.10
Fe_2O_3	0.11	0.03
CaO	50.64	55.71
MgO	3.12	0.39
K_2O	0.14	<0.02
LOF*	43.99	43.83
Sum	99.86	99.96

* LOF: Loss on Fusion

Cadomin limestone was crushed and sieved to a size range of 212-600 μm for the attrition test. Powdered Cadomin and Spanish limestones were used for the production of pellets. The pelletization work was carried out in a mechanical pelletizer (Glatt GmbH) in batch mode. Prior to pelletization, lime was produced by calcining the powdered limestone at 850°C in air in a muffle furnace. A batch of 90 wt% lime and 10 wt% cement were then mixed rigorously for a few seconds in the pelletization vessel followed by water spray from an ultrafine pore nozzle under continuous mixing. The mixing was facilitated by two blades; an agitator at the bottom of the vessel and a chopper on the side. The rotation speed of the blades is controllable, thus the mixing speed was tuned to obtain the desired product quality. The resultant batch of pellets were sieved to a size range of 250-600 μm, and then left to dry in air. The pellets were designated according to their starting limestone, i.e., CD pellets and SP pellets. Table 7.3.2 presents the specifications of sorbents used in this work.

Table 7.3.2: Sorbent specifications.

Sorbent	Designation	Addition mode	Particle size (μm)
Cadomin limestone	CD	Batch	212-600
Cadomin pellets	CD-B	Batch	250-600
Cadomin pellets	CD-C	Continuous	250-600
Spanish pellets	SP-C	Continuous	250-600

7.3.2 – Dual fluidized bed system setup

Calcium looping tests were carried out in a 0.1 MW_{th} pilot plant developed at Natural Resources Canada – CanmetENERGY. The schematic of the facility is shown in Figure 7.3.1. A more detailed description of the setup is provided elsewhere (Symonds, et al., 2016). In general the system consists of two interconnected fluidized bed reactors, a calciner which is a circulating fluidized bed with capacity to operate in oxy-fuel firing conditions, and a carbonator which is a bubbling bed. Both the calciner and carbonator are constructed out of SS310 and have an internal diameter of 0.1 m, and heights of 5.1 and 3.0 m, respectively. In addition, the reactors are outfitted with electric heaters capable of operating at temperatures up to 1100°C.

Each reactor is equipped with a high efficiency cyclone to re-entrain the sorbent during circulating fluidized bed operation; thus, minimizing sorbent elutriation from the system. The feeding system is comprised of two feed hoppers for fuel and limestone with the capacity to operate in batch or continuous mode. This feature enables investigating the effect of materials addition mode on the rate of attrition of sorbent.

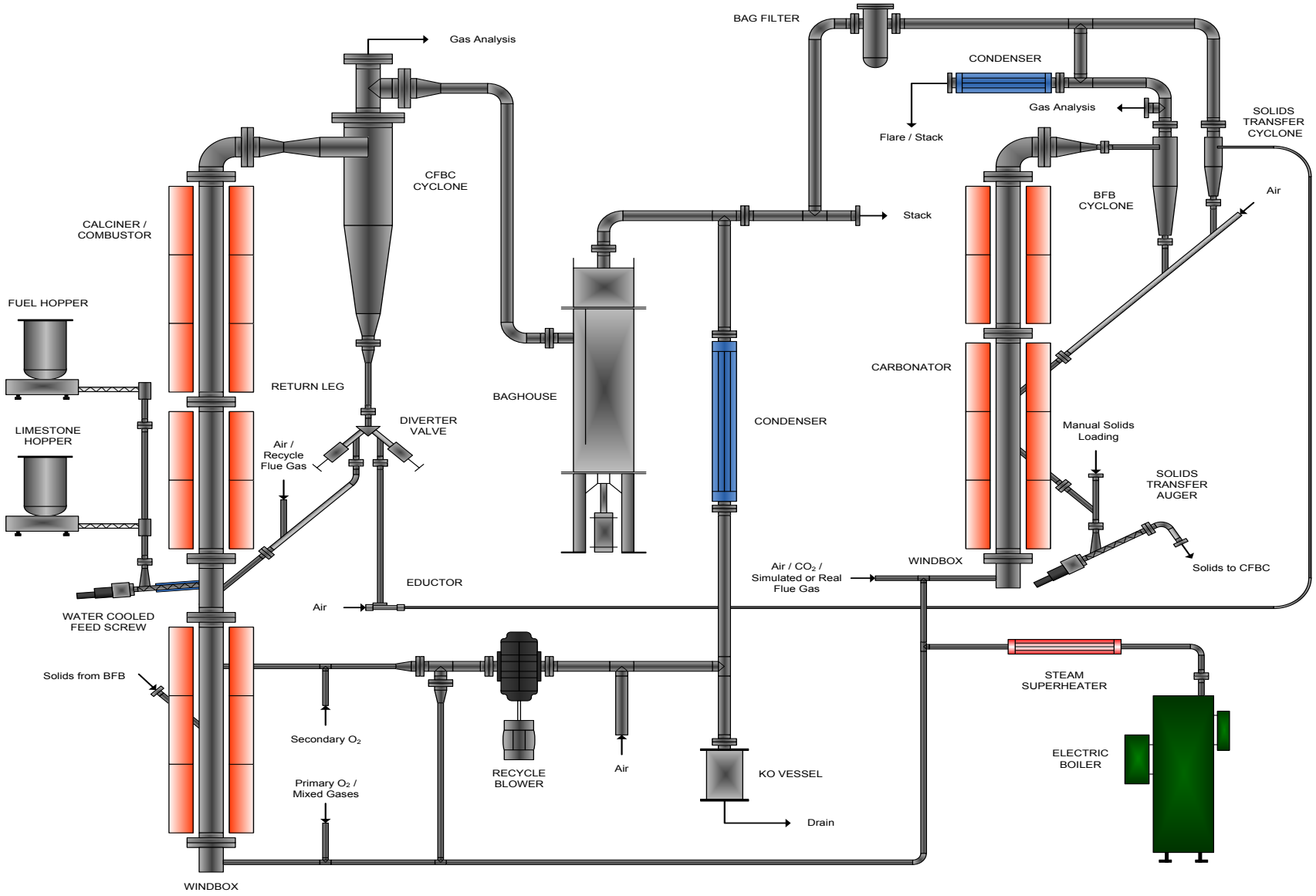

Figure 7.3.1: A schematic of the CaL pilot-plant at Natural Resources Canada – CanmetENERGY

The method for transferring the solids from the calciner to the carbonator and *vice versa* is a critical part in the system due to the fact that the system should try to minimize any particle attrition or fragmentation. The solids transfer system is comprised of two main components: (1) transfer of solids from the carbonator to the calciner by a mechanical auger, and (2) transfer of solids from the calciner to the carbonator by a pneumatic conveying system. The pneumatic educator uses compressed air to transfer the solids vertically through a 19 mm line to a high-efficiency cyclone, which discharges into a return-leg and is gravity feed into the carbonator. The transfer rate can be adjusted by changing the flow rate of compressed air to the educator. Additional compressed air is used to ensure the material exiting the transfer cyclone flows smoothly into the carbonator. All solids transfer and flue gas lines are constructed of high temperature stainless steel and are externally insulated to minimize heat loss to the surroundings.

7.3.3 – Methods

7.3.3.1 – Pilot plant test

Prior to the start of a test, the calciner was charged with 4.5 kg olivine sand with a particle size in the range of 525-1180 μm to help absorb and distribute heat while heating up the system to the desired temperatures (~650°C for the carbonator and ~900°C for the calciner). On the other hand, ~5 kg of sorbent was loaded to the carbonator while heating up and upon reaching a steady condition the sorbent was circulated to the calciner for calcination. Fluidization velocities in the calciner and carbonator were 2.0-2.6 and 0.5-0.8 m/s, respectively. The flue gas supplied to the carbonator was generated using an air-fired natural gas burner. The calciner operated under oxy-firing conditions using wood pellets as a fuel at a feeding rate of 5-7 kg/h. A more detailed description of the operation method is available in Chapter 6 (Symonds, et al., 2016).

The cycle begins when the calcined sorbent travels from the calciner through the cyclone and educator to the carbonator where carbonation takes place. The carbonated sorbent then leaves the carbonator and is transferred back to the calciner for the next calcination. In the batch addition test, ~1 kg of sorbent was added to the system when the carbonator outlet CO_2 concentration reached 1.5 vol% (dry basis). This amount was translated to an input make-up flow rate in the continuous addition test. Shortly after starting the test, a CO_2 concentration of 90% was achieved in the calciner, indicating a suitable oxy-firing condition was attained. This condition was maintained throughout the test campaign in order to eliminate the effect of oxy-firing condition on the attrition of the sorbents. CO_2 capture efficiencies in all tests were in the range of 80-90% while average molar calcium looping ratios (CaO/CO_2) were in the range of 9.2-12.3. The test was stopped when the CO_2 capture capacity started declining after the last injection of sorbent. In general, all tests were run for a minimum of 5 h of continuous, steady-state operation. A sample (~30 g) was withdrawn from the carbonator and the calciner every 1 h for conversion analysis. Attrition analysis was made with samples withdrawn from the system at the end of the test, and thus no replacement with fresh material was required.

7.3.3.2 – Analysis

The setup in Figure 7.3.1 enabled an efficient fluidization and circulation of solids between the reactors; thus, the solids were assumed to be thoroughly mixed throughout the entire system. Accordingly, particle size distribution (PSD) in the carbonator is assumed to be identical to that in the calciner, and sampling from either reactor is adequate for the assessment of attrition. Whenever possible, a sample of 200 g was extracted from the carbonator and analyzed for PSD. The sample was loaded into sieving trays placed inside a mechanical shaker, and

sieving was allowed to continue for 20 min. The analysis was performed twice for each sample to determine the standard errors.

7.4 – Results and Discussion

The quantitative analysis of the PSD of limestone is shown in Figure 7.4.1. In Figure 7.4.1a, it can be seen that the sizes of raw limestone particles are evenly distributed (with nearly equivalent fractions) over the 250-600 μm size range. It can also be noted that 8.5% of the initial sorbent batch contains particles of a size smaller than 250 μm (the lower size of particles fed to the system is 212 μm, Table 7.3.2). After the test, the limestone displayed a completely different distribution where the proportion of large particles decreased considerably, while small particles increased showing singularity at particle size smaller than 250 μm, which represents 50.6% of the collected sample (corrected against the faction with size <250 μm in the raw limestone). The fractional mass of particles with size smaller than 250 μm was also analyzed for size distribution to provide more complete information on the attrition, and the results are shown in Figure 7.4.1b. This figure indicates that ~47% of this size fraction are particles with a size smaller than 150 μm.

(a)

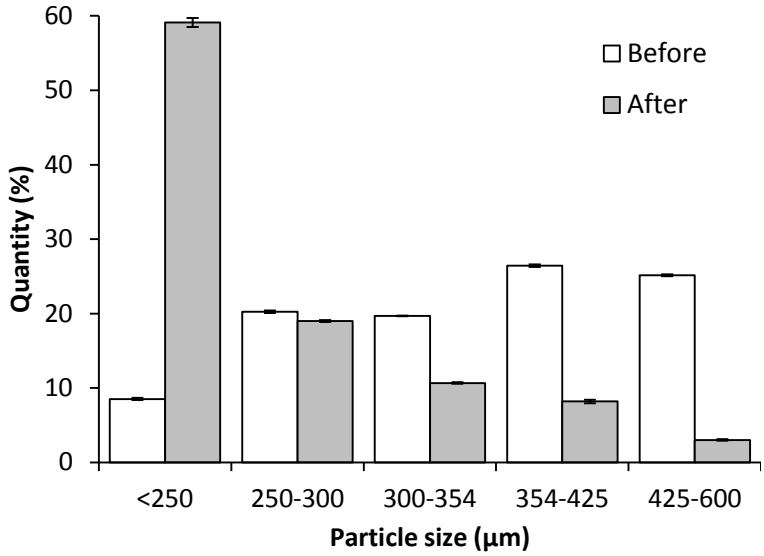

(b)

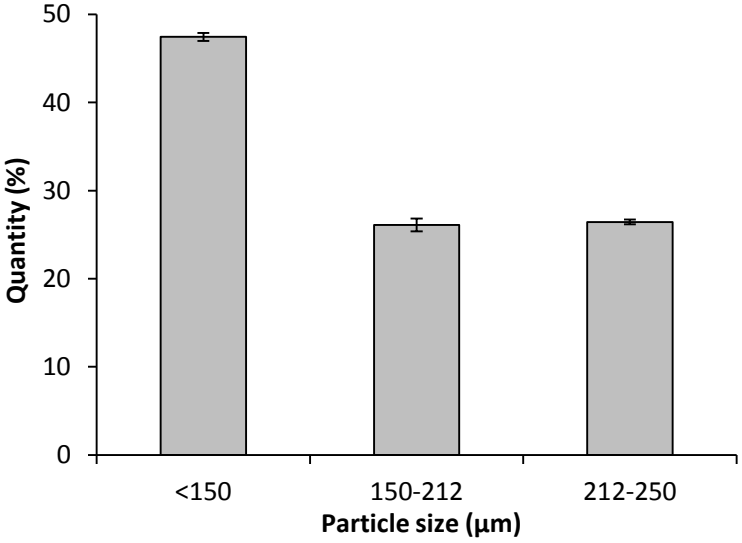

Figure 7.4.1: CD from the carbonator; (a) before and after the test, and (b) fraction with size <250 µm after the test.

It has been postulated (Scala, et al., 2010) that olivine sand has a much higher resistance to attrition than sorbents (limestone or pellets); thus, attrition of sand has been considered negligible. However, some sand particles were observed in the fraction with size 425-600 µm, whereas no sand particles were observed in the smaller size fractions. Sand particles collected in this size fraction are due to the fact that the size range of olivine sand particles used in this work

(i.e., 525-1180 μm) overlaps with the upper size fraction of the sorbent (i.e. 600-428 μm). As can be seen in Figure 7.4.1 (and all the subsequent figures), the quantity of the fraction with size 425-600 μm is fairly small. Accordingly, the effect of the presence of sand particles in this size fraction has an insignificant effect on the trends. It is worth addressing that the presence of sand in the bed may enhance sorbent attrition (Scala, et al., 1997). However, as all tests in this work were conducted in the presence of sand, it was not possible to verify this matter. Nonetheless, in reality the effect of sand on attrition, if any, will diminish gradually with the gradual and continuous discharge of materials from the system during operation (e.g., sintered sorbent and ash).

It must be noted that attrition by abrasion tends to take place at the beginning of the operation, shortly after injecting the sorbent, due to initial rounding off of angular raw limestone particles. The abrasion generates very fine particles that are quickly elutriated from the system (Scala, et al., 2000). Accordingly, the fractional mass of particles with size smaller than 250 μm in Figure 7.4.1 is the attrition that is most likely due to fragmentation of particles as a result of impacts against walls, bed materials, and internals of the bed (Scala, et al., 2000). As Figure 7.4.1 illustrates the development of the PSD after ~5 h of cyclic operation, it demonstrates the occurrence of severe attrition of limestone particles. Surface wear due to abrasion is expected to be much less with pellets compared to raw Cadomin because of their regular spherical shape.

Figure 7.4.2 highlights the PSD of CD-B (batch addition of pellets) before and after the test. In Figure 7.4.2a, it can be observed that the PSD patterns of pellets resemble to a large extent those of limestone. CD-B experienced a significant extent of impact fragmentation with 46% of the total mass was found to be particles with size smaller than 250 μm. Also, pellets of intermediate size between 300-600 μm were rarely present. Further analysis of the fractional

mass with pellets smaller than 250 μm in Figure 7.4.2b revealed that ~46% of this fraction is pellets with size smaller than 150 μm.

A comparison of these results with those obtained with limestone indicates that the pellets are indeed stronger than limestone particles, with extent of attrition slightly lower (by ~4.6%) than that of limestone. Furthermore, it is well acknowledged that CaO-based particles shrink under severe cyclic operation. A previous study (Manovic and Anthony, 2009c) noted that the volume of CaO-based pellets shrank by 15-20% after 300 carbonation/calcination cycles, whereas an earlier study (Alvarez and Abanades, 2005) also reported shrinkage in limestone particle size after multiple cycles. However, the effect of such phenomenon was assumed negligible compared to the effect of attrition. Therefore, it is concluded that the enhancement in the mechanical strength of these pellets was not to the point of outperforming limestone significantly, and thus the alteration in the mechanical strength of CD-B due to pelletization with 10% cement appears marginal.

(a)

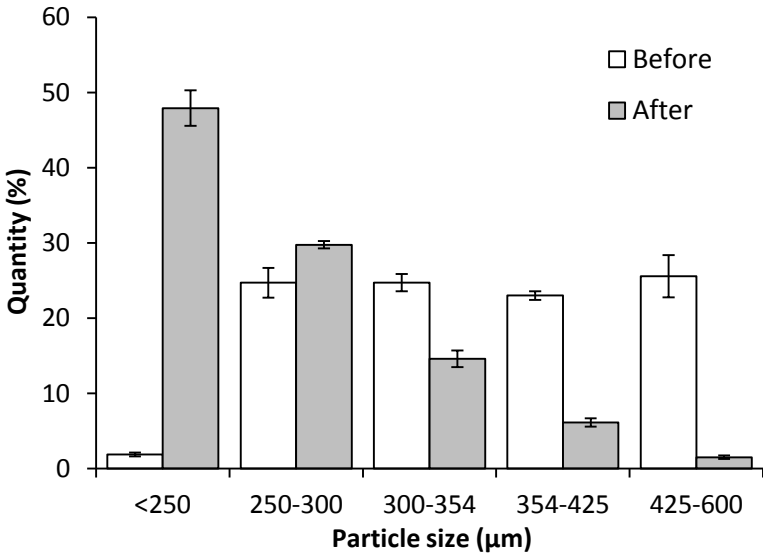

(b)

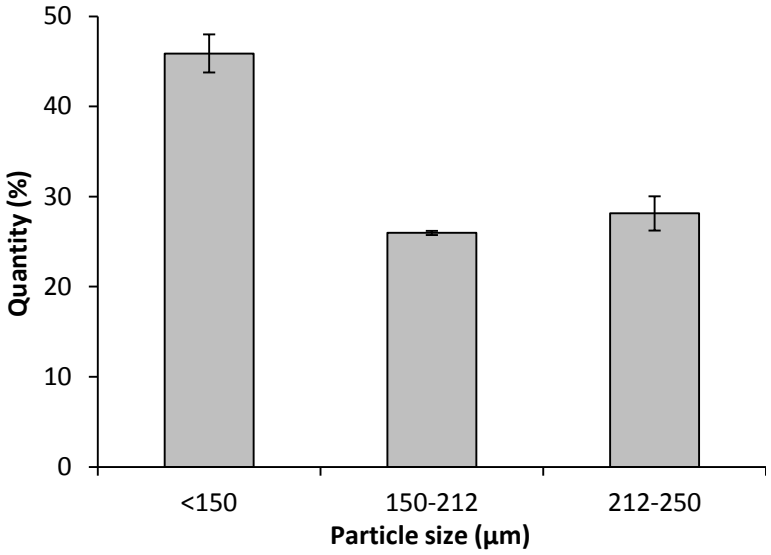

Figure 7.4.2: CD-B from the carbonator (batch addition of pellets-biomass, no steam); (a) before and after the test, and (b) fraction with size <250 μm after the test.

The effect of the direct and continuous injection of pellets to the calciner on the extent of attrition is shown in Figure 7.4.3. It can be seen that PSD pattern of the fragments is qualitatively similar to that Figure 7.4.2a. However, Figure 7.4.3a reveals that 54.3% of the sample is pellets with size smaller than 250 μm, representing an increase of 8.3% compared to that from the batch injection. Furthermore, 48.3% of the fractional mass with pellets smaller than 250 μm belongs to fragments with size smaller than 150 μm, as shown in Figure 7.4.3b. These results indicate that the method of feeding the pellets into the system affects their fragmentation pattern, and in the current case, it shifted the PSD of the pellets towards finer fragments. This effect can be rationalized by the fact that in the batch injection, about half of the total mass of the pellets was fed to the carbonator prior to the test (during warming up stage). As the pellets composed mainly of $Ca(OH)_2$, they saw a slow and gradual dehydration. In comparison, under continuous injection testing the pellets were fed directly to the calciner; thus, subjected to a sudden and rapid

dehydration due to the enhanced heating rate. Although the sudden dehydration may cause the pellets to undergo a pop-corn effect, this method of injection is more realistic than injection in batch mode. Considering this fact, it seems that the pellets did survive the sudden dehydration with fairly low fragmentation, as can be noticed from the comparison of the results in Figure 7.4.2 and Figure 7.4.3.

(a)

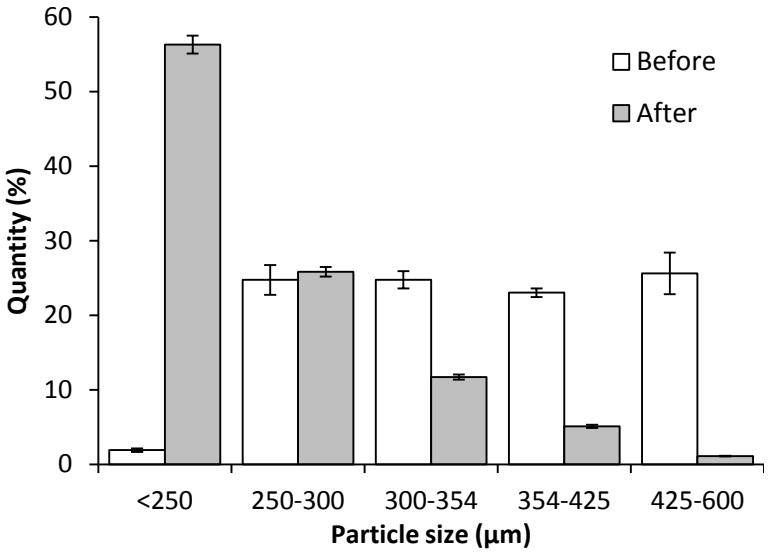

(b)

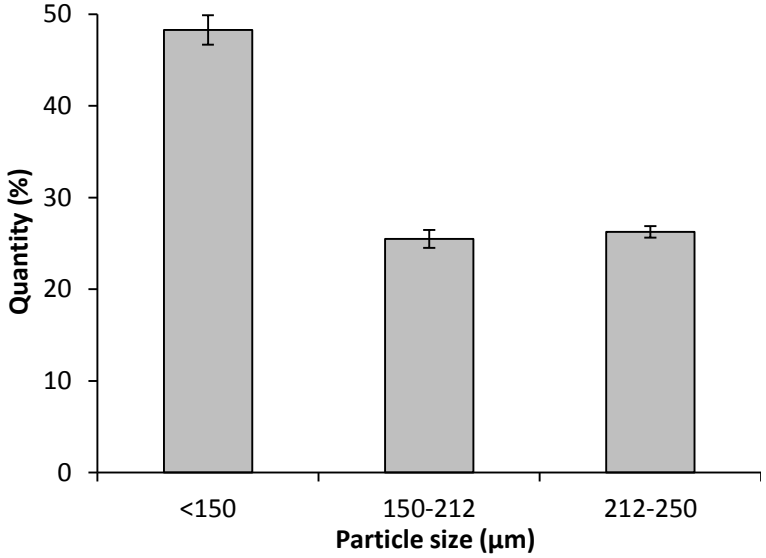

Figure 7.4.3: CD-C from the carbonator; (a) before and after the test, and (b) fraction with size <250 µm after the test.

To illustrate the effect of the parent limestone on the attrition of the resultant pellets, PSD of SP pellets injected continuously to the system during the test (SP-C) are presented in Figure 7.4.4 . Figure 7.4.4a highlights the way the size of pellets and fragments before and after the test are distributed. The most obvious observations are the near eliminations of the fractional mass of pellets with size in the range of 425-600 μm, representing 39.2% of the initial ~9 kg material before the test, and the significant increase in the fractional mass of pellets with size smaller than 250 μm (52% after the test). Figure 7.4.4b also shows that ~44.1% of the total fractional mass of pellets with size smaller than 250 μm are composed of fragments with a size smaller than 150 μm. An examination of the PSD patterns of SP-C and CD-C reveals a fair agreement between the attrition of both groups of pellets in the same injection mode. According to Table 7.3.1, Spanish limestone has a higher purity than Cadomin limestone (higher CaO content), nonetheless, a comparison of attrition extents in Figure 7.4.3 and Figure 7.4.4indicates that pellets prepared from these two limestones exhibited similar tendencies for attrition when tested under similar conditions. These lead to two main conclusions: (1) the type of limestone used in the preparation of pellets does not seem to play a significant role in the attrition of the corresponding pellets, and (2) pellets prepared with 10% calcium aluminate cement as a binder appear to have mechanical strength comparable to that of limestone. Accordingly, the improvement gained from pelletization appeared marginal, and thus pelletization under the specified conditions used here is of limited benefit for CaL process due to the increase cost of preparation.

(a)

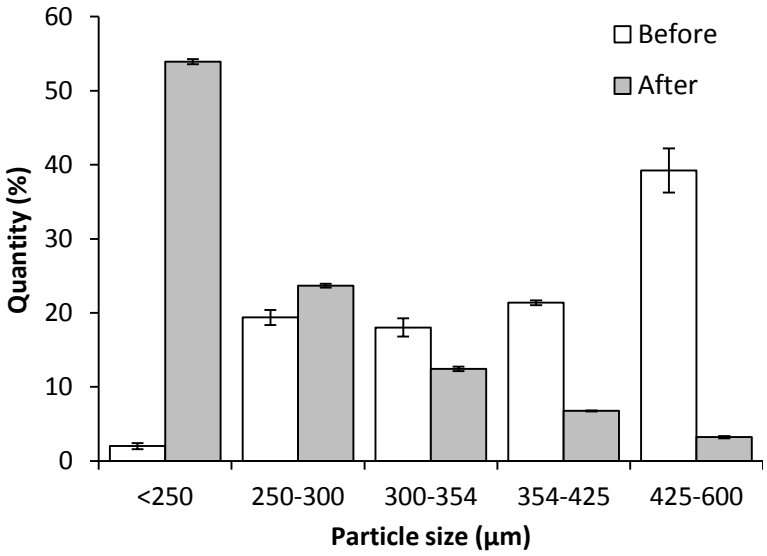

(b)

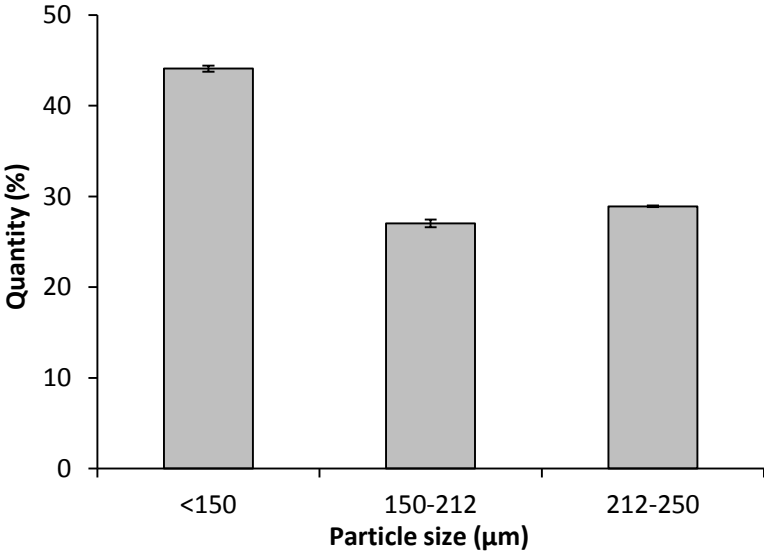

Figure 7.4.4: SP-C from the carbonator; (a) before and after the test, and (b) fraction with size <250 µm after the test.

It is worth addressing that, despite the high attrition extents observed with these sorbents, low elutriation rates (percentage of make-up rate) were obtained with CD-C and SP-C pellets, as shown in Figure 7.4.5. The elutriation data presented in this figure represent materials accumulated in the horizontal line and baghouse, i.e., fines with size < 5 µm not captured by the

cyclone. These relatively low elutriation rates explained to some extent the good CO_2 capture performance of these sorbents presented in our previous work (Symonds, et al., 2016). This implies that the elutriation of the very fine fraction is not expected to significantly influence the performance of these pellets due to the fact that the mass of this fraction is small compared to that of the make-up, which agrees well with results from a previous study (Dieter, et al., 2013). It can be concluded here that the current pellets have high attrition, but low elutriation after 5 h of continuous steady operation, and hence most of the sorbents remained within the DFB system. This is a desirable feature in these pellets, as high elutriation in potential commercial facilities would causes economic penalties and technical difficulties.

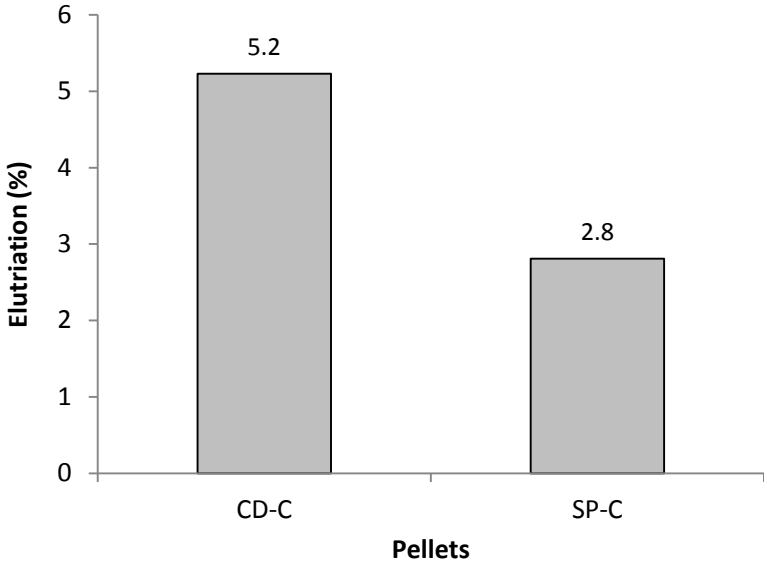

Figure 7.4.5: Elutriation of pellets in continuous addition mode.

7.5 – Conclusions

The attrition of CaO-based pellets in a pilot DFB system was studied and the results were presented in this work. Two different groups of pellets, 250-600 μm in size, prepared from Cadomin and Spanish limestones with 10% calcium aluminate cement as a binder were examined. The results revealed that ~50% of the sorbent, by mass, is smaller than 250 μm after

the test is completed. Furthermore, ~45% of the sorbent by mass, smaller than 250 μm is in fact smaller than 150 μm. The particle size distribution of pellets indicated high attrition, and the attrition extent was comparable to that of limestone tested under similar conditions. Batch and continuous injection of pellets to the system showed insignificant effect of injection method on the attrition of the pellets. The similarity of particle size distribution patterns of pellets is indicative of similar attrition tendencies, and appears to be a characteristic of these pellets regardless of limestone type and injection method. It was concluded that pelletization of CaO-based sorbents using limestone and 10% cement results in a marginal improvement in the mechanical strength of the resultant pellets in comparison to unmodified limestone. Accordingly, pelletization of sorbent for CO_2 capture in the CaL process is considered an inadequate approach for reducing the attrition of sorbent.

7.6 – Acknowledgements

This research and experimental test campaign was funded by Natural Resources Canada, through the Program of Energy Research and Development (PERD).

7.7 – References

Alvarez, D., Abanades, J.C. (2005). Pore-size and shape effects on the recarbonation performance of calcium oxide submitted to repeated calcination/recarbonation cycles. *Energy & Fuels,* 19, 270–278.

Arias, B., Diego, M. E., Abanades, J. C., Lorenzo, M., Diaz, L., Martinez, D. Alvarez, J., Sanchez-Biezma, A. (2013). Demonstration of Steady State CO_2 Capture in a 1.7 MWth Calcium Looping Pilot. *Int. J. Greenhouse Gas Control*, 18, 237-245.

Bernstein, A.L., Lee, Crookshank, S. (2006). Carbon dioxide capture and storage: A status report, *Climate Policy,* 6, 241-246.

Boot-Handford, M.E, Abanades, J.C., Anthony, E.J., Blunt, M.J., Brandani, S., Mac Dowell, N., Fernández, J.R., Ferrari, M.-C., Gross, R., Hallett, J.P., Haszeldine, R.S., Heptonstall,

P., Lyngfelt, A., Makuch, Z., Mangano, E., Porter, R.T.J., Pourkashanian, M., Rochelle, G.T., Shah, N., Yao, J.G. (2014). Carbon capture and storage update. *Energy and Environmental Science,* 7, 130-189.

Blamey, J., Anthony, E.J., Wang, J., Fennell, P.S. (2010a) The calcium looping cycle for large-scale CO2 capture. *Progress in Energy and Combustion Science,* 36, 260-279.

Blamey, J., Paterson, N.P.M., Dugwell, D.R., Fennell, P.S. (2010b). Mechanism of particle breakage during reactivation of CaO-based sorbents for CO2 capture. *Energy Fuels,* 24, 4605–4616.

Chen, Z., Lim, C.J., Grace, J.R. (2007). Study of limestone particle impact attrition, Chemical *Engineering Science,* 62, 867–877.

Dieter, H., Hawthorne, C., Zieba, M., Scheffknecht, G. (2013). Progress in calcium looping post combustion CO_2 capture: successful pilot scale demonstration. *Energy Procedia,* 37, 48–56.

Giuffrida, A., Bonalumi, D., Lozza, G. (2013). Amine-based post-combustion CO2 capture in air-blown IGCC systems with cold and hot gas clean-up. *Applied Energy,* 110, 44-54.

González, B., Alonso, M., Abanades, J.C. (2010). Sorbent attrition in a carbonation/calcination pilot plant for capturing CO_2 from flue gases. *Fuel,* 89, 2918–2924.

Hu, N., Scaroni, A.W. (1995). Fragmentation of calcium-based sorbents under high heating rate, short residence time conditions. *Fuel,* 74, 374–382.

Lu, D. Y., Hughes, R. W., Anthony, E. J. (2008). Ca-based Sorbent Looping Combustion for CO2 Capture in Pilot-Scale Dual Fluidized Beds. *Fuel Process. Technol*., 89, 1386-1395.

MacKenzie, A., Granatstein, D. L., Anthony, E. J., & Abanades, J. C. (2007). Economics of CO2 capture using the calcium cycle with a pressurized fluidized bed combustor. *Energy & Fuels*, 21, 920-926.

Manovic, V., Anthony, E.J. (2009a). Screening of binders for pelletization of CaO-based sorbents for CO2 capture. *Energy Fuels,* 23, 4797–4804.

Manovic, V., Anthony, E.J. (2009b). CaO-based pellets supported by calcium aluminate cements for high-temperature CO_2 capture. *Environmental Science and Technology,* 43, 7117–7122.

Manovic, V., Anthony, E.J. (2009c). Long-term behavior of CaO-based pellets supported by calcium aluminate cements in a long series of CO_2 capture cycles. *Industrial and Engineering Chemistry Research,* 48, 8906–8912.

Manovic, V., Anthony, E.J. (2010). CO_2 Carrying behavior of calcium aluminate pellets under high-temperature/high-CO_2 concentration calcination conditions. *Industrial and Engineering Chemistry Research,* 49, 6916–6922.

Manovic, V., Anthony, E.J. (2011). Reactivation and remaking of calcium aluminate pellets for CO_2 capture. *Fuel,* 90, 233–239.

Manovic, V., Harland, J.P., Blamey, J., Fennell, P.S., Lu, D.Y., Anthony, E.J. (2009). Influence of calcination conditions on carrying capacity of CaO-based sorbent in CO2 looping cycles. *Fuel,* 88, 1893–1900.

Materic, V., Holt, R., Hyland, M., Jones, M.I. (2014). An internally circulating fluid bed for attrition testing of Ca looping sorbents. *Fuel*, 127, 116–123.

Nittaya, T., Douglas, P.L., Croiset, E., Ricardez-Sandoval, L.A. (2014). Dynamic modelling and control of MEA absorption processes for CO2 capture from power plants. *Fuel,* 116, 672–691.

Ridha F.R., Manovic, V., Macchi, A., Anthony, E.J. (2012). High-temperature CO2 capture cycles for CaO-based pellets with kaolin-based binders. *International Journal of Greenhouse Gas Control*, 6, 164–170.

Romeo, L. M., Lara, Y., Lisbona, P., & Escosa, J. M. (2009). Optimized make-up flow in a CO2 capture system using CaO. *Chemical Engineering Journal*, 147 (2-3), 252-258.

Scala, F., Cammarota, A., Chirone, R., Salatino, P. (1997). Comminution of limestone during batch fluidized-bed calcination and sulphation. *AIChE Journal,* 43, 363-373.

Scala, F., Montagnaro, F., Salatino, P. (2007). Attrition of limestone by impact loading in fluidized beds. *Energy & Fuels,* 21, 2566–2572.

Scala, F., Salatino, P., Boerefijn, R., Ghadiri, M. (200). Attrition of sorbents during fluidized bed calcination and sulphation. *Powder Technology,* 107, 153–167.

Symonds, R. T., Champagne, S., Firas, N., & Lu, D. (2016). CO2 capture performance of CaO-based pellets in a 0.1 MWth pilot-scale calcium looping system. *Powder Technology*, 124-131.

Chapter 8 – Discussion, Conclusions, and Recommendations

The overall objective of this work was to develop a process for continuous CO_2 capture *via* calcium looping by filling in the missing information between what had previously been explored at the bench-scale and what can be expected at the commercial-scale. Although bench-scale testing, such as thermogravimetric and fixed bed analyses, provide general trends for CaO-based sorbent CO_2 carrying capacity deactivation, they fail to provide actual values expected when operating as a real dual fluidized bed reactor at the commercial-scale. The effects of proper gas-solid contacting, high heating rates, realistic reactive environments, and sorbent attrition must be considered in order to provide accurate information for process modeling and techno-economic analysis required for technology scale-up. Therefore, experimental measurements of key calcium looping process parameters were obtained *via* a combination of bench-scale, batch pilot-scale, and continuous pilot-scale testing at the 100 kW_{th} scale.

Economic analyses and simulation of the calcium looping process have shown that three process parameters are critical to the viability of this technology for post-combustion CO_2 capture technology, namely:

1) The sorbent deactivation rate;
2) The Ca/C molar ratio; and
3) The rate of sorbent attrition.

Taking this into consideration, not only were these parameters explored from a process improvement standpoint, but significant efforts were made to accurately determine them under conditions expected at the commercial-scale.

Chapter 3 explored the effect of the presence of HCl during carbonation and calcination on the CO_2 carrying capacity of a naturally occurring limestone. This series of experimental

tests represents the first time the impact of HCl on the calcium looping process has been considered under realistic operating conditions. Many fuels such as coal, biomass, refuse derived fuel, and biofuels contain significant quantities of chlorine, which principally converts to gaseous HCl during combustion or gasification. In an effort to move away from more carbon intensive fuels (i.e., coal), many of these bio-related fuels could very well end up as the primary fuel source for both post-combustion fuel gas generation and calcination; and therefore, HCl could become the major gaseous contaminate (as opposed to SO_2, for example).

Preliminary testing under a pure N_2 calcination environment resulted in the irreversible formation of $CaCl_2$, reducing the active portion of the sorbent surface over repeated calcination / carbonation cycles. Ultimately, this increased the CO_2 diffusional resistance to the active CaO sites, since diffusion through the $CaCl_2$ product layer became the rate controlling step. This lowered the cyclic carbonation conversion by a measured ~3 percentage points in comparison to without HCl present and would be expected to drop further as the number of cycles is increased.

When testing moved to a more realistic carbonation / calcination gaseous environment containing varying levels of steam, the results were dramatically different. When steam was added during calcination to levels anticipated during oxy-fuel combustion, the carbonation conversions over multiple cycles were in fact higher when HCl was present. This was attributed to the decomposition of $CaCl_2$ to CaO during calcination, causing the formation of larger pores at the particle surface and decreasing the CO_2 diffusional resistance during carbonation. This mechanism was supported by both phase equilibria analysis using FactSage and the difference in molar volumes between $CaCl_2$ and that of $CaCO_3$. Confirmation that full decomposition of $CaCl_2$ to CaO could be expected under typically oxy-fuel calcination conditions (both gaseous environment and reaction duration) was determined *via* fixed bed testing. Changes in particle

morphology were also observed, further reinforcing the hypothesis that dechlorination during calcination results in a particle structure that increases carbonation reactivity.

The major result from testing under gaseous environments containing HCl was that greater than 99% HCl capture can be attained without adversely affecting sorbent CO_2 capture performance when steam is present during calcination. This is significantly different in comparison to SO_2 that reacts with CaO and $CaCO_3$ to form $CaSO_4$, which cannot decompose under any conditions expected for calcium looping systems. From an experimental testing point of view, pilot-scale testing with HCl containing fuels becomes far less critical since its effect on sorbent deactivation is minimal at best. Referring back to Figure 3.4.10, there is a significant drop in carbonation conversion *via* fixed bed testing in comparison to thermogravimetric analysis, but this decrease can be attributed only to sorbent sintering caused by more severe calcination conditions (higher local CO_2 concentrations and higher heating rates). While this sintering effect will become more pronounced at the pilot-scale, by using the rationale above, the presence of HCl should not impact the sorbent CO_2 carrying capacity over repeated cycles under normal oxy-fuel calcination conditions.

Although the effect of HCl on sorbent performance does not appear to be critical to the successful development of calcium looping, there is still one major concern that has yet to be addressed. Due to HCl capture during carbonation, and its subsequent release *via* $CaCl_2$ decomposition during calcination, HCl concentrations in the concentrated CO_2 product stream could be relatively high (>2000 ppm). This could lead to potential corrosion related equipment failures in downstream process components such as the condenser, baghouse, and CO_2 scrubber / compressor. Therefore, the following future work is recommended:

- HCl concentration at the outlet of the calciner measurement during high chlorine fuel testing.
- Downstream process component materials testing under high HCl and steam gaseous environments.

The effect of both SO_2 addition and high CO_2 partial pressure calcination within the calcium looping process has been thoroughly investigated at the bench-scale. What was still required was the actual CO_2 carrying capacity of CaO-based sorbents over repeated cycles under these conditions at the pilot-scale. Hence, a series of batch pilot-scale fluidized bed calcium looping experiments were performed on the effect of SO_2 addition on CO_2 capture by limestone-based sorbents calcined under oxygen-enriched air and oxy-fuel conditions, with and without SO_2 addition during calcination (Chapter 4).

The higher CO_2 partial pressure associated with full oxy-fuel combustion conditions dropped the rapid kinetically-controlled CO_2 capture stage by approximately 80% and reduced the sorbent carrying capacity by 15 percentage points to 25%. This value was further reduced to only 11% after the second cycle. The addition of SO_2 during calcination also caused a dramatic reduction in the initial rapid kinetically-controlled CO_2 capture stage and dropped the carbonation conversion further to less than 15% after the first cycle. By the end of the third cycle, only a diffusion-controlled regime was observable. This was attributed to both enhanced sorbent sintering and the formation of a solid $CaSO_4$ layer/shell, which increases the diffusion resistance. These results are significant in comparison to TGA experiments conducted under similar conditions which showed carbonation conversions above 45% for the first cycle, with a more gradual decay in carbonation conversion over multiple cycles as predicted by Equation 2.2.

As described in Chapter 3, the presence of steam during carbonation has been shown to enhance the CO_2 capture performance of CaO-based sorbents. Again, pilot-scale experimental testing was required to provide quantitative values for carbonation conversions under conditions expected at the commercial-scale. The addition of steam during carbonation not only increased the fast CO_2 capture period by approximately 300%, but also resulted in an increase in average carbonation conversion to over 20% over three cycles (Cadomin limestone), with the presence of SO_2 and high CO_2 partial pressure during calcination. These findings were confirmed by TGA experiments, but careful attention should be made to avoid misleading results and conclusions related to sorbent performance under these less severe TGA calcination conditions.

One of the key objectives of the batch pilot-scale testing was to provide sorbent performance information required to determine sizing and operating parameters for a fully continuous calcium system operating under realistic conditions. By measuring the carbonation conversion over repeated cycles and the duration of the fast kinetically-controlled regime during batch testing, this could now be achieved. From this test campaign, it was now apparent that using a sorbent decay model, such as the one provided in Equation 2.2, was not a reasonable representation of true sorbent performance over repeated cycles. The assumption that the sorbent conversion would start out above 50% and gradually drop down to around 10% over 75 to 100 cycles would result in smaller than required Ca/C ratio and underestimation of the required sorbent make-up rate. Additionally, the reduction in the high efficiency CO_2 capture period could lead to an undersized carbonator in terms of gas-solid residence time. It is important to note that a higher Ca/C molar ratio than reported in literature would be required at the pilot-scale: 9-12 versus 4-8, where the latter is based solely off of bench-scale data.

With the lower than expected sorbent conversion, coupled with a reduced high efficiency CO_2 capture period, design calculations for a fully continuous calcium system could now be initiated. As explained in Chapter 2, a bubbling fluidized bed carbonator is the most reasonable choice when residence times in the order of minutes are required; and therefore, was selected as part of the design criteria for the system. Using a nominal thermal input of 100 kW to the calciner and the sorbent performance information gathered in Chapter 4, a complete heat and mass balance of the system was accomplished (not shown here) using UniSim process simulation software. All major process stream conditions (flowrate, temperature, pressure, etc.) such as fuel input, oxidant input, sorbent make-up, flue gas input carbonator, concentrated CO_2 product, recycle gas, and solids circulation rate were determined. These values, when combined with the fluidized bed hydrodynamic models, allowed for carbonator and calciner reactor sizing that (1) provided the appropriate gas-solid residence time to meet the desired CO_2 capture target (>90%) and (2) a reactor configuration that provided a controllable sorbent circulation rate (i.e., Ca/C molar ratio).

Chapter 5 provided detailed information on the design, construction, and commissioning of the dual fluidized bed system for continuous CO_2 capture. All information related to reactor geometry and limits of system operability were included based on experimental results contained in Chapter 4. A commissioning campaign showed that the calcium looping system could handle a variety of solid feedstocks for sorbent regeneration in oxy-fired combustion mode, CO_2 capture efficiencies greater than 90% could be achieved with simulated flue gas, and a concentrated CO_2 product stream of over 90 vol.% CO_2 could be achieved during oxy-fired combustion. Moreover, the system reliability related to solids transfer rates between reactors was not an issue and the transfer rate could not only be controlled, but accurately measured.

After the successful completion of the commissioning trials, CO_2 capture experiments were conducted using a variety of different CaO-based sorbents to examine the effect of realistic operating conditions on sorbent performance over long duration continuous operation (Chapters 6 and 7). It was determined that a natural occurring limestone (Cadomin) performed better than pelletized sorbents over a steady-state operating period of ~5 hours. The average carbonation conversion of the pellets was 6.0-6.8% compared to 7.8% achieved by limestone. The Ca/C molar ratio (F_{CaO}/F_{CO_2}) required to maintain >90% CO_2 capture ranged from approximately 9.2 for the limestone to 9.7-10.7 for the pellets. Additionally, sorbent make-up rates between 0.64 kg/h for the pellets and 0.93 kg/h for the limestone were determined, which after correcting for Ca content, result in a fresh sorbent make-up to circulating sorbent molar ratio of approximately 0.040 to 0.057. Based on these values, the average sorbent particle experiences ~18 to 25 cycles within the calcium looping process before being rejected from the system.

Analysis of the physical properties of the sorbents showed a significant loss of surface area and shift of pore size distribution to a wider range of pore size. These morphological changes occurred shortly after injecting the pellets into the system, suggesting rapid sintering of the pellets that reduced their CO_2 capture capacity. It was concluded that pelletization of CaO-based sorbents for CaL processes does not appear to be a practical approach, due to the high production cost of such pellets and the marginal improvement in CO_2 capture performance compared to natural non-modified limestones. In conjunction with published works on CO_2 capture performance of synthetic / modified CaO-based sorbents at the bench-scale; this work highlighted the fact that such sorbents would most likely have a significantly different performance when utilized at the commercial-scale. Thus, the assessment of such relatively

expensive sorbents should be performed at the pilot-scale under realistic operating condition to evaluate their performance against their production cost.

In conjunction with determining the sorbent performance from a CO_2 capture perspective, the rate of attrition of both limestone and synthetic pelletized sorbents was also tested using the pilot-scale dual fluidized bed system. The results revealed that, regardless of sorbent type ~50 wt.% of the sorbent attrited to smaller than 250 μm after the test had completed. Furthermore, ~45 wt.% of the sorbent smaller than 250 μm is in fact smaller than 150 μm. The particle size distribution of pellets indicated high attrition, and the attrition extent was comparable to that of limestone tested under similar conditions. Although the measured rates of attrition were relative high, sorbent elutriation rates (percentage of make-up rate) were quite low. The elutriation rates varied between 2.8 and 5.2% and had a minimal impact on the CO_2 capture performance. This would suggest that particle fragmentation is the dominant attrition mechanism since the majority of the attrited material could be captured using a high-throughput cyclone.

It is believed that the high attrition rate of limestone and pelletized sorbent occurred in the first calcination, caused by high calcination temperatures and heating rates. Batch and continuous injection of pellets to the system showed an insignificant effect of injection method on the attrition of the pellets. The similarity of particle size distribution patterns of pellets is indicative of similar attrition tendencies, and appears to be a characteristic of these pellets regardless of limestone type and injection method. Further to the performance results, it was concluded that pelletization of CaO-based sorbents only has a marginal improvement in the mechanical strength of the resultant pellets in comparison to that of naturally occurring limestone and the increased production cost would lead to the conclusion that pelletized sorbents are not a viable option.

The combination of bench-scale / batch pilot-scale testing and analysis led to the design and operation of a fully continuous dual fluidized bed reactor system for calcium looping. By operating under proper gas-solid contacting, high heating rates, and realistic reactive environments, key process parameters such as the deactivation rate, Ca/C molar ratio, and rate of sorbent attrition could be experimentally validated. Nevertheless, the following list summarizes suggestions for future work that is required for scale-up of the technology to the commercial-scale:

- Perform detailed techno-economic analyses *via* process simulation using the experimentally validated data provided in this work:
    - Cyclic sorbent carrying capacity = 6 to 8%
    - Ca/C molar ratio = 9 to 11
    - Sorbent make-up to circulating sorbent molar ratio = 0.040 to 0.057
    - Rate of sorbent elutriation (percentage of make-up rate) = 3 to 5%
- Perform continuous pilot-scale testing using a high sulphur content fuel and quantify the level of polycyclic aromatic hydrocarbons (PAH) in the waste sorbent.
- Explore options for decreasing the calciner operating temperature, such as the addition of steam, to increase average sorbent carbonation conversion and minimize particle attrition.
- Test a variety of synthetic or modified CaO-based sorbents that are more resistant to sintering at the pilot-scale for potential use at the commercial-scale.